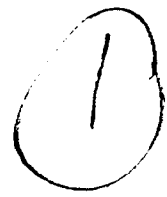


PL-TR-92-2054



AD-A247 625



PROCEEDINGS OF THE 13TH ANNUAL REVIEW
CONFERENCE ON ATMOSPHERIC TRANSMISSION
MODELS, 5-6 JUNE 1990

Editors:
F. X. Kneizys
L. W. Abreu

DTIC
ELECTE
MAR 11 1992
S D D

June 1990

APPROVED FOR PUBLIC RELEASE; DISTRIBUTION UNLIMITED



PHILLIPS LABORATORY
AIR FORCE SYSTEMS COMMAND
HANSCOM AIR FORCE BASE, MASSACHUSETTS 01731-5000

98 3 09 028

92-06101



"This technical report has been reviewed and is approved for publication"


WILLIAM A. BLUMBERG, Chief
Simulation Branch
Optical Environment Division


ALAN D. BLACKBURN, Col, USAF, Director
Optical Environment Division

This report has been reviewed by the ESD Public Affairs Office (PA) and is releasable to the National Technical Information Service (NTIS).

Qualified requestors may obtain additional copies from the Defense Technical Information Center. All others should apply to the National Technical Information Service.

If your address has changed, or if you wish to be removed from the mailing list, or if the addressee is no longer employed by your organization, please notify GL/TSI, Hanscom AFB, MA 01731-5000. This will assist us in maintaining a current mailing list.

Do not return copies of this report unless contractual obligations or notices on a specific document requires that it be returned.

REPORT DOCUMENTATION PAGE

1a. REPORT SECURITY CLASSIFICATION UNCLASSIFIED		1b. RESTRICTIVE MARKINGS	
2a. SECURITY CLASSIFICATION AUTHORITY		3. DISTRIBUTION/AVAILABILITY OF REPORT Approved for public release; distribution unlimited	
2b. DECLASSIFICATION/DOWNGRADING SCHEDULE			
PERFORMING ORGANIZATION REPORT NUMBER(S) PL-TR-92-2054		5. MONITORING ORGANIZATION REPORT NUMBER(S)	
6a. NAME OF PERFORMING ORGANIZATION Geophysics Laboratory (AFSC)	6b. OFFICE SYMBOL (if applicable) OP	7a. NAME OF MONITORING ORGANIZATION	
6c. ADDRESS (City, State, and ZIP Code) Hanscom AFB, MA 01731-5000		7b. ADDRESS (City, State, and ZIP Code)	
8a. NAME OF FUNDING/SPONSORING ORGANIZATION	8b. OFFICE SYMBOL (if applicable)	9. PROCUREMENT INSTRUMENT IDENTIFICATION NUMBER	
8c. ADDRESS (City, State, and ZIP Code)		10. SOURCE OF FUNDING NUMBERS	
		PROGRAM ELEMENT NO 62101F	PROJECT NO. 7670
		TASK NO. 09	WORK UNIT ACCESSION NO. 10
11. TITLE (Include Security Classification) Proceedings of the 13th Annual Review Conference on Atmospheric Transmission Models.			
12. PERSONAL AUTHOR(S) Editors, F.X. Kneizys and L.W. Abreu			
13a. TYPE OF REPORT Reprint	13b. TIME COVERED FROM _____ TO _____	14. DATE OF REPORT (Year, Month, Day) June 1990	15. PAGE COUNT
16. SUPPLEMENTARY NOTATION			
17. COSATI CODES		18. SUBJECT TERMS (Continue on reverse if necessary and identify by block number)	
FIELD	GROUP	Atmospheric Transmittance; Aerosols; Atmospheric Propagation	
20	06	Clouds; Radiative Transfer; Optical Turbulence; Molecular	
04	01	Absorption; Ultraviolet; Visible; Infrared; Spectroscopy.	
19. ABSTRACT (Continue on reverse if necessary and identify by block number) Contains the viewgraphs and other materials for the 31 papers presented at the Thirteenth Annual Review Conference on Atmospheric Transmission Models held at the Geophysics Laboratory (AFSC), Hanscom AFB, MA, 5-6 June 1990.			
20. DISTRIBUTION/AVAILABILITY OF ABSTRACT <input checked="" type="checkbox"/> UNCLASSIFIED/UNLIMITED <input type="checkbox"/> SAME AS RPT <input type="checkbox"/> DTIC USERS		21. ABSTRACT SECURITY CLASSIFICATION UNCLASSIFIED	
22a. NAME OF RESPONSIBLE INDIVIDUAL Leonard W. Abreu		22b. TELEPHONE (Include Area Code) 617-377-3654	22c. OFFICE SYMBOL GL/OPE

Contents

Introduction

vi

Session on Atmospheric Propagation Models

"Status of the LOWTRAN and MODTRAN Models"

L.W. Abreu, F.X. Kneizys, G.P. Anderson, E.P. Shettle, J.H. Chetwynd

1

"Modeling Solar and Infrared Radiation Fields for BTI/SWOE"

J.R. Hummel

13

"PCTTRAN 7 - An Implementation of the GL's LOWTRAN 7 Model for the Personal Computer"

J. Schroeder

26

"Spectral Modeling of Off-axis Leakage Radiance Using the MODTRAN Code"

N. Grossbard and D.R. Smith

34

"Cloud Opacity Retrievals Using LOWTRAN and the Stamnes Scattering Model"

B.L. Lindner and R.G. Isaacs

45

"Calculated Cloud Edge SWIR Radiance Gradients as Viewed by Satellite"

L.L. Smith

54

"The Department of Energy Initiative on Atmospheric Radiation Measurements (ARM): A Study of Radiative Forcing and Feedbacks"

R.G. Ellingson, G.M. Stokes and A. Patrinos

62

"The HITRAN Molecular Database in 1990"

Lt. S. Shannon and L.S. Rothman

71

"Line Coupling Calculations for Infrared Bands of Carbon Dioxide for FASCOD3"

M.L. Hoke, F.X. Kneizys, J.H. Chetwynd and S.A. Clough

80

"FASCOD3: An Update (with NLTE Emphasis)"

G.P. Anderson, F.X. Kneizys, E.P. Shettle, J.H. Chetwynd, L.W. Abreu,

M.L. Hoke, S.A. Clough and R.D. Worsham

88

Session on Line-By-Line Applications

"RAD: A Line-by-Line Non-LTE Radiative Excitation Model" R.H. Picard, R.D. Sharma, J.R. Winick, P.P. Wintersteiner, A.J. Paboojian, R.A. Joseph and H. Nebel	99
"Non-LTE CO ₂ Vibrational-Temperature Profiles for FASCOD3" P.P. Wintersteiner, A.J. Paboojian, J.R. Winick, R.H. Picard	112
"Non-LTE CO Infrared Emission in the Mesosphere and Lower Thermosphere and Its Effect on Remote Sensing" J.R. Winick, R.H. Picard and P.P. Wintersteiner	125
"Path Characterization Algorithms for FASCODE" R.G. Isaacs, S.A. Clough, R.D. Worsham, J.-L. Moncet, B.L. Lindner and L.D. Kaplan	137
"Temperature Retrievals with Simulated SCRIBE Radiances" J.-L. Moncet, S.A. Clough, R.D. Worsham, R.G. Isaacs and L.D. Kaplan	145

Session on Turbulence

"Validation of Random Phase Screens" A.E. Naiman and T. Goldring	155
"Recent Advances in Modeling of Boundary Layer Refractivity Turbulence" V. Theirmann, A. Kohnle	173

Session on Aerosols

"Visibility Data Filters for Europe" B.A. Schichtel and R.B. Husar	185
"Comparison of XSCALE 89 Vertical Structure Algorithm with Field Measurements" R.P. Fiegel	193
"Spatial Non-Uniformity of Aerosols at the 15,500 ft Level" L.A. Mathews and P.L. Walker	208
"A Method of Estimating Surface Meteorological Ranges from Satellite Aerosol Optical Depths" D.R. Longtin, J.R. Hummel and E.P. Shettle	219

Session on UV Modeling

"A Comparison of the UVTRAN and LOWTRAN7 Aerosol Models" S. O'Brien	226
"High Resolution Solar Spectrum Between 2000 and 3100 Angstroms" L.A. Hall and G.P. Anderson	237
"Predissociation Line Widths of the Schumann-Runge Absorption Bands of Some Isotopes of Oxygen" W.H. Parkinson, J.R. Esmond, D.E. Freeman, K. Yoshino, A.S-C. Cheung, S.L. Chiu	245
"AURIC: Atmospheric Ultraviolet Radiance Integrated Code" R.L. Hugueinin, M.A. LeCompte and R.E. Huffman	252
"Measurement Needs for AURIC: Atmospheric Ultraviolet Radiance Integrated Code" R.E. Huffman	264
"Modeling of Ultraviolet and Visible Transmission with the UVTRAN Code" E. Patterson and J. Gillespie	272

Session on LIDAR

"SABLE: A South Atlantic Aerosol Backscatter Measurement Program" S.B. Alejandro, G.G. Koenig, J.M. Vaughn and P.H. Davies	280
"The RSRE Laser True Airspeed System (LATAS)" J.M. Vaughn	281
"Measurements of Aerosol and Cloud Lidar Backscatter Profiles in the Equatorial South Atlantic" Lt. Col. G.G. Koenig, E.P. Shettle, S.B. Alejandro and J.M. Vaughn	282
"Comparisons Between SAGE 11 0.2 um Extinction and SABLE 10.6 um Backscatter Measurements" E.P. Shettle, G.G. Koenig, S.B. Alejandro, J.M. Vaughn, and D.W. Brown	283

Appendix

Call for Papers	284
Agenda	286
List of Attendees	293
Author Index	304

Acquisition For	
NTIS - CRA&I	<input checked="" type="checkbox"/>
DDIC - TAB	<input type="checkbox"/>
Unannounced	<input type="checkbox"/>
Justification	
By _____	
Date _____	
Acquisition For	
Dist	Acquisition For
A-1	

INTRODUCTION

The Thirteenth DoD Tri-Service Review Conference on Atmospheric Transmission Models was held at the Geophysics Laboratory, Hanscom AFB, Massachusetts on 5-6 June 1990. The purpose of the meeting was to review progress in the modeling of radiation propagating through the earth's atmosphere, identify deficiencies in these models, and make recommendations for improvements.

Approximately 100 scientists and engineers, representing DoD, other government agencies, industry, and the academic community were in attendance. The agenda consisted of thirty-one papers with sessions on turbulence, atmospheric propagation models, aerosols, UV modeling, and LIDAR.

This proceedings volume summarizes the technical presentations at the conference. The main part of the report consists of the abstracts and copies of the viewgraphs or slides and other material as provided by the authors for the presentations. The Appendix includes the original call for papers and invitation to the meeting, a copy of the Agenda for the meeting, a list of the attendees, and an author index.

A special thanks is extended to Ronald G. Isaacs, Betty Stenhouse and Atmospheric and Environmental Research, Inc.

Francis X. Kneizys

Leonard W. Abreu

STATUS OF THE LOWTRAN AND MODTRAN MODELS

L.W. Abreu, F.X. Kneizys, G.P. Anderson, E.P. Shettle*, and J.H. Chetwynd
Geophysics Laboratory/OPE, Hanscom AFB, MA 01731

LOWTRAN 7 (1988, AFGL-TR-88-0177) calculates atmospheric transmittance and background radiance for any given atmospheric path using spherical refractive geometry. The calculations are done at low spectral resolution (20 cm^{-1} full width-half maximum). The effects of single solar/lunar scattering and multiply scattered thermal and solar radiation are included. Enhancements and modifications to LOWTRAN will be discussed.

MODTRAN (presently beta-test version) is a 2 parameter band model (P & T) code with moderate spectral resolution (2 cm^{-1} full width-half maximum). The MODTRAN band model parameters were developed by utilizing the HITRAN data base. Full compatibility with LOWTRAN 7 is maintained and the code can be degraded to between 2 and 50 wavenumber spectral resolution.

*Now at Naval Research Laboratory (NRL), Code 6520, Washington, D.C. 20375

STATUS OF THE LOWTRAN AND MODTRAN MODELS

L.W. Abreu, F.X. Kneizys, G.P. Anderson,
E.P. Shettle and J.H. Chetwynd

ANNUAL REVIEW CONFERENCE ON
ATMOSPHERIC TRANSMISSION MODELS

5-6 June 1990

Geophysics Laboratory
Hanscom Air Force Base

ATMOSPHERIC PROPAGATION MODELS

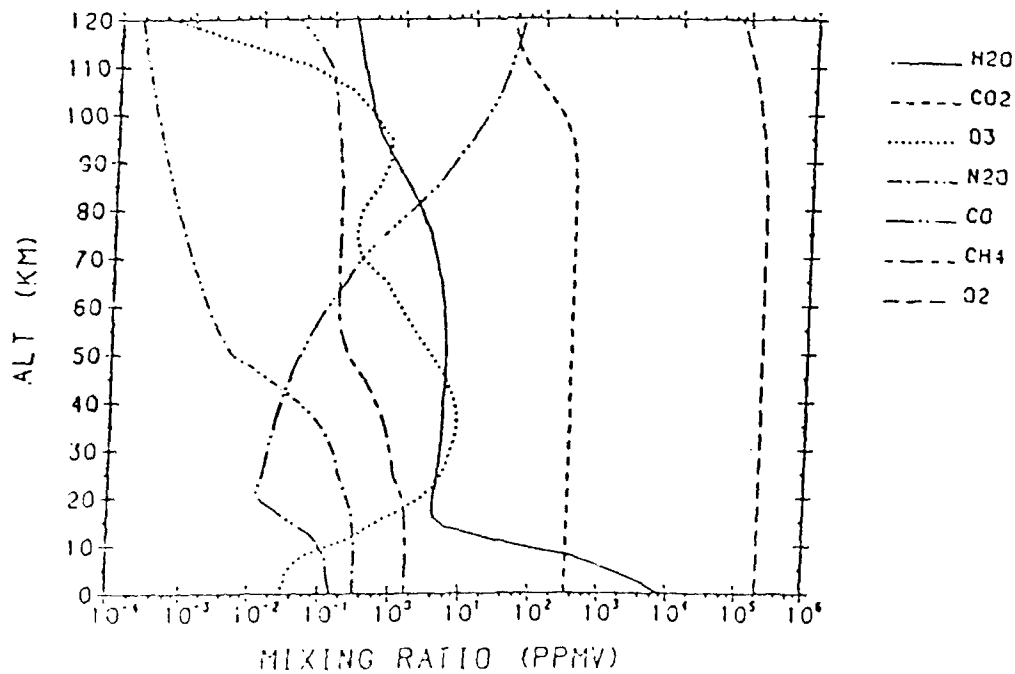
- * COMMON ELEMENTS
- * LOWTRAN (LOW)
- * MODTRAN (MODERATE)
- * FASCODE (HIGH)

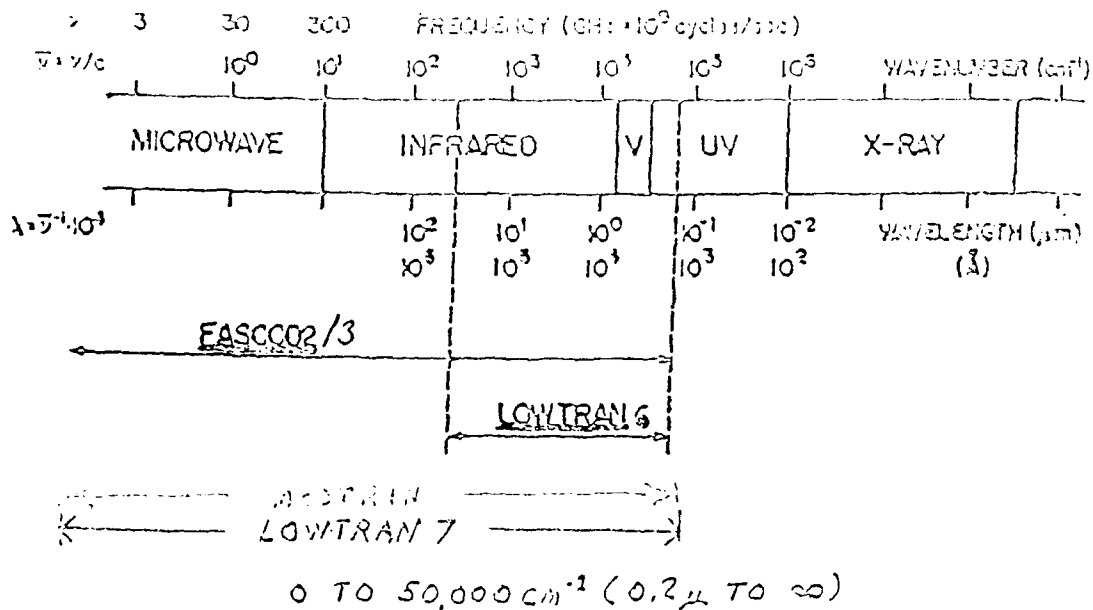
ATMOSPHERIC PROPAGATION MODELS

* COMMON ELEMENTS

- TRANSMITTANCE, RADIANCE
- GEOMETRY, THERMAL SCATTERING
- DEFAULT ATMOSPHERIC PROFILES
(MOLECULAR, AEROSOLS)
- SPECTRAL RANGE: 0 TO 50,000 CM-1
- INTERPOLATION, SCANNING, AND
FILTER FUNCTIONS

U.S. STD. PROFILES (1976)





ATMOSPHERIC PROPAGATION MODELS

* LOWTRAN 7 (1989)

RESOLUTION: 20 CM⁻¹ (LOW)

PHYSICS: 1-PARAMETER BAND MODEL

ALTITUDE RANGE: GROUND TO 40 KM

(LIMITED BY BAND MODEL)

APPLICATIONS: BROAD BAND SIMULATIONS (TDA ETC)

TARGET CONTRAST, LOOK-ON RANGE

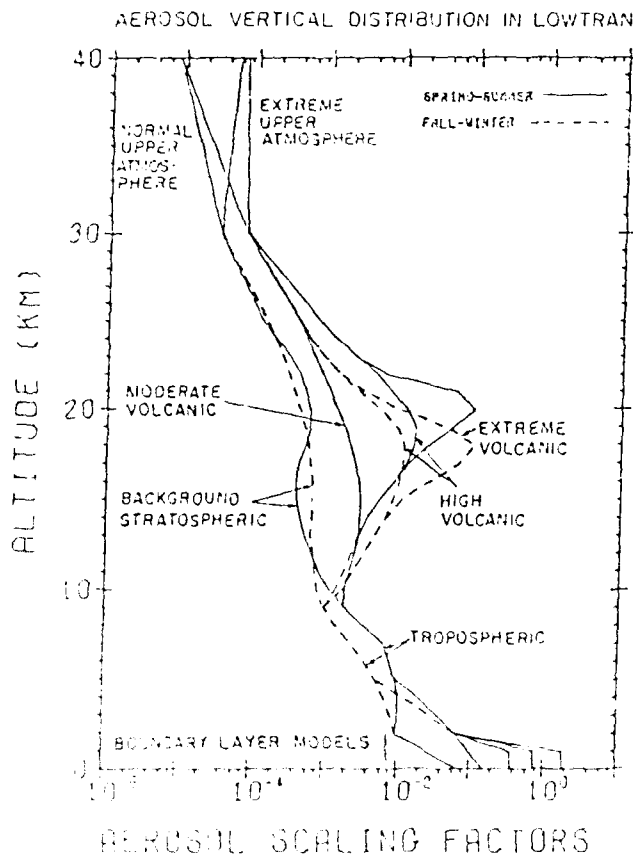
SOLAR (DIRECT, SCATTERED)

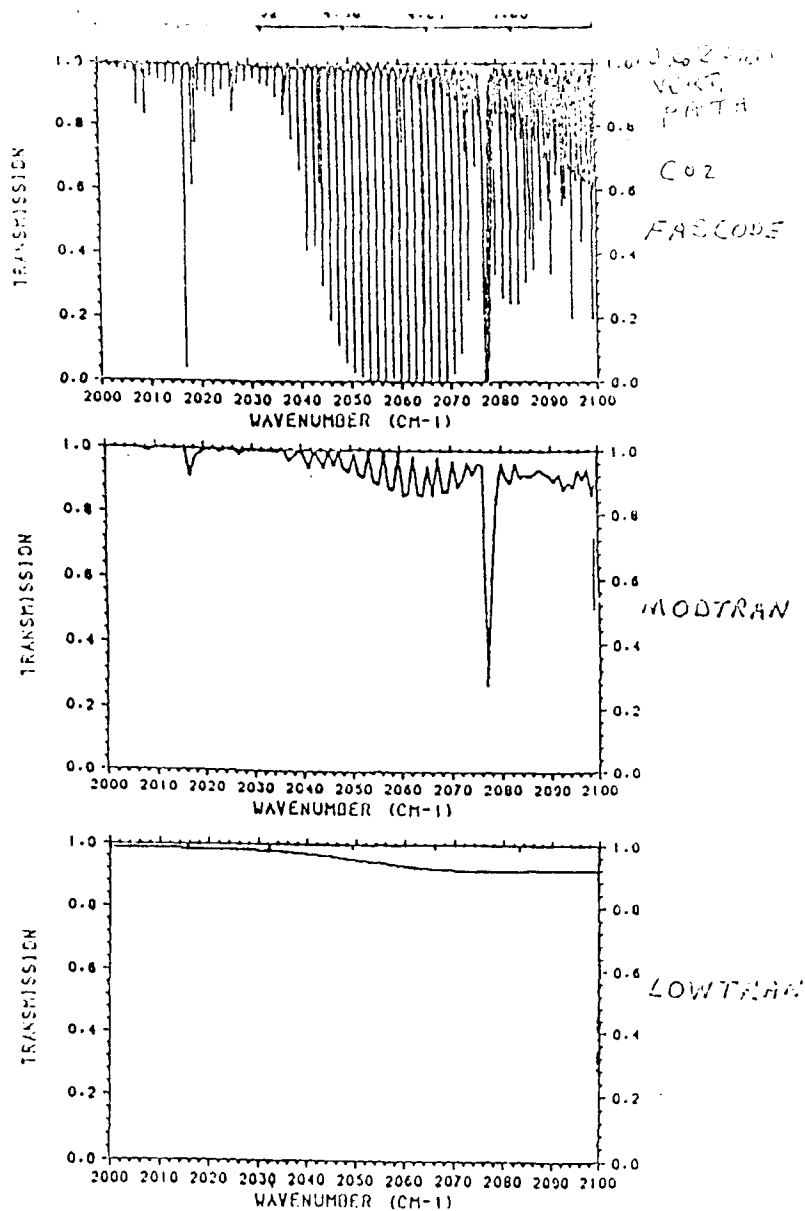
COMMENTS: EFFICIENT (NO TIME PENALTY)

ATMOSPHERIC PROPAGATION MODELS

* MODTRAN (1991)

RESOLUTION: 2 CM-1 (MODERATE)
PHYSICS: 2-PARAMETER BAND MODEL
ALTITUDE RANGE: GROUND TO 60 KM
(LIMITED BY LTE)
APPLICATIONS: BACKGROUND SIMULATIONS
+PLUMES, SOLAR (DIRECT, SCATTERED)
COMMENTS: MODERATE TIME CONSUMPTION
USES EXTERNAL DATABASE
IN 1 CM-1 BINS





MODTRAN Is An Atmospheric Transmittance And Radiance Model With:

- * Moderate Spectral Resolution; 2 cm^{-1}

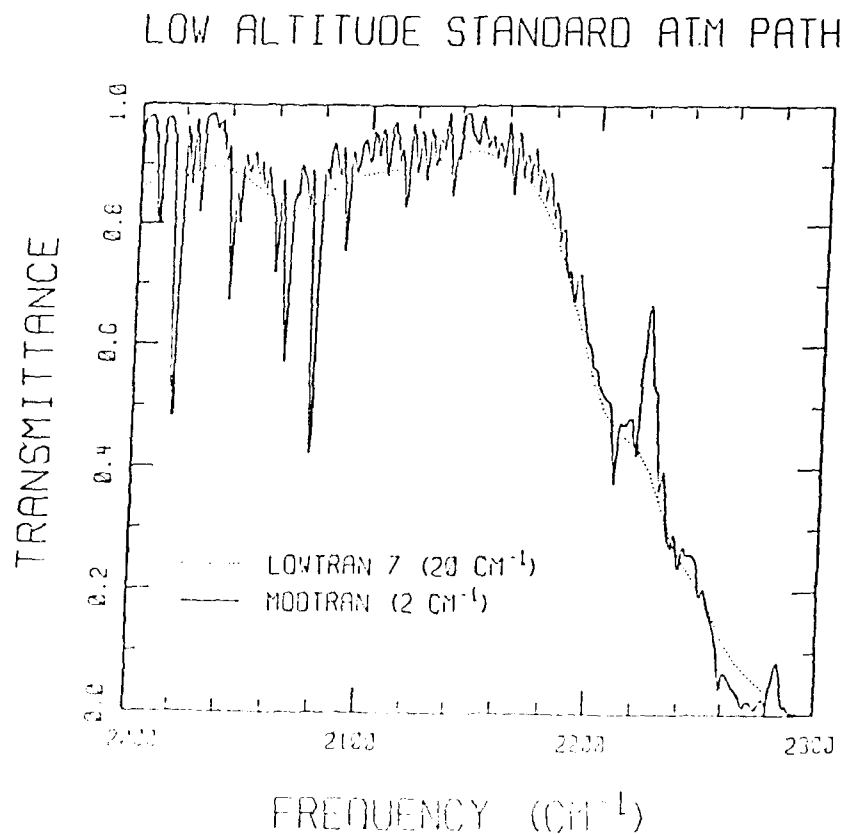
Appropriate For Transmittance Of
Plume Radiation

- * All LOWTRAN 7 Options Are Retained
- * Utilizes The LOWTRAN 7 Input Stream Plus
Two Additional Parameters
- * Run Times Are An Order Of Magnitude
Slower Than LOWTRAN 7

INCREASED SPECTRAL RESOLUTION

MOLECULAR TRANSMITTANCE ALGORITHMS WERE IMPLEMENTED WHICH PRODUCED 2 cm^{-1} Full Width/Half Maximum SPECTRAL RESOLUTION BY USING

- * 1 cm^{-1} BAND MODEL PARAMETERS FROM $0 - 17900 \text{ cm}^{-1}$
- * THE CURTIS-GOODSON APPROXIMATION FOR MULTIPLE LAYERS
- * AN EQUIVALENT WIDTH TRANSMITTANCE FORMALISM, AND
- * AN INTERNAL TRIANGULAR SLIT FUNCTION



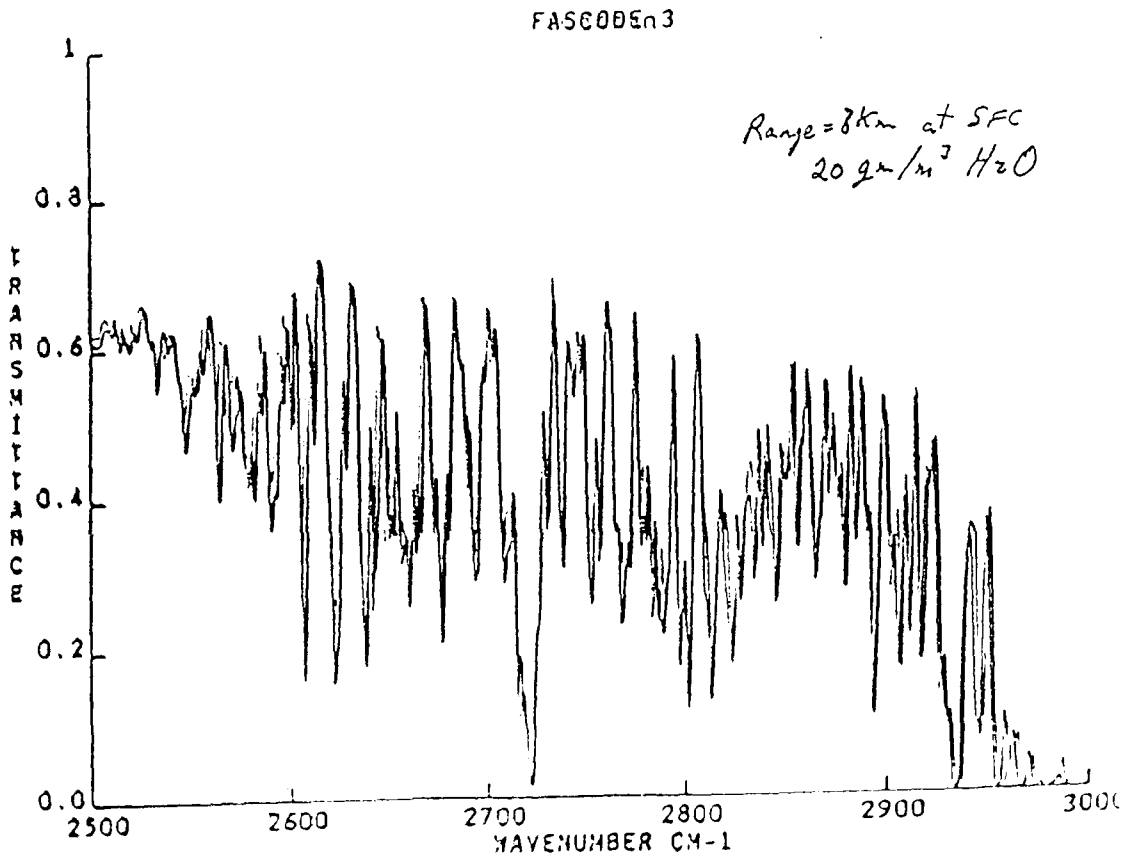
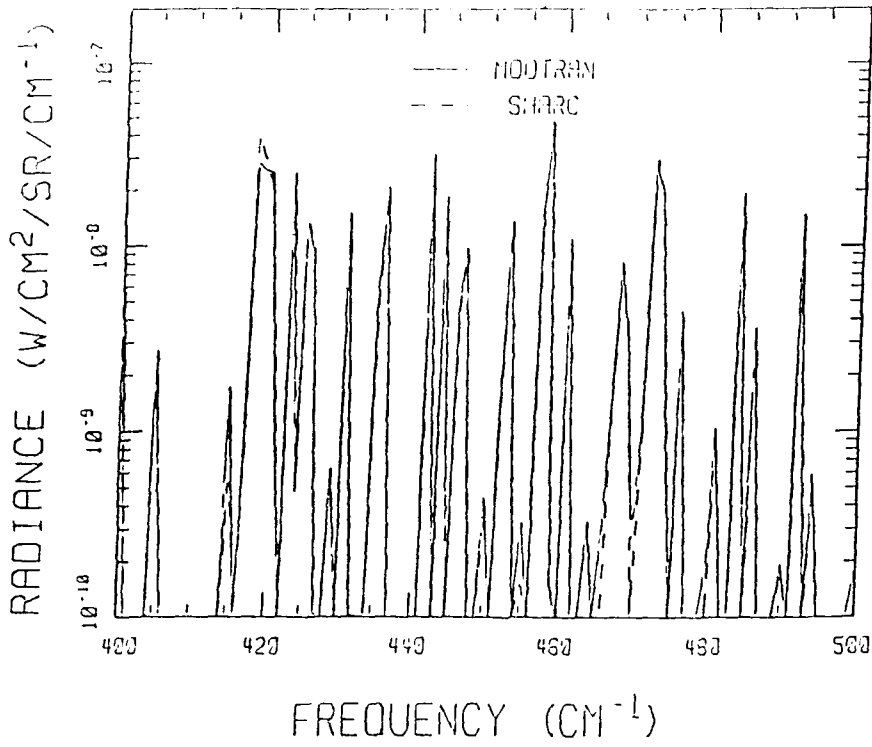
PHYSICS OF THE MODEL

- o Absorption Due To Lines Within Each 1cm-1 Bin Is Calculated By Integrating Over A Voigt Line Shape
- o The Curtis-Godson Approximation Is Used To Replace Multilayered Paths By An Equivalent Homogenous One
- o A Collisional Broadened Or Lorentz Line Width Parameter Is Defined At STP

EXPANDED APPLICABILITY

- * MODTRAN IS BETTER SUITED THAN LOWTRAN FOR ATMOSPHERIC PATHS ABOVE 30 KM
 - Band Model Parameters Are Both Temperature and Pressure Dependent
 - Transmittance Is Modeled With A Voigt Lineshape
- * HOWEVER, MODTRAN STILL ASSUMES LOCAL THERMODYNAMIC EQUILIBRIUM

H₂O 60 KM LIMB



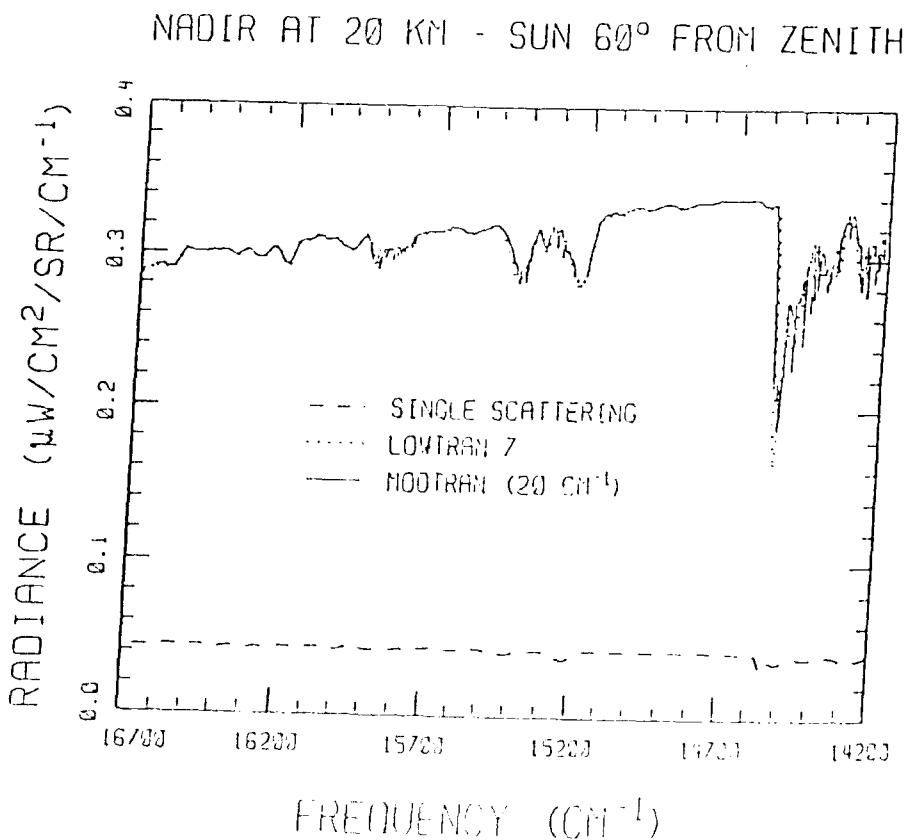
LOWTRAN 7 COMPATIBILITY

- o UTILIZING THE 1986 HITRAN DATA BASE SEPARATE ABSORPTION CALCULATIONS WERE PERFORMED FOR THE TWELVE MOLECULAR SPECIES IN LOWTRAN 7:

H2O CO2 O3 N2O CO CH4
O2 NO SO2 NO2 NH3 HNO3

- o THE THERMAL AND SOLAR MULTIPLE SCATTERING OPTION IS RETAINED

- The K-Distribution Method Is Replaced By 1 cm⁻¹ Calculations



MODTRAN 4.2.2003

FREQ (cm ⁻¹)	ALT (km)	T (K)	RANGE (km)	MEAN TR	MEAN TR	MEAN DIF	STAND DEV
2500-3300	45	300	1000000	.84432	.79373	.05059	4.55035E-3
	45	260	5000000	.71771	.55393	.04379	2.47046E-3
	30	300	50000	.75351	.71130	.04731	2.79251E-3
	30	260	10000	.87633	.85317	.01355	5.74034E-4
	15	300	1000	.72777	.70590	.02037	8.53067E-4
	15	260	500	.80402	.78934	.01419	5.24139E-4
	0	300	5	.72628	.72325	.00303	1.28832E-3
	0	260	1	.90095	.89974	.00121	3.40102E-4
3000-3500	45	300	1000000	.30033	.75677	.04340	8.55081E-3
	45	260	5000000	.65032	.65345	.03132	7.07845E-3
	30	300	50000	.72111	.68996	.03116	6.62731E-3
	30	260	5000	.88298	.87224	.01075	3.73268E-3
	15	300	100	.89267	.89470	.00203	2.57844E-3
	15	260	500	.77240	.76725	.00515	4.81810E-3
	0	300	.1	.79237	.78358	.00878	1.74617E-4
	0	260	1	.37106	.36653	.00453	2.50858E-4
3500-4000	45	300	50000	.74048	.66359	.07689	3.61090E-3
	45	260	50000	.73666	.67860	.05806	2.95129E-3
	30	300	1000	.73107	.68537	.04569	2.12370E-3
	30	260	500	.78857	.75784	.03073	1.42861E-3
	15	300	10	.74690	.72506	.02184	9.66237E-4
	15	260	100	.50990	.48951	.02038	1.06107E-4
	0	300	.001	.85431	.85948	.00483	2.24640E-4
	0	260	.01	.51742	.50799	.00943	5.12483E-4

GL ATMOSPHERIC PROPAGATION MODELS

GENERAL PROPERTIES	FABCODE	MODTRAN	LOWTRAN
SPECTRAL RESOLUTION			
HIGH	X		
MODERATE	X	X	
LOW	X	X	X
CAPABILITIES			
TRANSMITTANCE	X	X	X
BACKGROUND RADIANCE			
THERMAL	X	X	X
SOLAR/LUNAR		X	X

SPECIFIC APPLICATIONS	FASCODE	MODTRAN	LOWTRAN
LASER PROPAGATION	X		
PLUME SIGNATURES	X	X	
TARGET CONTRAST	X	X	X
REMOTE SENSING	X	X	X

GL ATMOSPHERIC PROPAGATION MODELS
POINTS OF CONTACT

- * LOWTRAN 7 (1989)
FRANCIS X. KNEIZYS
(617) 377-3654 /AV 478
 - * MODTRAN (1991)
LEONARD W. ABREU
(617) 377-2337 /AV 478
 - * FASCODE (FASCODE2-1986; FASCODE3-1990)
GAIL P. ANDERSON
(617) 377-2335 /AV 478
- GL/OPE (AFSC)
HANSCOM AFB, MA 01731

MODELING SOLAR AND INFRARED RADIATION FIELDS FOR BTI/SWOE

J.R. Hummel

SPARTA, Inc., 24 Hartwell Avenue, Lexington, MA 02173

The Balanced Technology Initiative (BTI) on Smart Weapons Operability Enhancement (SWOE) has a goal to model the radiant field from complex natural backgrounds. In order to achieve this goal, one must be able to model the thermal structure of the background. Two of the inputs to the energy budget of the background are solar and infrared radiation.

A review of approaches to calculate the solar and infrared fields has been made. The goal of this study has been to provide recommendations to the SWOE modeling community on the appropriate techniques to use for calculating the solar and infrared inputs to the background energy budgets.

MODELING SOLAR AND INFRARED RADIATION FIELDS FOR BTI/SWOE

John R. Hummel

SPARTA, Inc.
24 Hartwell Avenue
Lexington, MA 02173

June 5, 1990

Presented to:

Annual Review Conference on Atmospheric Transmission Models
Geophysics Laboratory, Hanscom AFB, Massachusetts

SPARTA INC.



SPARTA INC.

BRIEFING OUTLINE

- Background and Purpose of the Research
- Solar and Infrared Modeling Requirements of the BTI/SWOE Program
- Review of Representative Techniques
- Results
- Summary and Recommendations



SPARTA INC.

BACKGROUND AND PURPOSE OF THE RESEARCH

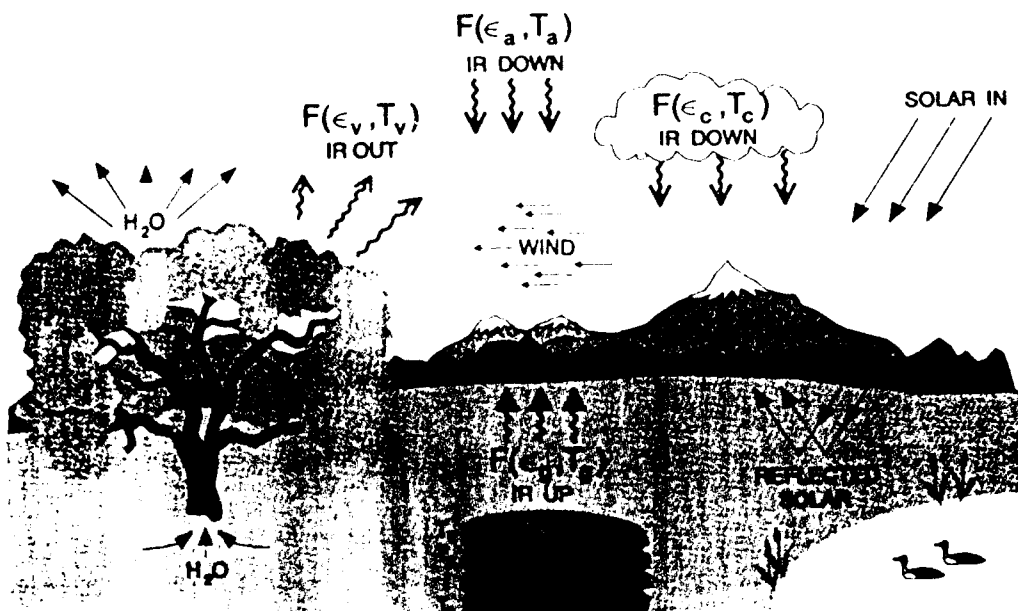
- **BACKGROUND**

- A Goal of the Balanced Technology Initiative (BTI) on Smart Weapons Operability Enhancement (SWOE) is to Model the Radiant Field From Complex Natural Backgrounds.
- One Must be Able to Model the Thermal Structure of the Background.
- Two of the Inputs to the Energy Budget are Solar and Infrared Radiation.

- **PURPOSE OF THE RESEARCH**

- Review Approaches to Calculate the Solar and Infrared Fields and Provide Recommendations to the BTI/SWOE Modeling Community on Appropriate Techniques.

RADIATION SCENE STRUCTURE





SOLAR AND INFRARED MODELING REQUIREMENTS FOR BTI/SWOE

- **FLUX INPUTS ARE REQUIRED TO:**
 - Thermally Load Scenes Prior to Time of Scene Simulation
 - Calculate Radiant Components Along Arbitrary Lines-of-Sight At Time of Scene Simulation

- **MODELS MUST:**
 - Valid for Wide Range of Environmental Conditions
 - Account for Cloud Reflections, Emissions, and Shadowing
 - Allow Variable Atmospheric Composition (H₂O, Aerosols,...)
 - Include Multiple Reflections and Emissions from Scene Elements

- **INPUTS MUST:**
 - Simple Enough for the SWOE User to Understand
 - Easily Obtainable (i.e., Surface Weather Observations)

SOLAR MODELS



COMPARISON OF SOLAR TREATMENTS

- Techniques to be Compared:
 - Solar Treatment in the Terrain Surface Temperature Model (TSTM)
 - ILUMA (EOSAEL 87)
 - LOWTRAN 7

- Results will be Compared for Clear and Cloudy Sky Conditions



SOLAR TREATMENT IN TSTM GENERAL BACKGROUND

- Based on Early Techniques Used by General Circulation Models

- Assumes Rayleigh Scattering Dominates Below 0.9 μm and H_2O Absorption Dominates Above

- Does Not Account for Aerosol Effects

- Includes Adjustments for Cloud Cover and Slope of Receiving Surface

- Cloud Adjustment Tied to Cloud Type

- Does not Separate Direct and Diffuse Components



SOLAR TREATMENT IN ILUMA GENERAL BACKGROUND

- Based on Shapiro Model (1982) for Calculating Solar Fluxes From Standard Surface Meteorological Observations
- Input Parameters Tied to:
 - Location
 - Time of Day
 - Type of Surface
 - State of Surface (Wet, Dry, Frozen,...)
 - State of Weather (Precip, Clouds, Presence of Obscurants,...)
- **Not** Tied to Temperature or RH
- No Accounting for Aerosols
- Does Not Separate Direct and Diffuse Components
- Model Evaluated for Limited Locations and Seasons



COMPARISON OF SOLAR MODELING FEATURES

FEATURE	TSTM	ILUMA	LOWTRAN 7
Wavelength Dependent	No	No	Yes
Separate Direct and Diffuse Terms	No	No	Yes
Adjustments for Clouds	Yes (Empirical)	Yes (Implicit)	Yes (Explicit)
Cloud Layering	No	Yes	No
Calculates Directional Radiances	No	No	Yes
Includes Weather Effects	No	Yes (Implicitly)	Yes (Explicitly)

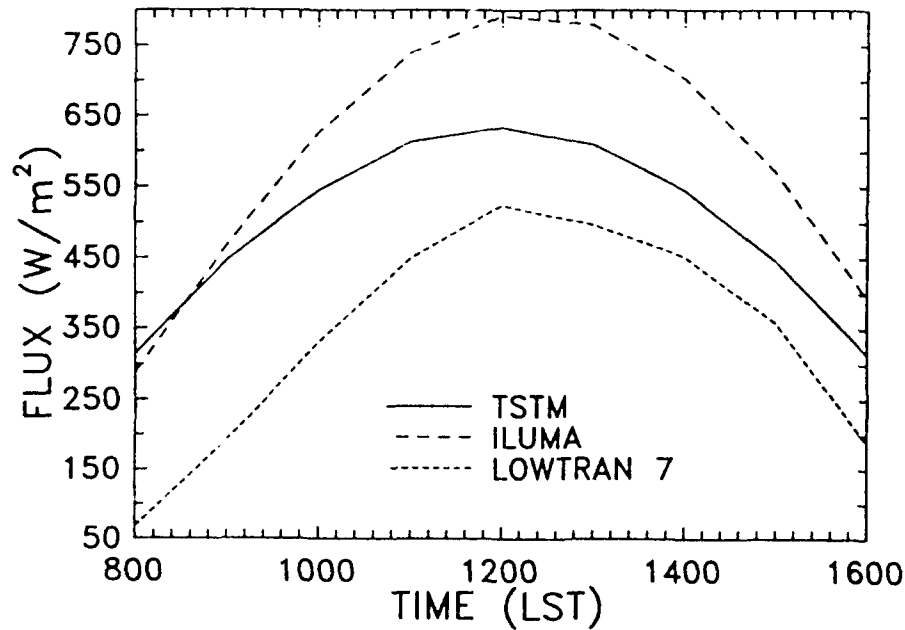
Trans 02/090490



RESULTS OF COMPARISONS SOLAR FLUXES

SPARTA INC.

CLEAR SKIES, 10 SEPT 1982



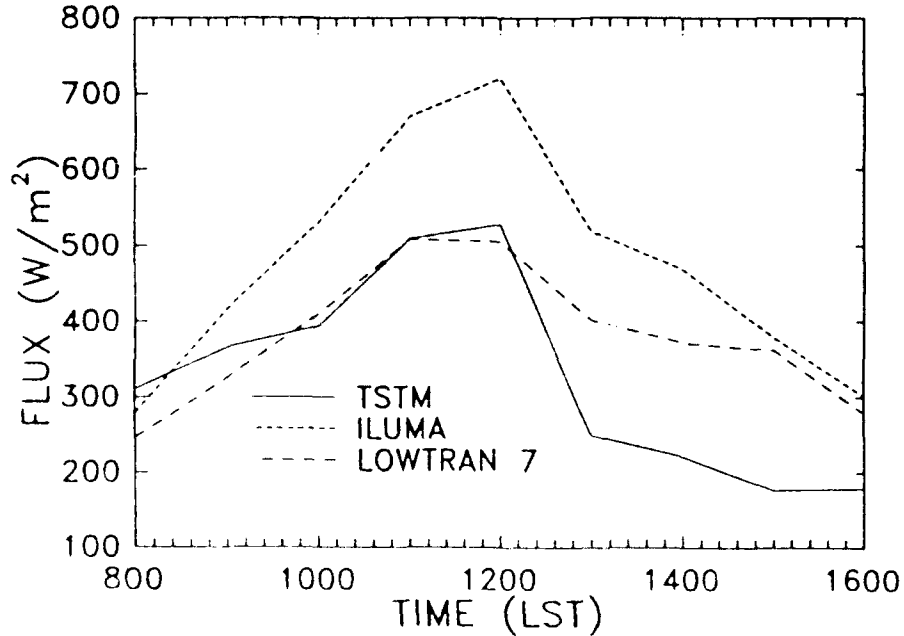
Trans 10/090490



RESULTS OF COMPARISONS SOLAR FLUXES

SPARTA INC.

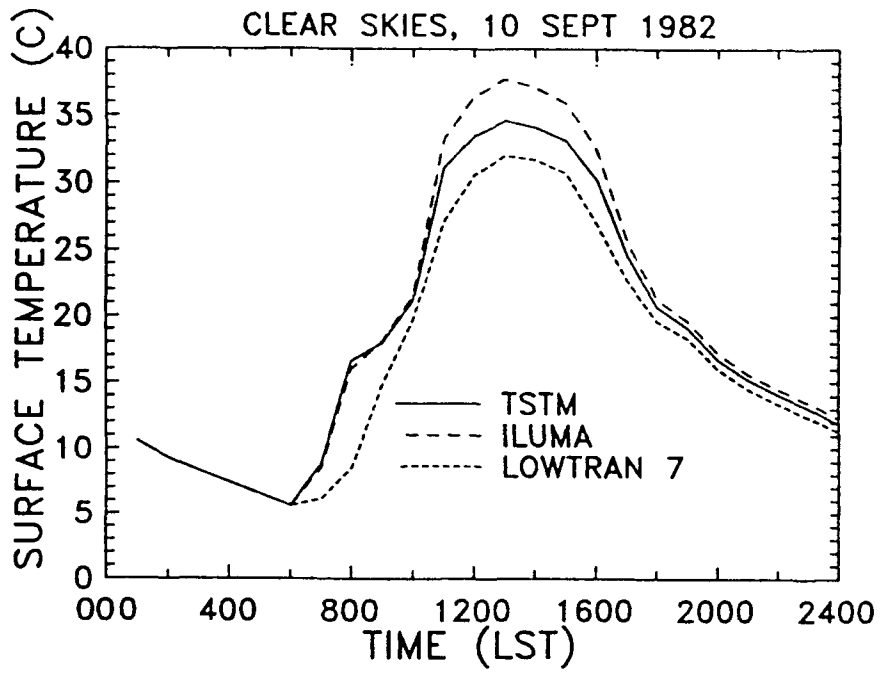
CLOUDY SKIES, 7 SEPT 1982





RESULTS OF COMPARISONS IMPACT OF SOLAR FLUX DIFFERENCES

SPARTA INC.



INFRARED MODELS



COMPARISON OF INFRARED TREATMENTS

SPARTA INC.

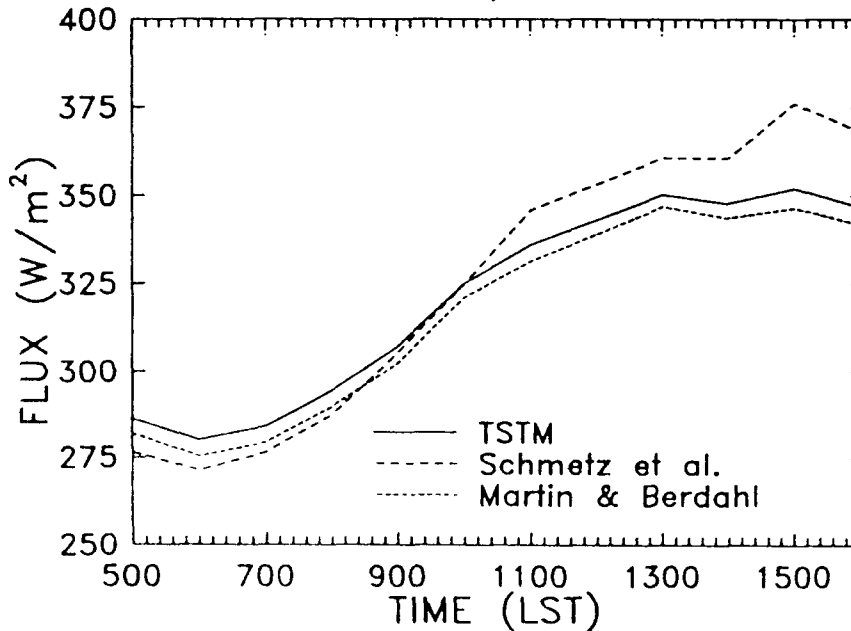
FEATURE	TSTM	Martin & Berdahl	Schmetz et al.	LOWTRAN 7
Clear Sky Emissivity Tied To	Air Temp, RH	Dew Point Temp	Air Temp (Idso & Jackson)	Model Atmosphere
Adjustments for Clouds	Yes (Empirical)	Yes (Empirical)	Yes (Empirical)	Yes (Explicit)
Cloud Layering	No	No	No	No
Calculates Directional Radiances	No	No	No	Yes
Wavelength Dependent	No	No	No	Yes
Includes Weather Effects	No	No	No	Yes (Explicitly)



RESULTS OF COMPARISONS IR FLUXES

SPARTA INC.

CLEAR SKIES, 10 SEPT 1982

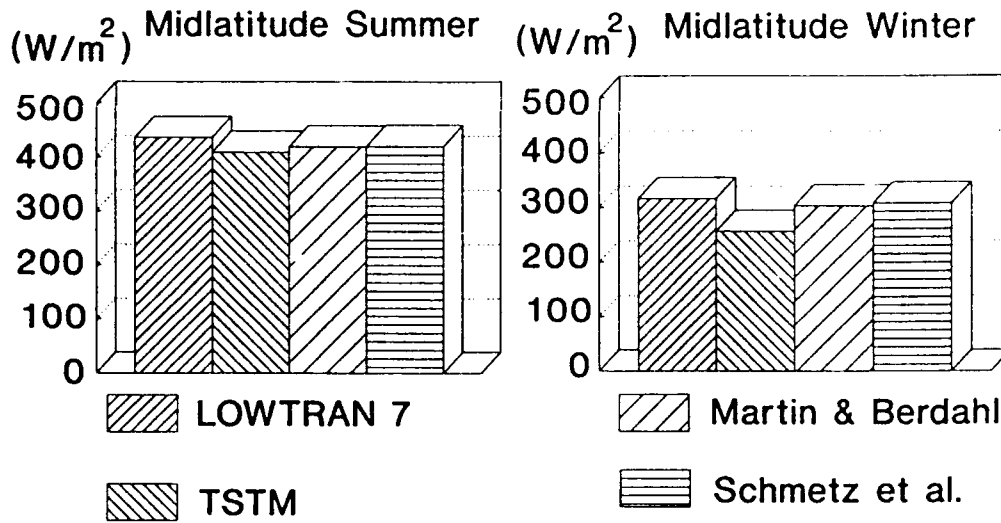




SPARTA INC.

RESULTS OF COMPARISONS IR FLUXES - CLOUDY SKIES

Cumulus Clouds



SUMMARY AND
CONCLUSIONS



SPARTA INC.

SUMMARY OF MODELING REQUIREMENTS FOR BTI/SWOE

AREA	REQUIREMENT
Energy Budget Calculations	Direct & Diffuse Solar Terms
	Account for Reflections Off Scene Elements
	Account for Absorption & Scattering by Atmospheric Gases, Aerosols, & Clouds
	Cloud Contributions Including Shadowing
Radiant Field Calculations	Wavelength Dependence
	Directional Scattering, Reflection, and Emission Along Arbitrary Lines-of Sight
Environmental	Valid for All SWOE Scenarios
Data	Obtainable From Routine Surface Weather Observations



SPARTA INC.

SUMMARY OF SOLAR MODELS STUDIED

MODELING REQUIREMENT	TSTM	ILUMA	LOWTRAN 7
ENERGY BUDGETS			
Wavelength Dependent	No	No	Yes
Separate Direct and Diffuse Terms	No	No	Yes
Adjustments for Clouds	Yes	Yes	Yes
Cloud Layering	No	Yes	No
Cloud Shadowing	No	No	No
Includes Aerosol Effects	No	No	Yes
RADIANT FIELDS			
Calculates Directional Radiances	No	No	Yes
Calculates for Specific Wavebands	No	No	Yes
ENVIRONMENTAL			
Valid for SWOE Locations	??	??	??
DATA			
Uses Conventional Surface Weather Data	Yes	Yes	Yes
Uses Radiosonde Data	No	No	Yes



SUMMARY OF INFRARED MODELS STUDIED

SPARTA INC.

MODELING REQUIREMENT	TSTM	Martin & Berdahl	Schmetz et al.	LOWTRAN 7
ENERGY BUDGETS				
Wavelength Dependent	No	No	No	Yes
Adjustments for Clouds	Yes	Yes	Yes	Yes
Cloud Layering	No	No	No	No
Includes Weather Effects	No	No	No	Yes
RADIANT FIELDS				
Calculates Directional Radiances	No	No	No	Yes
Calculates for Specific Wavebands	No	No	No	Yes
ENVIRONMENTAL				
Valid for SWOE Locations	??	??	??	??
DATA				
Uses Conventional Surface Weather Data	Yes	Yes	Yes	Yes
Uses Radiosonde Data	No	No	No	Yes



CONCLUSIONS AND RECOMMENDATIONS

SPARTA INC.

CONCLUSIONS

- Solar and Infrared Models Sampled From the Research Community do not Satisfy BTI/SWOE Requirements

RECOMMENDATIONS

- An Approach Similar to LOWTRAN 7 Should be Used to Provide Solar and IR Inputs to BTI/SWOE
- Modifications and Enhancements Required, but Within the Framework of LOWTRAN Concept
- Validation Studies With Field Data Mandatory



SPARTA INC.

CONCLUSIONS AND RECOMMENDATIONS

CONCLUSIONS

- Solar and Infrared Models Sampled From the Research Community do not Satisfy BTI/SWOE Requirements

RECOMMENDATIONS

- An Approach Similar to LOWTRAN 7 Should be Used to Provide Solar and IR Inputs to BTI/SWOE
- Modifications and Enhancements Required, but Within the Framework of LOWTRAN Concept
- Validation Studies With Field Data Mandatory

**PCTRAN 7 — AN IMPLEMENTATION OF THE GL's
LOWTRAN 7 MODEL FOR THE PERSONAL COMPUTER**

J. Schroeder

Ontar Corporation, 129 University Road, Brookline, MA 02146

PCTRAN 7 is an implementation of the Geophysics Laboratory's LOWTRAN 7 model, and associated software, for the IBM, and compatible, family of personal computers. The package contains software for setting inputs, help capability for LOWTRAN parameters, viewing of output files, screen graphics and hard copy graphics. The software has been validated by the GL under a cooperative IR &D agreement with Ontar.

This paper will describe PCTRAN 7, Version 2, and demonstrate the capabilities of the package.

**PCTRAN 7 [c]: An Implementation of the GL's
LOWTRAN 7 Model for the Personal Computer**

ANNUAL REVIEW CONFERENCE ON ATMOSPHERIC TRANSMISSION MODELS

Geophysics Laboratory, Hanscom AFB, MA

5 June 1990

Paul V. Noah, and John Schroeder

Ontar Corporation

129 University Road

Brookline, MA 02146 - 4532

Tel: 617-739-6607 FAX: 617-277-2374



Cooperative R & D Agreement

With Geophysics Laboratory - Hanscom AFB, MA

September 1988

PC Implementation of a Software Package - LOWTRAN 7 - PCTRAN 7 [c]



PCTRAN 7 [c] * Version 2

PC Version of the AFGL LOWTRAN 7 Atmospheric Radiance & Transmission Code

Complete Implementation of the LOWTRAN 7 Code - 7.37

Interactive User Input Software

Help Screens for All Input Variables

Screen and Hard Copy Graphics Output

Tabular Output in ASCII Format

Batch Processing Input Software

Plotting from Different LOWTRAN Calculations

***CERTIFIED for ACCURACY by the GEOPHYSICS LABORATORY**

Hardware and Software Requirements

Personal Computer - XT, AT, 80386, 80486 (Compatible, Clone)

1.2 Mbyte Diskette Drive, Hard Disk

640 Kbytes of Memory

CGA, EGA, or VGA Graphics Board and Monitor - for Screen Plots

Printer - for Hard Copy

Numeric Co-processor Highly Recommended

LITERATURE AVAILABLE

SOFTWARE DEMONSTRATION

Ontar Corporation

129 University Road

Brookline, MA 02146 - 4532

Tel: 617-739-6607 FAX: 617-277-2374 Bulletin Board: 617-277-6299



ONTAR's LOWTRAN Program Suite -- Version 7.2

- a. LOWTRAN Input -- LOWIN
- b. Execute LOWTRAN
- c. LOWTRAN Plotting -- LOWPLT
- d. Printer Plotting -- PRTPLT
- e. View LOWTRAN Output -- VIEWOUT
- f. View FILE7 -- VIEWOUT
- g. View FILE8 -- VIEWOUT
- h. LOWFIL Input -- LFILIN
- i. Execute LOWFIL
- j. View LOWFIL Output -- VIEWOUT
- k. Execute LOWSCAN
- l. LOWSCAN Plotting -- LOWPLT
- m. View FILE9 -- VIEWOUT
- n. Multiple LOWTRAN Plots -- LOWMPIN & LOWPLT

- o. Return to DOS

Input Function:

29



PC-TRAN7 Batch Mode Manager.

- ESC - Quit LOWIN (write LOWIN and LOWPLT.DAT)**
- F2 - Edit current run.**
- F3 - Edit next run.**
- F4 - Edit previous run.**
- F5 - Add new run (to end) and go to that run**
- F6 - Delete current run.**
- F7 - Go to run.**

Database name MCASE3

Number of runs in this database 4 Current run 3

LOWTRAN7 Card 5



Initial Altitude (km)	1.500
Final Altitude/Tangent Height (km)	10.000
Initial Zenith Angle (degrees)	.000
Path Length (km)	.000
Earth Center Angle (degrees)	.000
Radius of Earth (km) [.000 - default]	.000
Type of Path	Short
Initial Frequency 2000.000 cm-1	Wavelength 4.000 m
Final Frequency 2500.000 cm-1	Wavelength 5.000 m
Frequency Increment (wavenumber)	5.000

Run # 2 of 4 LOWTRAN7 Cards 3 & 4



Plot Type	Transmittance in m
Type of X Axis	Linear
Type of Y Axis	Linear
Number of Decimal Digits for Y Axis	2
Length of X Axis (In Inches)	7.0000
Beginning Wavenumber/Wavelength	4.0000 m
Ending Wavenumber/Wavelength	5.0000 m
X Axis Annotation Interval	.2000 m
X - Number of Minor Ticks / Division	5
Length of Y Axis (In Inches)	6.0000
Autoscale Y Axis	No
Minimum Transmittance/Radiance	.00E+00
Maximum Transmittance/Radiance	1.00E+00
Y Axis Annotation Interval	2.00E-01
Y - Number of Minor Ticks / Division	5
Plot Grids (Graph Paper)	Coarse Grid

Run # 2 of 4

LOWPLT Scaling

Plot # 1

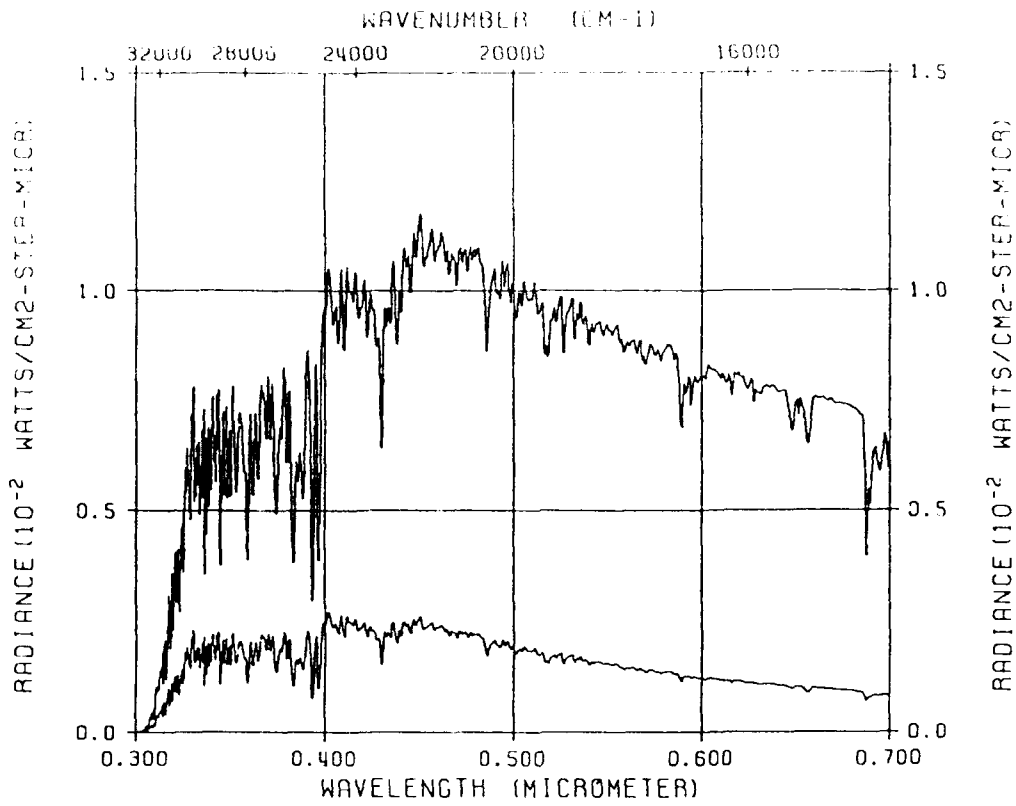


Multiple Run Plotting Inputs

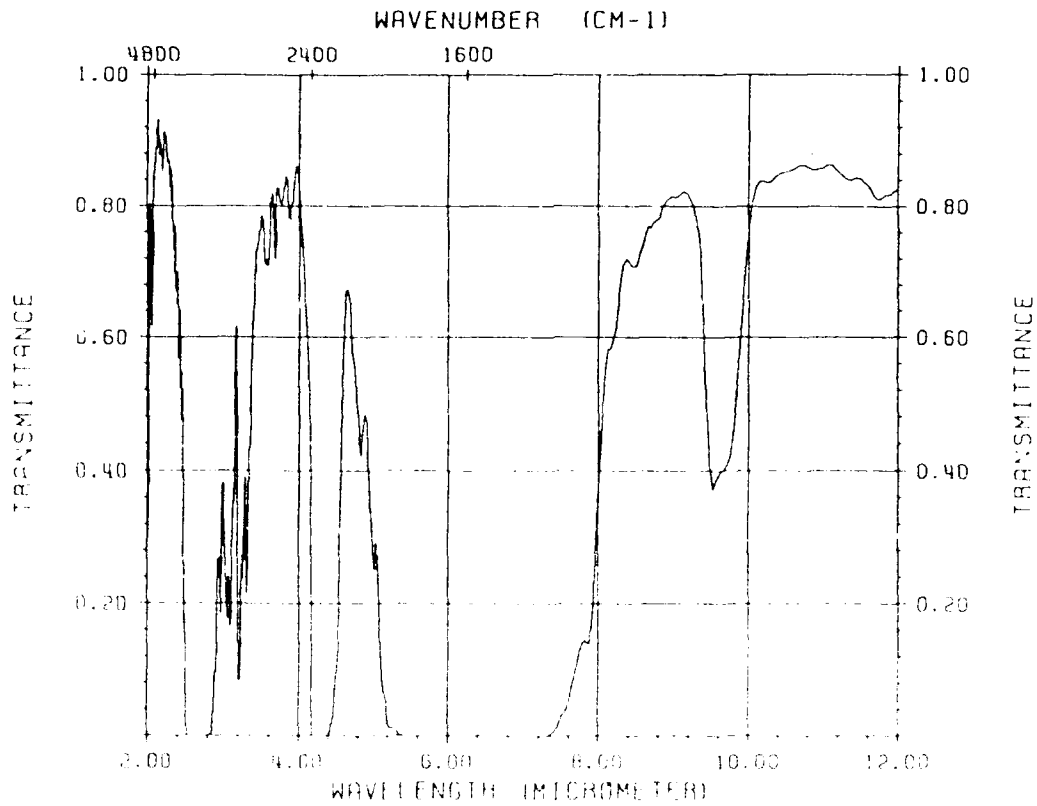
Filename	Run	Plot Mode	Title
CASE-A	1	Transmittance	1976 U S STANDARD
CASE-A	2	Transmittance	SUBARCTIC WINTER
CASE-A	3	Radiance /w Scattering	SUBARCTIC SUMMER
CASE-A	4	Radiance	MIDLATITUDE SUMMER
CASE-B	1	Transmittance	1976 U S STANDARD
CASE-B	2	Radiance	TROPICAL MODEL
CASE-B	3	Radiance /w Scattering	MIDLATITUDE SUMMER
CASE-B	4	Transmittance	SUBARCTIC SUMMER
CASE-C	1	Transmittance	1976 U S STANDARD
CASE-C	2	Radiance	TROPICAL MODEL
CASE-C	3	Radiance /w Scattering	New Model Atmosphere
CASE-C	4	Transmittance	Met Data (Hor Path)

LOWMPIN Select Runs

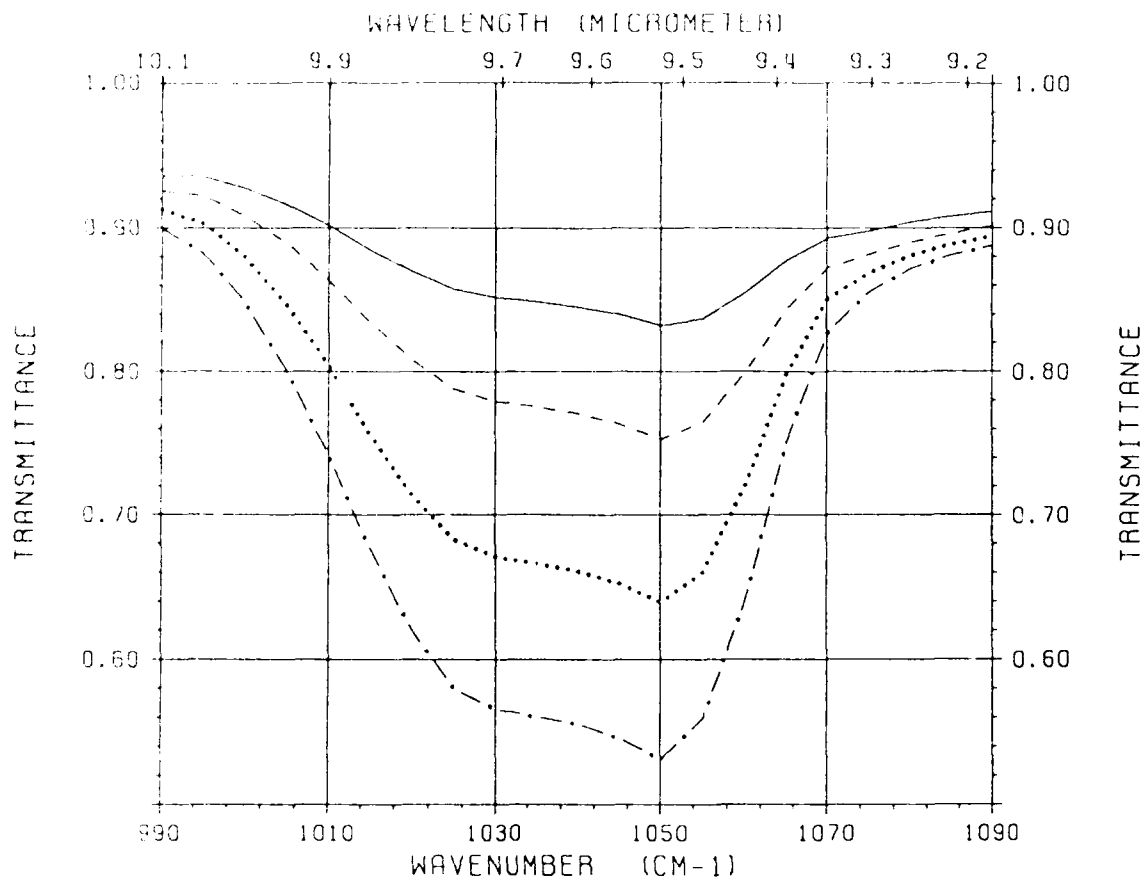




MULTIPLE AND SINGLE SCATTERED SOLAR RAD



SEA LEVEL TO SPACE



MULTIPLE PLOT TEST CASE



**SPECTRAL MODELING OF OFF-AXIS LEAKAGE
RADIANCE USING THE MODTRAN CODE**

N. Grossbard

Boston College, 885 Centre Street, Newton, MA 02159

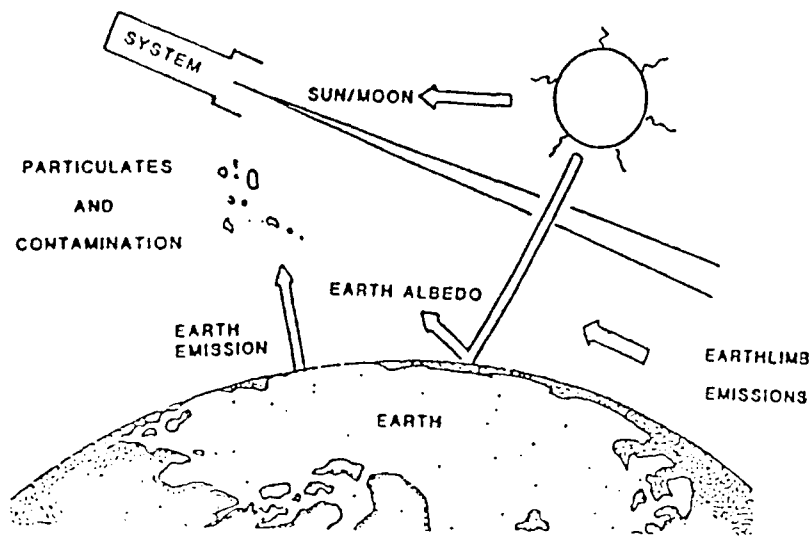
D.R. Smith

Geophysics Laboratory, Hanscom AFB, MA 01731

MODTRAN has been used together with the Degges High Altitude Infrared Radiance Model for the purpose of modeling the off-axis leakage spectra obtained from the HIRIS and SPIRE rocketborne atmospheric experiments. Off-axis leakage spectra for numerous angular shells around the sensor FOV were calculated using nominal or pre-flight estimates of the telescope's off-axis rejection (OAR) performance. Each leakage contribution was weighted to obtain a best least squared fit to the actual flight data. The resulting weighting functions were then applied as correction factors to the initial estimates of the off-axis rejection performance to obtain estimates of the inflight OAR performance of the telescope. The computed spectra are in good agreement with the flight data in each case and the resulting OAR performance curves, though considerably worse than initial estimates based on laboratory measurements, are reasonable for inflight conditions and in good agreement with other inflight estimates of OAR performance.

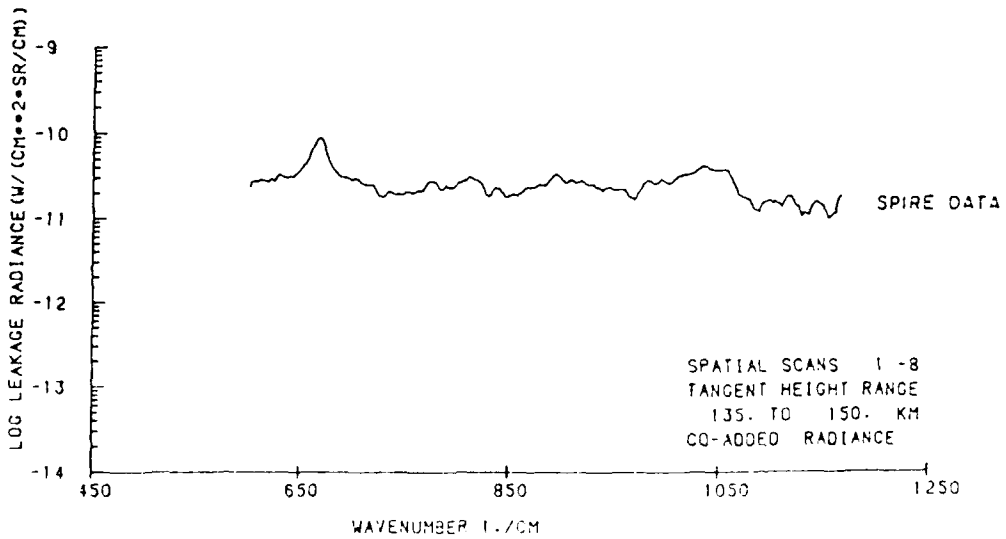
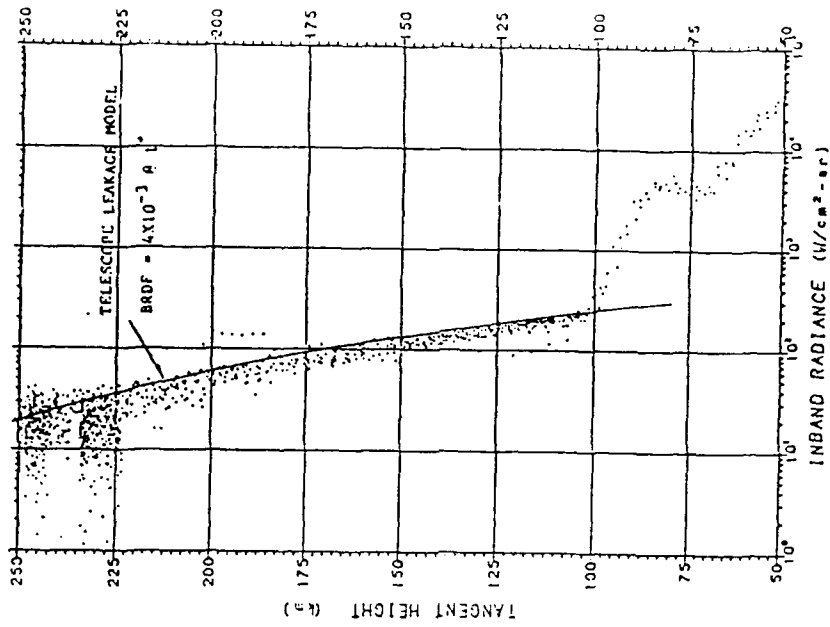
Spectral Modeling of Off-Axis Leakage Radiance Using the MODTRAN Code
N. Grossband (Boston College) and D.R. Smith (Geophysics Laboratory)

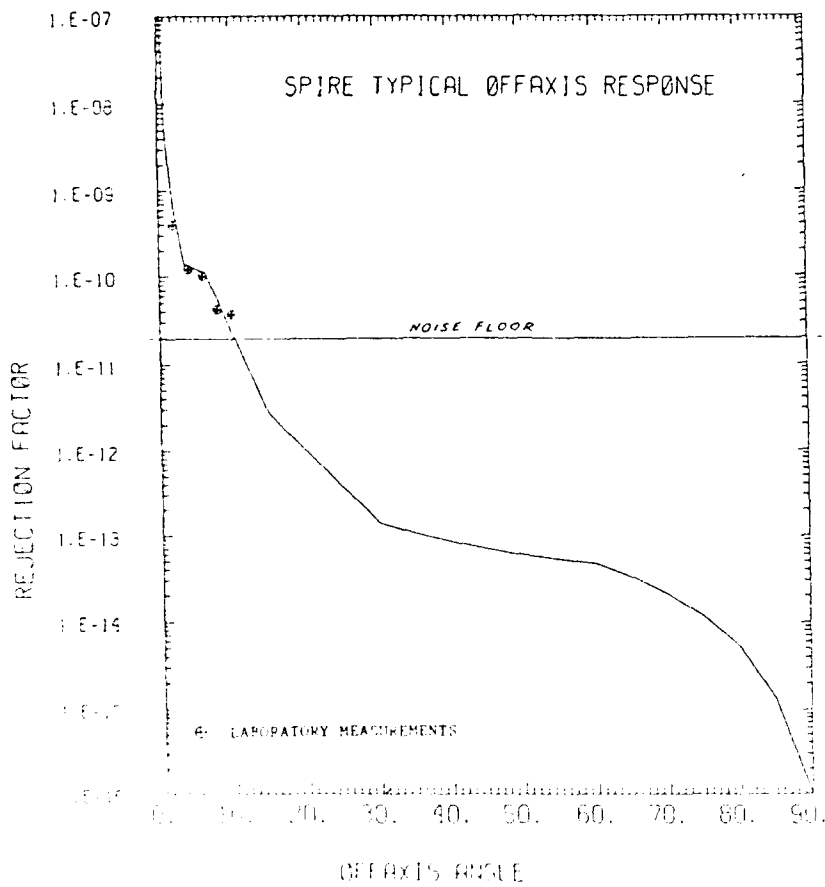
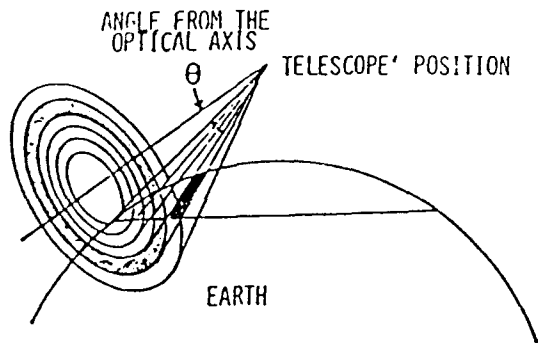
STRAYLIGHT



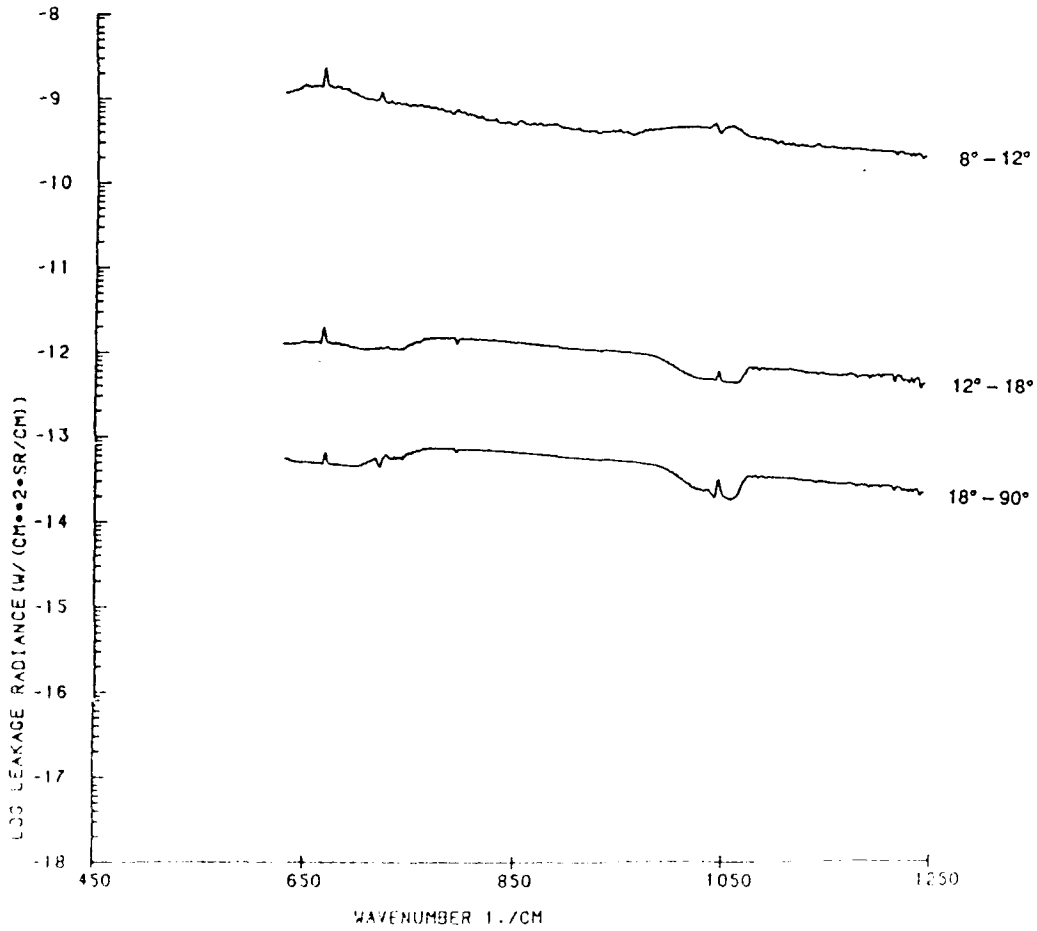
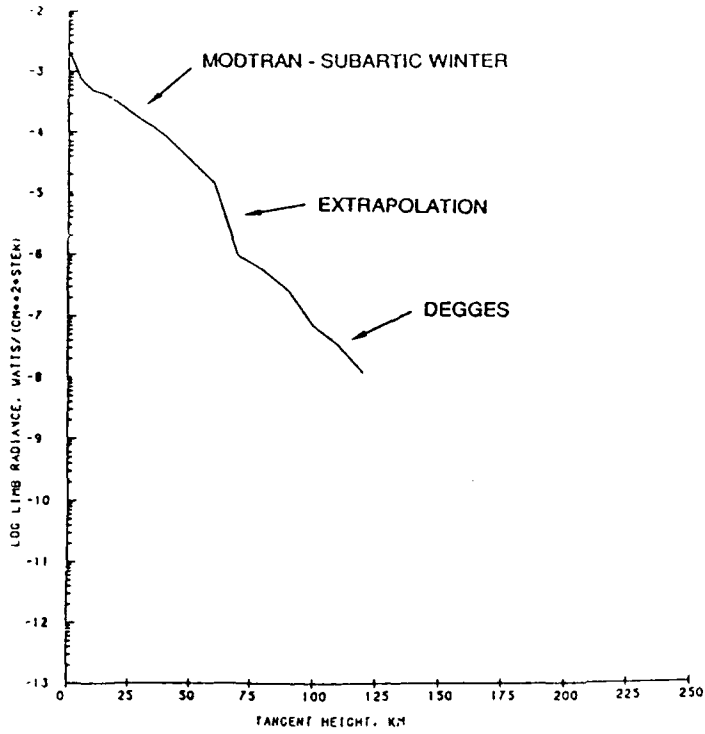
87/12/12.

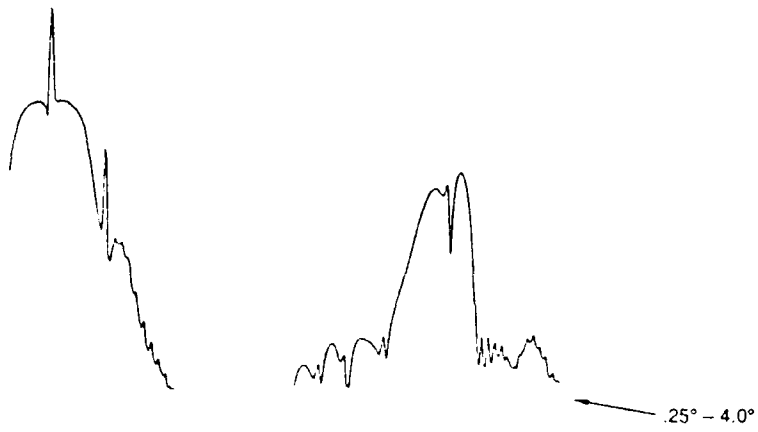
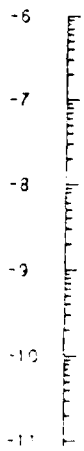
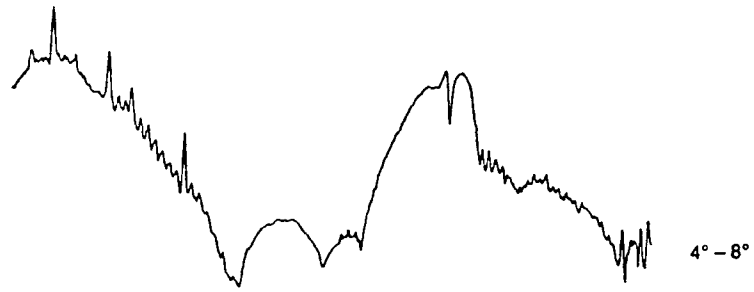
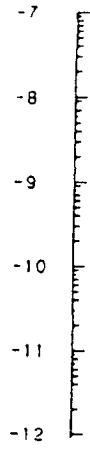
ELC FLIGHT 1 TANGENT HEIGHT VERSUS RADIANCE
CHANNEL 13 194.0 TO 403.0 SECONDS



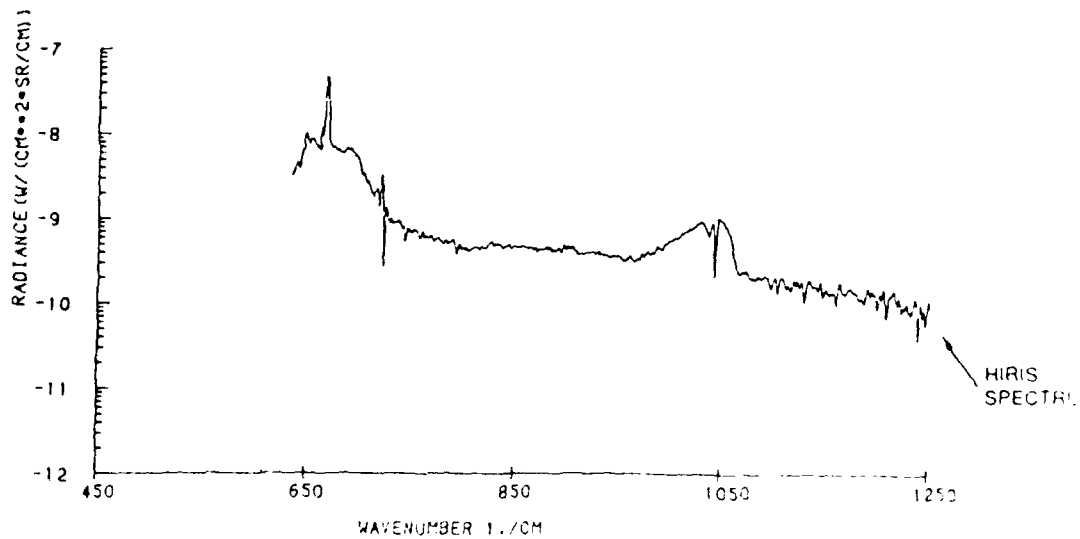
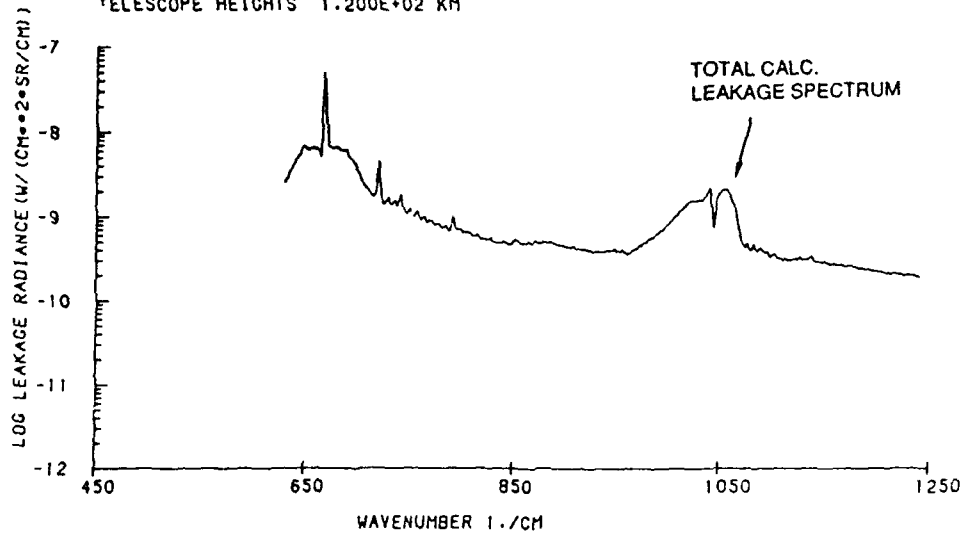


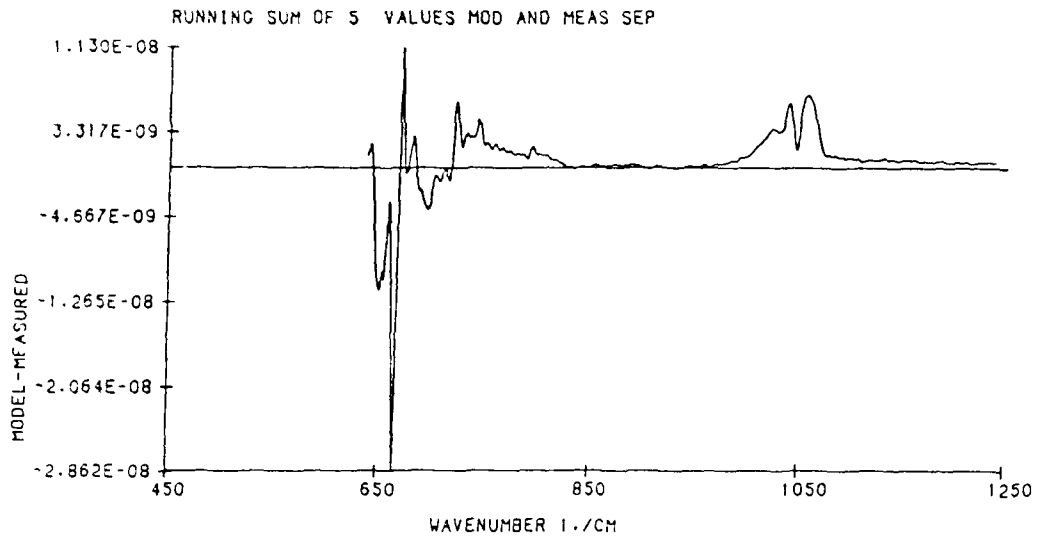
ATMOSPHERIC MODEL



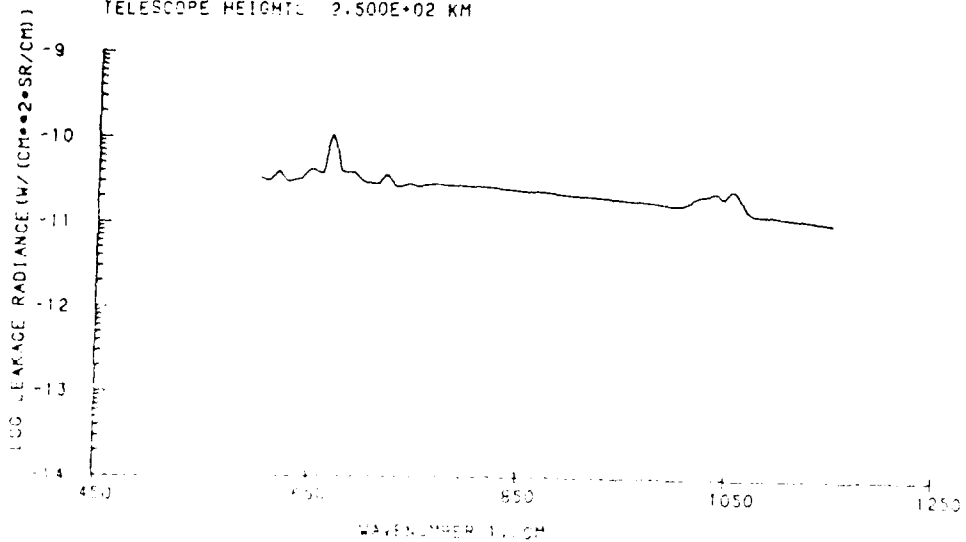


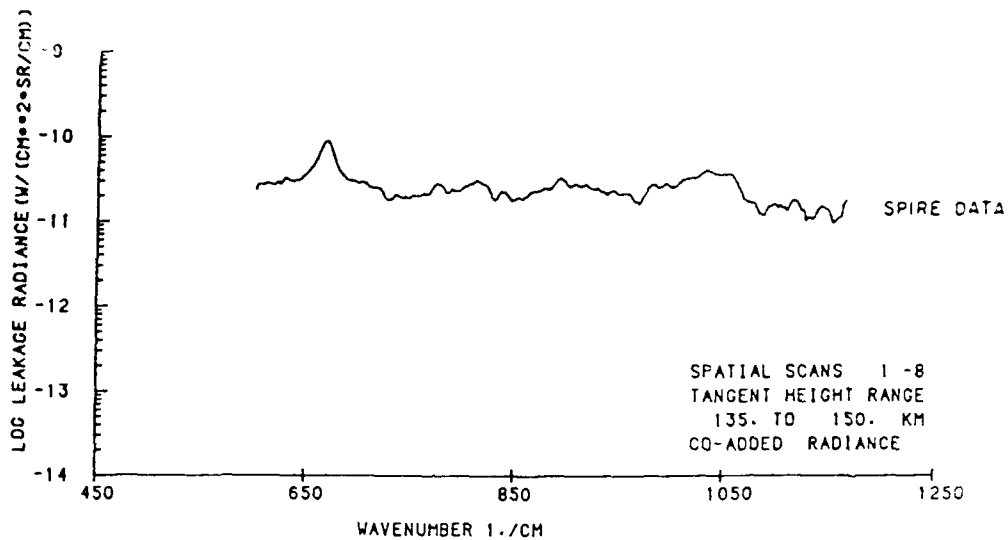
ELEVATION ANGLE -3.50 DEGREES
TANGENT HEIGHT 107.89 KM
89/06/02. RUN NUMBER 259 TELESCOPE MODEL 9 (HIRIS)
RESOLUTION (3 WAVENUMBERS)
INTEGRATE FROM 2.500E-01 THRU 90. DEGREES SMOOTH OVER 3 WAVENUMBERS
MINIMUM ALTITUDES 0. KM
TELESCOPE HEIGHTS 1.200E+02 KM



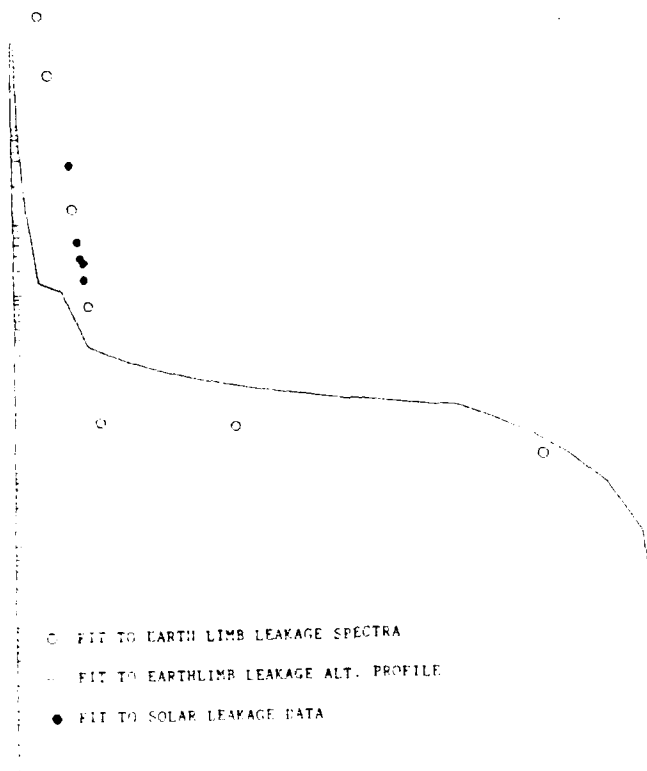
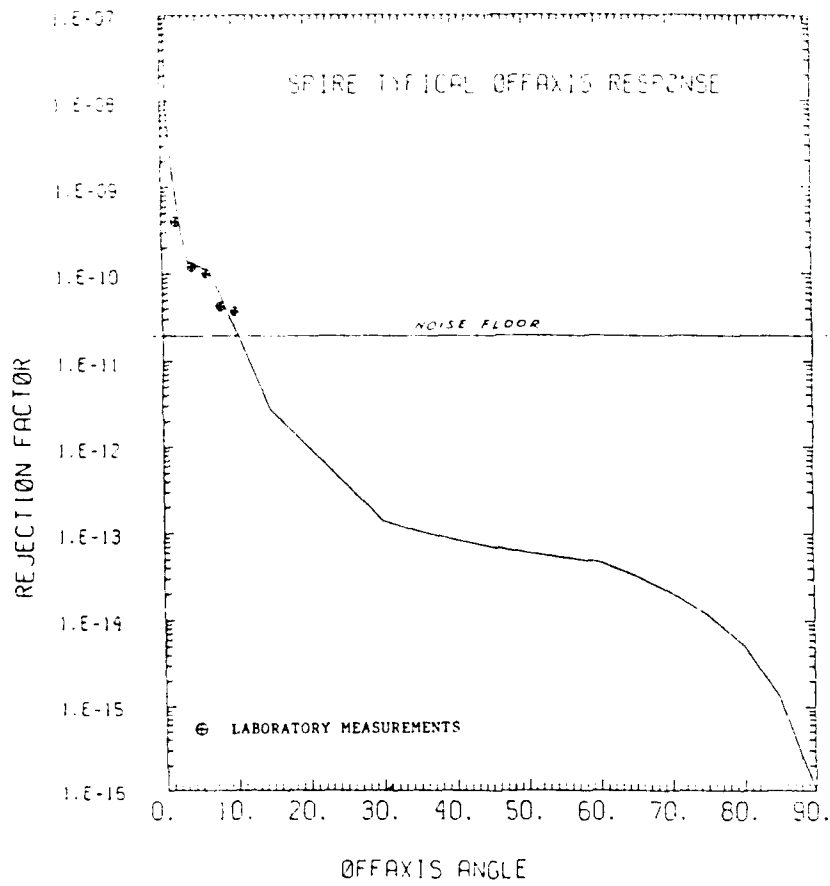


ELEVATION ANGLE -10.00 DEGREES
 TANGENT HEIGHT 149.35 KM
 89/09/12. RUN NUMBER 344 TELESCOPE MODEL 10(SPIRE)
 LOW RESOLUTION (15 WAVENUMBERS)
 INTEGRATE FROM 2.500E-01 THRU 90. DEGREES SMOOTH OVER 15 WAVENUMBERS
 MINIMUM ALTITUDES 0. KM
 TELESCOPE HEIGHT 2.500E+02 KM

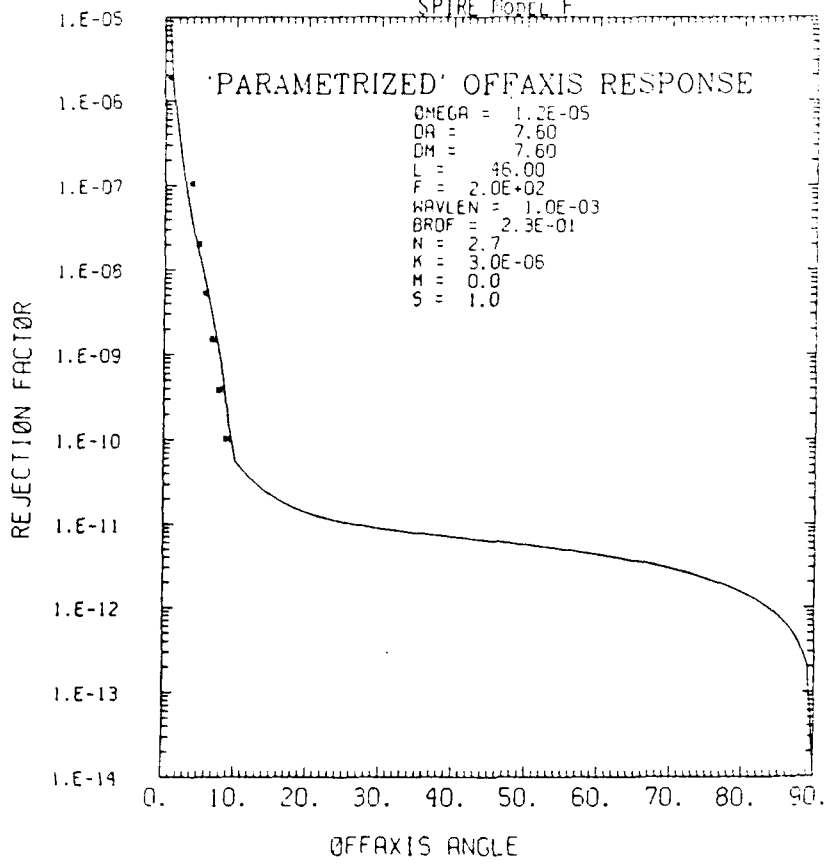




WEIGHT=1.22	INTEGRAL STARTING AT 2.500E-01	FORCE CONSTANT= 4.000E-02
WEIGHT=1.56	INTEGRAL STARTING AT 2.000E+00	FORCE CONSTANT= 4.000E-02
WEIGHT=0.01	INTEGRAL STARTING AT 4.000E+00	FORCE CONSTANT= 4.000E-02
WEIGHT=0.18	INTEGRAL STARTING AT 8.000E+00	FORCE CONSTANT= 4.000E-02
WEIGHT=0.94	INTEGRAL STARTING AT 1.200E+01	FORCE CONSTANT= 4.000E-01
WEIGHT=0.95	INTEGRAL STARTING AT 1.800E+01	



SPIRE Model F



**CLOUD OPACITY RETRIEVAL USING LOWTRAN
AND THE STAMNES SCATTERING MODEL**

B.L. Lindner and R.G. Isaacs

Atmospheric and Environmental Research, Inc., 840 Memorial Drive, Cambridge, MA, 02139

The AFGL LOWTRAN atmospheric transmittance model and an efficient Mie theory algorithm have been combined with the Stamnes discrete ordinate method multiple-scattering model, and used to simulate multispectral sensor intensities for a variety of cloud properties, surface types, sun and sensor geometries, and background atmospheres, from visible to infrared wavelengths. These intensities are stored in a lookup table, and a minimization procedure has been developed to most efficiently and accurately match observed intensities with those in the lookup table, and hence retrieve cloud properties. The minimization procedure has been used to retrieve cloud optical depth from LANDSAT TM data.

CLOUD OPACITY RETRIEVALS USING LOWTRAN
AND THE STAMNES SCATTERING MODEL

B. L. LINDNER and R. G. ISAACS

Atmospheric and Environmental Research, Inc.

COMBINE MODELS:

LOWTRAN

AFGL MIE CODE (Shettle)

STAMNES MULTIPLE SCATTERING CODE

SIMULATE SENSOR RADIANCES AS FUNCTION OF:
WAVELENGTH

CLOUD PROPERTIES (TYPE, THICKNESS, PARTICLE SIZE, PHASE)
SURFACE TYPE

SUN-SENSOR GEOMETRY (SZA, VIEW ANGLE)

ATMOSPHERE TYPE (LOWTRAN BASE ATMOSPHERES)

INVERT DATA

MATCH DATA RADIANCE TO SIMULATED RADIANCE

RADIATIVE TRANSFER MODEL

RADIATIVE TRANSFER MODEL (cont Inued)

DISCRETE ORDINATE METHOD (DOM) OF STANNES AND CONKLIN (1984) TREATS:

- MULTIPLE SCATTERING BY ATMOSPHERE AND CLOUDS
- GAS ABSORPTION
- VERTICAL STRUCTURE
- ARBITRARY SURFACE REFLECTANCE
- COMBINED SCATTERING AND THERMAL SOURCE FUNCTION

FORMULATION: DISCRETE ORDINATES (Angles μ_l , 1-2 to 64)

RADIANCE R_{ν} CALCULATED BY SOLVING:

$$\mu_l \frac{\partial R_{\nu}}{\partial r}(r, \mu_l, \phi) - R_{\nu}(r, \mu_l, \phi) - J_{\nu}(r, \mu_l, \phi)$$

$$J_{\nu}(r, \mu_l, \phi) = (1 - \omega(r)) B_{\nu}(T) + \frac{\omega(r) P_{\nu} e^{-r/\mu_0}}{4}$$

$$+ \frac{\omega(r)}{4\pi} \int_{\Omega} P_{\nu}(r, \mu_j, \phi, \mu_j', \phi') R_{\nu}(r, \mu_j, \phi) d\Omega$$

APPROXIMATE ANGULAR INTEGRAL USING:

$$\int_{\Omega} P_{\nu} R_{\nu} d\Omega \approx \frac{\omega}{4\pi} \sum_l \epsilon_l R_l$$

RADIATIVE TRANSFER MODEL (continued)

DATA PROCESSING (continued)

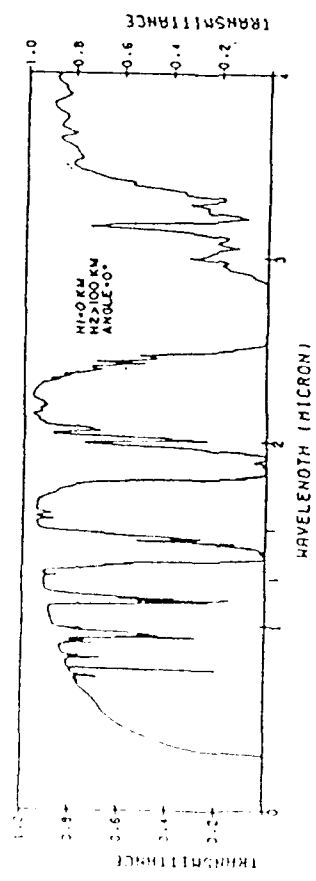
OPTICAL PARAMETERS (r, w, P) RELATED TO:

- METEOROLOGICAL PARAMETERS (TEMPERATURE PROFILE, WATER VAPOR MIXING RATIOS, ETC.) USING THE AFGL LOWTRAN ATMOSPHERIC TRANSMISSION ALGORITHM
- CLOUD PARAMETERS USING AER CLOUD MODELS (E.G. STRATUS, ALTOSTRATUS, CIRRUS, ETC.)

STEP	PARAMETER	APPROACH
1	CLOUD COVER CLOUD TOP	HISTOGRAM IR EBBT
2	CLOUD TYPE	CLASSIFICATION
3	THICKNESS PHASE PARTICLE SIZE	MINIMIZATION PROCEDURE

Atmospheric Vertical Opacity at Selected
Wavelengths for Midlatitude Summer Conditions

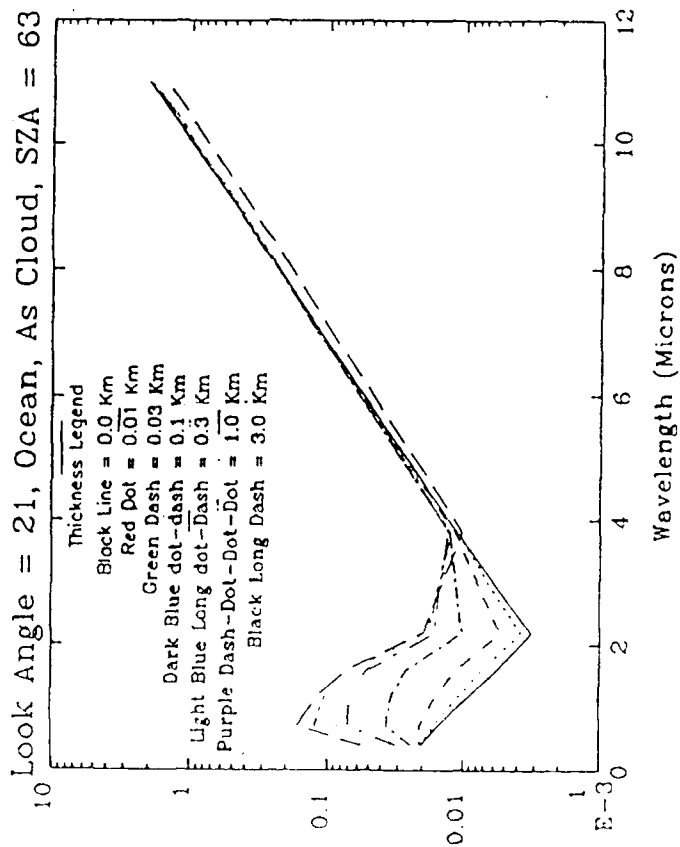
Wavelength (μm)	Opacity
0.4	0.8
0.7	0.6
1.13	60.0
1.25	0.15
1.6	1.5
2.2	2.7
2.47	85.0
3.13	130.0
3.6	6.1
3.8	3.9
4.7	17.0
11.0	1.8



Transmittance Spectra for a vertical path from ground to space from 0.25 to 4 μm , using the Rural Aerosol Model, 23-km VIS and the U.S. Standard Model Atmosphere in the AFGL LOWTRAN model.

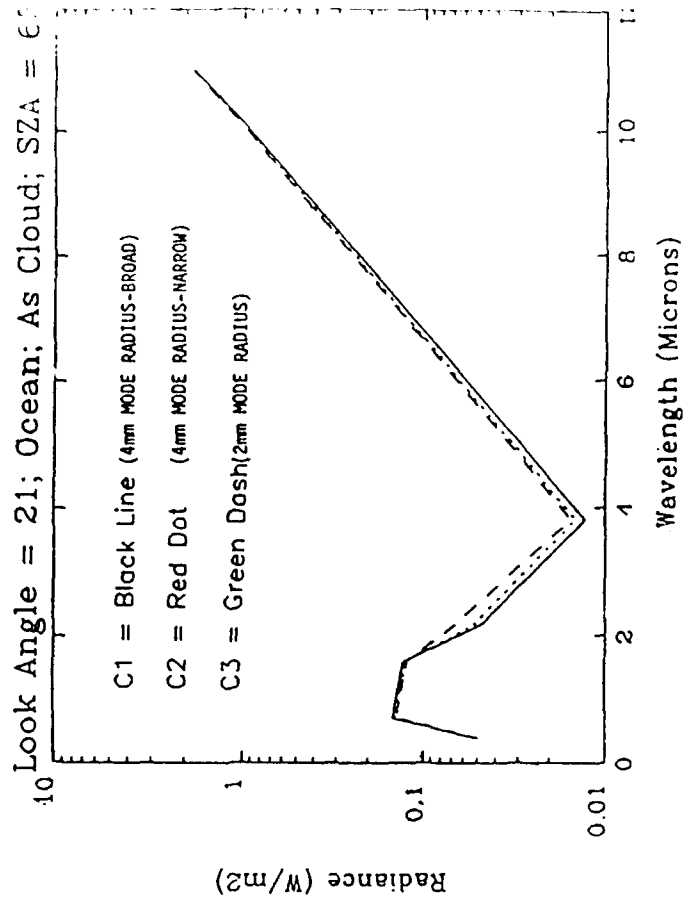
RADIANCE DEPENDENCE ON CLOUD THICKNESS

• NEAR INFRARED OPTIMAL FOR CLOUD THICKNESS RETRIEVAL



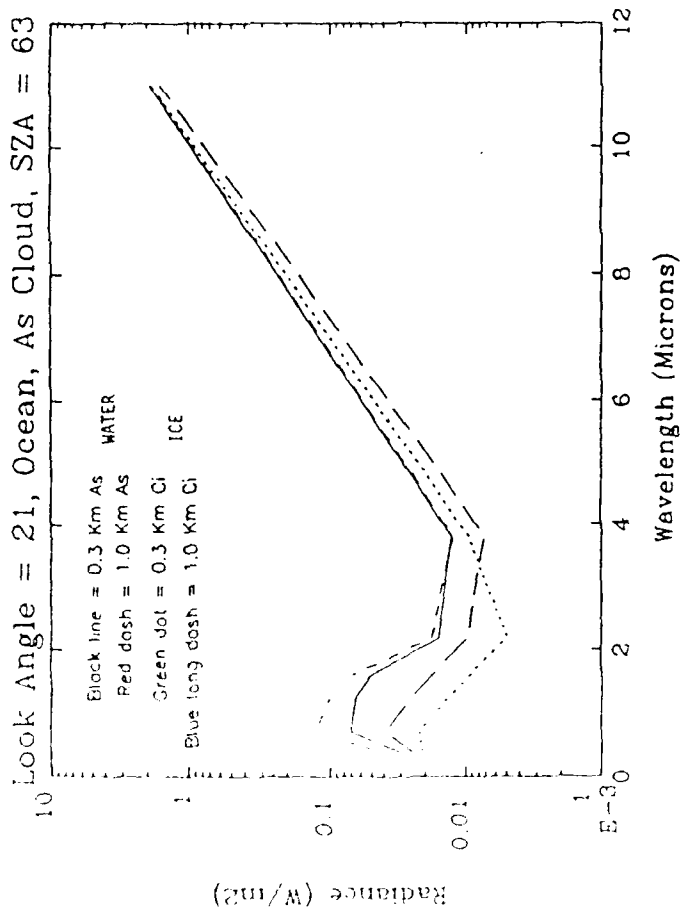
RADIANCE DEPENDENCE ON PARTICLE SIZE

• NEAR INFRARED CHANNELS OPTIMAL FOR PARTICLE SIZE RETRIEVAL

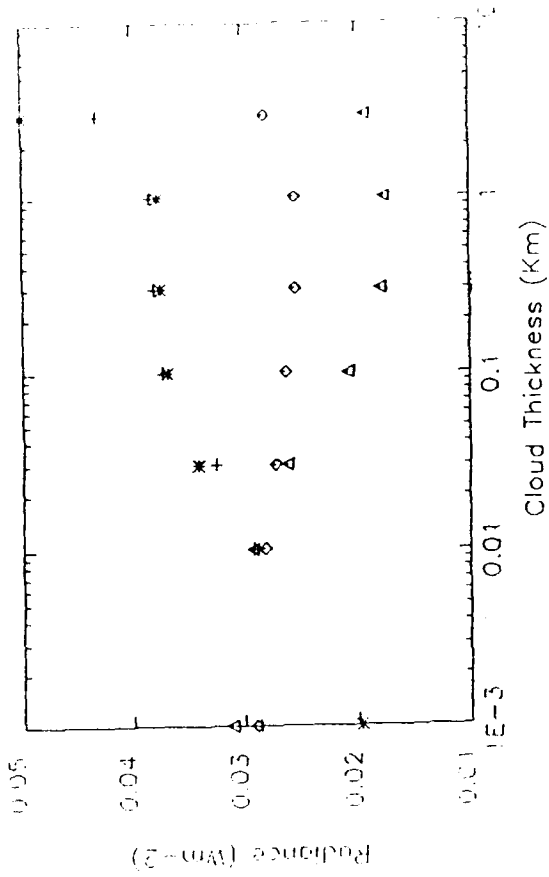


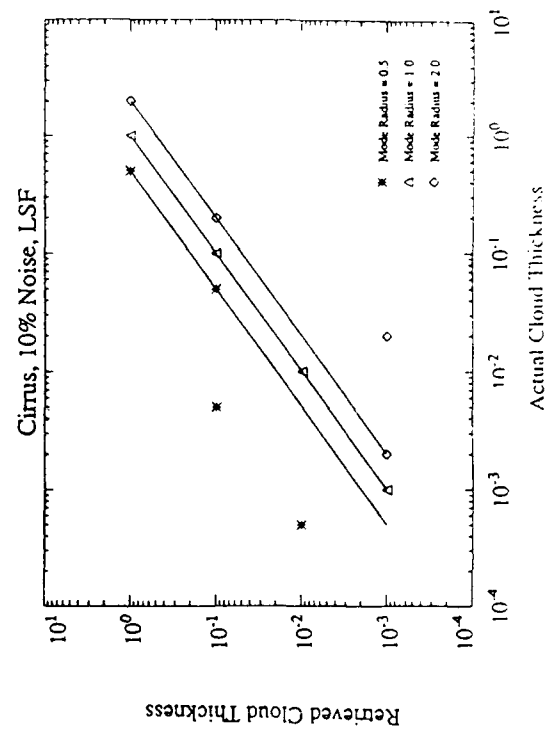
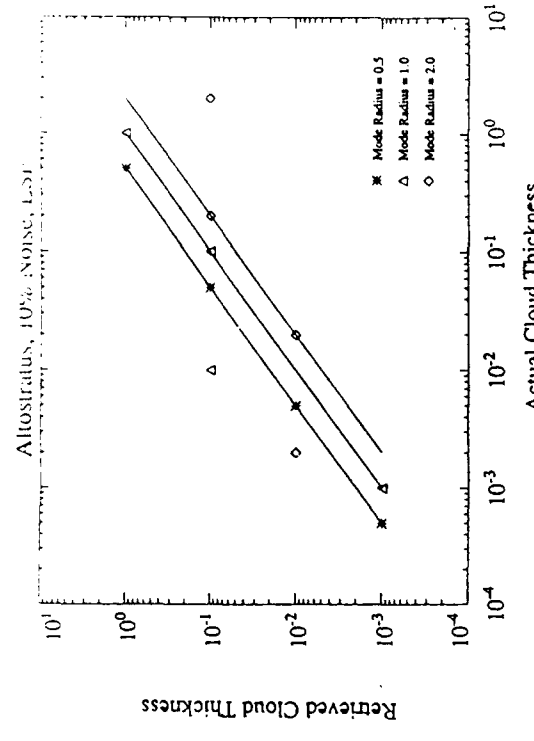
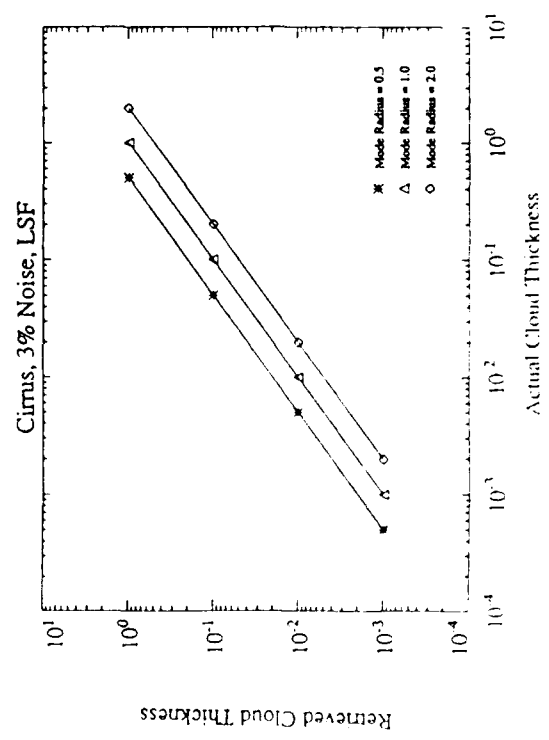
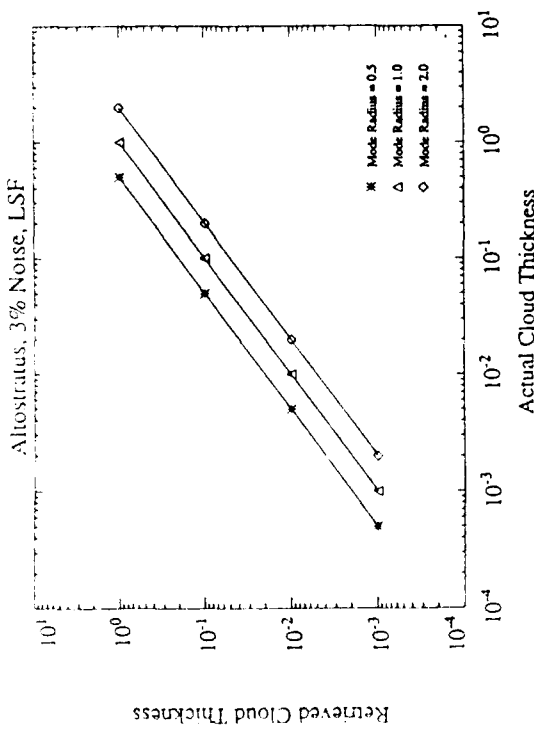
RADIANCE DEPENDENCE ON CLOUD PHASE

• VISIBLE THROUGH NEAR INFRARED SIGNATURE DISTINGUISHES CLOUD PHASE



Bare Soil, Solar Zenith Angle of 63°, 2.2 μm, as Cloud





1 8 9



2.3

4

5

7

6

LANDSAT TM Image taken off the coast of South Carolina

Cloud Thickness Inferred for Each Subimage

Index	Cloud_Thickness (ft)
1	3.0
2	1.0
3	1.0
4	0.3
5	0.1
6	0.01
7	0.01
8	0.01

CALCULATED CLOUD EDGE SWIR RADIANCE GRADIENTS AS VIEWED BY SATELLITE

L.L. Smith

Grumman Corporate Research Center, Bethpage, NY 11714

As surveillance systems become more capable and more sophisticated, knowledge of the effects of clouds as background clutter becomes an increasing stressing factor on performance. Cloud edge radiance gradients in the SWIR are calculated using the LOWTRAN 7 code for multiple satellite-cloud-sun viewing geometries. As expected, the gradient, defined as the change in cloud radiance per degree in the detector focal plane, increases as the viewing position approaches the earth's limb. This is principally caused by the foreshortening of the cloud boundary as the limb is approached with a small effect due to an increase in cloud brightness. The gradient peaks in both the forward scattering and backscattering directions are due to the phase angle effect of the scattering particles.

Calculated Cloud Edge SWIR Radiance Gradients as Viewed by Satellite

Lewis L. Smith

Grumman Corporate Research Center

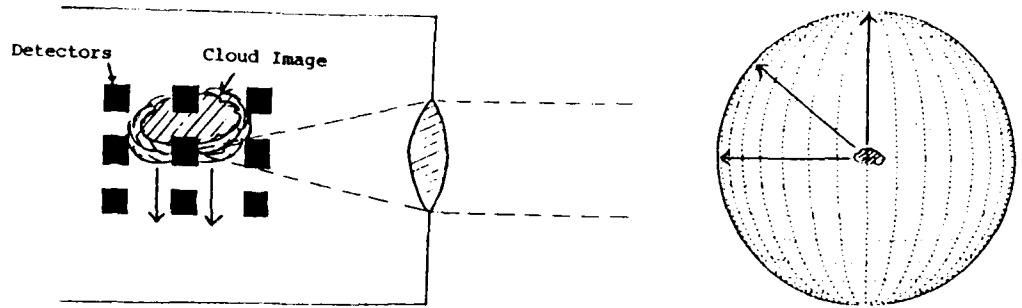
CALCULATED CLOUD EDGE SWIR RADIANCE GRADIENTS AS VIEWED BY SATELLITE

Lewis L. Smith

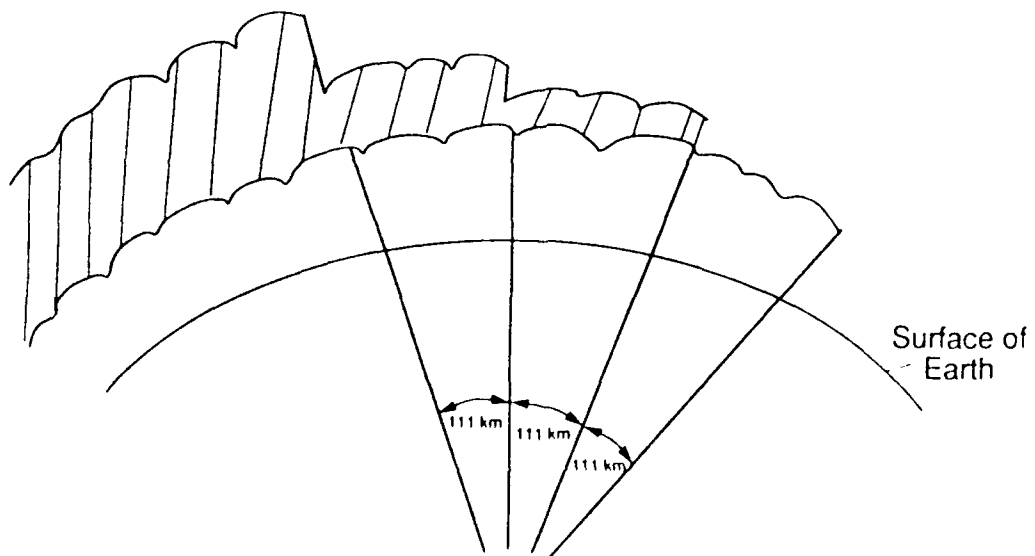
Grumman Corporate Research Center

As satellite systems become more capable and more sophisticated, knowledge of the effects of clouds as background clutter becomes an increasing stressing factor on performance. Cloud edge radiance gradients in the SWIR are calculated using the ATHAN code for multiple satellite-cloud-sun viewing geometries. As expected, the gradient (defined as the change in cloud radiance per degree in the detector focal plane) increases as the viewing position approaches the earth's limb. This is due to the foreshortening of the cloud boundary as the limb is approached with a similar effect due to an increase in cloud brightness. The gradient peaks occur in the forward scattering and backscattering directions due to the phase angle effect of the scattering pattern.

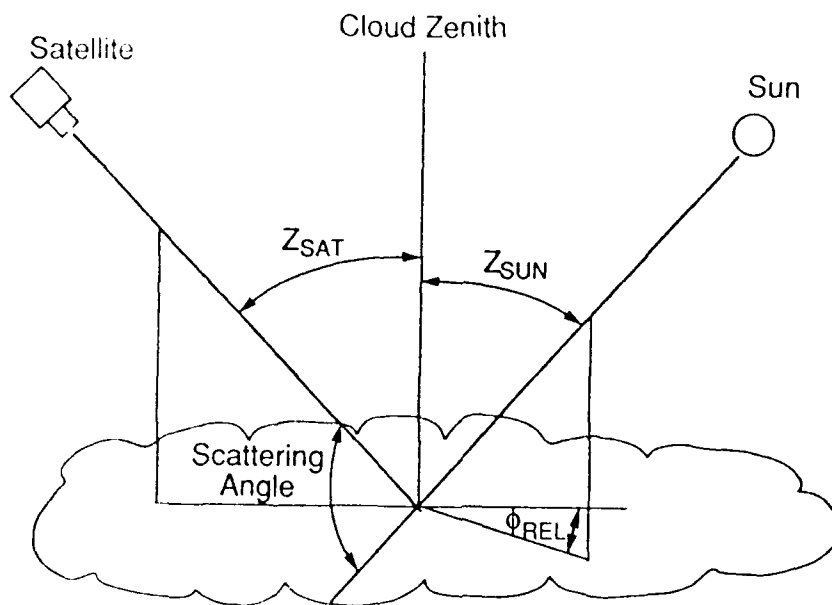
Cloud Projection on Globe
and
Cloud Image Motion in Satellite Focal Plane



Simplified Cloud Edge Model



Scattering Angle Definition



$$\text{SCATTERING ANGLE} = \cos^{-1}[\sin(Z_{\text{SAT}}) \sin(Z_{\text{SUN}}) \cos(\phi_{\text{REL}}) - \cos(Z_{\text{SAT}}) \cos(Z_{\text{SUN}})]$$

AV-9C 1896.004

Cloud Edge Gradient Model

- SWIR radiances calculated using standard cirrus cloud model from LOWTRAN7 w/multiple scattering & daytime conditions
- Cloud thickness varies in step size
 - 111 km in longitude (east)
 - 111 km in latitude (south)
- Maritime aerosols
- Sub-satellite point on equator

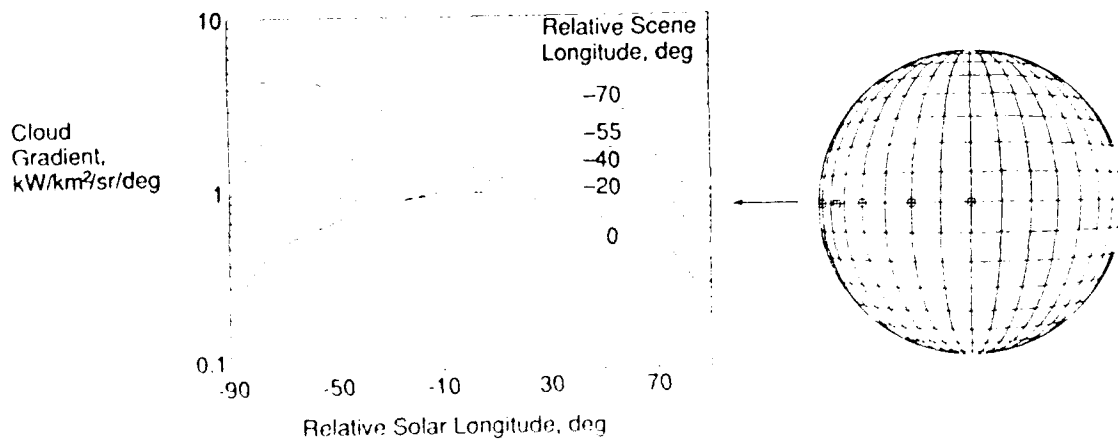
AV-9C 1896.004

Cloud Edge Gradient Model (Cont'd)

- Model atmospheres
 - 0-25° tropical
 - 25-55° midlatitude summer
 - 55-70° subarctic summer
- Cirrus cloud base altitude
 - 0-25° 11 km
 - 25-55° 10 km
 - 55-70° 7 km
- Cloud edge gradients calculated from changing radiance in satellite detector focal plane
- All gradients normalized to cloud at sub-satellite point

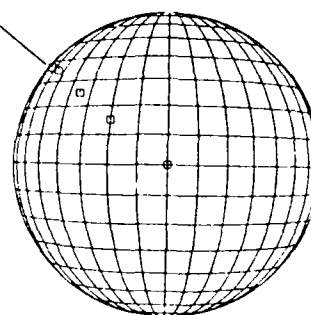
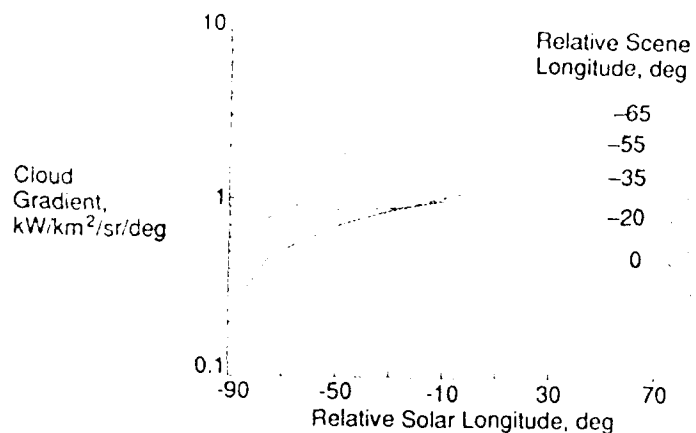
MVIO 2858-003

Cloud Gradients - South



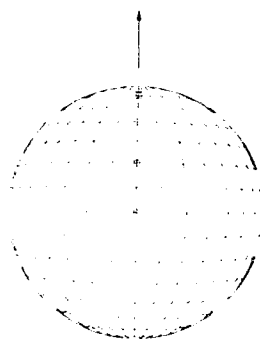
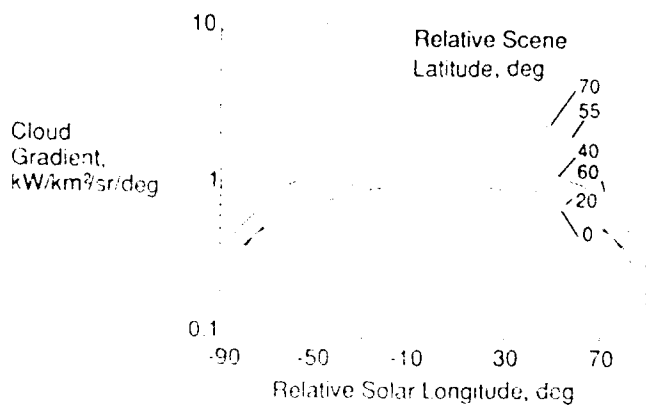
MVIO 2858-003

Cloud Gradients - South



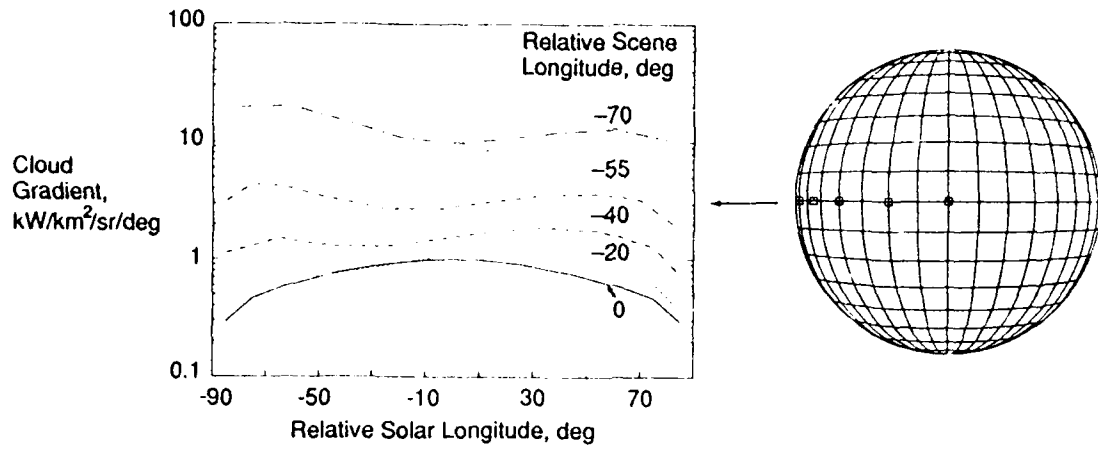
JULY 1968 010

Cloud Gradients - South



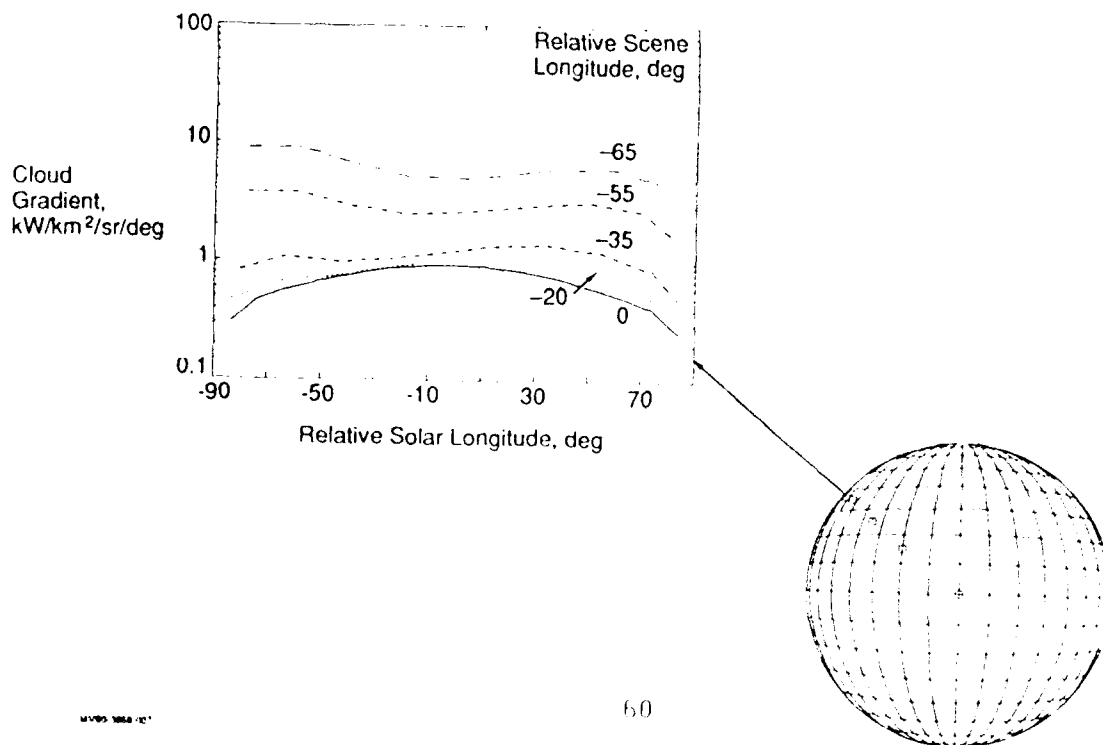
JULY 1968 010

Cloud Gradients - East



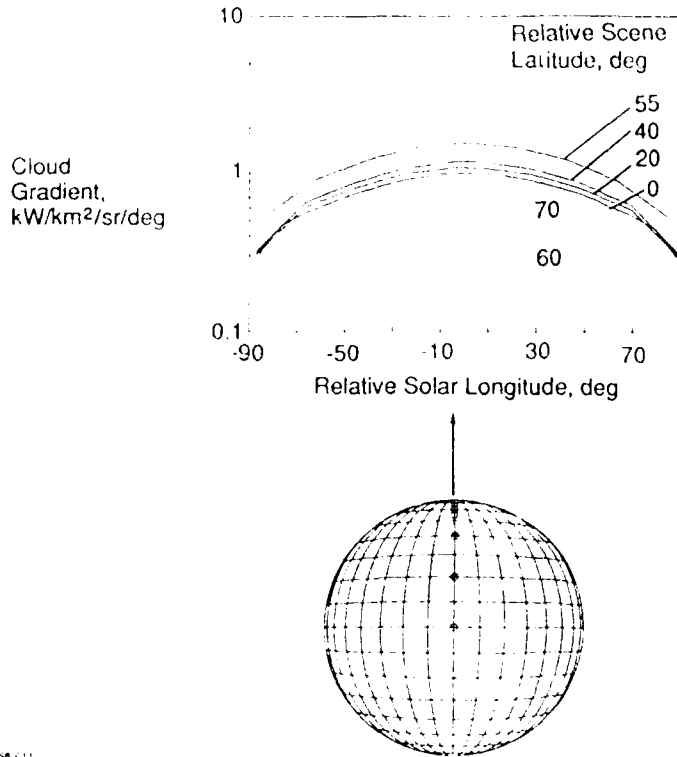
4499 1000 000

Cloud Gradients - East



4499 1000 000

Cloud Gradients - East



Conclusions

- Cloud edge SWIR gradient increases as viewing position approaches earth's limb - caused by foreshortening
- Gradient increases as cloud altitude increases due to decreased atmospheric absorption
- Gradient peaks in both forward and backscattered directions due to phase angle effect of scattering particles

**THE DEPARTMENT OF ENERGY INITIATIVE ON ATMOSPHERIC RADIATION
MEASUREMENTS (ARM): A STUDY OF RADIATIVE FORCING AND FEEDBACKS**

R.G. Ellingson

Department of Meteorology, University of Maryland, College Park, MD 20742

G.M. Stokes

Applied Physics Center, Pacific Northwest Laboratories, Richland, WA 99352

A.Patrnos

Division of Atmospheric and Climate Research, US Department of Energy, Washington, DC 20545

As a key component of the strategy to address global climate, the Department of Energy has launched the Atmospheric Radiation Measurements (ARM) initiative. The objectives of the ARM Program are to provide detailed measurements of radiative effects in the atmosphere, and to provide parameterizations of these effects for use in atmospheric models. Particular emphasis will be on those effects associated with clouds and greenhouse gases. The effort will support the continued and rapid improvement of GCM predictive capability. The presentation will summarize the science context, program requirements, measurement strategy, experimental approach, scientific management and site selection.



State of the Art in Radiation Models

ICRCCM has shown a wide range of disagreement among radiation models used in climate studies

There are no calibrated techniques for predicting and calculating the radiative effects of clouds for either homogeneous or broken conditions



Radiation and Climate - Important Facts

Radiation is a quantity to which Earth's climate is VERY sensitive -

1% changes are important



Atmospheric Radiation Measurement Program

**A Study of Radiative Forcing
and Feedbacks**



General Goals of ARM:

**Improve the Performance of
General Circulation Models
of the Atmosphere
as Tools for Predicting
Global and Regional Change**



Specific Goals of ARM

**Improve the Treatment of
Radiative transfer in GCMs Under
Clear Sky, General Overcast, and
Broken Cloud Conditions**

**Improve the Parameterization
of the Properties and Formation
of Clouds in GCMs**



ARM Design Strategy

Successive Approximation

Scientific Issues

Experiment Definition

Instrument, Model, Site

Selection (Process)

Data System Requirements



Experiment Definition

Key Organizing Concept

Model to be Tested (hypothesis)

Input Data

Test Data



Experimental Context

**Hypothesis-Oriented Radiation
Science Experiment**

Clouds and Radiation Testbed



Model Definition

**Numerical (computational)
representation of the
understanding of
a physical process**



Design Process Goals

**Rapid Deployment
Long-term Flexibility
Strong Coupling to Science**



CART Data System: Design Activities

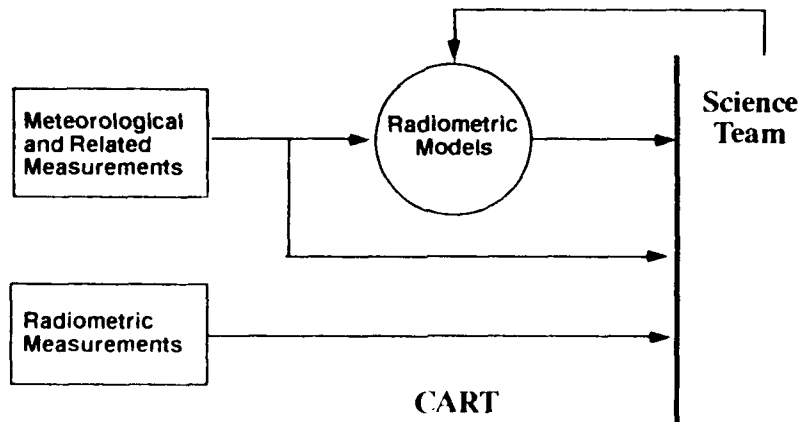


Data System Design: Objective

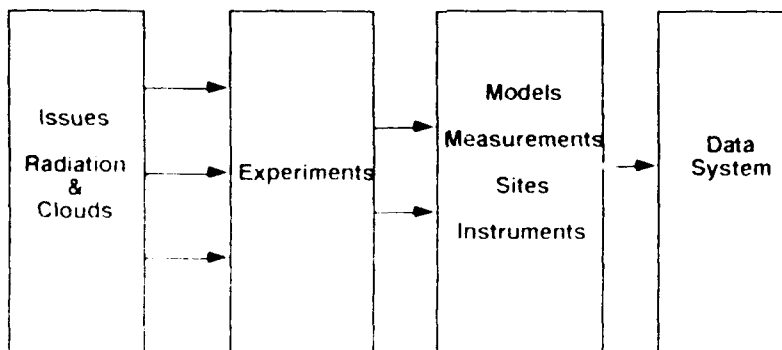
A data system that can provide streams of data (measurements and predictions) of known quality that can be compared to test the predictive power of radiometric and other models selected to be a part of the ARM program



Representative Intercomparison of Data



CART Design Process





Requirements Definition

- **Formal top-down design sessions to include representatives of Science Team and instrument developers**
- **Design reviews and workshops with Science Team and interagency working groups**
- **Formal design review with outside panel**



Summary of Design Process

- **Design driven by scientific requirements**
- **Focus on providing streams of measurements and predictions for intercomparison**
- **Creation of a process that supports evolution of ARM scientific activities**

THE HITRAN MOLECULAR DATABASE IN 1990

Lt. S. Shannon and L.S. Rothman

Geophysics Laboratory/OPI, Hanscom AFB, MA 01731-5000

The spectroscopic molecular database, HITRAN, is the DoD and international standard compilation of absorption parameters that enable the calculation of atmospheric spectral simulations from the microwave through the visible. HITRAN has been periodically improved and released; the current edition being 1986 (Applied Optics, 26, 4058 (1987)). This present edition contains over a third of a million transitions for some 28 species and their significant atmospheric isotopic variants. The new edition will have additional species and will contain many more transitions. Furthermore, there will be appended new cross-sections for heavy molecular species, with bands at several representative temperatures. This talk will summarize some of the major updates and modifications that will be available on HITRAN 1990.

The HITRAN Molecular Database in 1990

Lt Scott Shannon & Laurence S. Rothman
GL/OPI
Hanscom AFB, MA 01731-5000

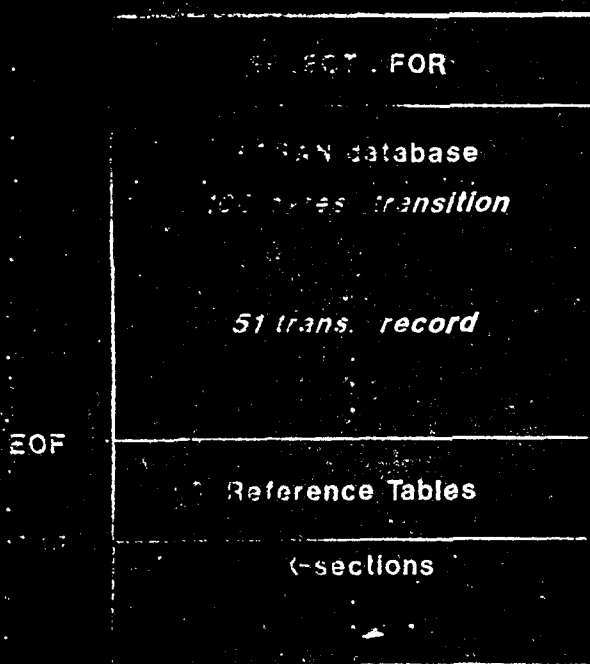
OUTLINE

- ① **Major Molecular Parameter Updates**
- ② **SELECT: Database Interface**
- ③ **Conclusions**

Major Molecular Parameter Updates

- ⊕ H₂O
- ⊕ CO₂
- ⊕ O₃
- ⊕ CH₄
- ⊕ CO, HNO₃, HCl, HF, HI, HBr...
- ⊕ Cross-sections (ClONO₂, CFC's, N₂O₅...)

HITRAN



Water Vapor (H_2O)

All new regions have been taken at the Kitt Peak Solar Observatory using the FTS and long path cell. These data replace older parameters that were observed using grating spectrometers and a path through the atmosphere. Most notable improvement in intensities of weak lines.

- ① Roth (JPL)
- ② Haud & G. (no), Deynat (JPL), F. (no) & corrections
- ③ FCP
- ④ Roth
- ⑤ FCP (data) & corrections & compilation

Data for the 1980-1985 period are available at the following URL:

Water Vapor (H₂O)

	V _{min}	V _{max}	# bands	# lines
①	5904	7965	9	3112
②	8036	9482	9	1874
③	9603	11 481	9	2484
④	11 661	12 741	5	714
⑤	13 238	22 657	41 (39,2)	4608

Carbon Dioxide (CO₂)

① **New Line Positions:** New fit of observed high resolution data by Hawkins & Rothman. New data includes very high vibrational 4.3- μ m observations of Bailly *et al.* (Orsay) and the 15- μ m observations of Esplin *et al.* (GL)

② **New intensities:** New intensity observations of Dana *et al.* (Paris) and Johns (NRC). Calculations by Wattson & Rothman for unobserved bands, include Herman-Wallis coefficients.

③ **Revised Halfwidths:** Re-evaluation of all halfwidth observations.

Ozone (O₃)

- ❶ New data for ν_2 and $2\nu_2 - \nu_2$ from Pickett (JPL) *et al.*
- ❷ Umpteenth revamping of 10- μm region. This time includes many new bands and hot bands.
- ❸ Isotopic bands of 10- μm region from FCP & Rinsland (NASA Langley)
- ❹ Many new combination bands from Goldman (Denver)

Ozone (O₃)

	ν_{min}	ν_{max}	# bands	# lines
❶	557	900	2	12 085
❷	919	1271	18	42 500
❸	934	1178	4	13 590
❹	1319	2322	19	44 926

Methane (CH₄)

- ① Major improvement by Brown (JPL)
- ② Updated mono-deuterated methane bands by Brown.

Methane (CH₄)

	<i>V_{min}</i>	<i>V_{max}</i>	# bands	# lines
①	0	6185	31 (21,6,4)	37 207
②	2902	3147	3	309

Other Molecular Species

- ⊛ CO (carbon monoxide): Update, primarily for HITEMP (*Tipping*)
- ⊛ NO (nitric oxide): Update of fundamental (*Ballard*)
- ⊛ HNO₃ (nitric acid): addition of new bands
(fundamentals and combinations, 410 to 1400 cm⁻¹)
(*Goldman, Maki, Rinsland, Perrin, et al.*)
- ⊛ HCl, HF, HI, HBr (hydrogen halides):
Update, primarily for HITEMP (*Tipping, et al.*)
- ⊛ H₂O₂ (hydrogen peroxide): ν_6 band, 138-1500 cm⁻¹ (*Hillman*)
- ⊛ C₂H₂ (acetylene): ν_5 band, 1192-1470 cm⁻¹ (*Rinsland*)
- ⊛ C₂H₆ (ethane). ν_9 and ν_7 bands, 0-833 and 2973-3000 cm⁻¹
(*Blass; Goldman, Dang-Nhu, et al.*)
- ⊛ COF₂, SF₆...: new species on compilation (*Goldman*).

Updates generally include all parameters of HITRAN format.

Cross-sections (Supplemental files)

CFC's now at six temperatures: 203, 213, 233, 253, 273, and 293K.
N₂O₅ at 233, 253, 273, and 293K. ClONO₂ at 213 and 296K.

Species	ν_{\min}	ν_{\max}	# lines
CFC-12 (CCl ₂ F ₂)	867	937	67 554
CFC-13 (CClF ₃)	765	805	
"	1065	1140	
"	1170	1235	72 822
CFC-14 (CF ₄)	1255	1290	14 160
CFC-22 (CHClF ₂)	780	840	
"	1080	1150	
"	1290	1335	70 806
CFC-113 (C ₂ Cl ₃ F ₃)	780	995	
"	1005	1232	5316

Cross-sections (continued)

Species	v_{\min}	v_{\max}	# lines
CFC-114 ($C_2Cl_2F_4$)	815	860	
"	870	960	
"	1030	1067	
"	1095	1285	146 442
CFC-115 (C_2ClF_5)	955	1015	
"	1110	1145	
"	1167	1260	76 056
N_2O_5	555	600	
"	720	765	
"	1210	1275	
"	1680	1765	2004
$ClONO_2$	555	600	
"	720	765	

SELECT OPTIONS

Input:

- ① v_1 and v_2 (Initial and final frequencies of selection)
- ② Molecule
- ③ Isotope
- ④ v' , v'' (upper and lower "global" quanta)
- ⑤ S_{crit} (Intensity cutoff)

Output:

- ⊙ Batch file for input
- ⊙ Files for input to subsequent programs
(direct image; '82 format; user defined)
- ⊙ Hard copy listing
(codes converted to spectroscopic and chemical notations;
80 or 132 columns printers)

SUMMARY

- ★ Improvements notable for remote sensing, laser transmission, climate modeling, use of heavy species...
- ★ New Edition of HITRAN to appear in fall 1990.
- ★ Users on mailing list will be notified through newsletter.
- ★ HITEMP due shortly after HITRAN.
- ☆ SELECT faster and more flexible.

HITRAN Database Distribution

Tape: 9 track, ASCII, 1600 BPI

Climatological Services Section
National Climatic Data Center of NOAA
Federal Building
Asheville, NC 28801
phone: (704) 259-0682

or

Dr. Laurence S. Rothman
AFGL/OPI
Hanscom AFB, MA 01731-5000
phone: (617) 377-2336

**LINE COUPLING CALCULATIONS FOR INFRARED
BANDS OF CARBON DIOXIDE FOR FASCOD3**

M.L. Hoke, F.X. Kneizys, S.A. Clough*, J.H. Chetwynd
Geophysics Laboratory/OP, Hanscom AFB, MA 01731

Second order perturbation theory line coupling parameters (y 's and g 's) have been calculated for the six most important Q-branches of carbon dioxide in the fifteen micron spectral region; those at 618, 667 (fundamental), 720, 741 and 791 cm^{-1} of the most abundant isotope $\text{O}^{16}\text{-C}^{12}\text{-O}^{16}$ and at 721 cm^{-1} of the less abundant isotope $\text{O}^{16}\text{-C}^{12}\text{-O}^{17}$. Line coupling parameters have also been calculated for the P and R branches of the 4.3 micron fundamental band. For each band the temperature dependence of the coefficients is accounted for by interpolation of a set of four pairs of coupling parameters (y, g) at the temperatures 200, 250, 296 and 340 K. These line coupling parameters are part of the new version (version 3) of the GL high resolution line-by-line computer code FASCODE. Details of the calculations, including the appropriateness of perturbation theory and the accuracy of the temperature interpolation scheme, will be discussed.

*Now at Atmospheric and Environmental Research, Inc., 840 Memorial Drive, Cambridge, MA

SOME THEORY

$$I(\nu) \propto \text{Im} \left\{ \sum_j d_j \langle j | [(\nu - \nu_0) - iPW]^{-1} | k \rangle d_{k\rho} \right\}$$

$(\nu - \nu_0)$ DIAGONAL $(n \times n)$

W RATE MATRIX $(n \times n)$

$$W_{jj} = \alpha_j^0$$

W_{ij}, W_{ji} GIVE COUPLING BETWEEN LINES (i, j) .

$W_{ij} \rho_j = W_{ji} \rho_i$ DETAILED BALANCE

IF $W_{ij} \rightarrow \delta_{ij} W_{ij} = \alpha_j^0$

THEN $I(\nu) \rightarrow \sum_j [P \alpha_j^0 / \{ (\nu - \nu_0)^2 + (P \alpha_j^0)^2 \}]$

1963 P. 1014
 1964 P. 1014
 1965 P. 1014
 1966 P. 1014
 1967 P. 1014
 1968 P. 1014
 1969 P. 1014
 1970 P. 1014
 1971 P. 1014
 1972 P. 1014
 1973 P. 1014
 1974 P. 1014
 1975 P. 1014
 1976 P. 1014
 1977 P. 1014
 1978 P. 1014
 1979 P. 1014
 1980 P. 1014
 1981 P. 1014
 1982 P. 1014
 1983 P. 1014
 1984 P. 1014
 1985 P. 1014
 1986 P. 1014
 1987 P. 1014
 1988 P. 1014
 1989 P. 1014
 1990 P. 1014
 1991 P. 1014
 1992 P. 1014
 1993 P. 1014
 1994 P. 1014
 1995 P. 1014
 1996 P. 1014
 1997 P. 1014
 1998 P. 1014
 1999 P. 1014
 2000 P. 1014
 2001 P. 1014
 2002 P. 1014
 2003 P. 1014
 2004 P. 1014
 2005 P. 1014
 2006 P. 1014
 2007 P. 1014
 2008 P. 1014
 2009 P. 1014
 2010 P. 1014
 2011 P. 1014
 2012 P. 1014
 2013 P. 1014
 2014 P. 1014
 2015 P. 1014
 2016 P. 1014
 2017 P. 1014
 2018 P. 1014
 2019 P. 1014
 2020 P. 1014
 2021 P. 1014
 2022 P. 1014
 2023 P. 1014
 2024 P. 1014
 2025 P. 1014

EIGEN ANALYSIS OF $(\psi_0 + iPW)$

EIGENVECTORS (COMPLEX) x ; MATRIX (x_{jk})

EIGENVALUES (COMPLEX) λ ; VECTOR (λ_j)

$$\langle j | (\psi - \psi_0) - iPW | k \rangle = \sum_l \langle x_{jl} | (\psi - \lambda_l) | x_{lk}^{-1} \rangle \langle x_{lk}^{-1} |$$

$$I(\psi) \langle j | k \rangle \text{Im} \sum_l d_j \langle x_{jl} | (\psi - \lambda_l) | x_{lk}^{-1} \rangle \langle x_{lk}^{-1} | d_k \rho_{jk}$$

$$= \sum_l \frac{\text{Im}(\lambda_l) \cdot \text{Re}(G_l) + (\psi - \text{Re}(\lambda_l)) \cdot \text{Im}(G_l)}{\{ (\psi - \text{Re}(\lambda_l))^2 + (\text{Im}(\lambda_l))^2 \}}$$

WHERE

$$G_l = \sum_k \langle x_{lk}^{-1} | \rho d_k^2 | x_{lk} \rangle \cdot \sum_j (d_j / d_k) \langle x_{jk} \rangle$$

PERTURBATION THEORY

$$G_l^p = \rho_l d_l^2 \{ (1 + P^2 g_l) + i P \gamma_l \}$$

SUM RULES

$$\sum_l \lambda_l = 0 ; \sum_l \lambda_l g_l = 0$$

EFFECTIVE COUPLING PARAMETERS (γ_l^c, g_l^c)

COMPARE (G_l) AND (G_l^p)

$$P \gamma_l^c = \text{Im}(G_l) / (\rho d_l^2)$$

$$P^2 g_l^c = \{ \text{Re}(G_l) / (\rho d_l^2) \} - 1$$

(γ_l^c, g_l^c) PROVIDES GENERAL DESCRIPTION OF EFFECT

FREQUENCY DEPENDENCE :

$$\frac{[(\psi - \psi_{0i}) \cdot (\psi - \psi_{0j}) + \alpha_i \cdot \alpha_j] \cdot (P W_{ij})}{[(\psi - \psi_{0i}) + \alpha_i] \cdot [(\psi - \psi_{0j}) + \alpha_j]}$$

$$\rightarrow \frac{(P W_{ij})}{(\psi - \psi_{0i})(\psi - \psi_{0j})} \rightarrow \frac{1}{\psi^2}$$

RATE MATRIX

$$W_{ij} = (W'_{ij} + W''_{ij}) / 2 \quad \begin{matrix} (') \text{ UPPER STATE (V.I.B.)} \\ (') \text{ LOWER STATE (V.I.B.)} \end{matrix}$$

$$W''_{ij} = A_1 \cdot (1/A_1) \cdot A_2 \cdot \text{Exp} \left\{ -A_3 |A_1 E''_{ij}| / kT \right\}$$

SIMILARLY FOR W'_{ij} ; (A_1, A_2, A_3) PARAMETERS

ASSUME $\alpha_j (= W'_{ij})$ RESULTS FROM ONLY ROTATIONALLY INELASTIC COLLISIONS ; $\alpha_j = W'_{ij}$ TRANSITION FROM LINE (j) TO ALL OTHER LINES (i)

W_{ij} TRANSITION RATE FROM LINE (i) TO LINE (j)

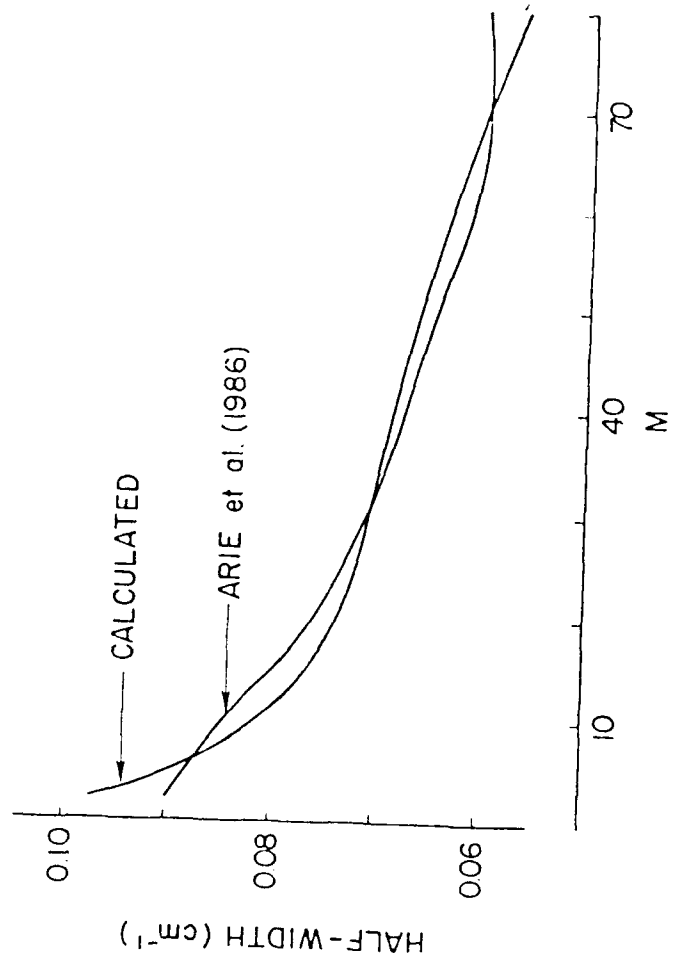
CONSERVATION OF TRANSITION PROBABILITY $\Rightarrow \sum_i W_{ij} = 0$

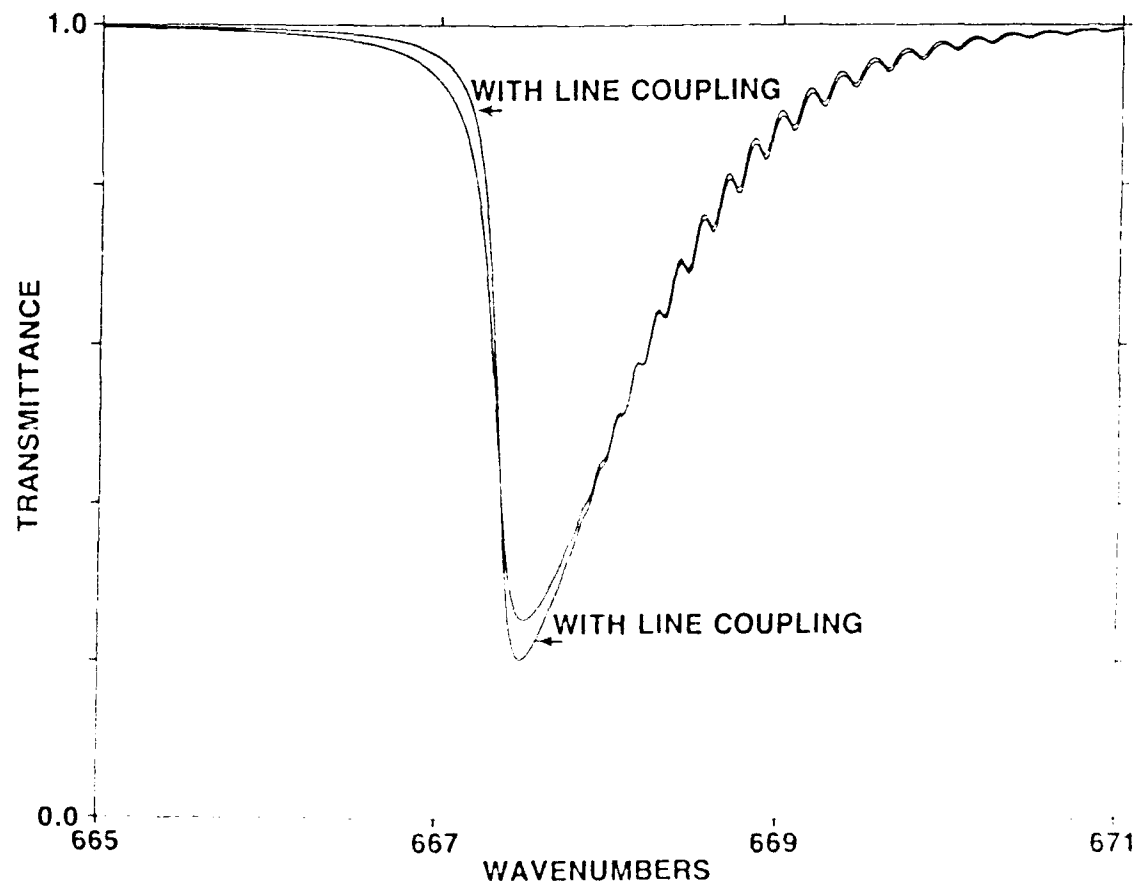
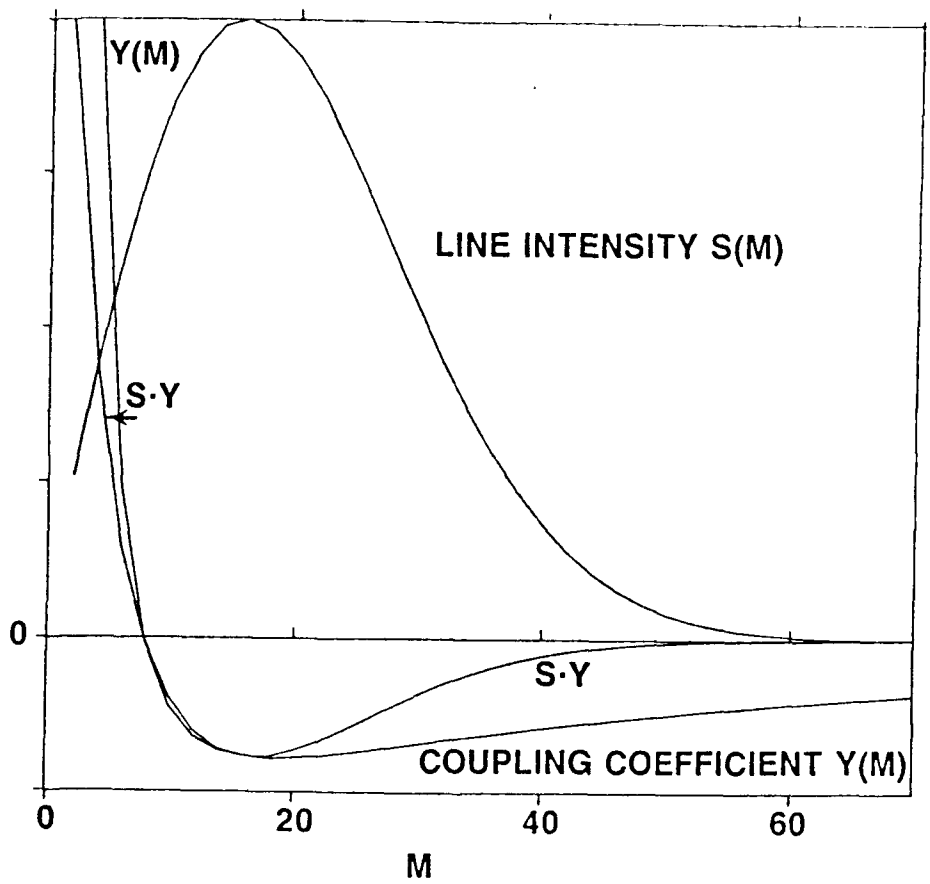
OR
$$W_{ij} (= \alpha_j) = - \sum_{i \neq j} W_{ij}$$

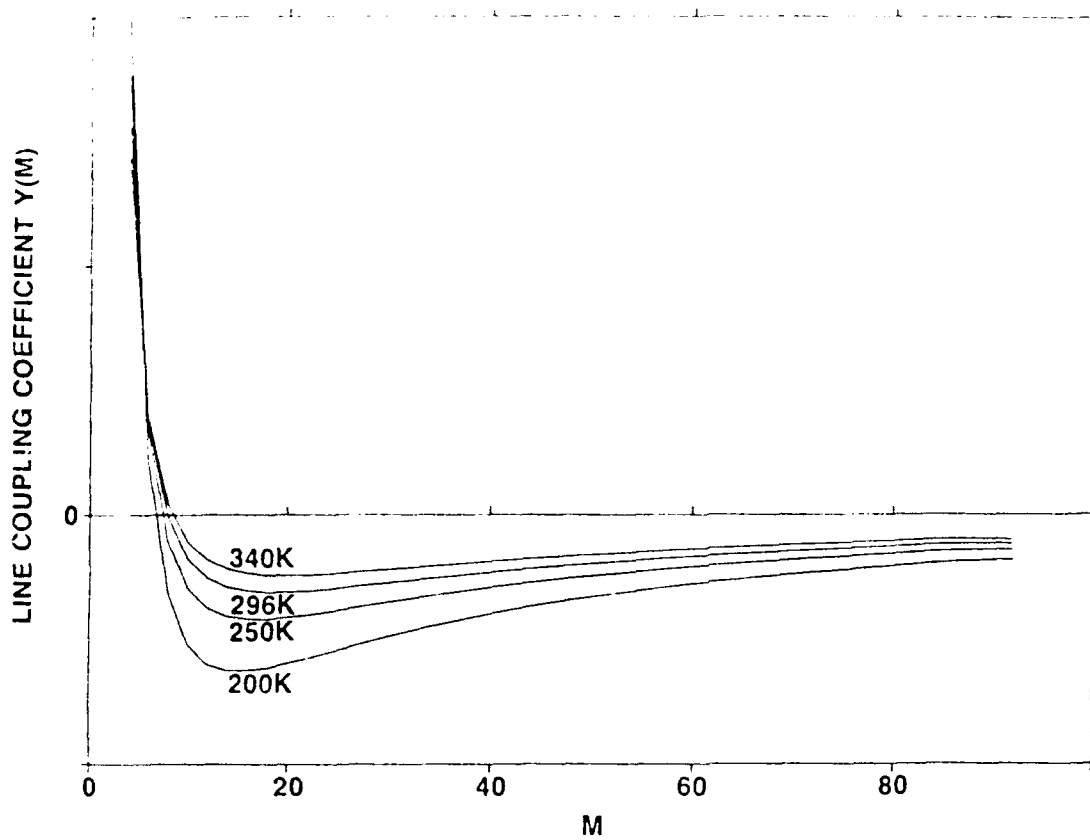
RATE PARAMETERS A_1, A_2, A_3 DETERMINED BY LEAST

SQUARES FIT.

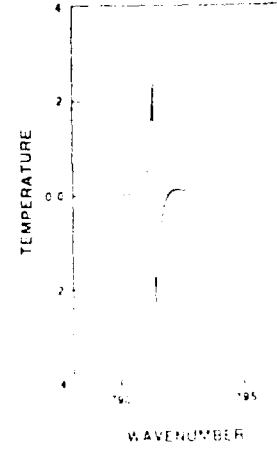
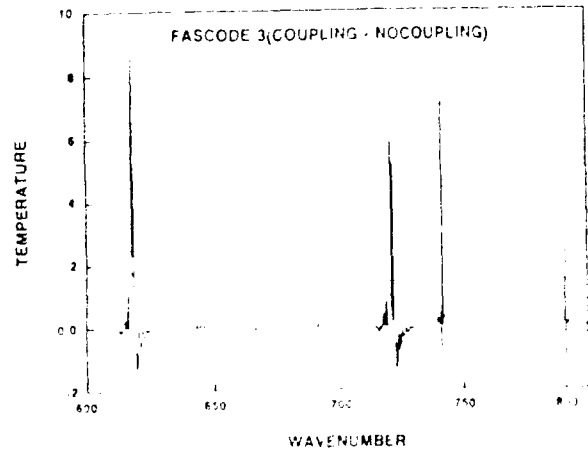
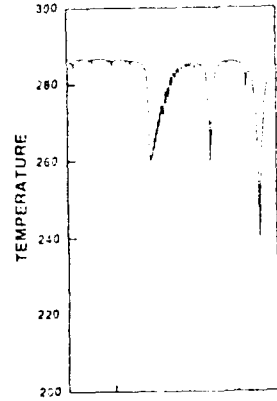
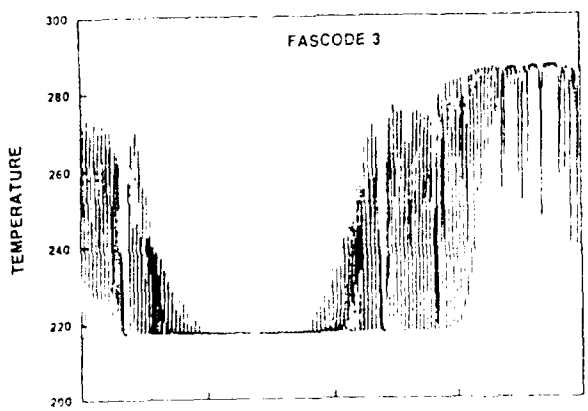
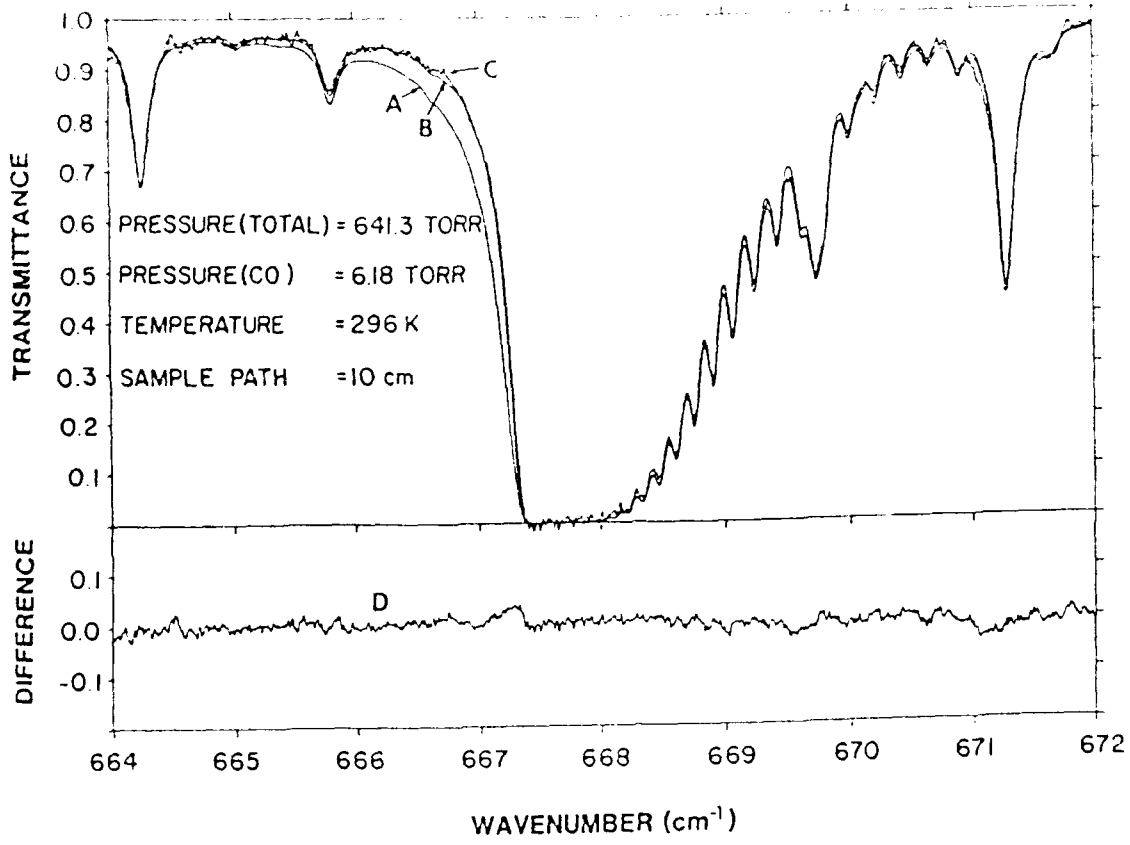
$$\left\{ \begin{matrix} \alpha_j^0 \text{ ARIE et al (1986)} \\ (B, D, H) \quad \nu_1 \nu_2 \end{matrix} \right\} \Rightarrow \begin{matrix} \langle A_1 \rangle = 0.0270 \\ \langle A_2 \rangle = 0.354 \\ \langle A_3 \rangle = 1.076 \end{matrix}$$



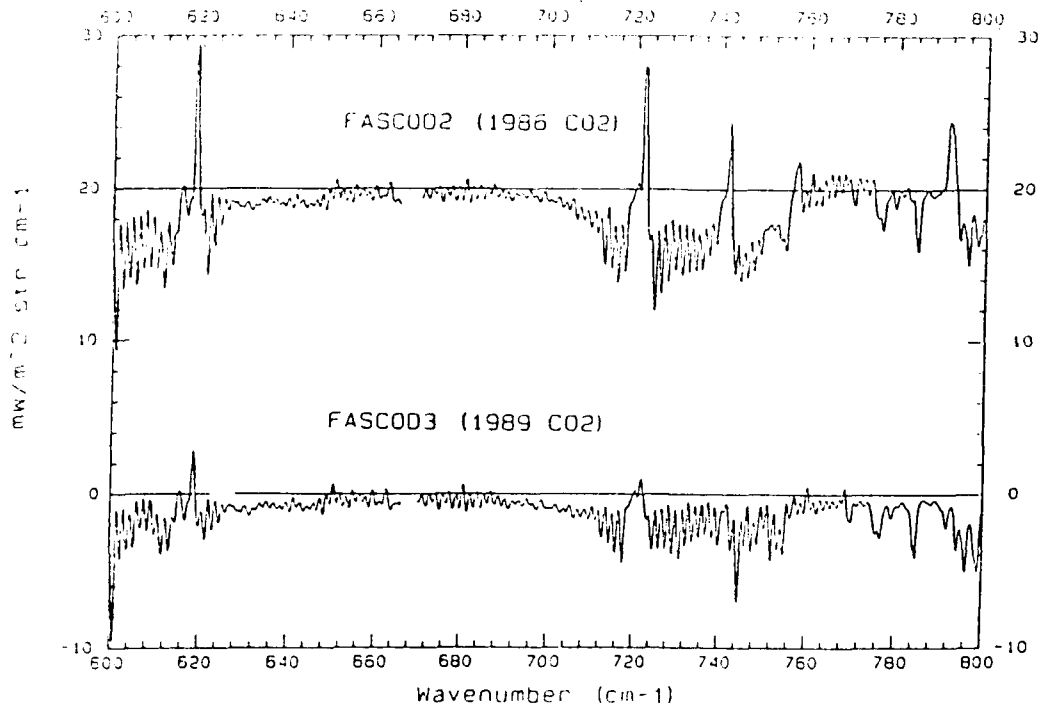




	TRANSITION		BAND CENTER	ISO.
	10002	01101	618	626
	01101	00001	667	626
	10001	01101	720	626
	10001	01101	721	636
(E ← F)	11101	02201	741	626
(F ← E)	11101	02201	741	626
	11101	10002	791	626



FASCODE-HIS



FIG(17)

FASCOD3: AN UPDATE (WITH NLTE EMPHASIS)

G.P. Anderson, F.X. Kneizys, E.P. Shettle*, J.H. Chetwynd, L.W. Abreu, M.L. Hoke
Geophysics Laboratory/OP, Hanscom AFB, MA, 01731

S.A. Clough, R.D. Worsham

Atmospheric and Environmental Research, Inc., 840 Memorial Drive, Cambridge, MA, 02139

FASCOD3, a line-by-line atmospheric radiance-transmittance code, is currently scheduled for a late summer release. As with FASCOD2, the program is applicable to spectral regions from the microwave to the middle ultraviolet, employing standard spectroscopic parameters supplied from external line atlases. New FASCOD3 capabilities include multiple scattering of thermal radiation, CO₂ and O₂ temperature-dependent line coupling, UV diffuse absorption (O₂ and O₃), improved weighting functions, and enhanced non-local thermodynamic equilibrium (NLTE) calculations. NLTE input requirements include temperature or population profiles for the specified excited vibrational states. Any auxiliary NLTE line positions, halfwidths, strengths and vibrational-rotational assignments must also be provided.

*Now at NRL.

FASCODE3: An Update

G.P. Anderson, F.X. Kneizys, E.P. Shettle,
J.H. Chetwynd, L.W. Abreu, M.L. Hoke
(Geophysics Lab (AFSC))

S.A. Clough, R.D. Worsham
(Atmospheric and Environmental Research, Inc.)

Presented at the:

Annual Review Conference on Atmospheric Transmission Models
5-6 June 1990

FASCODE: Fast Atmospheric Signature Code

Version 2 and Version 3

AFGL:	F.X. Kneizys] - Primary
	S.A. Clough ¹	
	G.P. Anderson	- UV, Constituent Profiles
	E.P. Shettle	- Aerosols/Hydrate
	J.H. Chetwynd	- Programming, Validation
	L.W. Abreu	- LOWTRAN7 Compatibility
	W.O. Gallery ¹	- Geometry
	L.S. Rothman	- Line Atlas
	M.L. Hoke	- Line Coupling

¹ Currently at Atmospheric and Environmental Research, Inc.

FASCOD3: Fast Atmospheric Signature Code

Version 3

FASCODE: Fast Atmospheric Signature Code

Version 2 and Version 3

Generic Capabilities:

- o Line-by-line molecular spectroscopy including line coupling
- o Uniform physical definitions (0-50000cm-1)
- o Full geometric path flexibility, 0-120+km, all lines of sight with spherical refraction
- o Access to arbitrary databases (HITRAN86, NLTE, etc.)
- o Voigt line shape at all altitudes and/or pressures
- o Mathematical optimization for layering and spectral sampling algorithms
- o Default or user-supplied atmospheric profiles, P, T, and mixing ratios for 28 constituents
- o Default or user-supplied aerosol and hydrometeor profiles; full LOWTRAN7 compatibility
- o Laser (monochromatic) options
- o Non-local thermodynamic equilibrium; NLTE populations must be provided from outside source (i.e. Degges, SHARC, AARC, etc.)
- o Weighting functions, merge options, ground reflection
- o Thermal multiple scattering, layer fluxes
- o Standard "user" options (plot, scan, filter, etc)

↳ interpolation
 ↳ differencing
 X-Y (ASCII)

- Visidyne: H.J.P. Smith - contributions to FASCODIC (1978)
 D.J. Dube
 M.E. Gardner
- T.C. Degges - NLTE theory (1977, 1985)
- Sonicraft: W.L. Ridgway - contributions to FASCOD2 (1985)
 R.A. Hoose
 A.C. Cogley
- AER, Inc.: R.G. Isaacs - Multiple Scattering (1987)
 R.D. Worsham - programming contributions to FASCOD3 & MS (1988)

• X-sections

PASCOD3: Fast Atmospheric Signature Code

Version 3

Applications:

- o Laser Propagation/
Ground Based Laser
- o Plume Signature/
Infrared Search and Track
- o Target Contrast/
Tactical Decision Aids
- o Remote Sensing/
Improved Point Analysis Models
- o Data Simulation/
UV, Visible, IR, microwave
MLTE, line coupling
- o Instrument design & development/
Information content, etc.

PASCOD3: Fast Atmospheric Signature Code

Version 3

Current Status (6/90):

- o Beta test version being debugged at AFGL;
also available to DoD users with special need
- o Contract with:
Atmospheric and Environmental Research, Inc.
for assistance with documentation:

Preliminary User Instructions (1/90)
User's Manual (5 months after release)
Scientific Report (10 months after release)

- o Expected DoD release: 2Q90
- o General release: 3Q90
- o Contact: Gail P. Anderson
AFGL/OPE
Hanscom AFB, MA 01731
(617)-377-2335
FAX (617)-377-4498

FASCOD3: Fast Atmospheric Signature Code

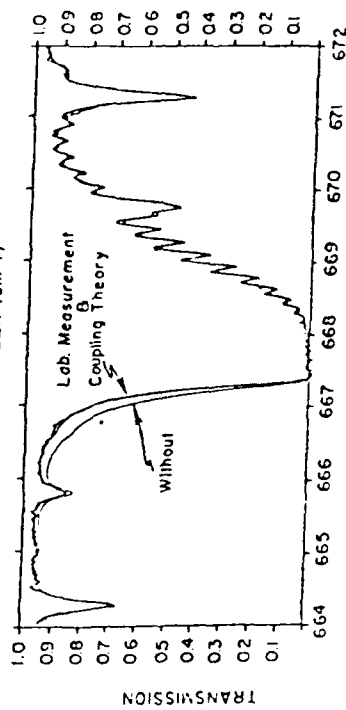
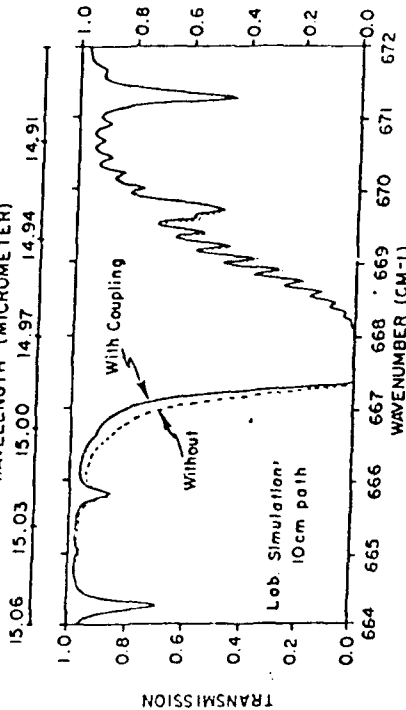
DOCUMENTATION:

- o "Instant" User Instructions (upon release)
 - Read tape
 - Unpack
 - Machine conversions
 - I/O "Parameter" definitions
 - Test cases
 - Sample output
 - Database access
 - (File management)
- o User's Manual (release plus 5 months)
 - Expansion of "Instructions"
 - Scientific definitions
 - References
 - Description/justification of "default" choices
 - Subroutine descriptions and flow charts
 - Segment load file
 - File management
- o Scientific Report (release plus 10 months)
 - All of the above AND:
 - Philosophy/history of FASCOD
 - Algorithm descriptions
 - Line-by-line functions *
 - Line shape *
 - Line coupling
 - Continua *
 - Diffuse functions
 - Geometry *
 - Layering selection *
 - Layer merging *
 - Weighting functions
 - Standard profiles (p, T, constituent) *
 - Aerosol/hydrometeor profiles (LOWTRAN7)
 - NLTE
 - Multiple scattering
 - Test cases/templates
 - Validation
 - Comparisons
 - References
 - Hints/cautions
 - etc.

(* mostly as in FASCOD2)

- o Line coupling - Optical depth, transmittance, and radiance important in vicinity of strong Q-branches and other "dense" band systems for which coupling coefficients are available (CO2 and O2 for now) moderate effects (contamination of remote sensing channels leading to T-determinations with errors > 5-10K) default option; activated whenever coef. are supplied new input parameters - coupling coef. as a fn(T) (recognized-by LNPL routines) embedded coding modifies line shape and continua small effect on runtime

FASCOD3: Line Coupling
WAVELENGTH (MICROMETER)



FASCOD3: Fast Atmospheric Signature Code

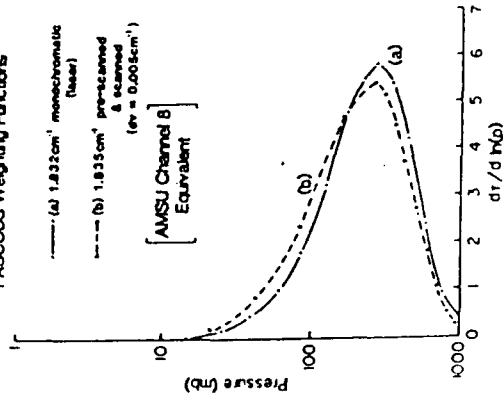
SPECIAL OPTIONS (con't #1):

o Weighting Functions

instrument design tool for ascertaining signature source regions as a fn(distance from observer) calculates cumulative transmittance from observer to points (layer boundaries) along the line-of-sight activated by IMF = 3-8, 13-18, 23-28 saves "layer-defined" monochromatic transmittances at dv(natural) for IMRG = 3-8; can consume large amnts of storage for moderate spectral range for IMRG = 13-18, will save only spectrally scanned cumulative transmittances while preserving proper line-by-line calculation for IMRG = 23-28, will save only filtered (spectrally integrated) cumulative transmittances, while preserving proper line-by-line calculation coding dependent on viewing geometry:

- line-by-line calc original pre-stored
- ground to space (IMRG = 4, 14, 24 6, 16, 26)
- space to ground (IMRG = 3, 13, 23 5, 15, 25)
- tangent (IMRG = 7, 17, 27 8, 18, 28)
- timing increases minimal to moderate
- does NOT work with IAERSL = 1,7 or IMS = 1

FASCOD3 Weighting Functions



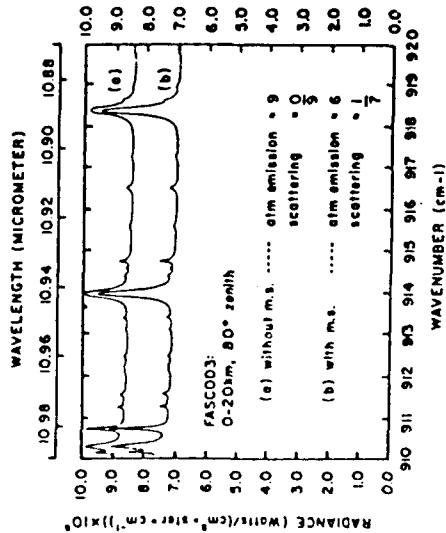
FASCOD3: Fast Atmospheric Signature Code

SPECIAL OPTIONS:

o Thermal multiple scattering - (Radiance ONLY)

encouraged for long slant paths at moderate to high pressure (i.e. below 15km) in the presence of scatterers (aerosols and/or clouds) 10-20% effect in IR activated by IMS=1 directionally dependent increases total radiance when looking down decreases " " " up strong function of viewing angle function of scattering opacity vs total opacity ** increases FASCOD3 runtime by at least a factor of 2-3 modularized coding (if IMS=0, normal FASCOD3 execution occurs)

new input parameters - surface T and emissivity - min and max altitudes for calc.



o Non-local thermodynamic equilibrium (NLTE) - Radiance

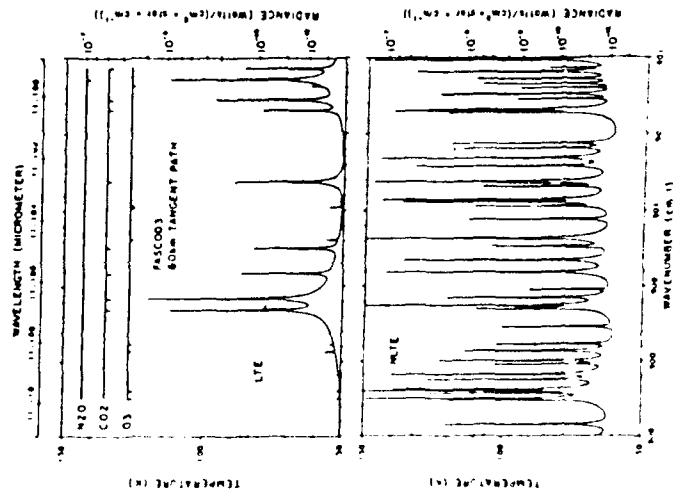
- appropriate for spectral ranges and altitudes where "hot" bands occur
- potentially large effects, particularly for paths above 50km
- activated by HIRAC=4
- new input parameters - vibrational ID's
 - vibrational T's or populations
 - standard line parameters (S, v)
- modularized coding
- improved line shape for far wings
- increases runtime in proportion to no. of lines

o Cross Section Capability - Radiance and Transmittance

- (activated by:)
- Currently reads HITRAN86 cross sections
- Will read HITRAN90 T-dependent cross sections
- Incorporates cross section into layer optical depths at the coarsest resolution possible:

- i.e. Function 1 ($\pm 4\alpha$)
- Function 2 ($\pm 16\alpha$)
- Function 3 ($\pm 64\alpha$)
- Function 4 ($\pm 256\alpha$)

Layer-dependent



Validation

FAAC002/1: Fast Atmospheric Signature Code

FAAC002/1: Fast Atmospheric Signature Code

Recent Comparisons/Validation:

Recent Comparisons/Validation:

o Theoretical

o Theoretical

WMO Intercomparison of Transmittance and Radiance Algorithms (ITRA) - 1985-1988

WMO Intercomparison of Transmittance and Radiance Algorithms (ITRA) - 1985-1988

- compared with 6 line-by-line codes for limb, nadir, and microwave test cases
- IR and mm wavelengths
- line shape (including continua)
- layering algorithm
- transmittance, radiance, and weighting functions

- compared with 6 line-by-line codes for limb, nadir, and microwave test cases
- IR and mm wavelengths
- line shape (including continua)
- layering algorithm
- transmittance, radiance, and weighting functions

SHARC - Strategic High Altitude Radiance Code for NLTE comparisons

o Laboratory (partial list; historic validation)

Line coupling (Lafferty & Hoke, 1986-87) etc.

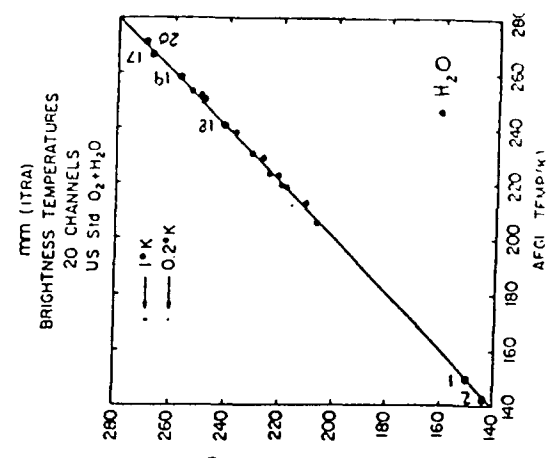
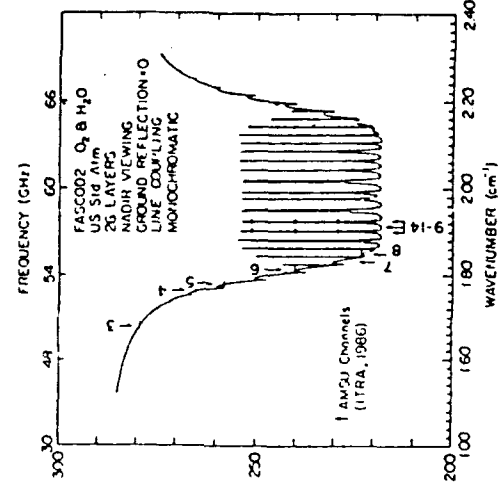
o Atmospheric Instruments

SCRIBE (Stratospheric Cryogenic Interferometric Balloon Experiment, AFGL) 1984-1988; multiple balloon flights with very high spectral resolution (0.06cm^{-1}); limb and nadir radiance

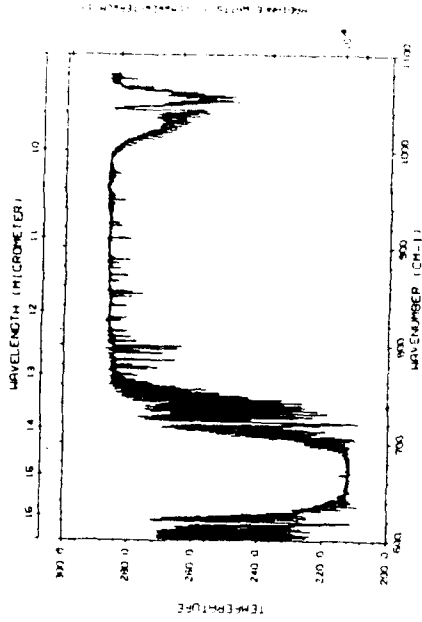
HIS (High-Resolution Interferometer Sounder, Univ. of Wisconsin) 1985-1988; multiple airborne (balloon, aircraft, and shuttle) flights with high spectral resolution (0.5cm^{-1}); limb and nadir radiance

ATMOS (Atmospheric Trace Molecule Spectroscopy instrument, JPL/NASA) 1985; spacelab (shuttle) flight with very high spectral resolution (0.01cm^{-1}); solar occultation (transmittance)

IMRLE (Infrared Mobile Optical Radiation Laboratory, NRL) 1976-1979; ground-based Fourier-transform spectrometer with very high resolution (0.06cm^{-1}); transmittance

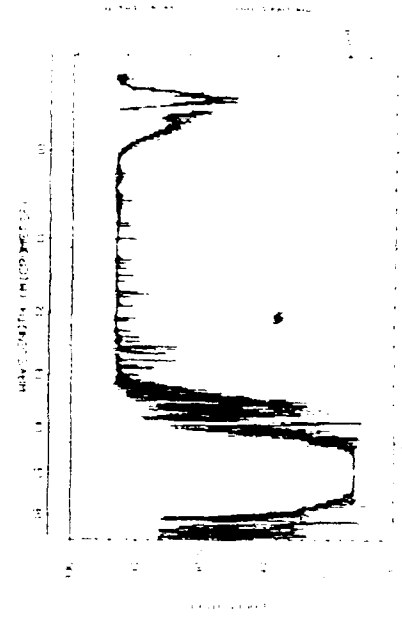


HIS Measurement



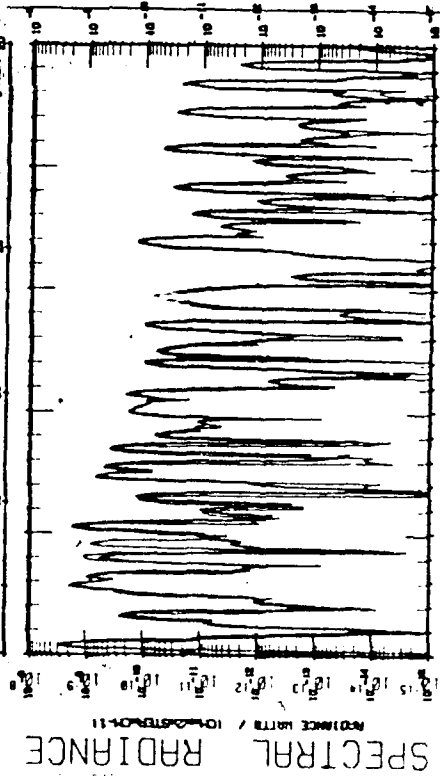
FSC3 Calculation

5 x s



SHARC-FASCODE COMPARISON

SPECTRAL SCIENCES INCORPORATED



SPECTRAL RADIANCE

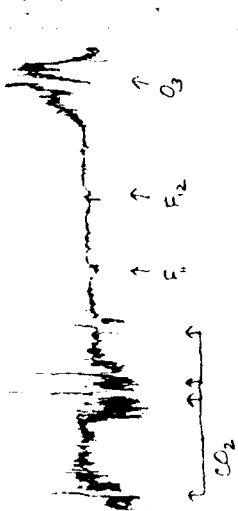
- H₂O ROTATION BANDS
- FASCODE CALC'S BY GL/OPE
- 20-40 μm
- SINGLE LAYER
- 90 km ALTITUDE

WAVENUMBER (CM⁻¹)

11000 10000 9000 8000 7000 6000 5000 4000 3000 2000 1000 0

FSC2

improved O₃ profile
to coupling (CO₂)
to x-sections (F₁ & F₂)



FSC3 - FSC2

improvements: new O₃ profile
new CO₂ coupling
x-sections



SOME REMAINING PROBLEMS:

X Incorporating the effects of "heavy molecules" in transmittance/radiance modelling:

Solutions

- o not conducive to line-by-line approach -
- o many anthropogenic in origin
- o "green house" gases; i.e. fill windows
- o partial solution provided by HITRAN x-sections

2. Inferring path variables (z, P, T, μ , clouds, etc) from E/O measurements:

- o measurement & "forward" calculation capabilities exist
- o requires iterative "inversion" algorithm
- o must provide a "quasi-realtime" solution

3. Determining sensitivity analyses for instrument design

- o identify spectral regions where E/O technologies will best meet specifications (i.e. most effective)
- o predictive
- o previously developed for LOWTRAN6

4. Understanding line shape theory & line coupling

- o H₂O far wing behavior particularly difficult in "window" regions
- o very small attenuation in transmittance; potentially large problem in non-linear absorption

SOME REMAINING PROBLEMS: (con't)

5. Describing effects of "hot" gases: plumes, etc.
 - o requires "hot gas" tape with higher vib-rot assignments
 - o requires NLTE estimates for populations (in addition to thermal)
 - o requires band model development

6. Improving NLTE high altitude models:
 - o additional spectral parameters, particularly O₃
 - o additional gas population estimates - not simple
 - o radiative transfer mechanisms

7. Establishing UV/Electronic transition capability
 - o airglow, night glow
 - o alternate source functions
 - o high altitude

RAD: A LINE-BY-LINE RADIATIVE EXCITATION MODEL, WITH APPLICATION TO CO₂

P.P. Wintersteiner*, R.H. Picard#, R.D. Sharma#, H. Nebel#+,
A.J. Paboojian*, J.R. Winick#, and R.A. Joseph*

*ARCON Corporation, 260 Bear Hill Road, Waltham, MA 02154

#Geophysics Laboratory/OPE, Hanscom AFB, MA 01731

+Permanent address: Alfred University, Alfred, NY 14802

In the non-LTE region of the atmosphere, the local kinetic temperature is not sufficient to determine molecular vibrational-level populations (or vibrational temperatures) as it is in the LTE atmosphere, and it is necessary to calculate these populations explicitly in order to determine the radiation fluxes. This requires a calculation of the excitation and loss processes for the molecular vibrational levels, which, in turn, requires a radiative-transfer calculation to determine the upwelling/downwelling fluxes responsible for the radiative excitation process. We have developed the RAD line-by-line radiative-transfer code to carry out this calculation in the atmosphere. This paper will first discuss the basic RAD algorithm and approach. Then we will show the results of calculations carried out for CO₂ 15 μm and 4.3 μm radiation under nighttime, daytime, and auroral conditions. Finally, we will validate the model by comparing the RAD predictions to data from the SPIRE and FWI experiments.

**RAD: A Line-by-Line Radiative Excitation Model
with Application to CO₂**

P.P. WINTERSTEINER⁽¹⁾, R.H. PICARD⁽²⁾, R.D. SHARMA⁽²⁾, H. NEBEL⁽²⁾,
A.J. PABOOJIAN⁽¹⁾, J.R. WINICK⁽²⁾, & R.A. JOSEPH⁽¹⁾

(1) ARCON CORPORATION
(2) GEOPHYSICS LABORATORY

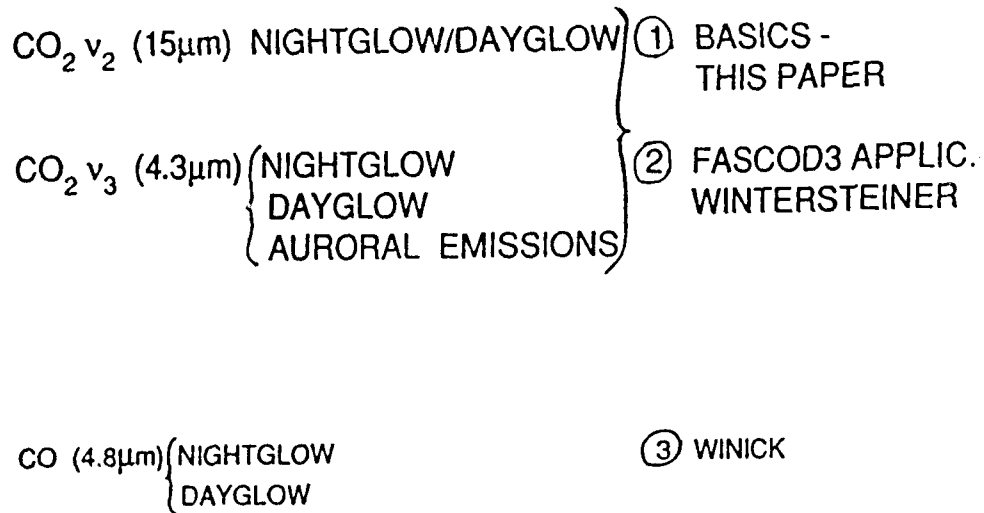
Annual Review Conference
on Atmospheric Transmission Models
Geophysics Laboratory
5-6 June 1990

PRESENTER: R.H. PICARD

LINE-BY-LINE RADIATIVE EXCITATION ALGORITHM
(RAD) - FEATURES

- ASSUMPTIONS
 - o PLANE - PARALLEL GEOMETRY
 - o NON-OVERLAPPING LINES
 - o COMPLETE FREQUENCY REDISTRIBUTION
 - o $T_{rot} = T_{kin}$
- FULL LINE-BY-LINE CALCULATION
- FINE LAYERING
- ALTITUDE-DEPENDENT EMISSION/ABSORPTION
LINESHAPE (VOIGT)
- MODULAR STRUCTURE / *ITERATIVE APPROACH*

LINE-BY-LINE RADIATIVE EXCITATION ALGORITHM
(RAD) - APPLICATIONS



RAD: A LINE-BY-LINE RADIATIVE EXCITATION ALGORITHM

OUTLINE

- NON-LTE EFFECTS
- RAD MODEL & ALGORITHM
- APPLICATIONS/COMPARISONS WITH DATA

NON-LTE EFFECTS

SOLVE SIMULTANEOUSLY FOR POPULATIONS & FLUXES

1) EQ. OF TRANSFER - FLUX

$$\frac{\partial I}{\partial \tau_y} = S - I \quad \leftarrow \text{FLUX}$$

SOURCE FUNCTION

$$S \equiv \frac{A}{B_{\uparrow}} \frac{N_2}{N_1}$$

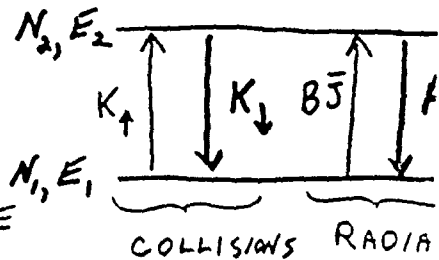
2) RATE EQ. - POPULATION (STEADY-STATE)

$$\frac{N_2}{N_1} \equiv e^{-\frac{E_2 - E_1}{k_B T_{vib}}} = \frac{K_{\uparrow} + B_{\uparrow} \bar{J}}{K_{\downarrow} + A}$$

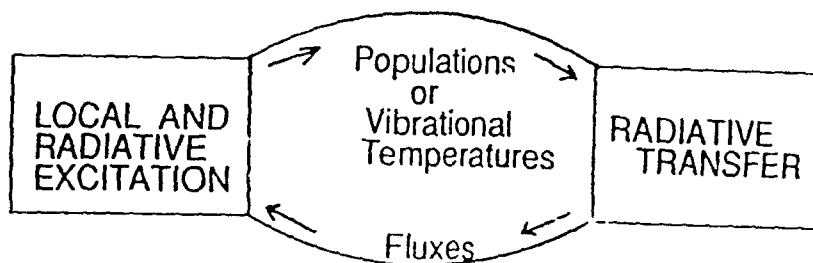
- DEFINITION OF T_{vib}

- LTE: $T_{vib} = T$

- \bar{J} = AVERAGE OF FLUX I OVER FREQUENCY, ANGLE



RAD MODULAR STRUCTURE



- ITERATIVE APPROACH \rightarrow SMALL EQUATION SET

- Method of Successive Substitution

- Provisional Vibrational Temperatures

\rightarrow Radiative Excitation Rates

\rightarrow New Vibrational Temperatures

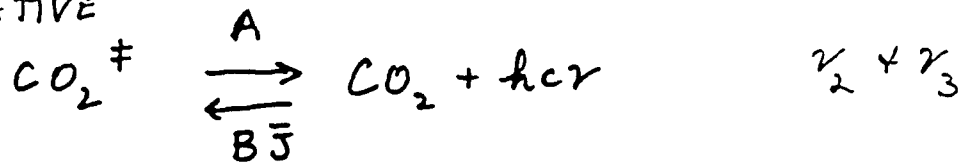
- Major & Minor Iterations

- Minor Iterations: Opacities Constant

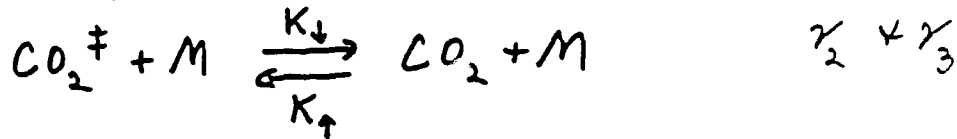
\rightarrow Transfer Function

PRODUCTION & LOSS PROCESSES - CO₂ VIBRATION

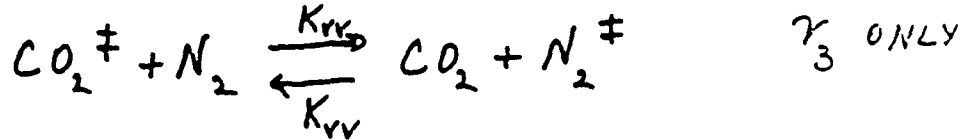
- RADIATIVE



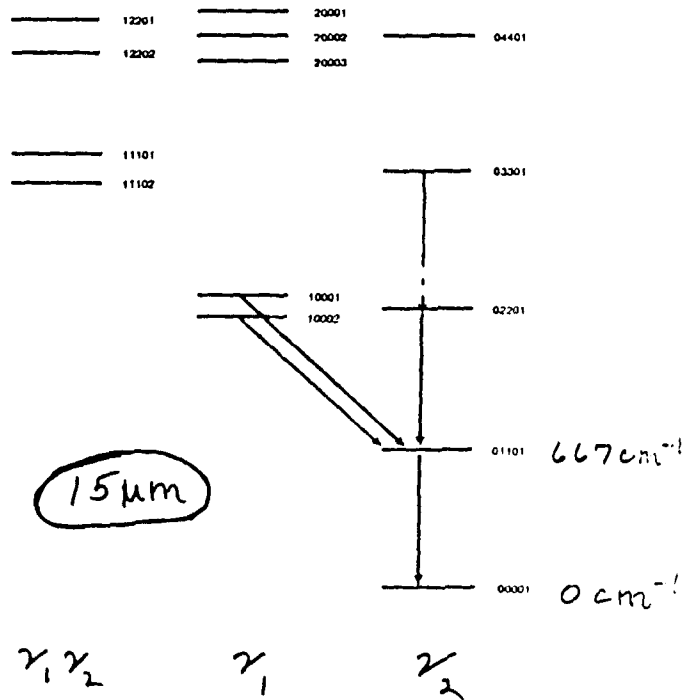
- COLLISIONAL (V-T)

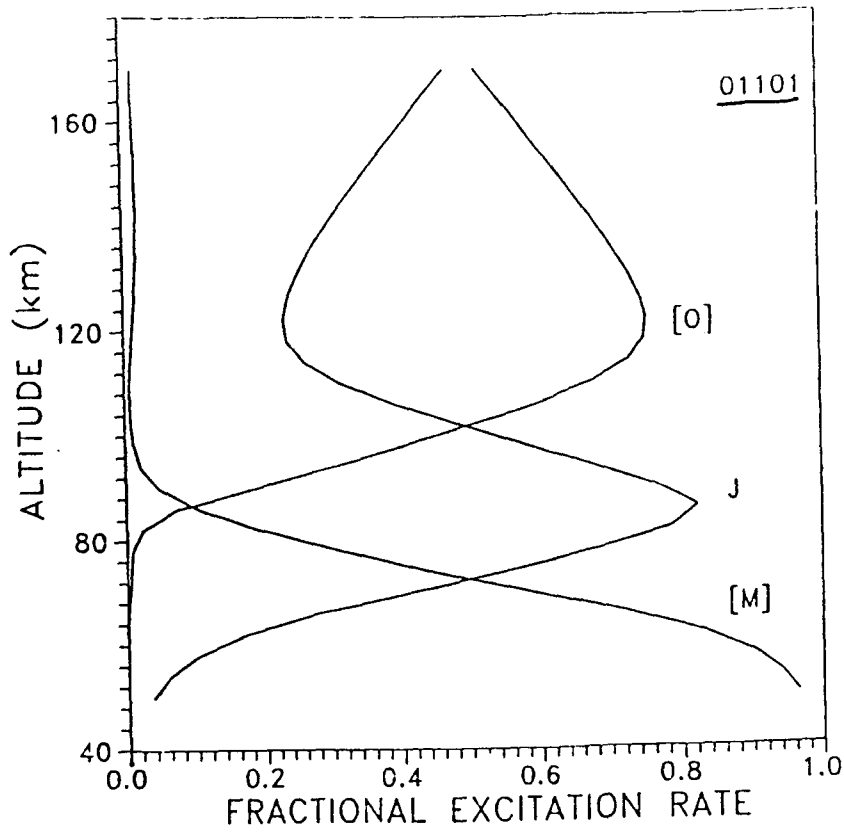


- VIBRATIONAL TRANSFER (V-V)



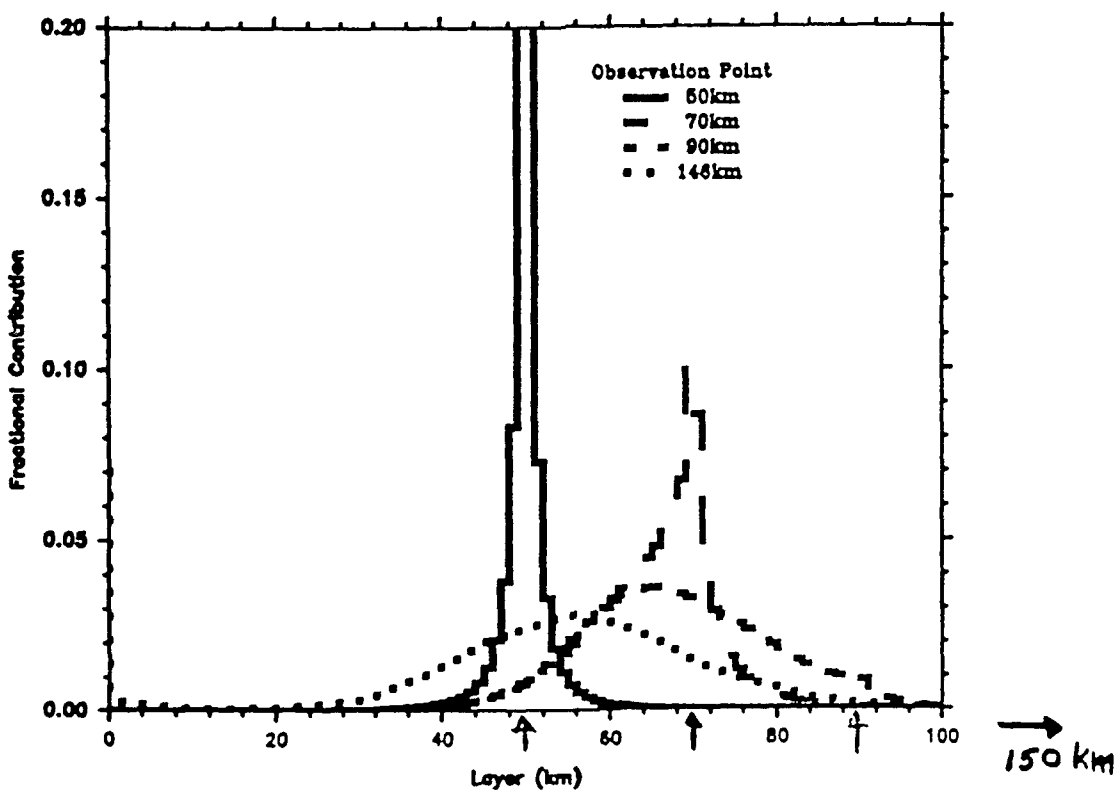
CO₂ BEND-STRETCH MANIFOLD





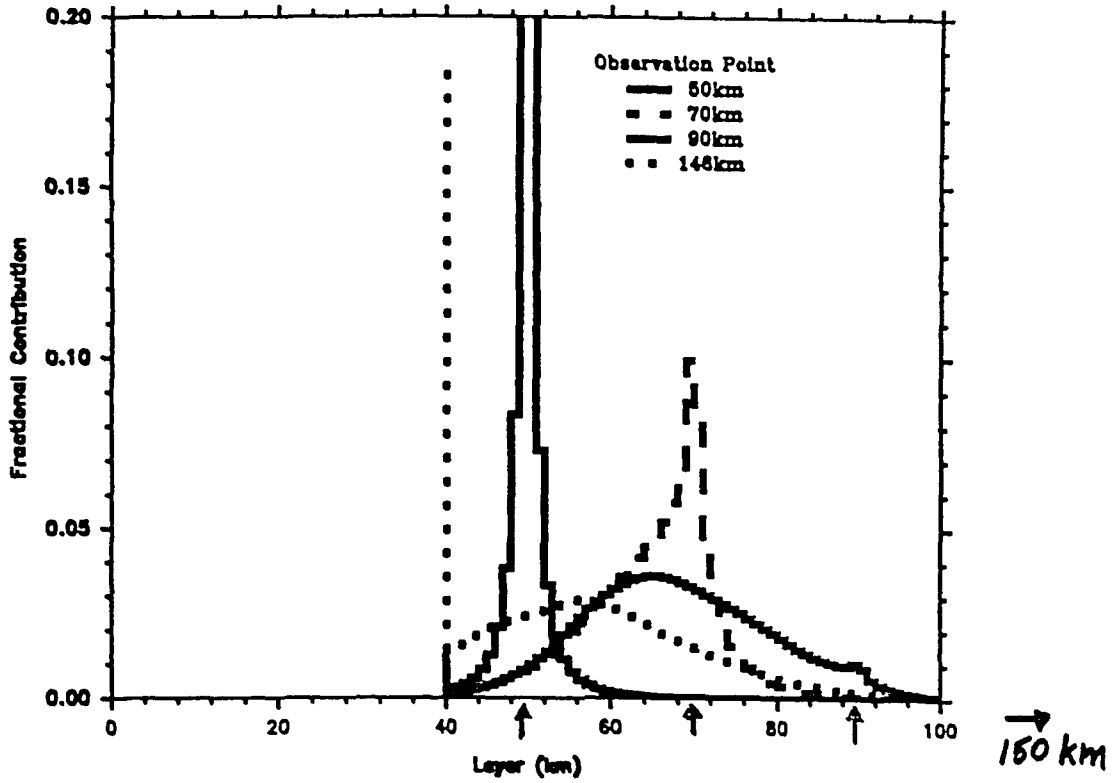
? $\frac{\uparrow \text{Non-LTE}}{\downarrow \text{LTE}}$

RADIATIVE TRANSFER FUNCTION - CO₂ 636 01101-00001
Ground boundary

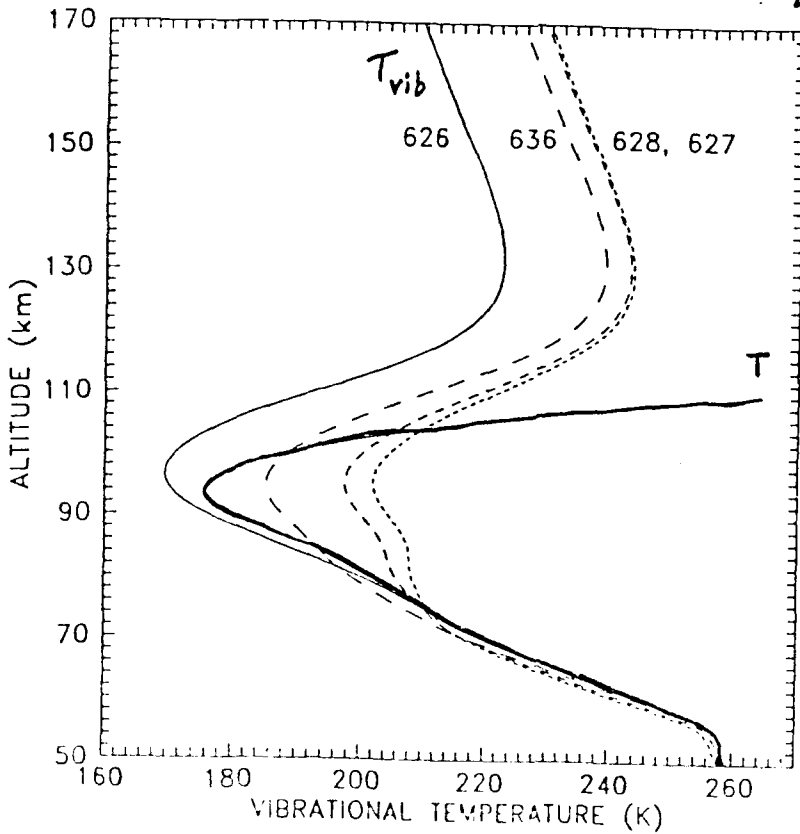


RADIATIVE TRANSFER FUNCTION - CO₂ 636 01101-00001

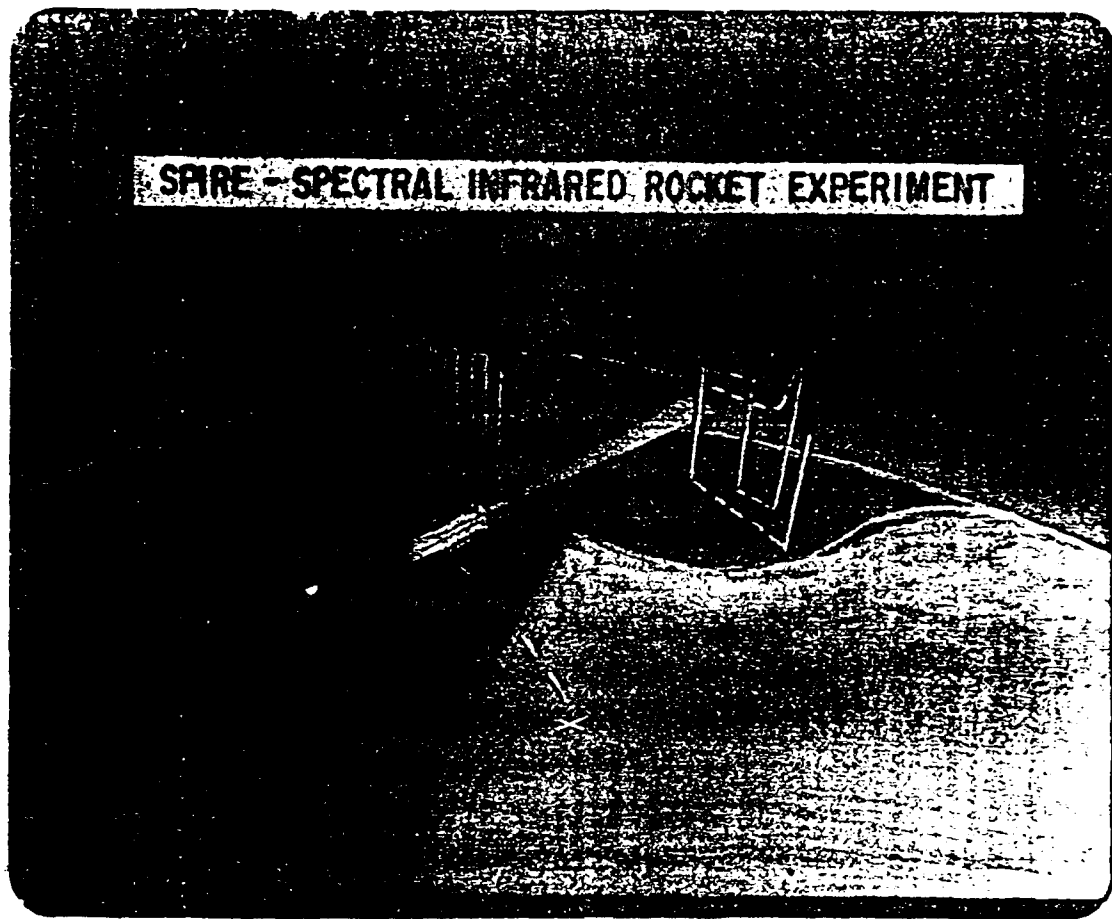
40 km boundary



CO₂ (01101) VIBRATIONAL TEMPERATURES γ_2

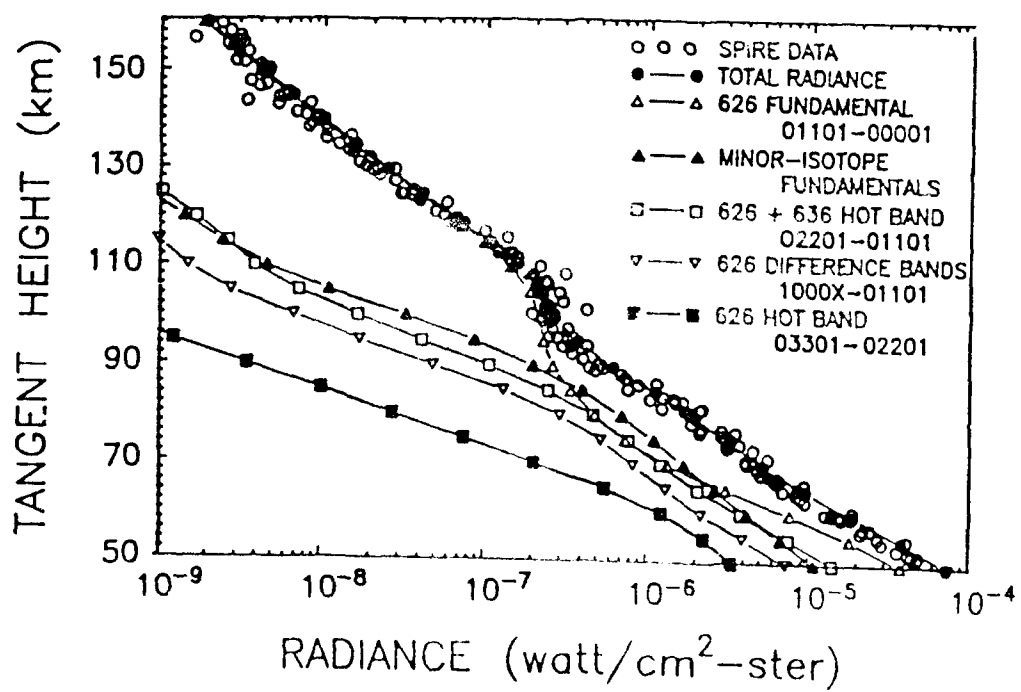


SPiRE - SPECTRAL INFRARED ROCKET EXPERIMENT

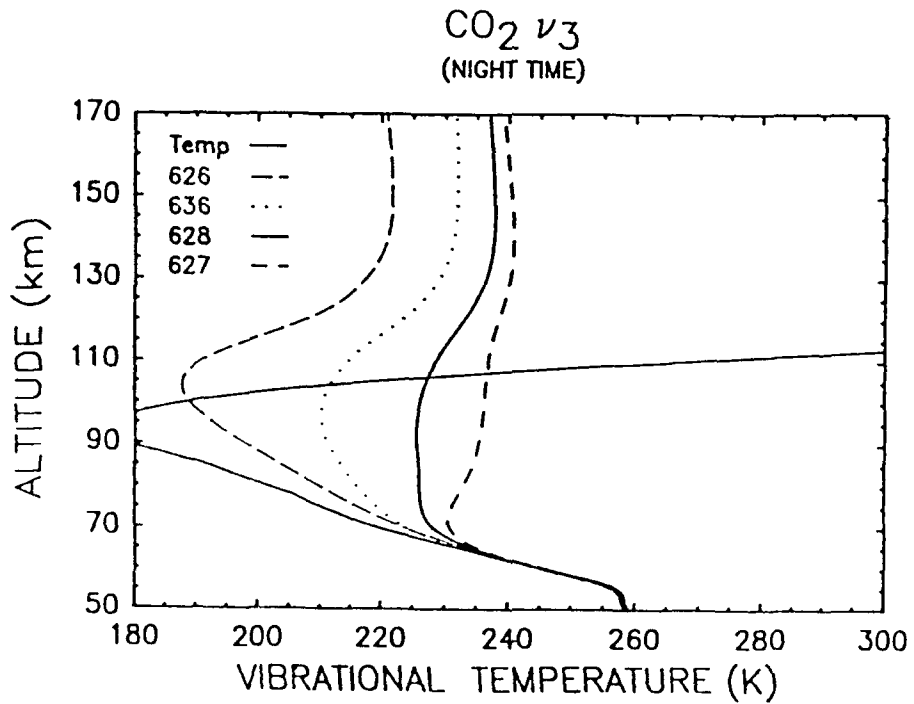
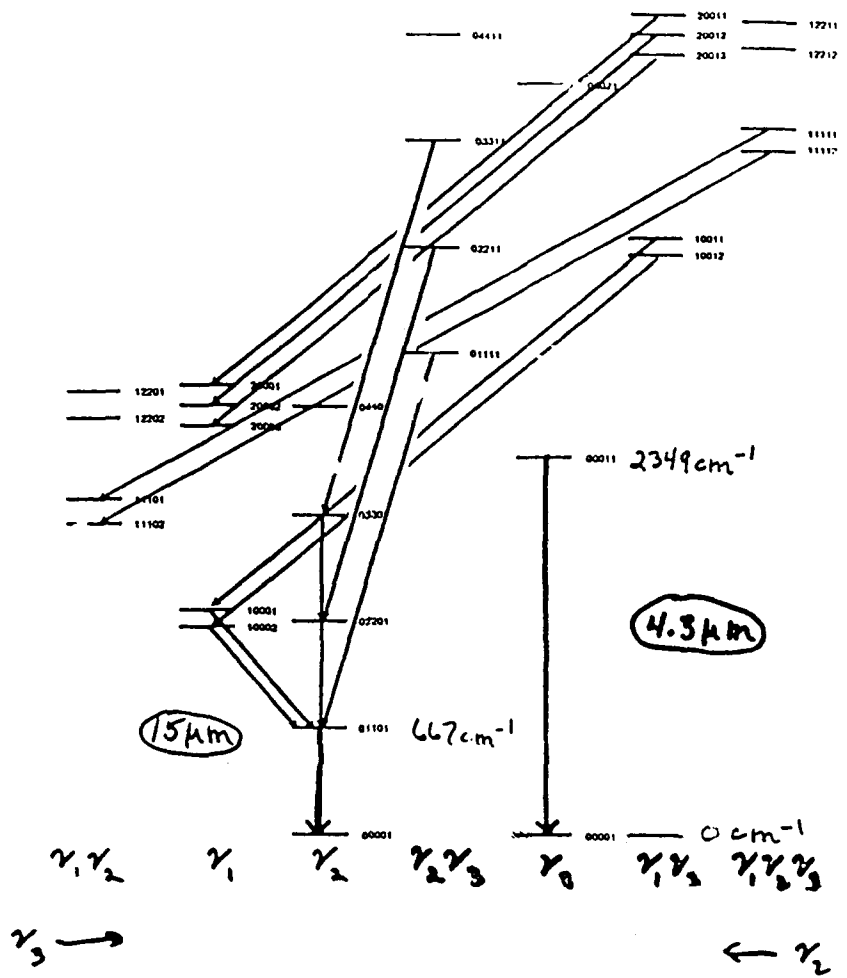


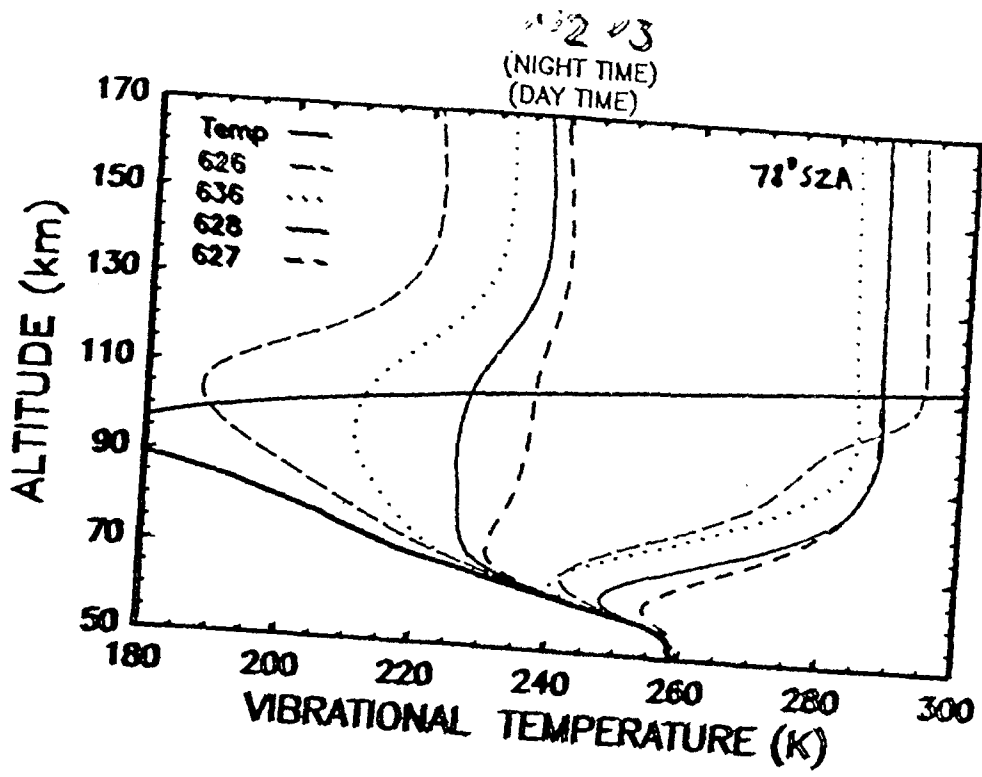
Poker Flat
Terminator

SPiRE BAND RADIANCE, 13-16.5 μm

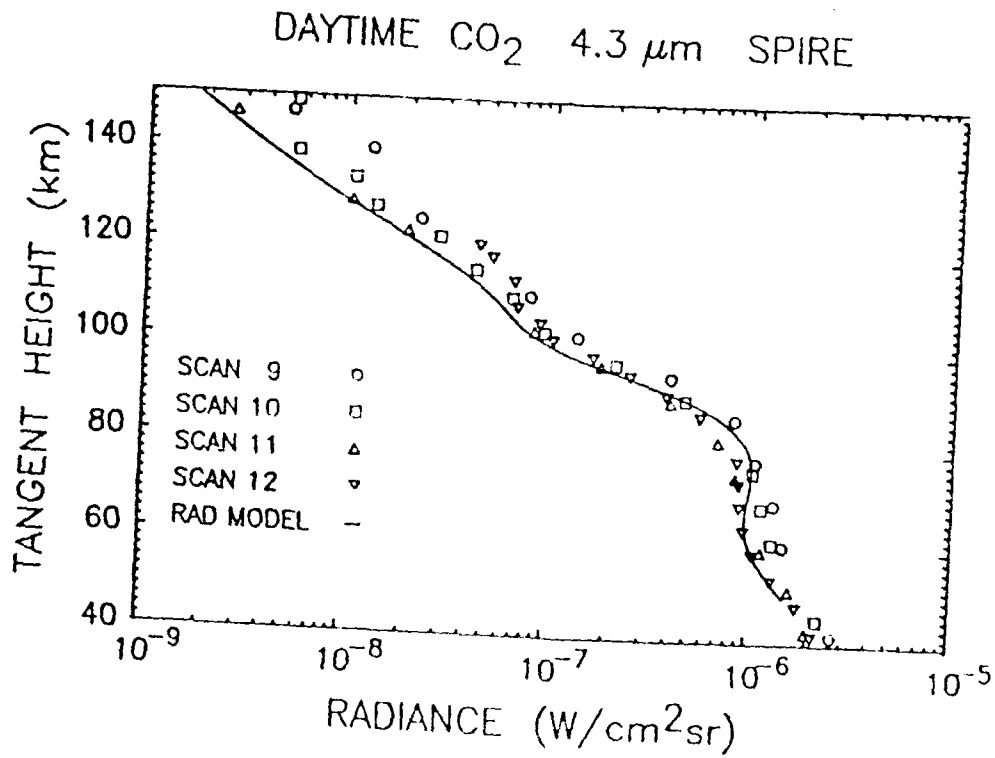


CO₂ VIBRATIONAL ENERGY LEVELS

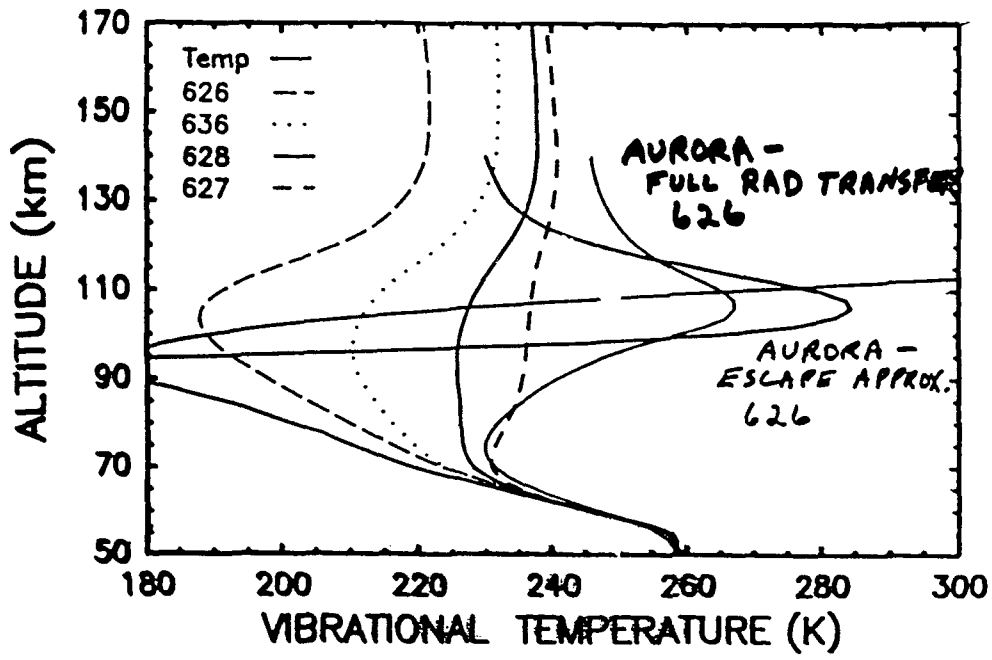




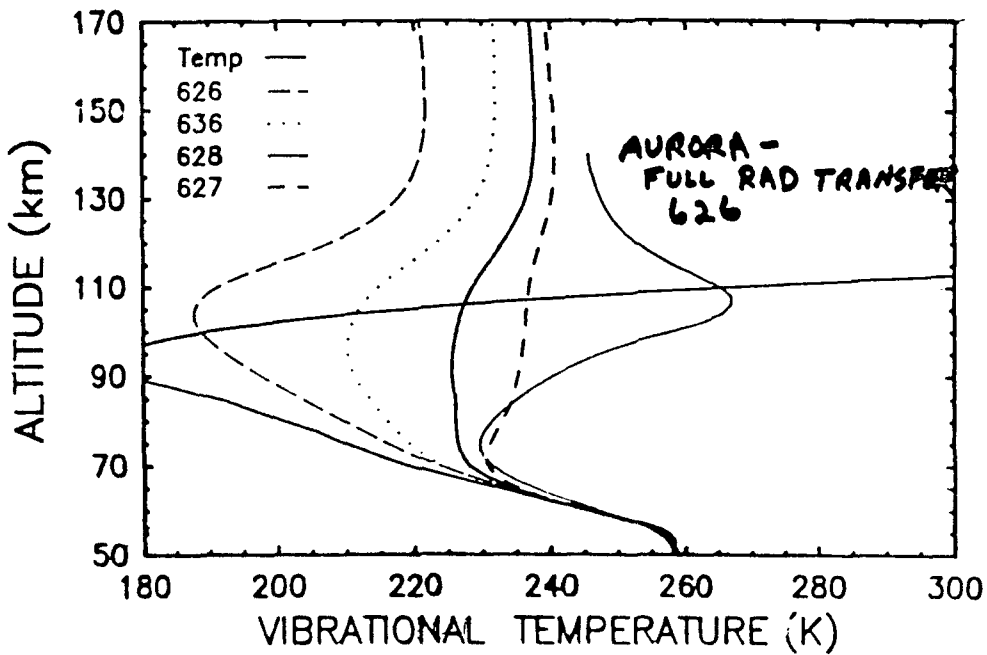
0-2

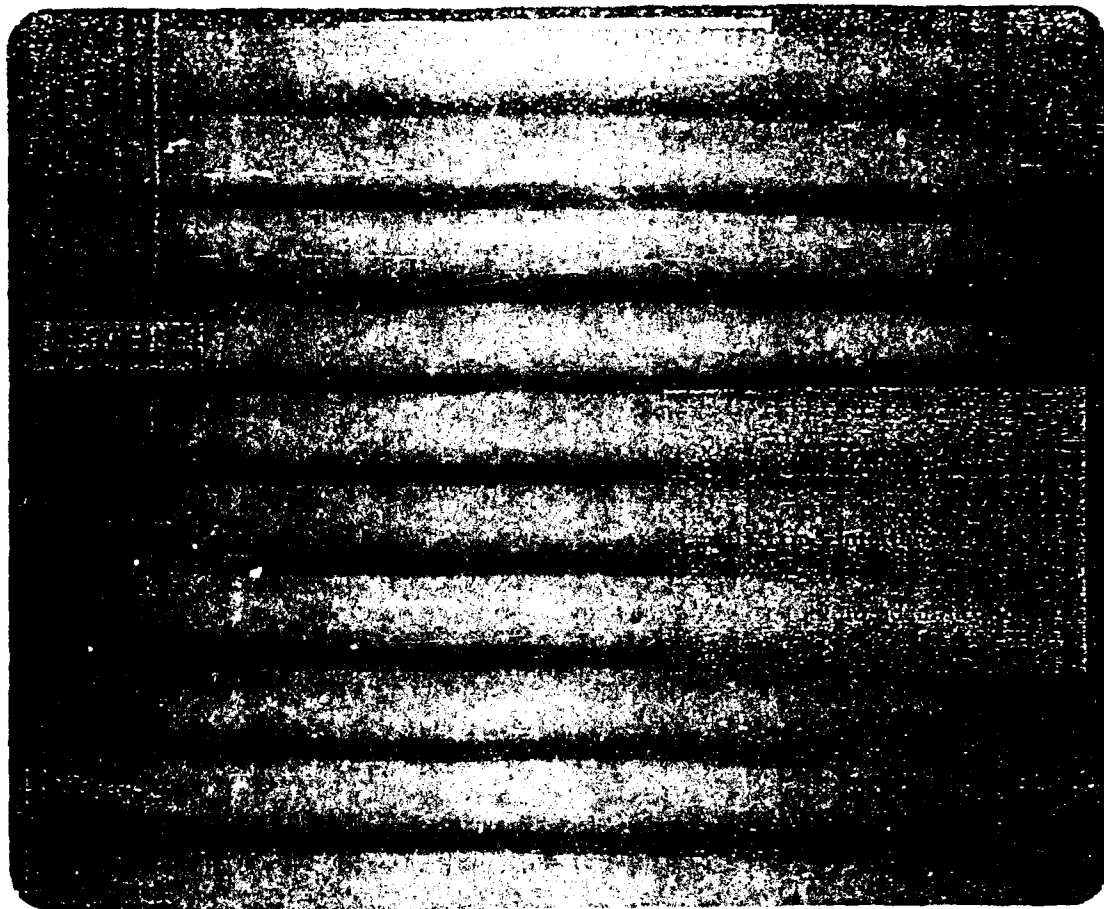


CO₂ ν₃
(NIGHT TIME)

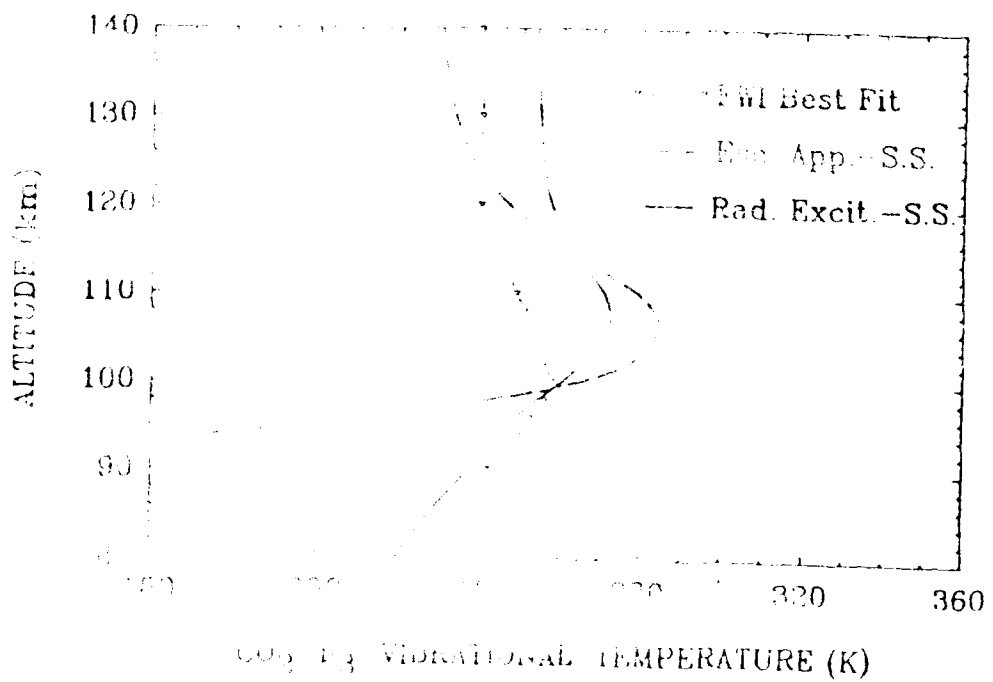


CO₂ ν₃
(NIGHT TIME)





CO₂ VIBRATION
 IN THE MIRA



RAD - LINE-BY-LINE RADIATIVE EXCITATION ALGORITHM

CONCLUSIONS

- POWERFUL LINE-BY-LINE RADIATIVE EXCITATION MODEL (RAD) DEVELOPED
- RAD APPLIED TO CO₂ 4.3 μ m & 15 μ m AIRGLOW PREDICTION
- MODEL PREDICTIONS AGREE WELL WITH SPIRE AND FWI DATA UNDER BOTH NIGHT AND DAY CONDITIONS
- NON-LTE EFFECTS ABOVE 60-70 KM (+/-)
- RAD MODEL PROVIDES BENCHMARK TO TEST VALIDITY OF MODELS WITH MORE APPROXIMATIONS, (HAIRM, SHARC)
- NEXT TWO TALKS: APPLICATION TO FASCOD3
APPLICATION TO 4.8 μ m CO

NON-LTE CO₂ VIBRATIONAL TEMPERATURE PROFILES FOR FASCOD3

P.P. Wintersteiner and A.J. Paboojian

ARCON Corp., 260 Bear Hill Road, Waltham, MA 02154

J.R. Winick and R.H. Picard

Geophysics Laboratory/OPE, Hanscom AFB, MA 01731

Using line-by-line radiative transport, we have developed procedures for evaluating non-LTE populations for all the infrared-emitting vibrational states of CO₂ that are important for atmospheric studies. We have calculated these populations, expressed as vibrational temperatures, for the six FASCODE model atmospheres for day and night conditions. We will outline the calculations, including the assumption and the data required for input, and present some of the results (e.g., vibrational temperatures, cooling rates, excitation/de-excitation rates). We will also discuss the qualitative differences arising from the different features of the model atmospheres.

Non-LTE CO₂ Vibrational Temperature Profiles for FASCOD3

P. P. Wintersteiner and A. J. Paboojian
VERGOS Corp., 260 Bear Hill Rd., Walham, MA, 02154

J. R. Menden, R. H. Picard, R. D. Sharma, and G. P. Anderson
Geophysics Laboratory/OPE, Hanscom AFB, MA, 01731

Using line-by-line radiative transport, we have developed procedures for evaluating non-LTE populations for all the infrared-emitting vibrational states of CO₂ that are important for atmospheric studies. We have calculated these populations expressed as vibrational temperatures for the six FASCOD3 model atmospheres for day and night conditions. We will outline the calculations, including the assumptions and the data requirements for input, and present an overview of the results. We will also discuss the radiative differences arising from the differing features of the model atmospheres.

Title

Objectives

Figure 1. Breadth and temperature of stratopause and mesopause regions strongly influence the CO₂ vibrational-temperature profiles. Models 4 and 5 are extremes in this regard, while Model 6 falls in between.

Figure 2. CO₂ levels for which we calculate vibrational temperatures are enclosed in boxes.

Figure 3. Substantial differences exist between bend-stretch vibrational temperatures for different model atmospheres.

(a) Model 6 (nighttime) profiles are typical in that:

- i. The 01101 vibrational temperature is slightly below the kinetic temperature above 80 km. The 1 to 3 K difference corresponds to a 3 to 5% lower volume emission rate (Is this "in LTE"?)
- ii. The 02201 vibrational temperature is a couple of degrees above 01101 due to lower atmospheric opacity through the mesosphere and (consequently) greater pumping from the lower, warmer regions.
- iii. The 03301 temperature is warmer still, for similar reasons. The 5 to 10 K difference gives approximately twice the volume emission (compared to LTE).

(b) Same as (a), but for Model 4. The 01101 vibrational temperature still tracks T. Higher states are more strongly pumped by a warmer stratopause, and thermal excitation at the cold mesopause is less significant.

(c) Same as (a), but for Model 5. The 01101 vibrational temperature still tracks T. For the higher states, changes seen in (b) are reversed.

Figure 4 ($CO_2/00011$) and $N_2(v=1)$ vibrational temperatures. Day/night differences are obvious as is the strong coupling of N_2 to CO_2 or the thermal reservoir. Departure from LTE is at a lower altitude than for the bend/stretch states.

Model 4. Noontime sun is at 37° , greater solar zenith angles would reduce the 0111 vibrational temperature in the 80-110 km region, but not elsewhere.

Model 5. Comparison with 4 shows the effect

of the wind velocity at 100 km.

The effect is small, but the 0111 vibrational temperature is primarily to produce a small increase in the 0111 vibrational temperature in the 80-110 km region. The effect is small, but the 0111 vibrational temperature is primarily to produce a small increase in the 0111 vibrational temperature in the 80-110 km region.

Model 6. The effect of the wind velocity at 100 km is small, but the 0111 vibrational temperature is primarily to produce a small increase in the 0111 vibrational temperature in the 80-110 km region. The effect is small, but the 0111 vibrational temperature is primarily to produce a small increase in the 0111 vibrational temperature in the 80-110 km region.

Model 7. The effect of the wind velocity at 100 km is small, but the 0111 vibrational temperature is primarily to produce a small increase in the 0111 vibrational temperature in the 80-110 km region.

Model 8. The effect of the wind velocity at 100 km is small, but the 0111 vibrational temperature is primarily to produce a small increase in the 0111 vibrational temperature in the 80-110 km region. The effect is small, but the 0111 vibrational temperature is primarily to produce a small increase in the 0111 vibrational temperature in the 80-110 km region.

Model 9. The effect of the wind velocity at 100 km is small, but the 0111 vibrational temperature is primarily to produce a small increase in the 0111 vibrational temperature in the 80-110 km region. The effect is small, but the 0111 vibrational temperature is primarily to produce a small increase in the 0111 vibrational temperature in the 80-110 km region.

Model 10. The effect of the wind velocity at 100 km is small, but the 0111 vibrational temperature is primarily to produce a small increase in the 0111 vibrational temperature in the 80-110 km region.

Figure 5. Low time vibrational temperatures for six high lying states, three of them pumped at $2.0 \mu m$ by solar flux.

Figure 8. Experimental CO_2 mixing ratios from the literature, and two model profiles. CO2D is the profile used in our calculations; CO2E, having significant depletion in the 80-110 km region, was used for comparison.

Figure 9. (Sensitivity to $[CO_2]$) Same as Figure 3(a), but for CO2E instead of CO2D. The comparison reveals that these vibrational temperature results are not very sensitive to $[CO_2]$ at altitudes where $[CO_2]$ is not well known. For $z < 110$, there are vibrational temperature differences of 2 K or less at the mesopause.

Figure 10. (Sensitivity to $[O]$) Comparison of the 0110 vibrational temperatures in Model F, with results obtained by doubling and halving $[O]$. 2.0% differences in $[O]$ correspond to 14% changes in volume emission differences of 15% correspond to roughly a 60% effect in vibrational temperatures and is about 10% less sensitive to $[O]$.

Figure 11. (Sensitivity to CO_2) Comparison of the 0110 vibrational temperatures in Model F, with results obtained by doubling and halving CO_2 . 2.0% differences in CO_2 correspond to 14% changes in volume emission differences of 15% correspond to roughly a 60% effect in vibrational temperatures and is about 10% less sensitive to CO_2 .

Figure 12. Nighttime $4.3 \mu m$ band radiance, using vibrational temperatures of 1100 K plus those for the 0111 state. Radiance from the 0111 band is the largest component of this sum for a considerable range of tangent altitudes. It is to higher vibrational temperatures at lower atmospheric density. Comparison of CO_2 and CO_2E vibrational temperatures shows that the major change by 40 K. This results in an order of magnitude difference in volume emission near the mesopause.

Summary

Non - LTE CO₂ Vibrational - Temperature
Profiles for FASCOD3

P. P. Wintersteiner, A. J. Paboojian
ARCON Corporation

J. R. Winick, R. H. Picard, R. D. Sharma,
G. P. Anderson
Geophysics Laboratory

OBJECTIVE

- Generate CO₂ vibrational temperature library profiles for FASCODE
- consistent with the six AFGL Atmospheric Constituent profiles
- all important emitting states
- night-time, local noon

OVERVIEW OF RESULTS FOR NON-LTE REGIONS

- vibrational temperatures
 - bend-stretch states (15 μm)
 - ν₃ states (4.3 μm)
 - ν₁ν₂ states (4.3, 2.7 μm)
- solar influence
- sensitivity to input profiles
- isotopes

Annual Review Conference on Atmospheric
Transmission Models
5 June 1990
Geophysics Laboratory

KINETIC TEMPERATURES

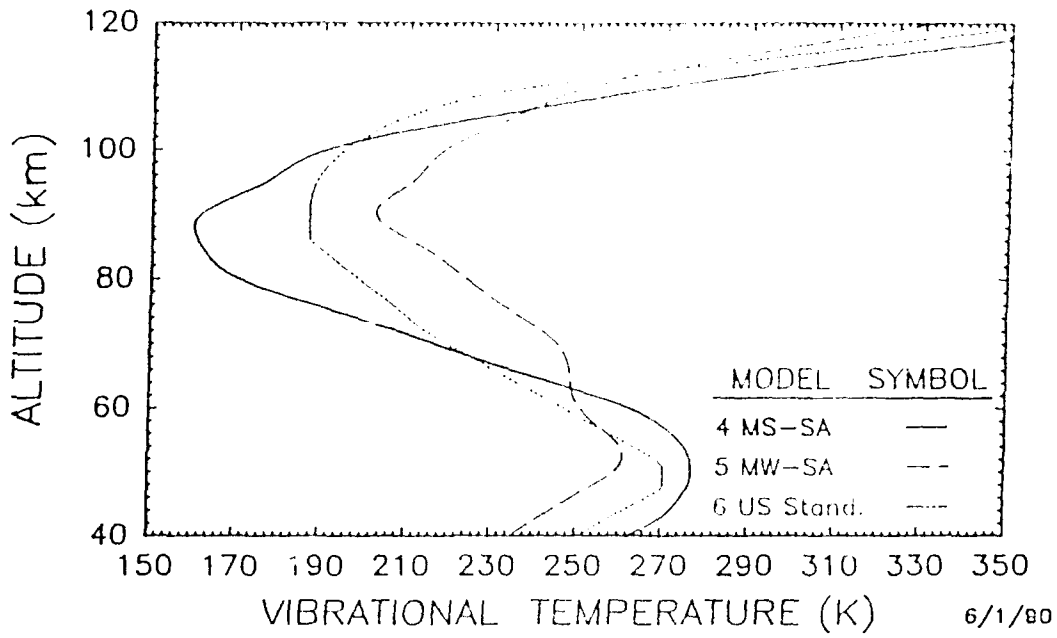


Figure 1

CO₂ VIBRATIONAL ENERGY LEVELS

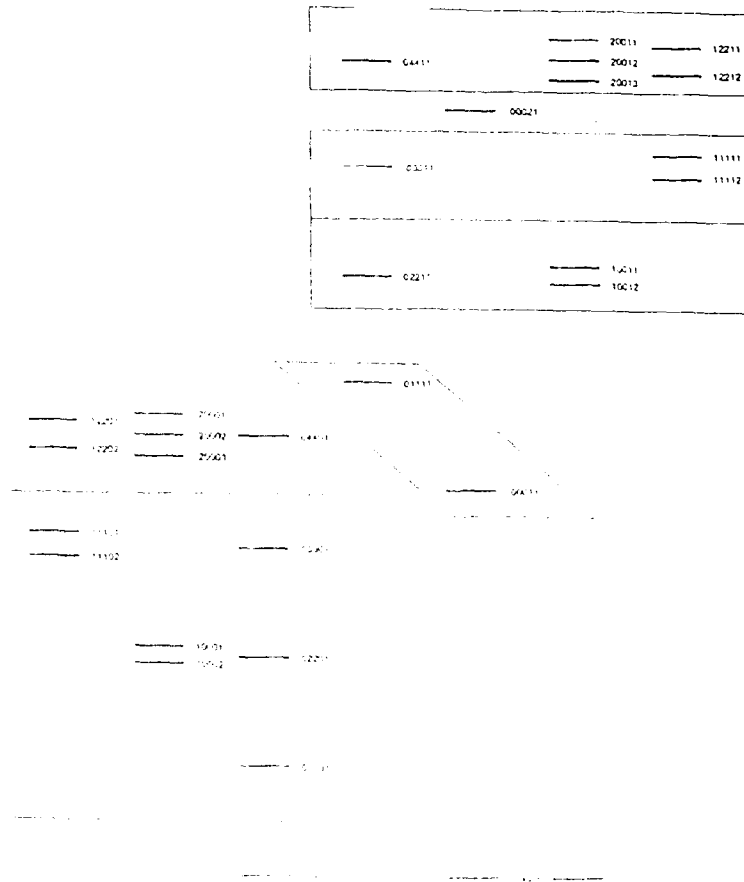


Figure 2

CO₂ VIBRATIONAL TEMPERATURES (FASCODE ATMOSPHERE 6)

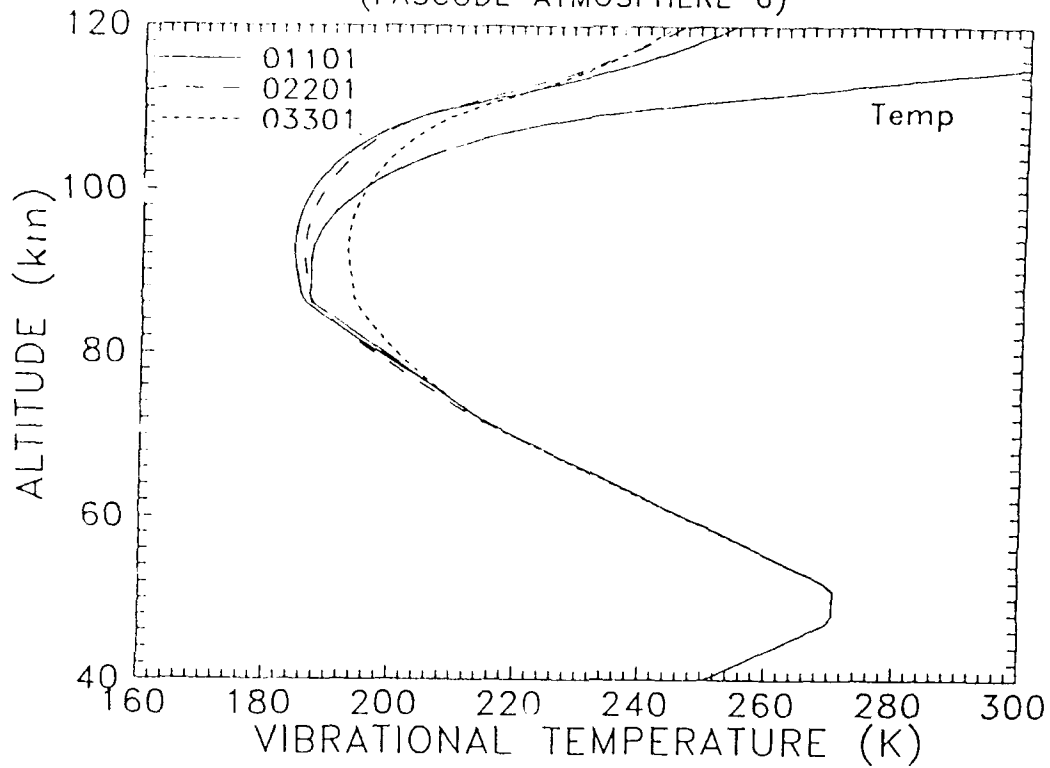
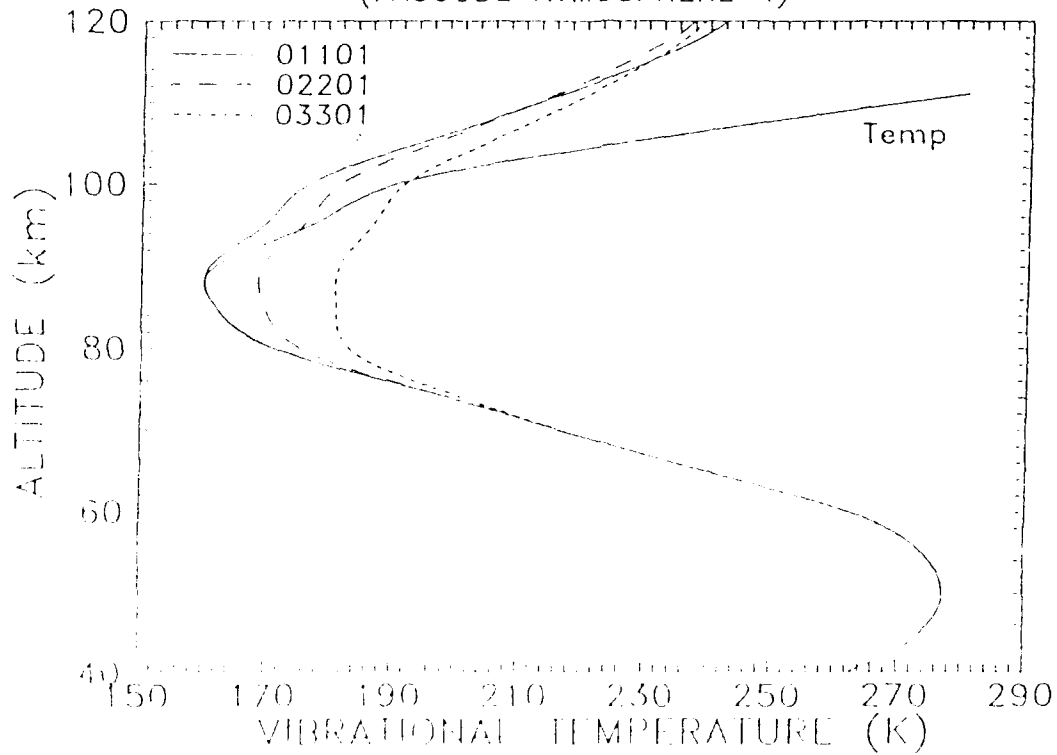


Figure 3(a)

CO₂ VIBRATIONAL TEMPERATURES (FASCODE ATMOSPHERE 4)



CO₂ VIBRATIONAL TEMPERATURES
(FASCODE ATMOSPHERE 5)

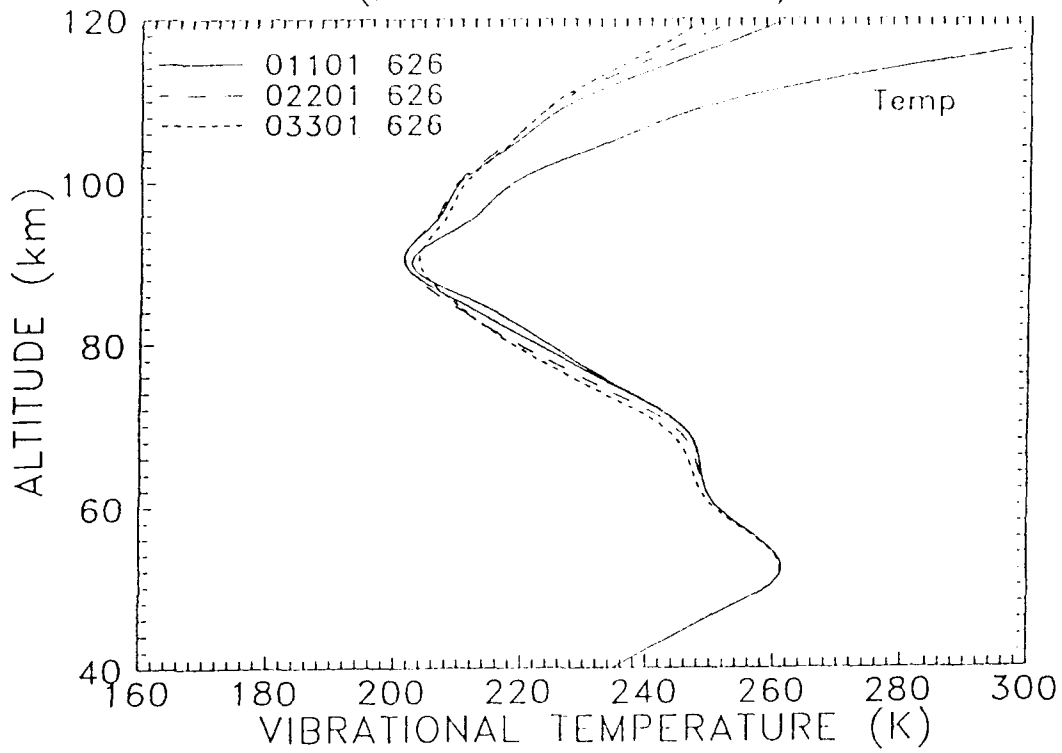
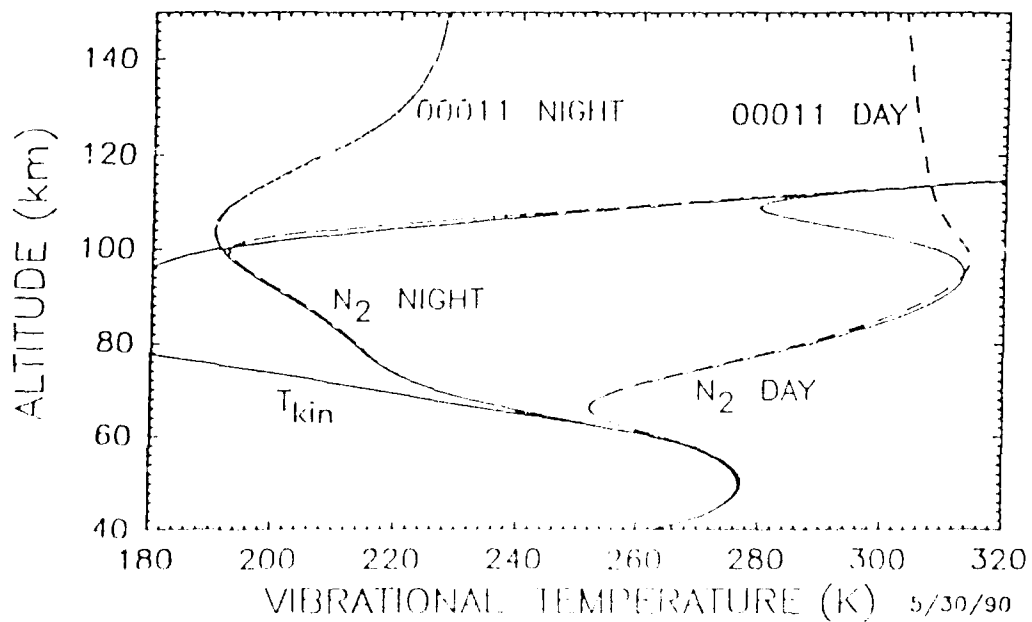


Figure 3(c)

TEMPERATURE
(FASCODE ATMOSPHERE 4)



TEMPERATURE
(FASCODE ATMOSPHERE 5)

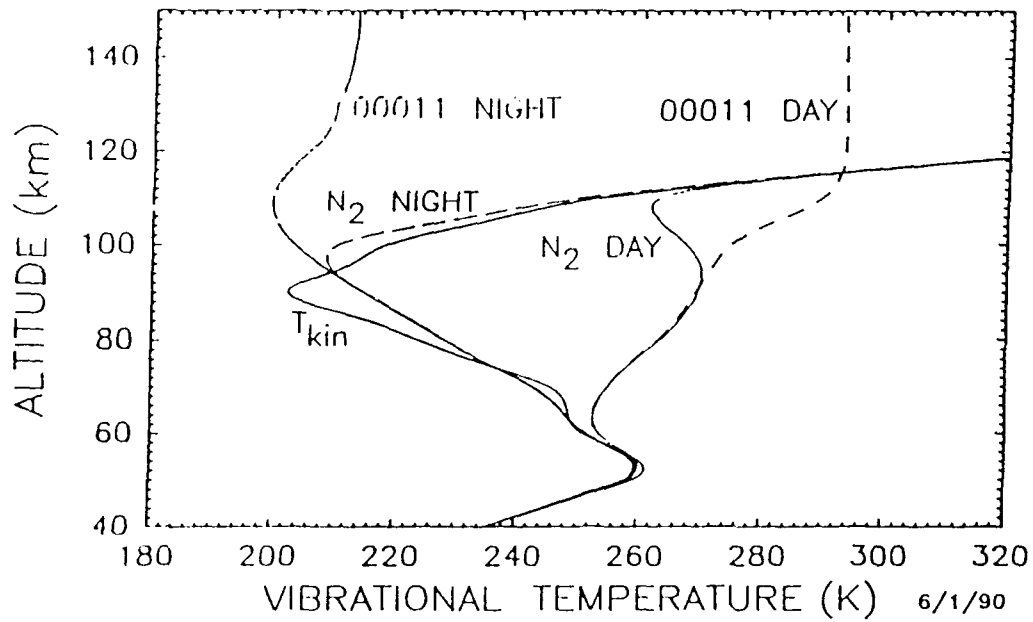
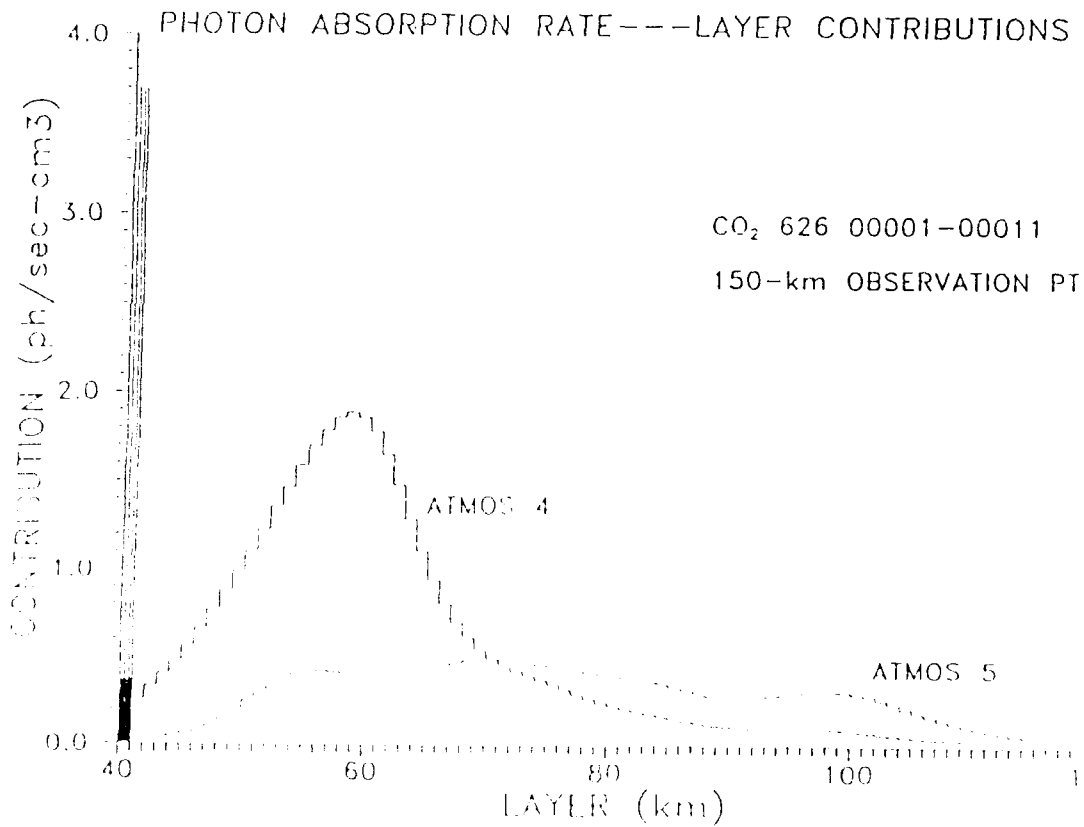


Figure 309



CO₂ 626 VIBRATIONAL TEMPERATURE
(FASCODE ATMOSPHERE 4)

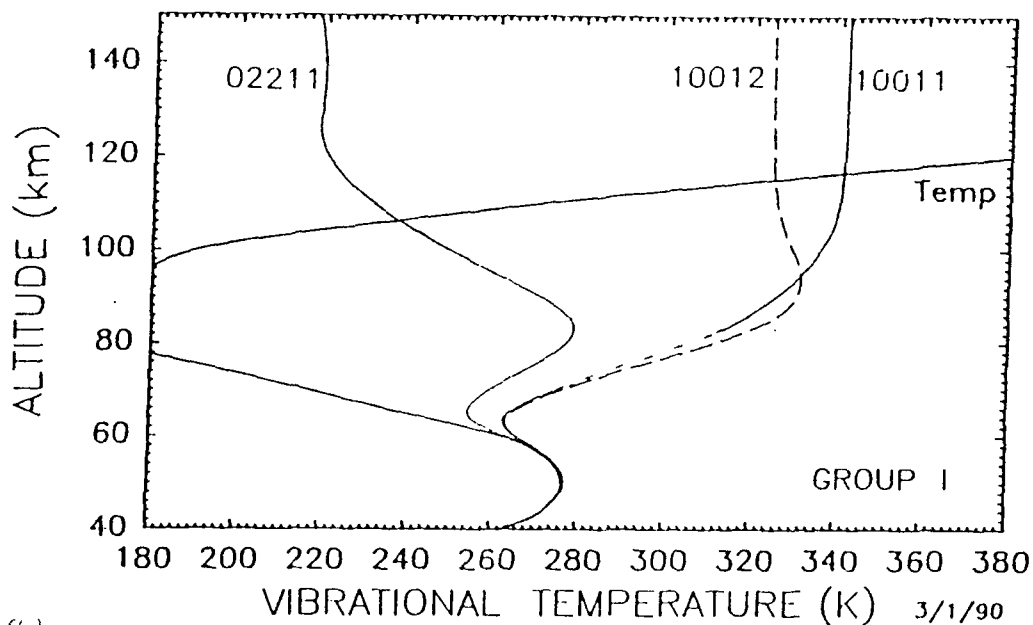
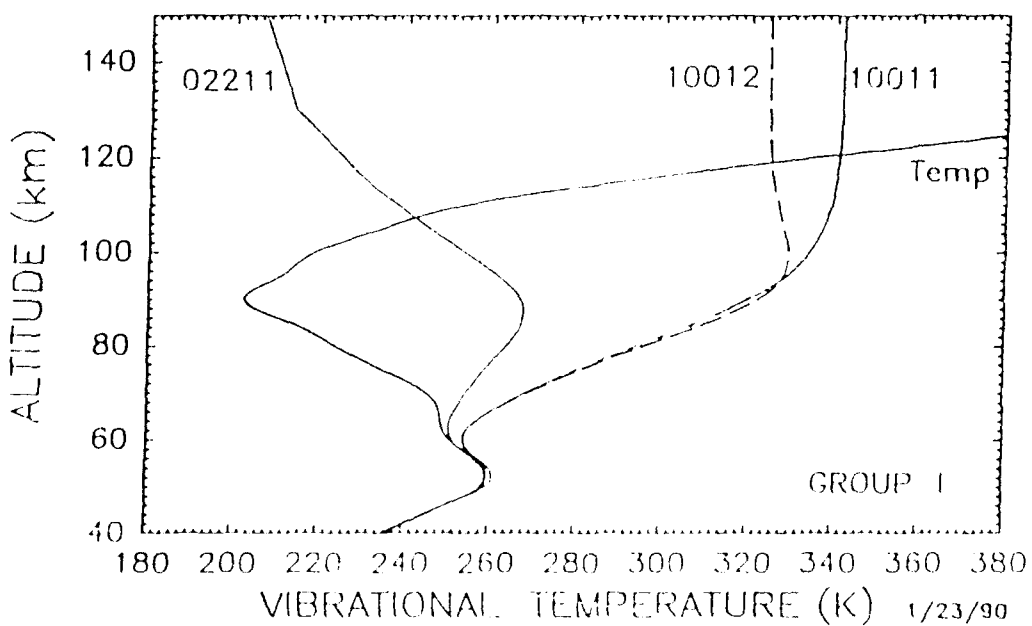


Figure 6(a)

CO₂ 626 VIBRATIONAL TEMPERATURE
(FASCODE ATMOSPHERE 5)



CO₂ 626 VIBRATIONAL TEMPERATURE
(US STANDARD ATMOSPHERE)

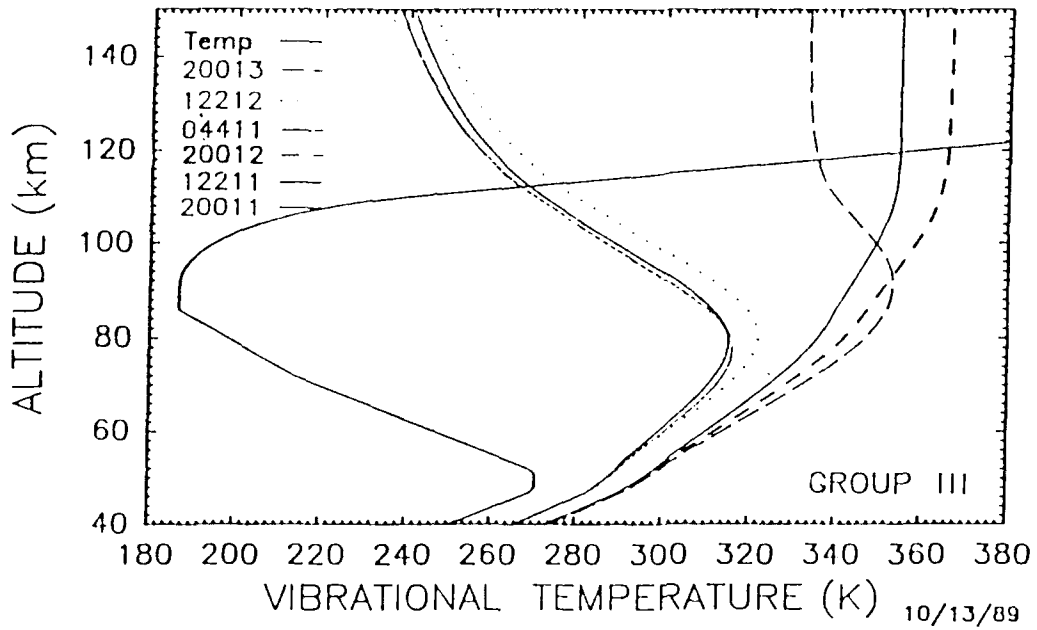
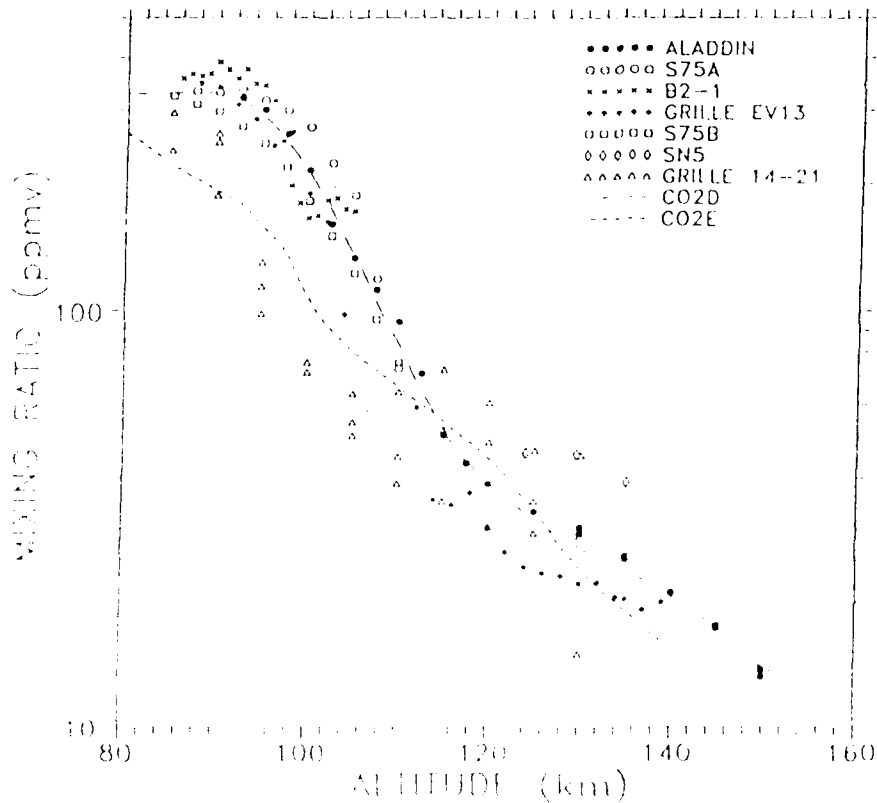


Figure 7

EXPERIMENTAL CO₂ MIXING RATIOS



CO₂ VIBRATIONAL TEMPERATURES
(FASCODE ATMOSPHERE 6)

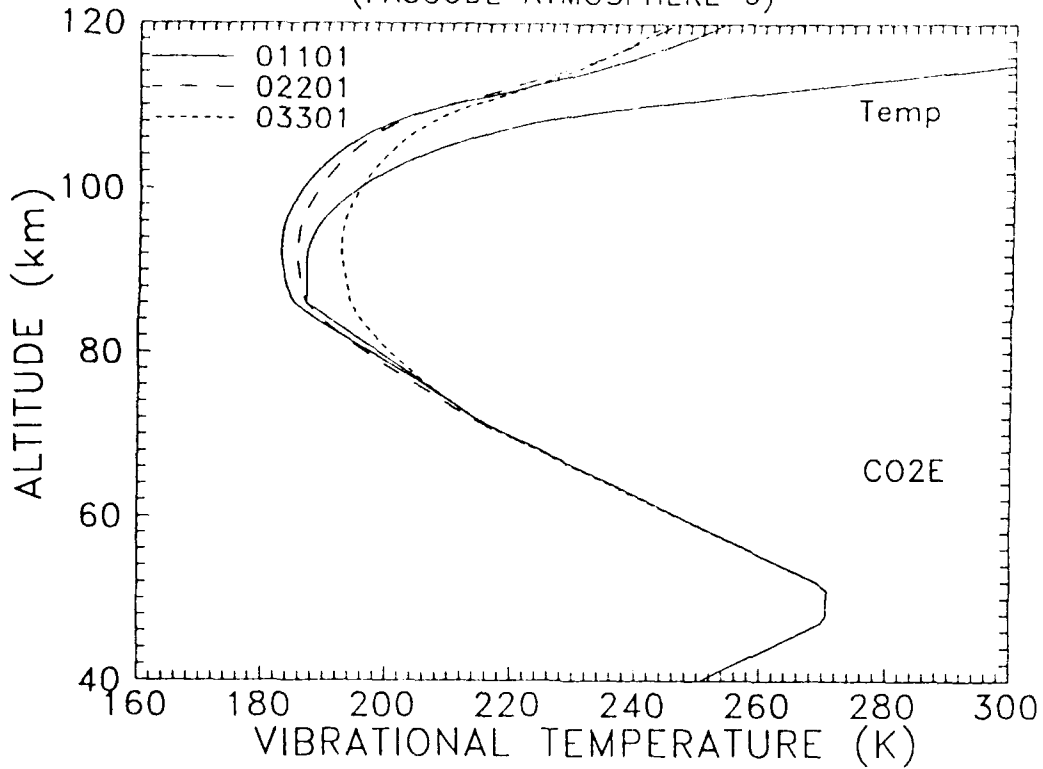
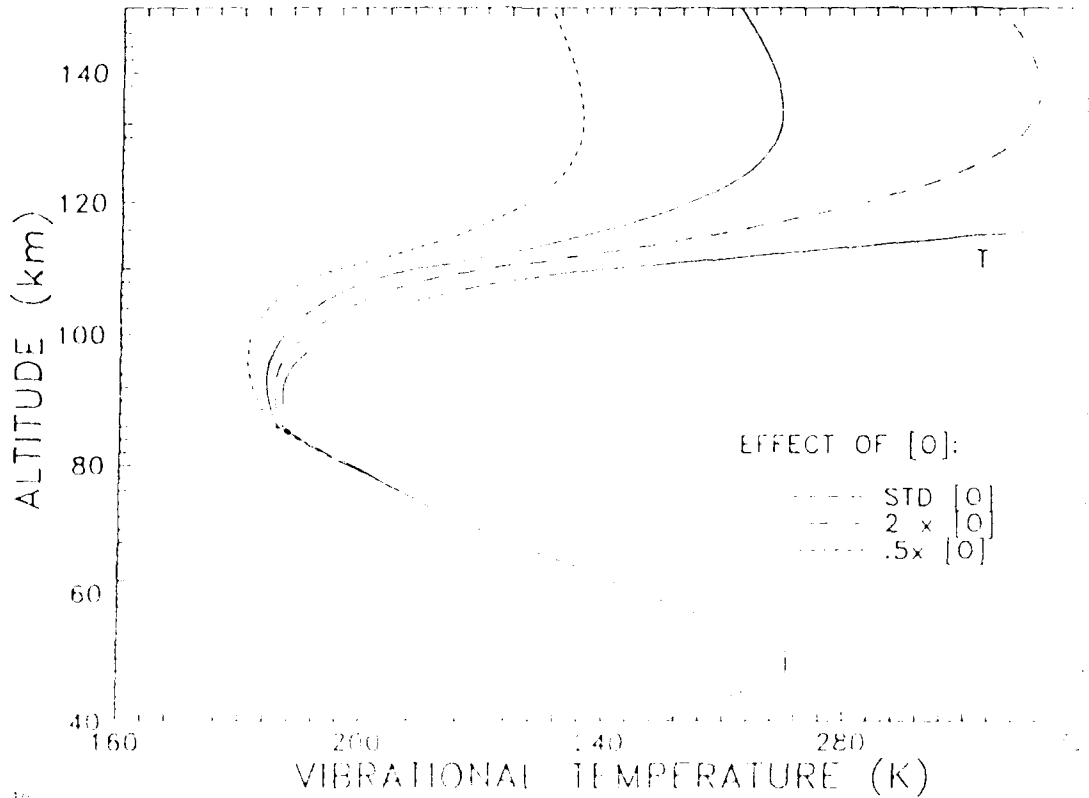


Figure 9

CO₂(01101) VIBRATIONAL TEMPERATURES
(FASCODE ATMOSPHERE 6)



CO₂ (01101) VIBRATIONAL TEMPERATURES
(FASCODE ATMOSPHERE 6)

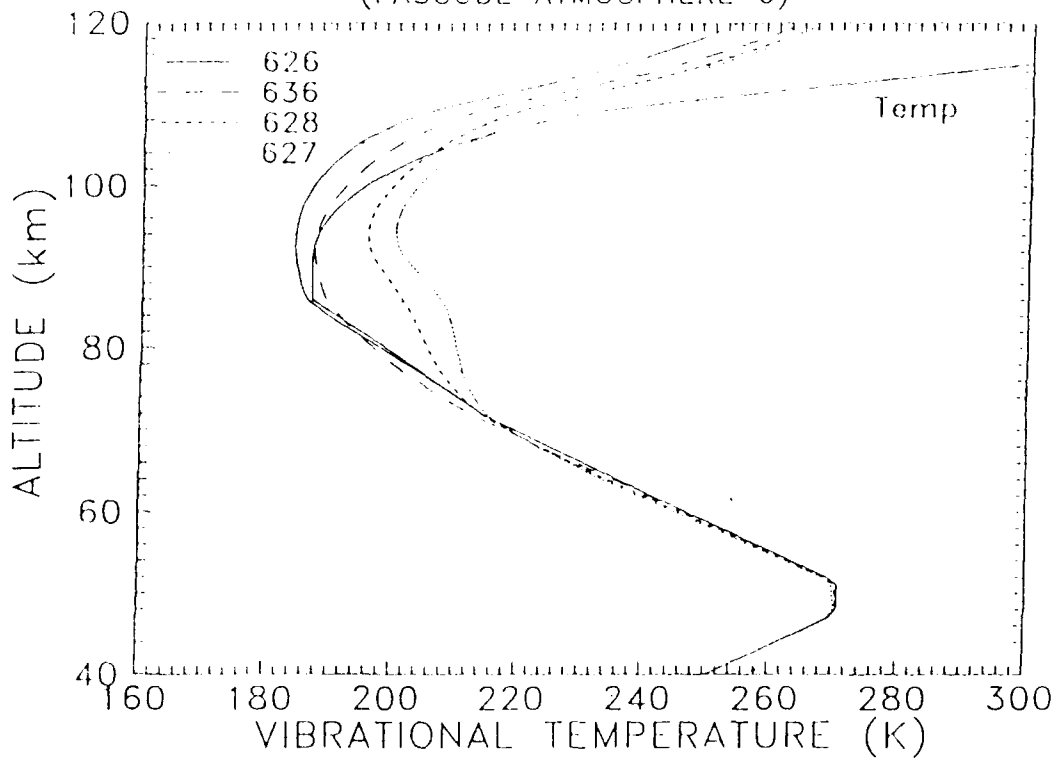
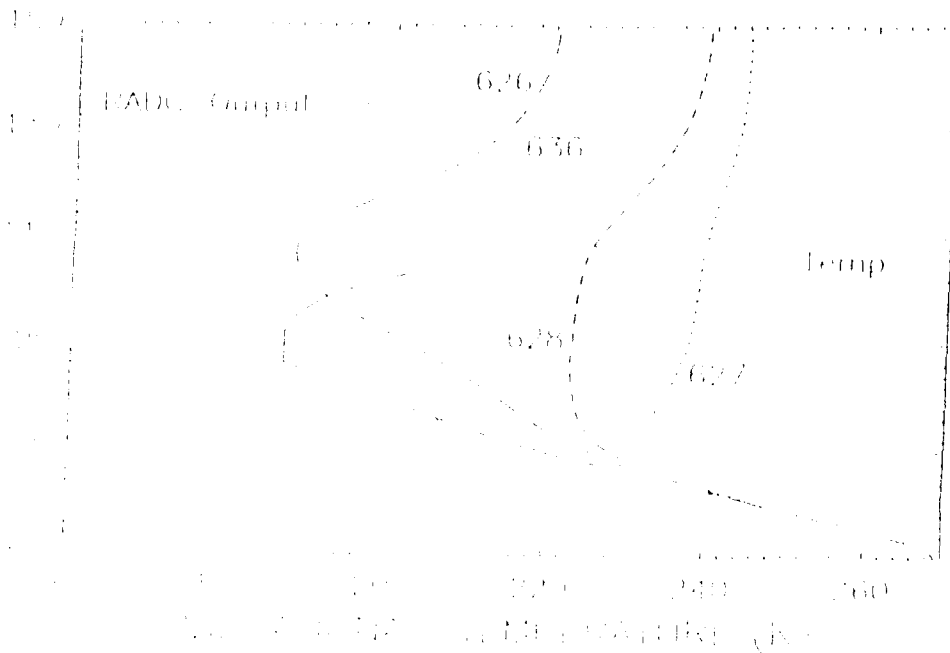


Figure 11-5

CO₂ (00011) VIBRATIONAL TEMPERATURES
(US STANDARD ATMOSPHERE)



CO₂ 4.3 MICRON LIMB RADIANCE
(FASCODE ATMOSPHERE 6, NIGHTTIME)

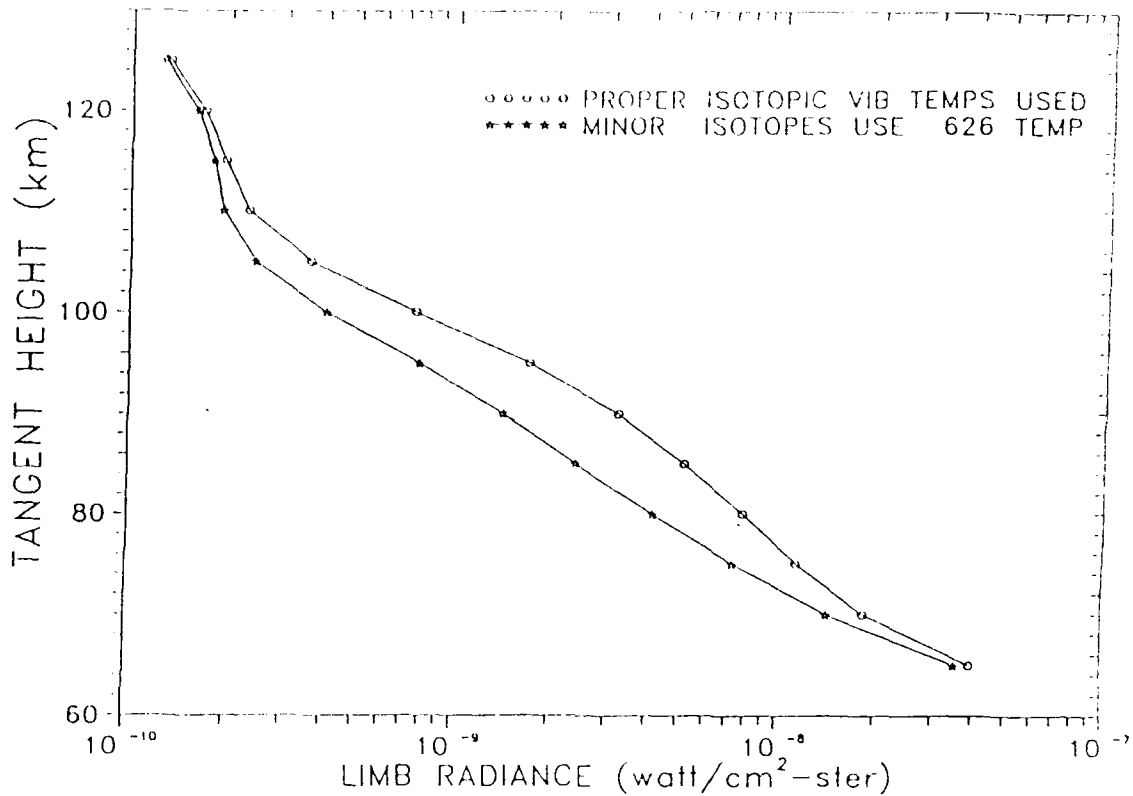


Figure 12

SUMMARY

ALL ABOUT NON-LTE CO₂ IN THE ATMOSPHERE
(or)
WHERE IS NON-LTE BEHAVIOR SIGNIFICANT ?

IMPROVED CO₂ VIBRATIONAL-TEMPERATURE LIBRARIES

- o ALL IMPORTANT EMITTING STATES
- o UP-TO-DATE MODEL
- o LINE-BY-LINE RADIATIVE TRANSPORT
- o CONSISTENT WITH FASCODE ATMOSPHERES

RESULTS

- o SUBSTANTIAL DIFFERENCES BETWEEN MODEL ATMOSPHERES
- o DIURNAL DEPENDENCE
- o DEPENDENCE ON [CO₂], [O]
- o ISOTOPIC DEPENDENCE

**NON-LTE CO INFRARED EMISSION IN THE MESOSPHERE AND
LOWER THERMOSPHERE AND ITS EFFECT ON REMOTE SENSING**

J.R. Winick, R.H. Picard
Geophysics Laboratory/OPE, Hanscom AFB, MA 01731

P.P. Wintersteiner, A.J. Paboojian
Arcon Corporation, 260 Bear Hill Road, Waltham, MA 02154

We will present a model of the non-LTE infrared emission from CO based upon the RAD computer code. This model uses a line-by-line radiative transfer algorithm to calculate the radiative contribution to the vibrational temperature. The CO emission departs from LTE at altitudes as low as 40 km at night and 30 km during daytime. The nighttime CO vibrational temperature above 60 km is most strongly dependent upon the radiative excitation emanating from the upper stratosphere and weakly dependent upon the CO density profile above 40 km. This introduces an additional seasonal and latitudinal dependence to the nighttime radiance beyond that caused by local variations in the CO density. The daytime vibrational temperature is dominated by direct absorption of solar radiation which has important structure imposed on it from solar CO absorption lines.

Non-LTE CO INFRARED EMISSION IN THE MESOSPHERE AND LOWER THERMOSPHERE AND ITS EFFECT ON REMOTE SENSING

Jeremy R. Winick and R. H. Picard
Geophysics Laboratory/OPE
Optical and Infrared Technology Division
Hanscom AFB, MA 01731

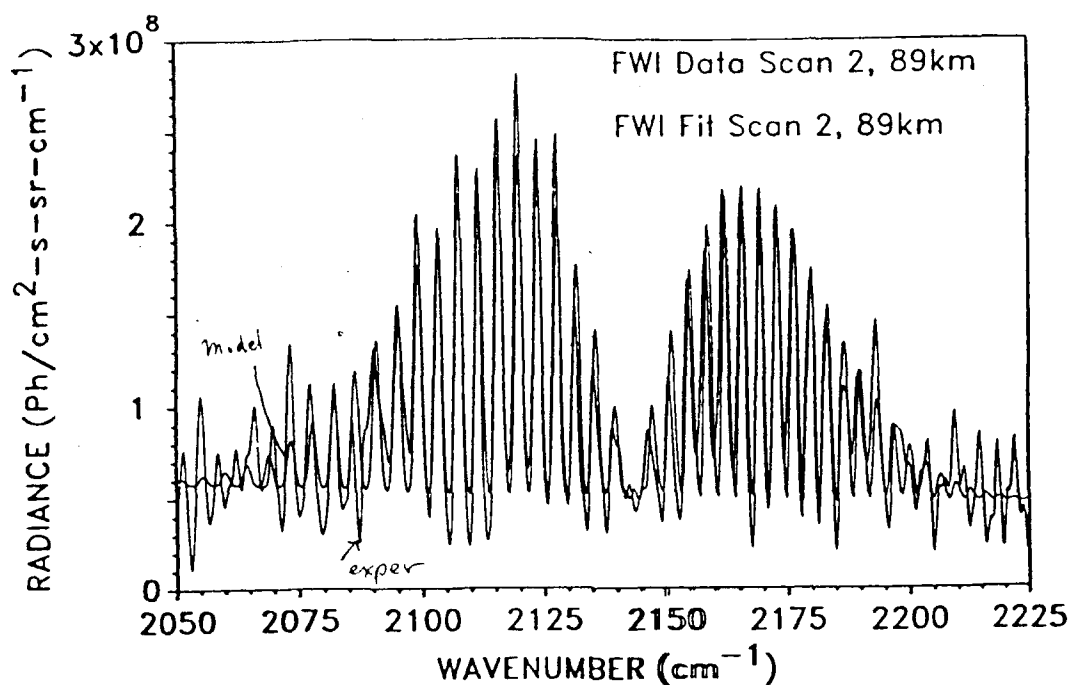
P. P. Wintersteiner and A. J. Paboojian
Arcon Corporation
260 Bear Hill Road
Waltham, MA 02154

*Annual Review Conference on Atmospheric Transmission Models
Geophysics Laboratory (AFSC)
5 June 1990*

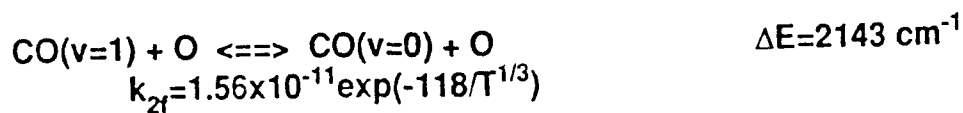
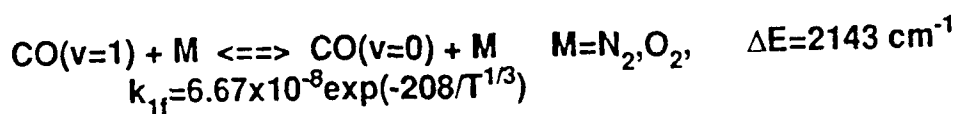
CO Non-LTE Emission

OUTLINE

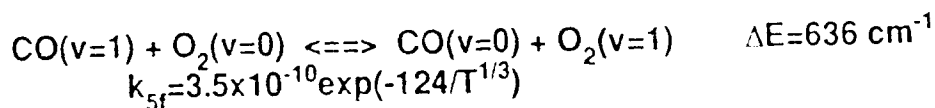
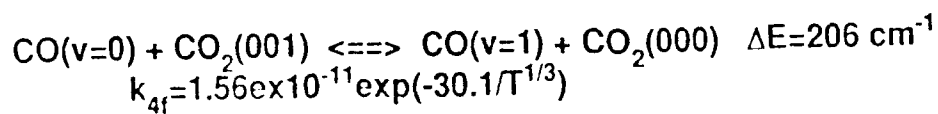
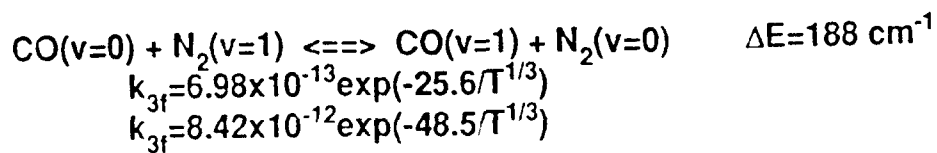
- Review of GL CO Infrared Observations (FWI)
- Use of line-by-line *non-LTE* model (RAD) for determination of CO vibrational temperature
- Important Processes Determining Nighttime *non-LTE* CO($v=1$)
 - Sensitivity Study of vibrational temperature
 - Comparison of CO Vibrational Temperature to Kinetic Temperature
- Important Processes Determining Daytime *non-LTE* CO($v=1$)
 - Solar Excitation
 - Solar CO absorption line structure in solar flux
- Can one develop retrieval algorithms?
 - Complex forward problem
- Conclusions



KINETIC MECHANISM FOR CO(V) NLTE EMISSIONS

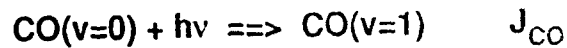
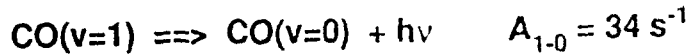


V-V processes:



KINETIC MECHANISM FOR CO(V) NLTE EMISSION(Continued)

Radiative Processes:



Calculation of Excitation coefficient in NLTE atmosphere done
by line-by-line Code RAD

In the mesosphere:

V-T is negligible $k_{1f}[\text{M}] < 10^{-3} \text{ s}^{-1}$, $k_{1r}[\text{M}] \ll 10^{-6} \text{ s}^{-1}$

V-V with O_2 (Reaction 5) is unimportant

k_3 is dominant collisional term and depends upon N_2
vibrational temperature

Reactions 4 is unimportant since CO_2 is a minor species

Reactions with atomic oxygen only important at high
temperatures, but above 150 km density is too low

RADIATIVE TRANSPORT - KINETICS CALCULATION

Line-by-Line Plane-Parallel Atmosphere Code

Lineshape changes with altitude: Voigt lineshape

Doppler broadening (temperature)

Lorentz broadening (pressure)

AFGL HITRAN Database using 79 $^{12}\text{C}^{16}\text{O}$ (1-0) lines

Vibrational temperature calculated by iterative method

Steady-state calculation of radiating state

Uses previous iteration radiation field

Combines collisional excitation and quenching

CO profile is unusual in that:

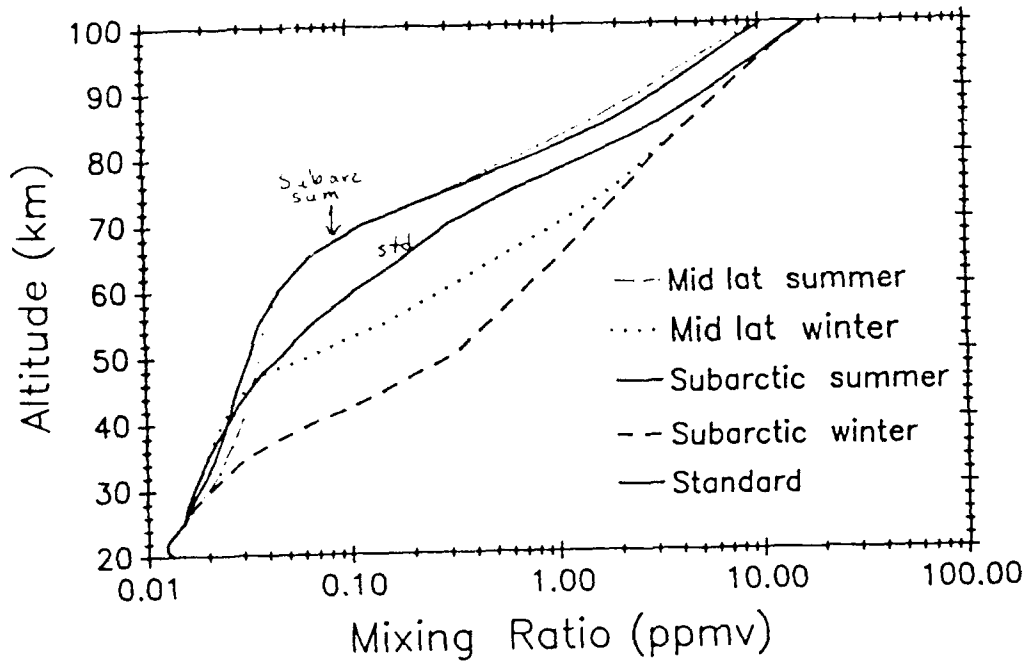
Mixing ratio increases above Tropopause

Latitudinal variation

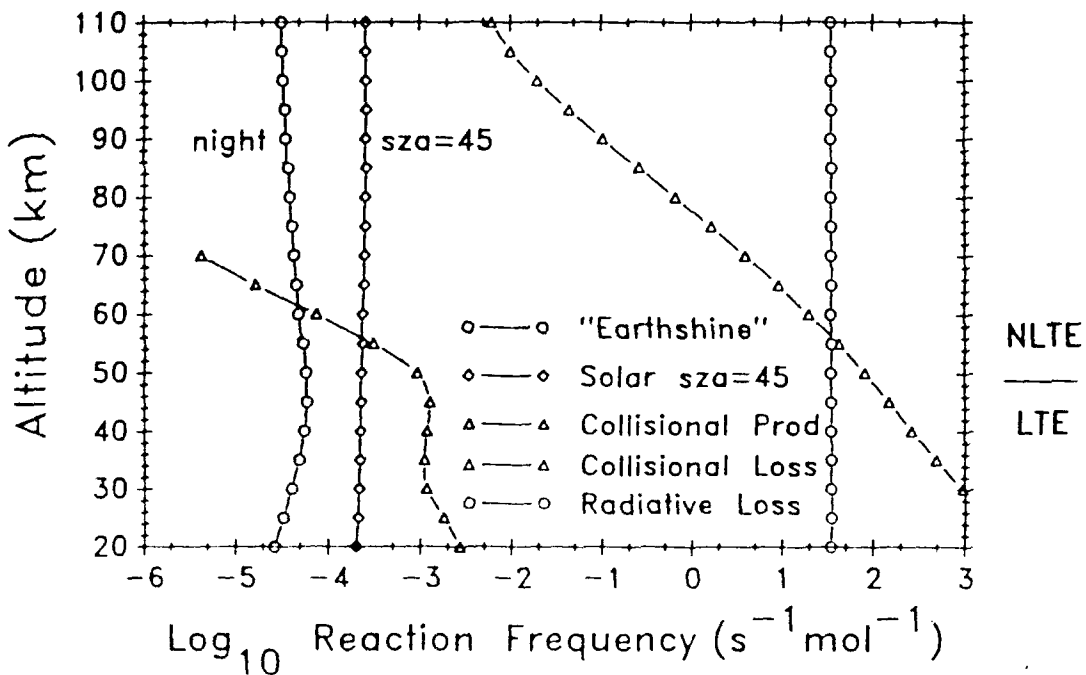
Seasonal variation

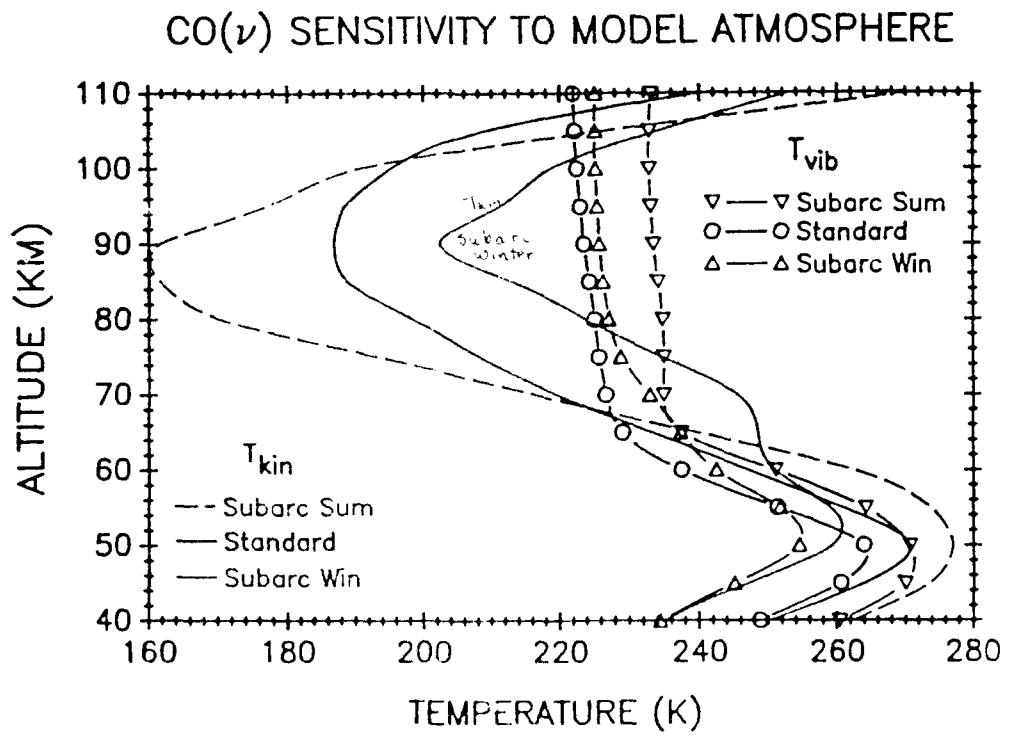
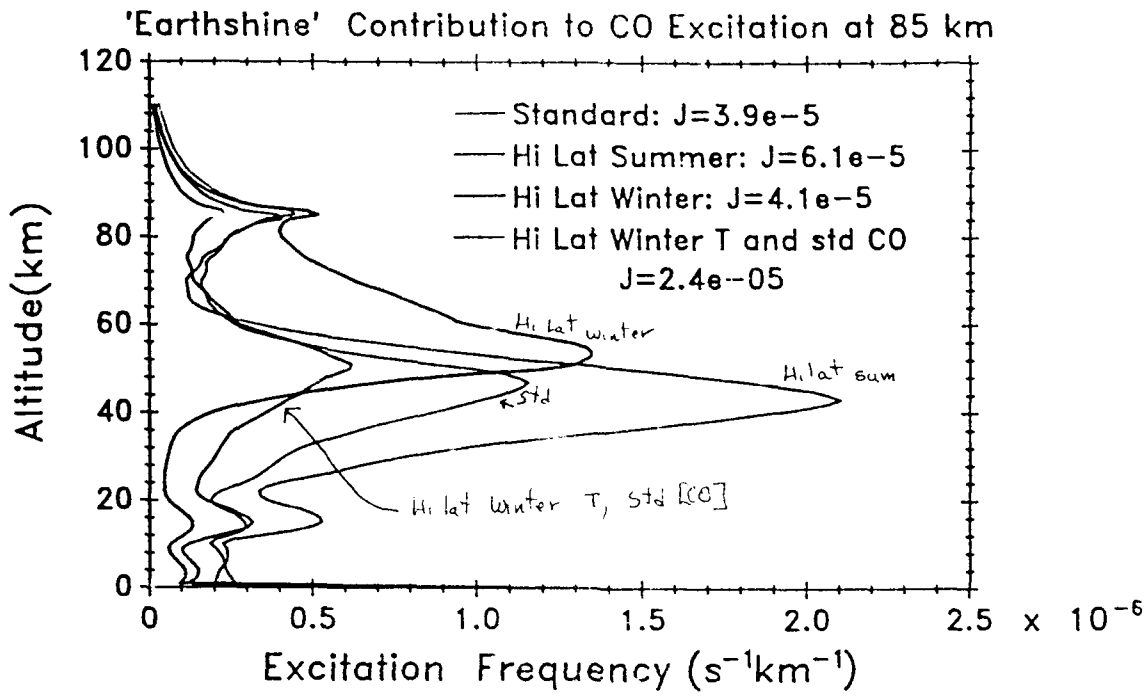
Collisional processes are inefficient

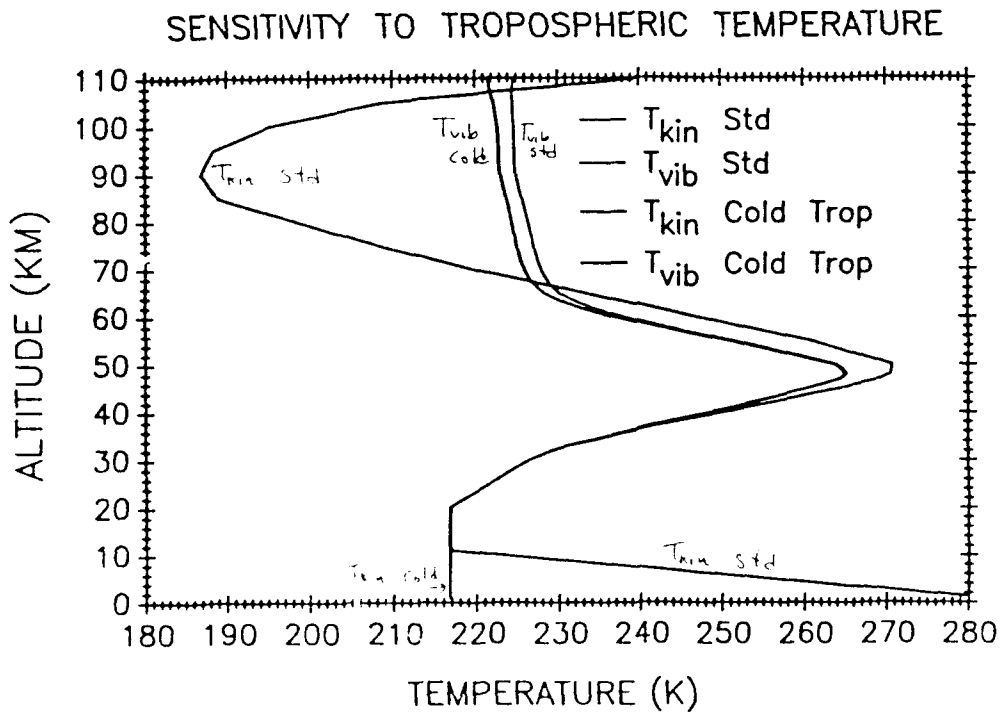
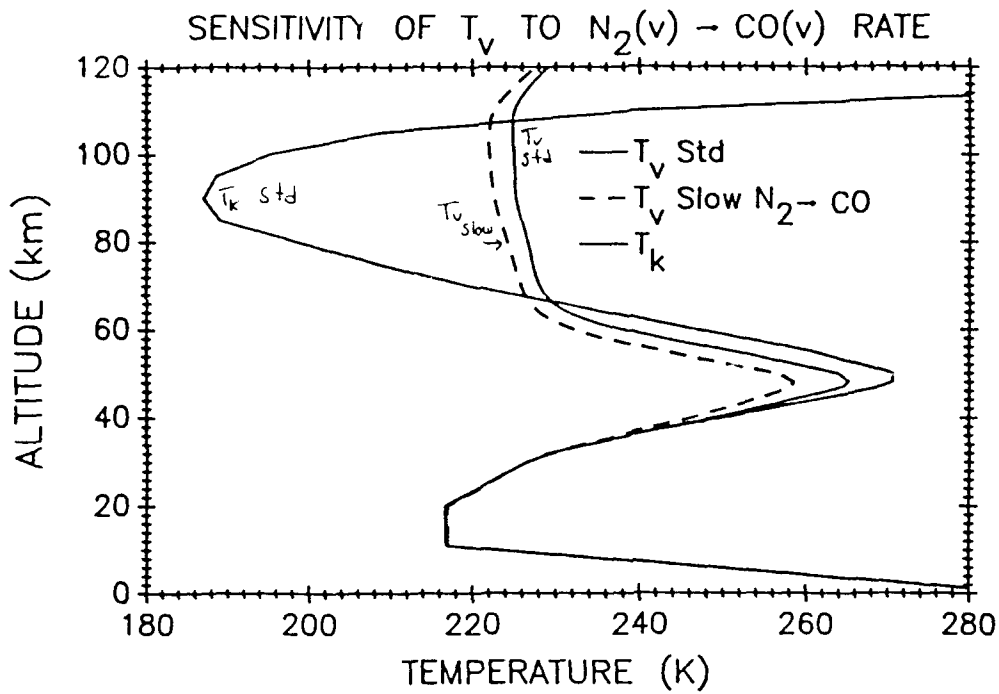
CO PROFILES

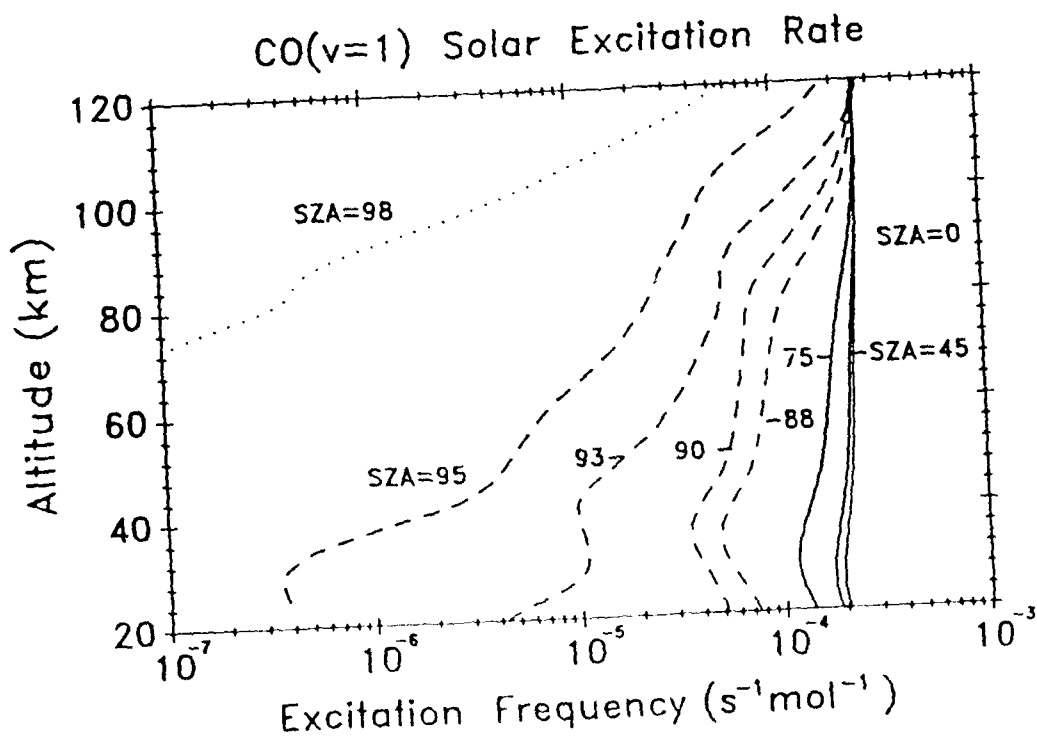
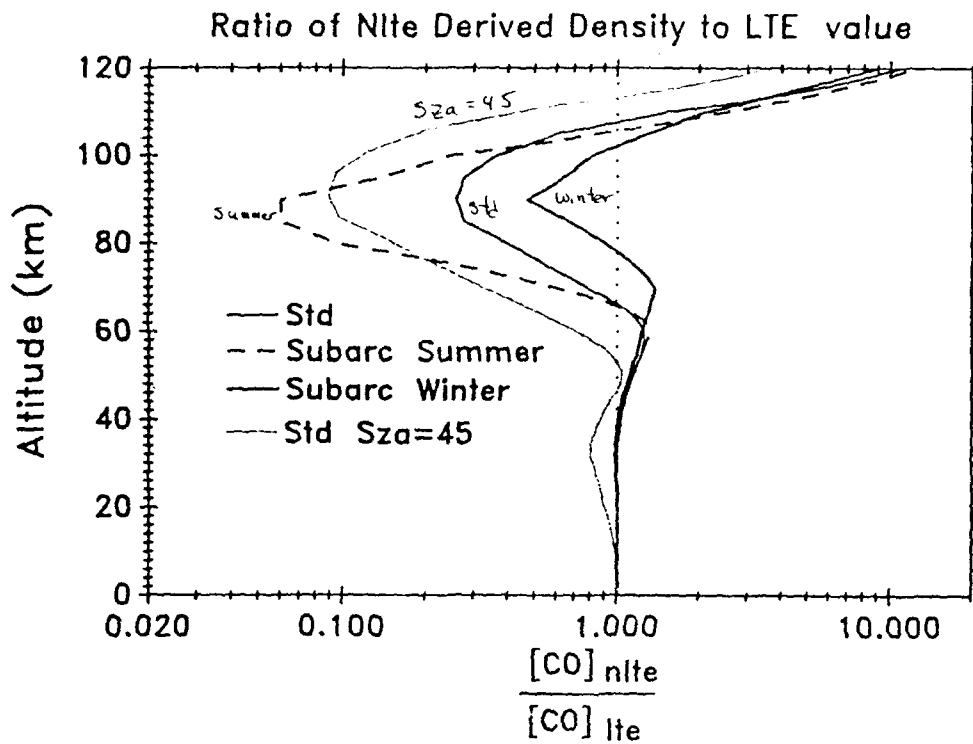


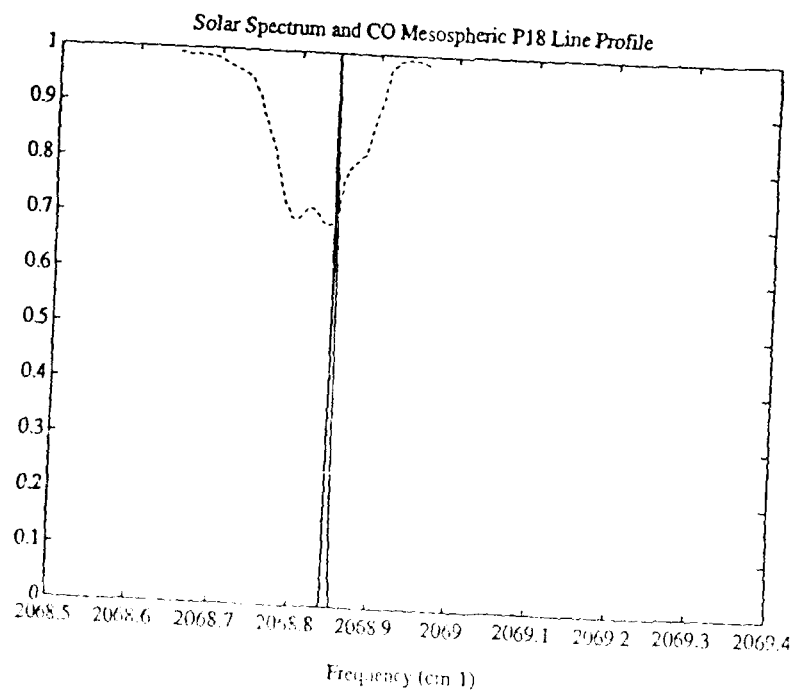
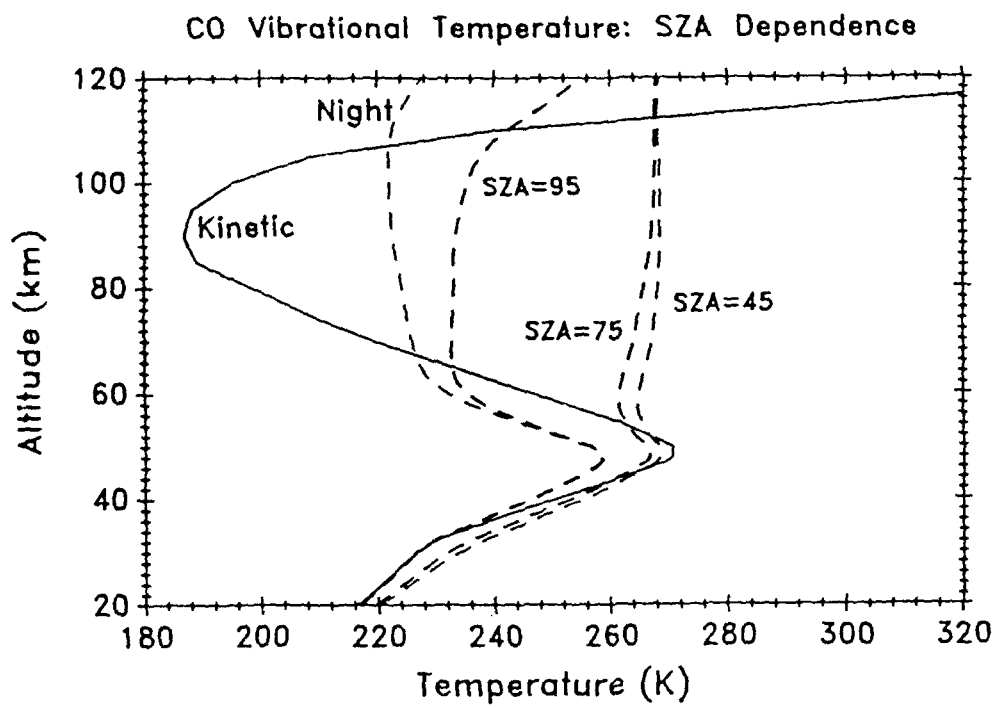
CO(v) Production and Loss

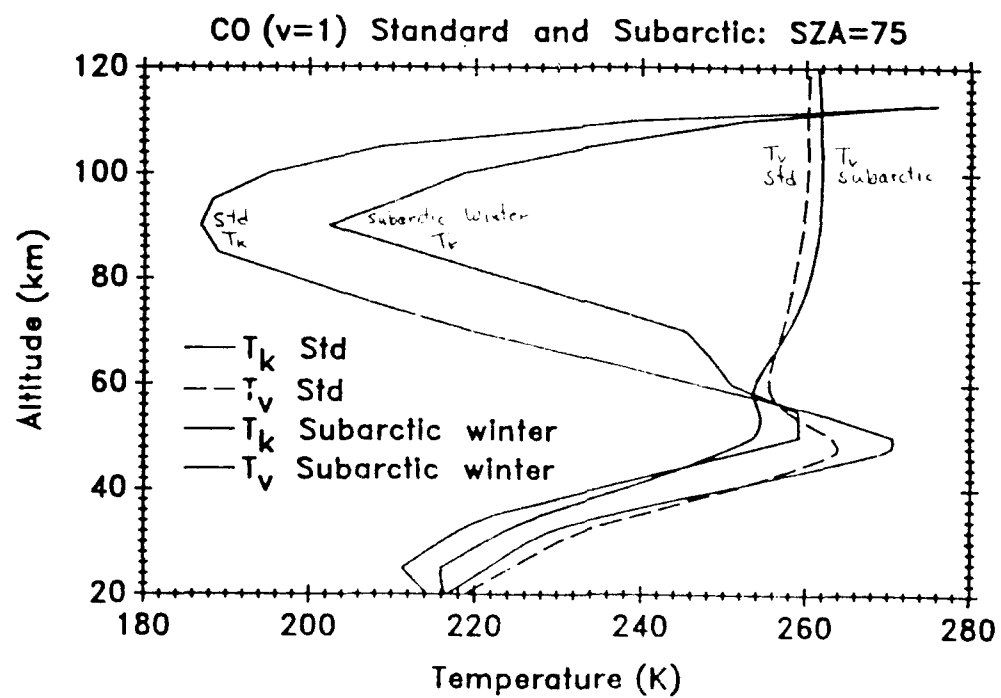
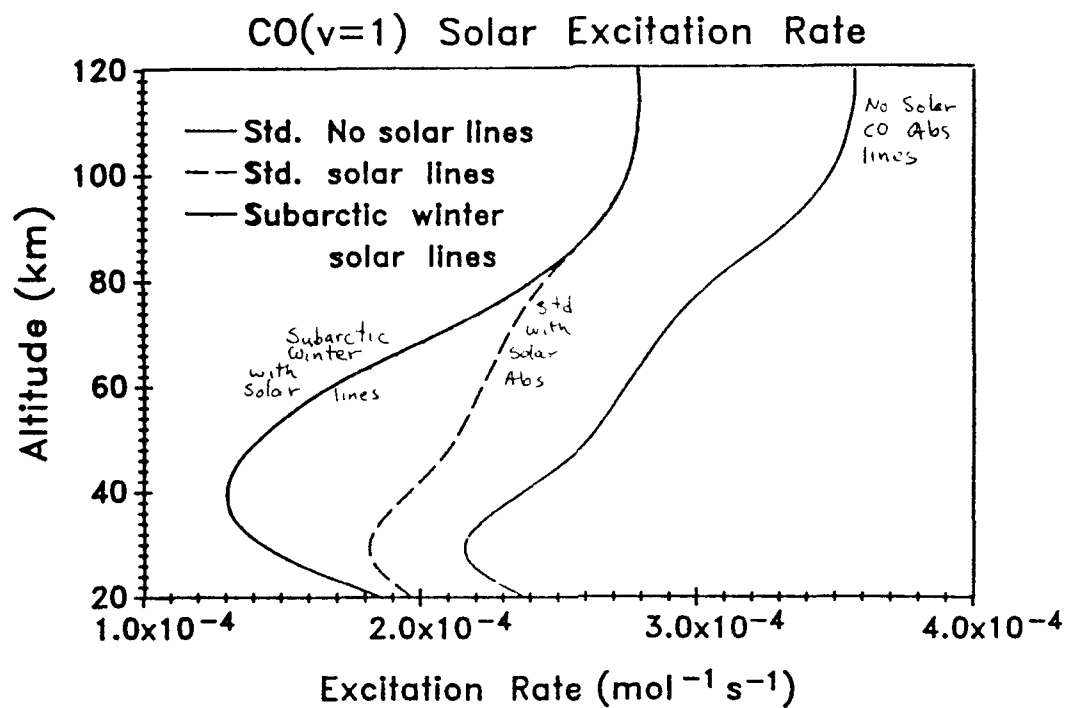












Conclusions

Nighttime:

CO 4.8 μm nighttime Emission is *non-LTE* above 45 km

Collisions are inefficient populating CO(v) which leads to the dominance of radiative processes above 50 km

CO has unusual profiles that make it a good test for radiative transfer codes

Latitudinal and seasonal variation in CO and T effect $T_{\text{vib}}(z)$

Large departures from LTE can lead to large errors in retrieved density if non-LTE model is not used

Limb radiance retrieval is especially difficult since the dependence upon the lower state density is partially non-local

This non-local problem may not be too important except for mid and high latitude winter situations where there is increased CO in the lower mesosphere

Conclusions (continued)

Daytime:

CO 4.8 μm daytime Emission is *non-LTE* above 30 km

Production of CO(v=1) is dominated by direct solar excitation

CO solar absorption lines must be included in excitation calculation

Daytime enhanced $\text{N}_2(v=1)$ and $\text{CO}_2(001)$ populations effect excitation (only weakly, rate constant and SZA dependent) in 60-80 km region

Vibrational Temperature profile depends upon SZA especially for SZA > 75

Mesospheric Emission is less sensitive to latitude and season (except for SZA dependence) than nighttime case.

Subarctic winter CO profile has less solar excitation due to slightly increased opacity at high SZA.



ACKNOWLEDGEMENTS

This work was supported by the Air Force Office of Scientific Research under task 2310G5.

PATH CHARACTERIZATION ALGORITHMS FOR FASCODE

R.G. Isaacs, S.A. Clough, R.D. Worsham, J.-L. Moncet, B.L. Lindner, and L.D. Kaplan
Atmospheric and Environmental Research, Inc., 840 Memorial Drive, Cambridge, MA 02139

We describe the results of a study undertaken at AER to identify and implement a state-of-the-art nonlinear retrieval approach to characterize line of sight variability of atmospheric thermal and constituent environments. This path characterization capability was designed to interface with the existing Geophysics Laboratory (GL) line-by-line radiance/transmittance code, FASCODE.



Path Characterization Algorithms for FASCODE

**R. G. Isaacs, S. A. Clough, R. D. Worsham, J.-L.
Moncet, B. L. Lindner, L. D. Kaplan**

**Atmospheric and Environmental Research Inc.
Cambridge, MA 02139**



Path Characterization

**Quantitative assessment of the relationship between path optical
properties and path thermodynamic properties:**

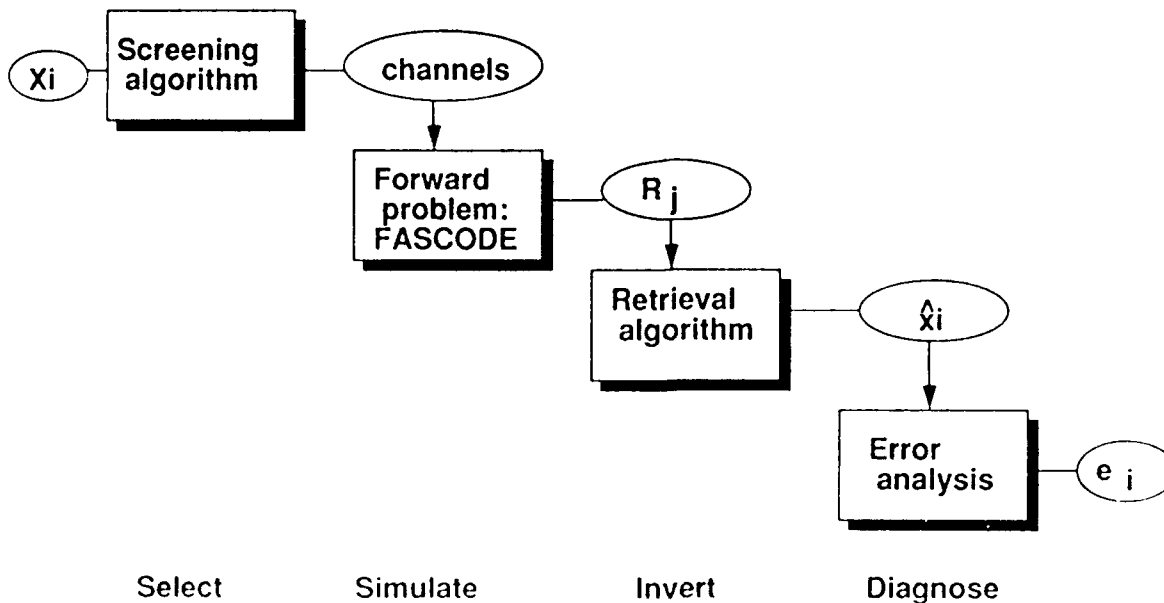
- **Path optical properties (data):**
 - optical depth
 - transmittance
 - emission (radiance, brightness temperature)

- **Path thermodynamic properties (desired parameters):**
 - temperature
 - concentrations of absorbers and scatterers
 - path boundary temperature and emissivity/reflectivity
 - pressure (surface, limb layer)

Objectives

- Identify and implement a state-of-the-art nonlinear retrieval approach to characterize line-of-sight variability of atmospheric path thermal and constituent environments;
- Interface with the existing Geophysics Laboratory (GL) line-by-line radiance/transmittance code, FASCODE
- Provide code and comprehensive documentation

Path Characterization Concept





Screening Algorithm

- Suggest fruitful spectral regions for the retrieval of desired atmospheric parameters;
- User selects temperature parameter or molecule of interest;
- Algorithm computes optical depth vs total optical depth for selected wavenumber region;
- HITRAN data base, FSCATN atmospheres (T, p, u), 1 cm^{-1} band model;
- Histogram capability to select wavenumber regions for best discrimination from background atmosphere.



Forward Problem (FASCODE)

- Provides simulated data set (radiance spectrum, channelized brightness temperature data, etc.) from initial guess;
- Provides required Jacobian of data sensitivity to variations in desired parameters: $\frac{d R_i}{d x_j}$
- Covers microwave to UV spectral domain;
- Interfaces provide all required FASCODE data files in standard format;
- Capability to control data spectral resolution;
- Computational liability potentially addressed via "rapid" algorithms for selected channel sets .



Retrieval Algorithm Selection

- Literature review (Isaacs, 1988, *SPIE*, 928, 136) prompted choice of Physical Least Squares (PLS) approach;
- Extensive heritage (Rodgers, 1976, 1987; Eyre, 1989);
- Incorporates the physics of the radiative transfer process through the FASCODE forward problem;
- Climatology not required (helpful in practice, null space, 1st guess)
- Applied iteratively;



Retrieval Algorithm Capabilities

- Choice of penalty function:
 - maximum likelihood (using error covariances of parameter and data)
 - ridge regression (minimum information);
- Choice of representation: radiance, brightness temperature;
- Option for eigenanalysis including retrieval via eigenvalues;
- Capability to include physical constraints e.g. superadiabaticity/supersaturation, etc. (not implemented);
- Capability to add realistic measurement noise to simulations.



Error Analysis

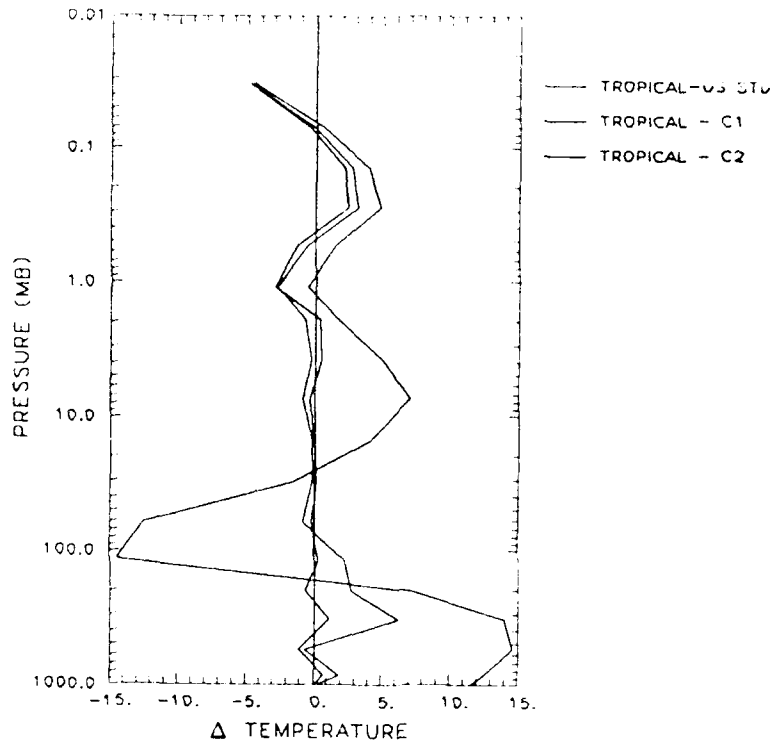
- **Provides comprehensive error analysis based on Rodgers (1987);**
- **Estimate of the covariance of the retrieval errors including the effects of:**
 - **measurement noise**
 - **uncertainties in the a priori information;**
- **Errors in forward problem not yet treated;**
- **Retrieval performance evaluated by comparing covariances of the state parameters before and after the measurement process:**
 - **information content**
 - **FUV**



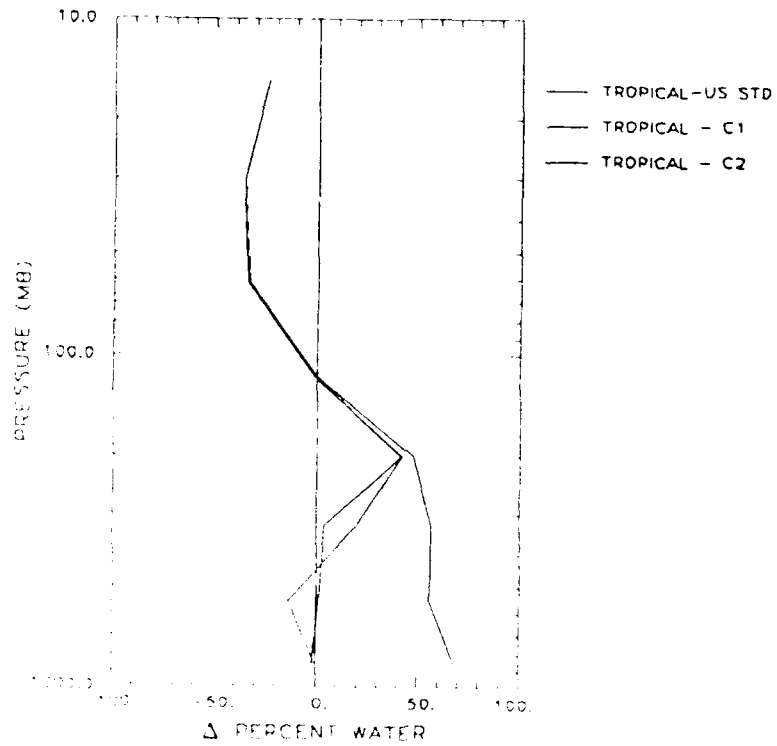
Test Cases

- **Microwave temperature and moisture sounding:**
Advanced Microwave Sounding Unit (AMSU);
- **Infrared temperature and constituent (ozone) sounding:**
SCRIBE and HIS;
- **Spectroscopic applications.**

SIMULTANEOUS RETRIEVALS



SIMULTANEOUS RETRIEVALS





Path Characterization Summary

- **implementation of a state-of-the-art nonlinear retrieval approach to characterize line-of-sight variability of atmospheric path thermal and constituent environments consistent with the FASCODE formalism;**
- **technical issues related to non-linearities, incorporation of physical constraints, forward problem;**
- **applications to other path parameters such as aerosol, cloud, and non-LTE.**
- **Final Report: Isaacs et al, 1990 (GL-TR-90-0080)**

TEMPERATURE RETRIEVALS WITH SIMULATED SCRIBE RADIANCES

J.-L. Moncet, S.A. Clough, R.D. Worsham, R.G. Isaacs and L.D. Kaplan
Atmospheric and Environmental Research, Inc., 840 Memorial Drive, Cambridge, MA 02139

The FASCODE path characterization algorithm has been applied to the retrieval of atmospheric temperature using simulated radiances for a nadir view from 31.3 km corresponding to a typical SCRIBE float altitude. The spectral region studied was 720 to 775 cm^{-1} with a resolution consistent with SCRIBE. The sensitivity of the retrievals to measurement noise, first guess error, and to systematic error including photometric calibration and line parameter error will be discussed.

Temperature Retrievals with Simulated SCRIBE Radiances

J.-L. Moncet, S.A. Clough, R.D. Worsham, R.G. Isaacs and L.D. Kaplan

Introduction

Goal of the study:

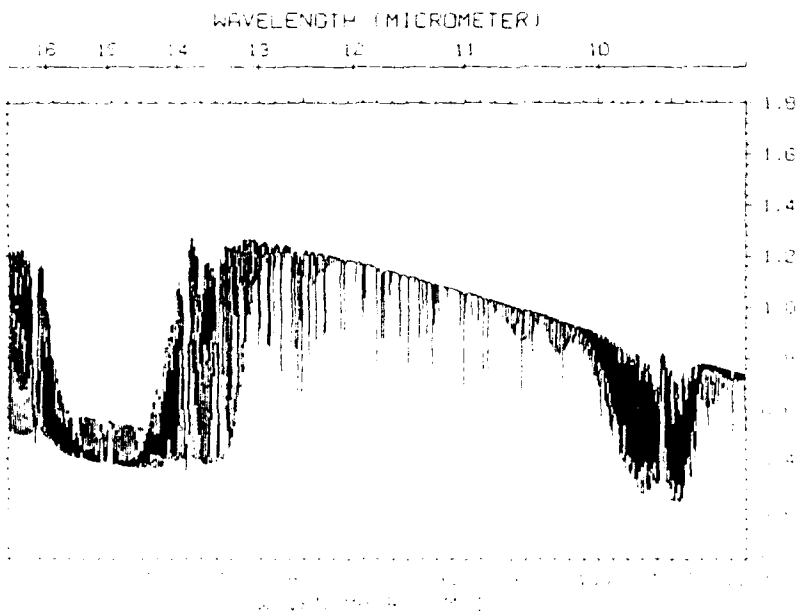
Assess the performance of path characterization algorithm for temperature retrievals based on SCRIBE data.

Study effects of:

- instrumental noise
- calibration errors
- uncertainties on line parameters

SCRIBE Instrument

- Cryogenic Michelson interferometer spectrometer
- Platform: Balloon
- Altitude: 32km
- Spectral range 600–1400 cm^{-1}
- Resolution: 0.06cm^{-1}



Non-Linear Retrieval Algorithm

Obtain best estimate \hat{x} of unknown state vector x^m from set of measured radiances y^m ,

$$y^m = F(x^m) + \varepsilon, \quad (1)$$

where ε (covariance S_ε) is the measurement error.

Newtonian Iteration:

- Expand forward model about guessed vector x_{n-1} :

$$y - y_{n-1} = K(x - x_{n-1}) + \mathcal{O}(x - x_{n-1})^2. \quad (2)$$

- Ignoring higher order terms in eq.(2), find x_n such that

$$E(x_n) = (y^m - y_n)^T W (y^m - y_n) + (x_n - x_0)^T \Gamma (x_n - x_0) \quad (3)$$

is minimized (here, $W = S_\varepsilon^{-1}$).

- Solution*:

$$x_n = x_{n-1} + H^{-1} [K^T W (y^m - y_{n-1}) + \Gamma (x_0 - x_{n-1})] \quad (4)$$

with

$$H^{-1} = (K^T W K + \Gamma)^{-1}. \quad (5)$$

* In Maximum Likelihood approach, $\Gamma = S_x^{-1}$, where S_x is the covariance of the first guess.

Error Analysis (Rodgers, 1990)

- Once convergence is reached, and provided that K does not change too rapidly within the error bounds of the solution,

$$y^m - y_{n-1} \simeq K(x^m - x_{n-1}) + \varepsilon. \quad (6)$$

- Combining equations (6) and (4), the retrieval error is expressed as the sum of a "null-space" error and the error due to instrumental noise:

$$x_n - x^m = H^{-1} \Gamma (x_0 - x^m) + H^{-1} K^T W \varepsilon. \quad (7)$$

- The total error covariance is,

$$S = S_N + S_I \quad (8)$$

with

$$S_N = H^{-1} \Gamma S_x \Gamma H^{-1} \quad (9)$$

and

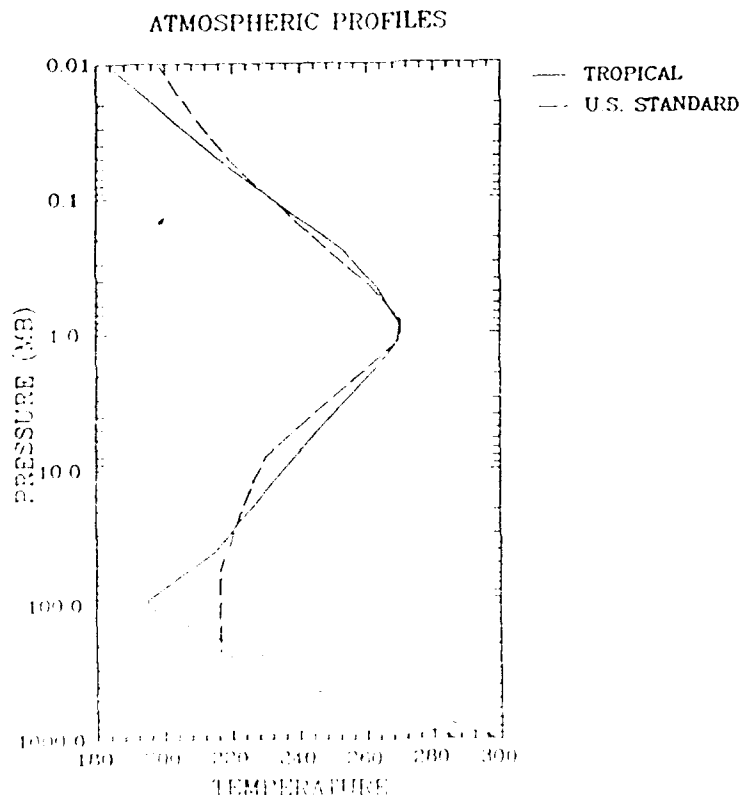
$$S_I = H^{-1} K^T W S_\varepsilon W K H^{-1}. \quad (10)$$

Conditions of the Experiment

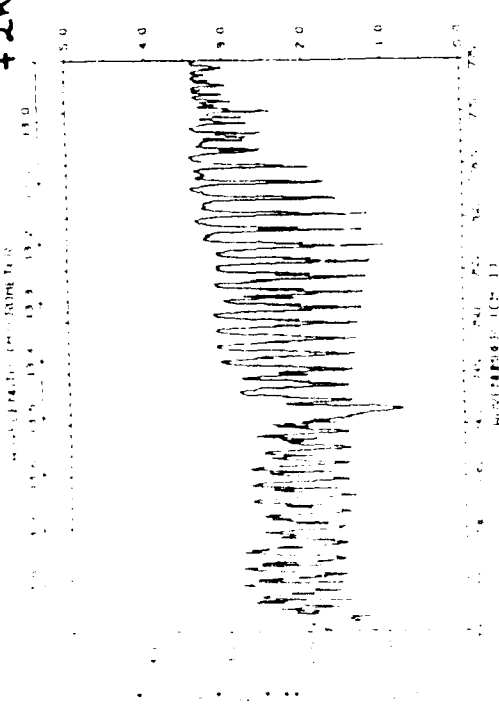
- Temperature retrieval in the CO₂ 15 μ m-band (720 – 775 cm⁻¹)
- Model: FASCOD3
- Line file: HITRAN 1988

Atmospheric Profiles:

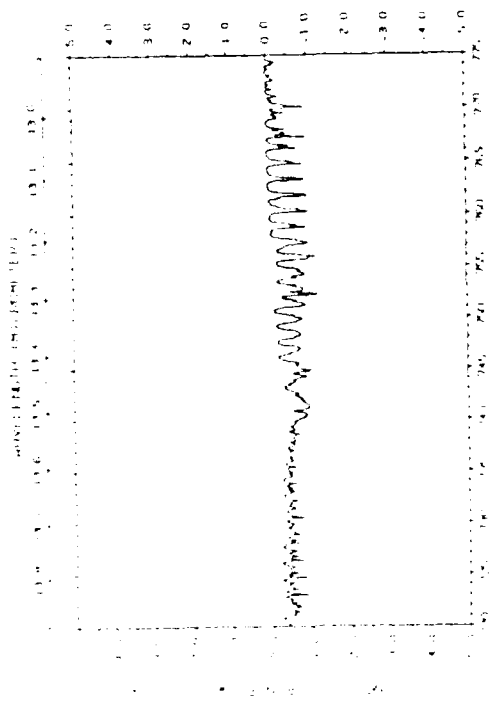
- Retrieved parameters: 18 layer temperatures (from 0 to 30.31km) + surface temperature
- Temperature profile:
 - Background: Tropical
 - Simulated: Background + 2K
- Water vapor profile: U.S. Standard



No Measurement Noise (Simulated = Base Case + 2K)

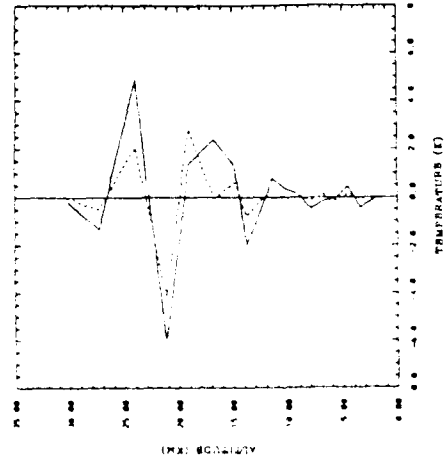


$$(y^m - y_0)$$

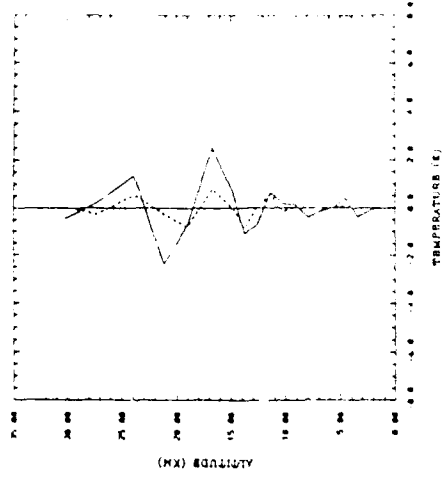


$$(y^m - y_0) - K(x^m - x_0)$$

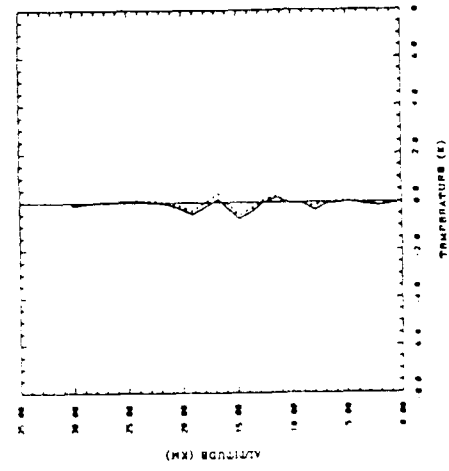
SCAIRE - Temperature Retrieval (720.775 cm⁻¹)
- NO MEASUREMENT NOISE -



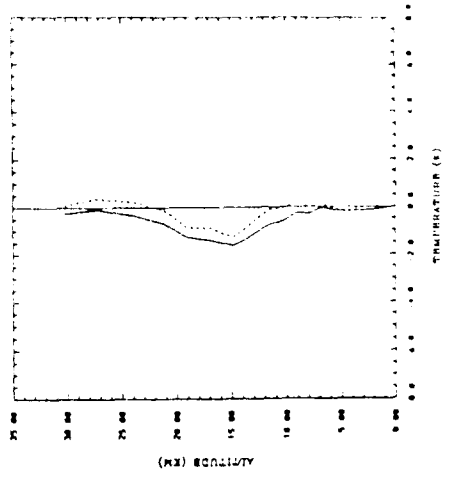
$\gamma = 0$ — 1st ITERATION
----- 5th ITERATION



$\gamma = 1.0 \cdot 10^{-20}$ — 1st ITERATION
----- 4th ITERATION



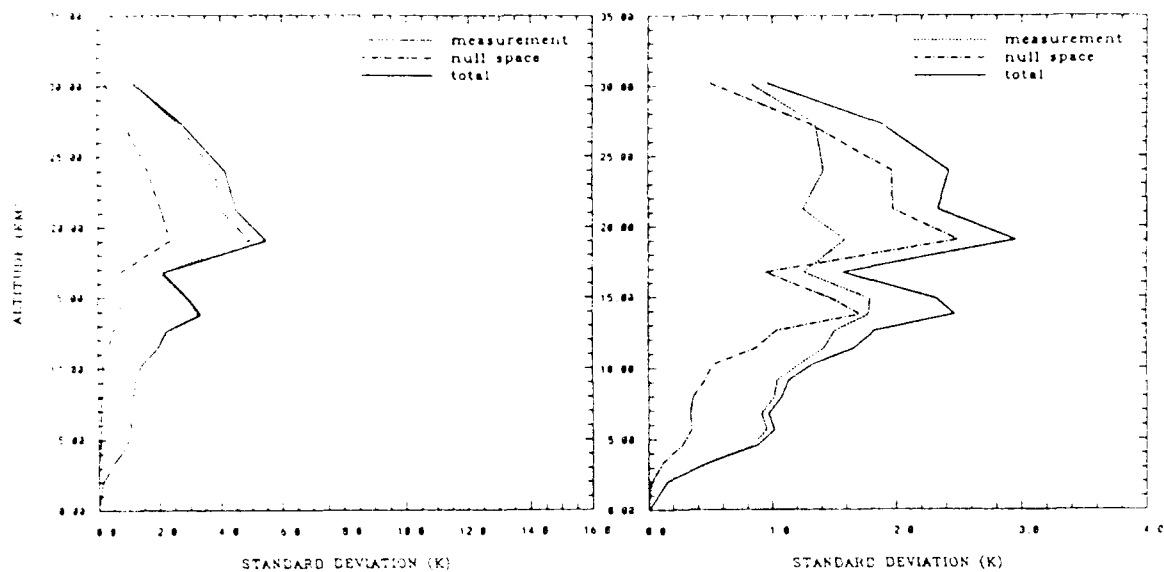
$\gamma = 6.5 \cdot 10^{-19}$ — 1st ITERATION
----- 3rd ITERATION



$\gamma = 1.6 \cdot 10^{-17}$ — 1st ITERATION
----- 3rd ITERATION

SCRIBE Temperature Retrievals (720-775cm⁻¹): Error Analysis

Maximum probability solution ($\sigma_\epsilon = 2.6 \times 10^{-8} \text{W/cm}^2/\text{ster/cm}^{-1}$).

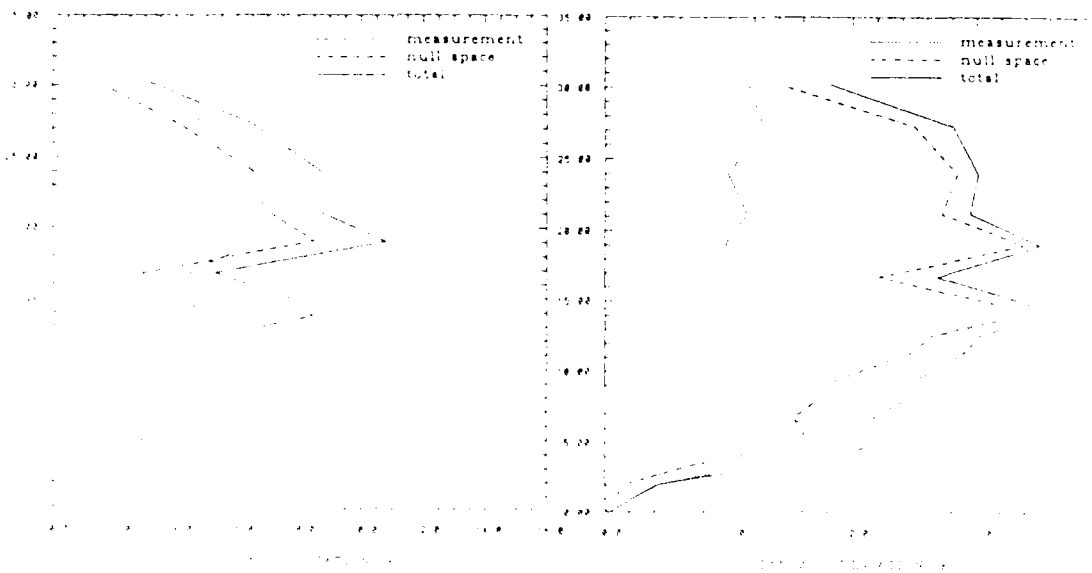


(a) $\sigma_x = 16\text{K}$

(b) $\sigma_x = 4\text{K}$

SCRIBE Temperature Retrievals (720-775cm⁻¹): Error Analysis

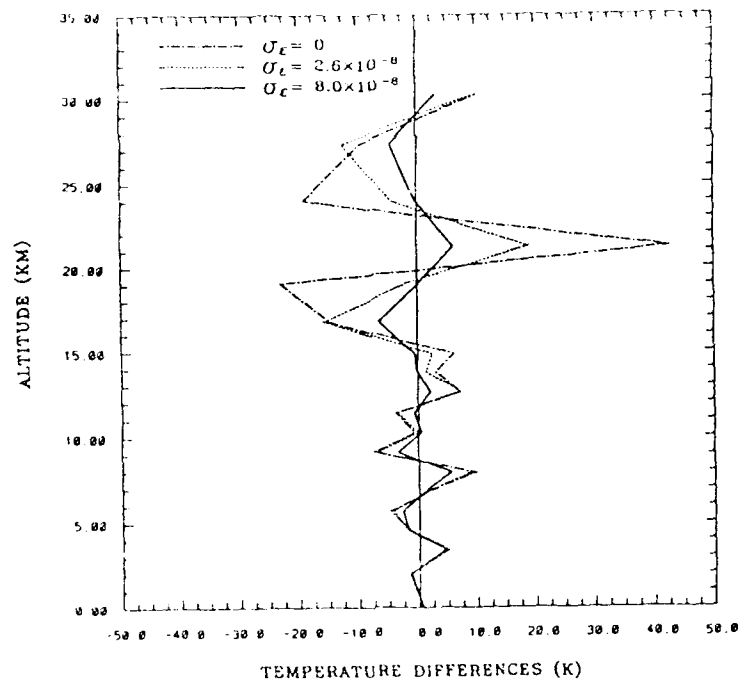
Maximum probability solution ($\sigma_\epsilon = 8.0 \times 10^{-8} \text{W/cm}^2/\text{ster/cm}^{-1}$).



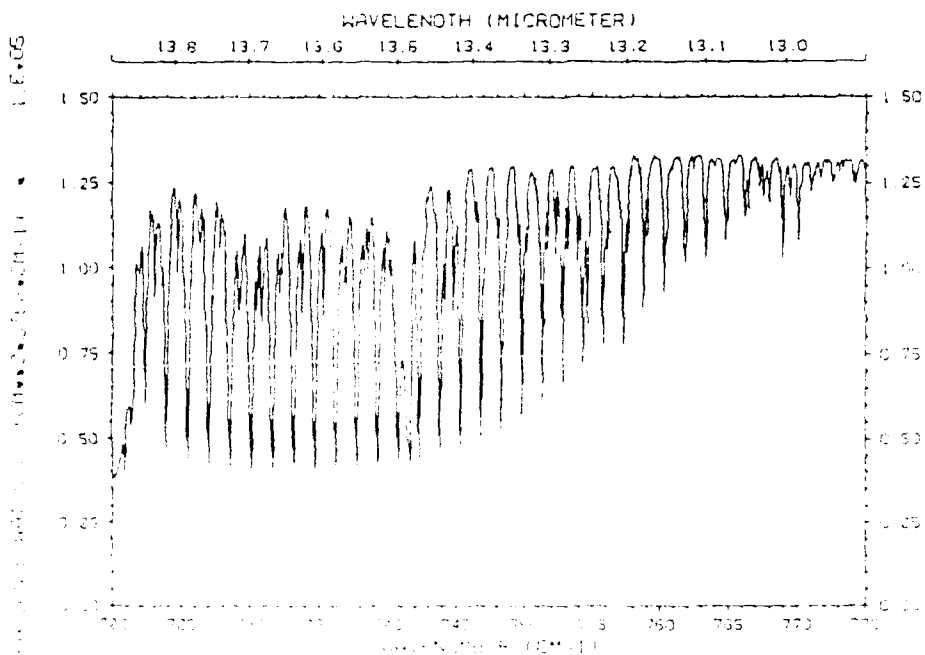
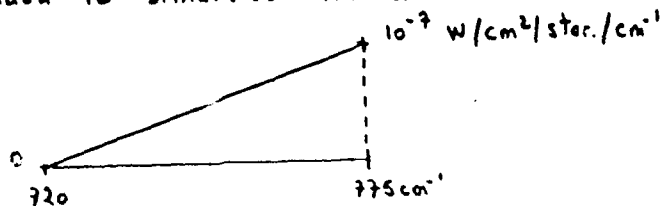
(a) $\sigma_x = 16\text{K}$

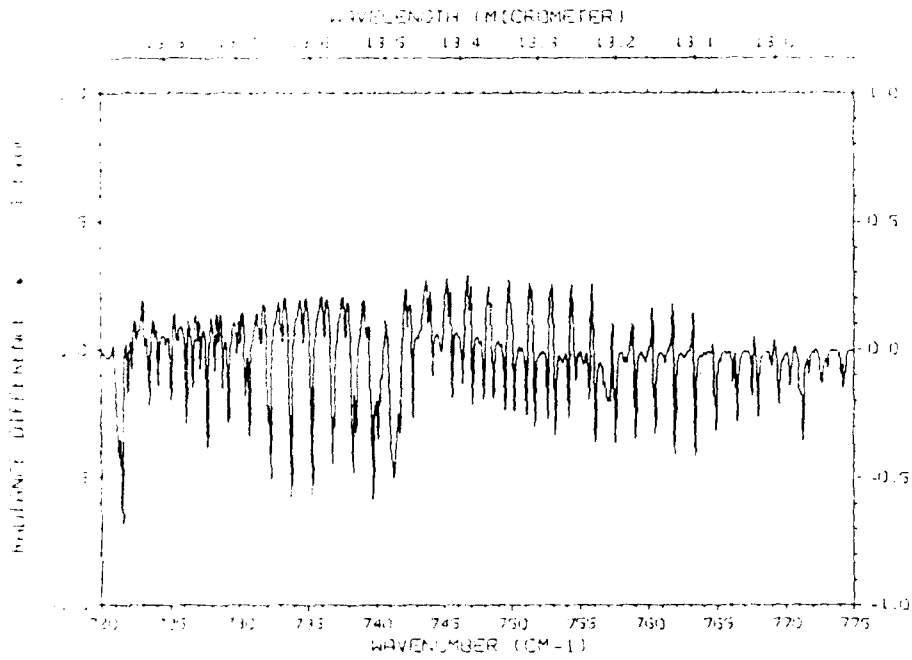
(b) $\sigma_x = 4\text{K}$

SO2 IR . TEMPERATURE RETRIEVAL (720-775 cm⁻¹)
 Effect of Calibration ERRORS *

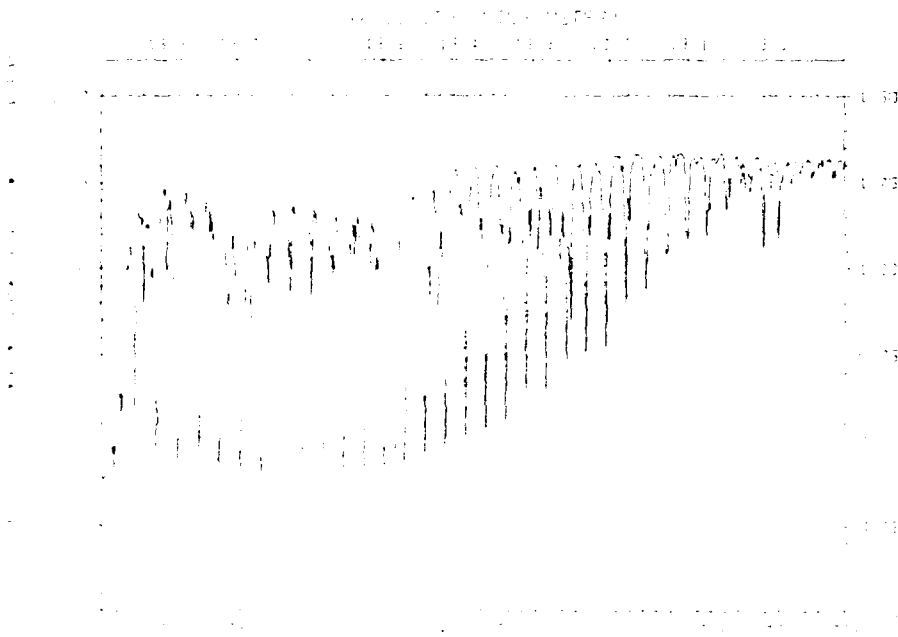


* (Ramp added to simulated Radiances:

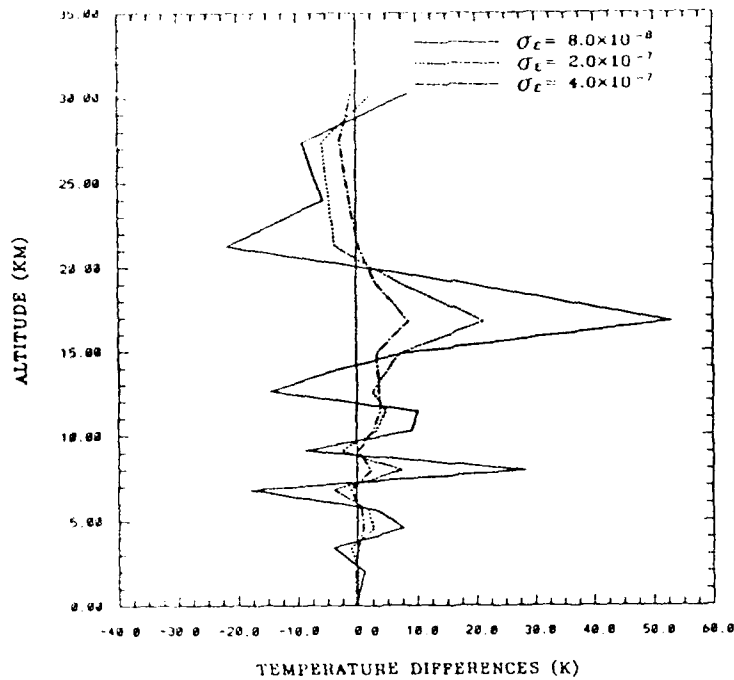




T115102
89



Temperature Retrievals ($720-775\text{cm}^{-1}$) Effect of errors on line Parameters *



* (Simulated Radiances generated with
HITRAN 86 line file + line coupling).

Summary

- Retrieval most effective in lowest atmospheric layers (below 5km) and at the surface. Above 5km the improvement depends on the quality of the *a priori* information (if short-range forecast is used, little improvement expected in the 10–30km layer).
- In an ideal situation (no model errors) expected accuracy is < 1–2K in the lowest 10km, depending on level of instrumental noise.
- Retrieval is very sensitive to calibration errors. These tend to affect all layers, including the surface.
- Current state of knowledge on line parameters seriously limits the quality of the physical retrieval (near the surface, retrieved temperatures remains little affected by errors on line intensities).

VALIDATION OF RANDOM PHASE SCREENS

A.E. Naiman and T. Goldring

W.J. Schafer Assoc., Inc., Arlington, VA 22209

A simple scheme for validating realizations of atmospheric turbulence phase screens is presented and critiqued. The statistics of interest are the first few Zernike modes. For screen generators based on the Fast Fourier Transform, computed and theoretical variances ([1]) are compared, and the discrepancy between them is analyzed. A method for quantifying the accuracy of Zernike mode variances, given grid size and resolution, is discussed. Finally, numerical results are presented for a specific turbulence spectrum.

Reference:

[1] R.J. Sasiela, *A Unique Approach to Electromagnetic Wave Propagation in Turbulence and the Evaluation of Multiparameter Integrals*, Lincoln Laboratory, Massachusetts Institute of Technology, Technical Report 807, 1 July 1988.



Validation of Random Phase Screens

Annual Review Conference on
Atmospheric Transmission Models
5-6 June 1990

by A. E. Naiman and T. Goldring
W. J. Schafer Associates
Arlington, VA 22209

ATM Conference
p 1



Outline

- ⇒ Introduction
 - Theoretical and Estimated Zernike Modes
 - Error Estimation and Effective Zernike modes
 - Numerical Example
 - Error Analysis --- Theory
 - Summary

ATM Conference
p 2



A Simple Validation Scheme

- Create ensemble of phase screens
- Extract desired Zernike modes directly from phases
- Estimate variances
- Compare with values expected from theory

Estimated and theoretical Zernike mode variances
can be compared directly -- **with inherent limitations, ...**

ATM Confer



Validation -- Definition

- Another validation criterion:
 - Comparing with structure function
- Zernike modes represent classical optical aberrations, e.g. tilt, focus \Rightarrow
 - Test if a phase screen generator realizes the Zernike modes properly



Purpose of Presentation

- Discuss inherent limitations of simple validation scheme
- These arise due to discretization \Rightarrow
 - * Discrepancies between numerical and theoretical results
- Analyze these errors
 - * Show method for quantifying them

ATM Conferen

P



Outline

- Introduction
- \Rightarrow Theoretical and Estimated Zernike Modes
- Error Estimation and Effective Zernike modes
- Numerical Example
- Error Analysis - Theory
- Summary



Zernike Expansions

Zernike expansion of a continuous 2-D function ϕ [Noll]:

$$\phi(r, \theta) = \sum_j a_j Z_j(\rho, \theta),$$

R --- aperture radius, $\rho = \frac{r}{R} \in [0, 1]$, and the coefficients are given by:

$$a_j = \iint \rho d\rho d\theta W(\rho) \phi(R\rho, \theta) Z_j(\rho, \theta),$$

$W(r) = \begin{cases} 1, & r \leq 1, \\ 0, & r > 1, \end{cases}$ is the radially symmetric step function

Any *continuous* 2-D phase realization,
can be expanded in terms of Zernike polynomials

ATM Confer
P



Variances of Theoretical Zernike Coefficients

Zernike coefficient phase variance [Sasiela]:

$$\sigma_0^2(a_j) = \iint d\vec{\kappa} W_\phi(\vec{\kappa}) F_j(\vec{\kappa}),$$

$W_\phi(\vec{\kappa})$ is the turbulence spectrum, $F_j(\vec{\kappa})$ is the filter function:

$$F_j(\vec{\kappa}) = (n' + 1) \left[\frac{2J_{n'+1}(\frac{\kappa D}{2})}{\frac{\kappa D}{2}} \right]^2 \begin{cases} 2 \cos^2(m'\varphi) & (x\text{-component}), \\ 2 \sin^2(m'\varphi) & (y\text{-component}), \\ 1 & (m' = 0), \end{cases}$$

D --- diameter of the aperture,

m', n' --- Zernike component indices (angular frequency and radial degree)

$$\kappa = |\vec{\kappa}|$$

$$F_j(\vec{\kappa}) = |\mathcal{F}(\text{Zernike polynomial } j)|^2 \text{ [Noll]}$$

ATM Confer



Effective vs. Theoretical Variances — Definition

- $\sigma_{\text{eff}}^2(a_j) \stackrel{\text{def}}{=} \text{variance of Zernike coefficients of phase screens}$
 - * i.e., *not* of realizations of the continuous random surface, which exist only in theory
- $\sigma_{\text{est}}^2(a_j) \stackrel{\text{def}}{=} \text{standard statistical estimate from a finite sample of phase screens, } \Rightarrow$
 - * $\sigma_{\text{est}}^2(a_j) \rightarrow \sigma_{\text{eff}}^2(a_j)$, as sample size increases
- However, $\sigma_{\text{eff}}^2(a_j) \neq \sigma_0^2(a_j)$ for a fixed computational grid
- For FFT-based methods, we quantify this error

ATM Conference
p. 9



Outline

- Introduction
- Theoretical and Estimated Zernike Modes
- \Rightarrow Error Estimation and Effective Zernike modes
- Numerical Example
- Error Analysis - Theory
- Summary

ATM Conference
p. 1



FFT Phase Screen Generator

- For grid length L , with N points in each direction, our phase realization is given by an inverse Discrete Fourier Transform (DFT):

$$\phi(x, y) = \sum_{n=-N}^{N-1} \sum_{m=-N}^{N-1} b_{nm} e^{-i\omega_0(nx+my)},$$

a continuous, doubly-periodic function of x and y .

- The inverse FFT efficiently computes the DFT on the grid $\{(x_j, y_k) : j, k = 0, \dots, N-1\}$ where:

$$x_j = y_j = \frac{jL}{N}.$$

ATM Conference
p. 11



FFT Phase Screen Generator — Continued

- The Fourier coefficients b_{nm} :
 - Random zero-mean Gaussian complex numbers
 - Occur in conjugate pairs \rightarrow
 - $\phi(x, y)$ is *real*
 - Have variance of:

$$\sigma^2(b_{nm}) = \omega_0^2 W_\phi(\kappa_{nm})$$

Note inclusion of ω_0^2

ATM Conference
p. 12



FFT Generator --- Choice of ω_0

- ω_0 determines periodicity and frequency content
 - Choose $\omega_0 = \frac{\pi}{L}$, so that:
 - * the period is $2L$
 - * Extracting any contiguous $N \times N$ submatrix of $\{\phi(x_j, y_k)\} \Rightarrow$
 - * Pairwise covariances will be correct for separation distances $\leq L$
 - * The continuous random surface $\phi(x, y)$ is sampled at precisely the Nyquist frequency corresponding to the band limiting assumption $W_\phi(\vec{\kappa}) \equiv 0, |\vec{\kappa}| > N\omega_0$.
- This is *implicit* in the discretization procedure.

These realizations $\phi(x, y)$ are distinct from the theoretically given ensemble $\hat{\phi}(x, y) = \iint_{-\infty}^{\infty} b(\vec{\kappa}) e^{-i\vec{\kappa} \cdot (x, y)} d\vec{\kappa}$, whose members are *not* periodic.



Effective Zernike Coefficients

We have, in general, the Zernike coefficients:

$$a_j = \iint \rho d\rho d\theta W(\rho) \phi(R\rho, \theta) Z_j(\rho, \theta),$$

and for the FFT method, the phase screen:

$$\phi(x, y) = \sum_{n,m=-N}^{N-1} b_{nm} e^{-i\omega_0(nx+my)},$$

or equivalently: $\phi(\vec{r}) = \sum_{n,m=-N}^{N-1} b_{nm} e^{i\vec{\kappa}_{nm} \cdot \vec{r}}$,

where $\vec{r} = (x, y)$ and $\vec{\kappa}_{nm} = (n\omega_0, m\omega_0)$. Substituting:

$$a_j = \sum_{n,m=-N}^{N-1} b_{nm} \iint d\vec{r} W(\rho) Z_j(\rho, \theta) e^{i\vec{\kappa}_{nm} \cdot \vec{r}}$$

The integral is the Fourier transform of the Zernike polynomial, over the aperture, computed analytically [Noll] as the filter function.



- Taking the variance:

$$\begin{aligned}\sigma_{\text{eff}}^2(a_j) &= \sum_{n,m=-N}^{N-1} \sigma^2(b_{nm}) F_j(\vec{\kappa}_{nm}) \\ &= \sum_{n,m=-N}^{N-1} \omega_0^2 W_\phi(\vec{\kappa}_{nm}) F_j(\vec{\kappa}_{nm})\end{aligned}$$

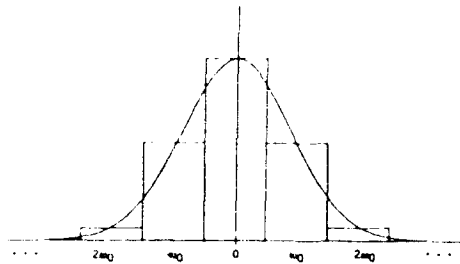
- Conclude: Effective variance is a standard numerical approximator to theoretical variance, i.e.:

$$\begin{aligned}\sigma_0^2(a_j) &= \iint d\vec{\kappa} W_\phi(\vec{\kappa}) F_j(\vec{\kappa}), \\ &\approx \sum_{n,m=-N}^{N-1} \omega_0^2 W_\phi(\vec{\kappa}_{nm}) F_j(\vec{\kappa}_{nm}) = \sigma_{\text{eff}}^2(a_j)\end{aligned}$$

$\sigma_{\text{eff}}^2(a_j)$ is "rectangle rule" approximation to $\sigma_0^2(a_j)$



- In one dimension:



- Note the error dependencies:

- "rectangle" error \downarrow as $\omega_0 \downarrow$ ($L \uparrow$)
- tail error \downarrow as $N \uparrow$

If ω_0^2 is *not* included in $\sigma^2(b_{nm})$,
then $\sigma_{\text{eff}}^2(a_j) \rightarrow \infty$, as $L, N \rightarrow \infty$



Example: Tilt Variances

- In general, two-axis tilt variance:

$$T^2 = \left(\frac{4}{kD} \right)^2 [\sigma^2(a_2) + \sigma^2(a_3)],$$

$\left(\frac{4}{kD} \right)^2$ — due to averaging the tilt *phase* variances over the aperture

- Theoretical and effective tilt variances:

$$T_0^2 = \iint d\vec{\kappa} W_\phi(\vec{\kappa}) \left[\left(\frac{16}{kD} \right) \frac{J_2\left(\frac{\kappa D}{2}\right)}{\frac{\kappa D}{2}} \right]^2$$

and

$$T_{\text{eff}}^2 = \sum_{n,m=-N}^{N-1} \omega_0^2 W_\phi(\vec{\kappa}_{nm}) \left[\left(\frac{16}{kD} \right) \frac{J_2\left(\frac{\kappa_{nm} D}{2}\right)}{\frac{\kappa_{nm} D}{2}} \right]^2$$

ATM Conference

p. 17



Outline

- Introduction
- Theoretical and Estimated Zernike Modes
- Error Estimation and Effective Zernike modes
- Numerical Example
- Error Analysis — Theory
- Summary

ATM Conference

p. 18



Turbulence Spectrum

2-D von-Kármán phase spectrum [Tatarski]:

$$W_{\phi}(\vec{\kappa}) = 2\pi k^2 \Delta z \frac{0.033 C_n^2}{[\kappa_0^2 + \kappa^2]^{11/6}},$$

where:

$$\begin{aligned} k &= \frac{2\pi}{\lambda}, \text{ the spatial wavenumber,} \\ \Delta z &= \text{the slab length,} \\ C_n^2 &= \text{the structure constant,} \\ \kappa_0 &= \frac{2\pi}{L_0}, \text{ and} \\ L_0 &= \text{the outer scale of turbulence.} \end{aligned}$$

ATM Conference
p. 19



Turbulence Spectrum — Continued

If C_n^2 is a function of z , then let:

$$\mu_0 = \int_0^{\Delta z} C_n^2(z) dz,$$

thereby:

$$W_{\phi}(\vec{\kappa}) = 0.2073 k^2 \mu_0 (\kappa^2 + \kappa_0^2)^{-11/6}$$

von-Kármán spectrum is widely used
and reduces to Kolmogorov spectrum when $L_0 \rightarrow \infty$

ATM Conference
p. 20



Tilt Variances -- Comparisons

- Sasiela derives a series approximation to T_0^2 for the von-Kármán spectrum:

$$T_0^2 = \frac{6.08\mu_0}{D^{\frac{1}{3}}} \left\{ 1 + 3.7 \left(\frac{D}{L_0}\right)^2 + \dots - \left(\frac{D}{L_0}\right)^{\frac{1}{3}} \left[1.42 + 4.01 \left(\frac{D}{L_0}\right)^2 + \dots \right] \right\}$$

- T_{eff}^2 is computed directly:

$$T_{\text{eff}}^2 = \sum_{n,m=-N}^{N-1} \sum_{n,m=-N}^{N-1} \omega_0^2 W_\phi(\vec{\kappa}_{nm}) \left[\left(\frac{16}{kD} \right) \frac{J_2\left(\frac{\kappa_{nm}D}{2}\right)}{\frac{\kappa_{nm}D}{2}} \right]^2$$

$$\approx 2095 \frac{\mu_0}{L^2 D^4} \sum_{n,m=-N}^{N-1} \sum_{n,m=-N}^{N-1} \left(\kappa_{nm}^2 + \left(\frac{2\pi}{L_0}\right)^2 \right)^{-\frac{11}{6}} \left[\frac{J_2\left(\frac{\kappa_{nm}D}{2}\right)}{\kappa_{nm}} \right]^2$$

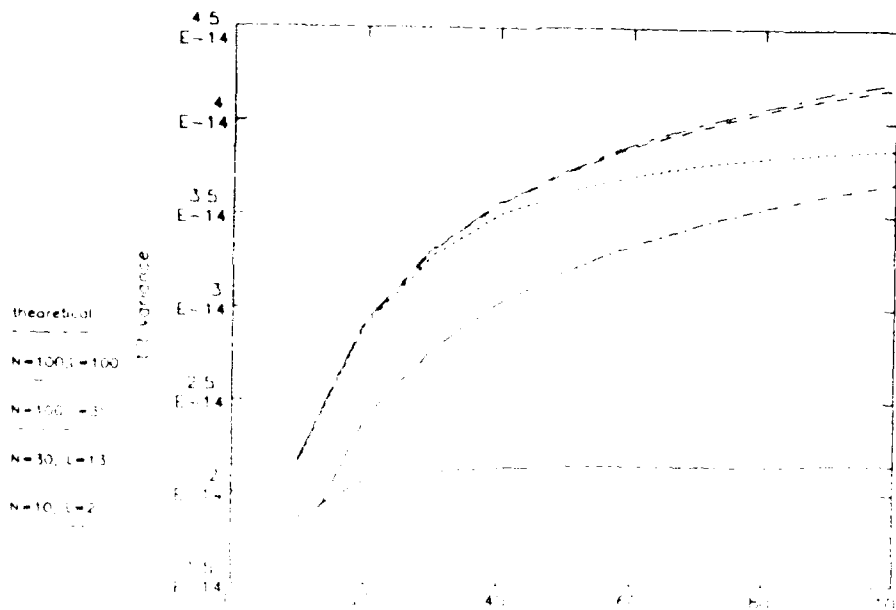
Recall: $\lim_{L,N \rightarrow \infty} T_{\text{eff}}^2 = T_0^2$

- Some examples, ...

ATM Conference
p. 21



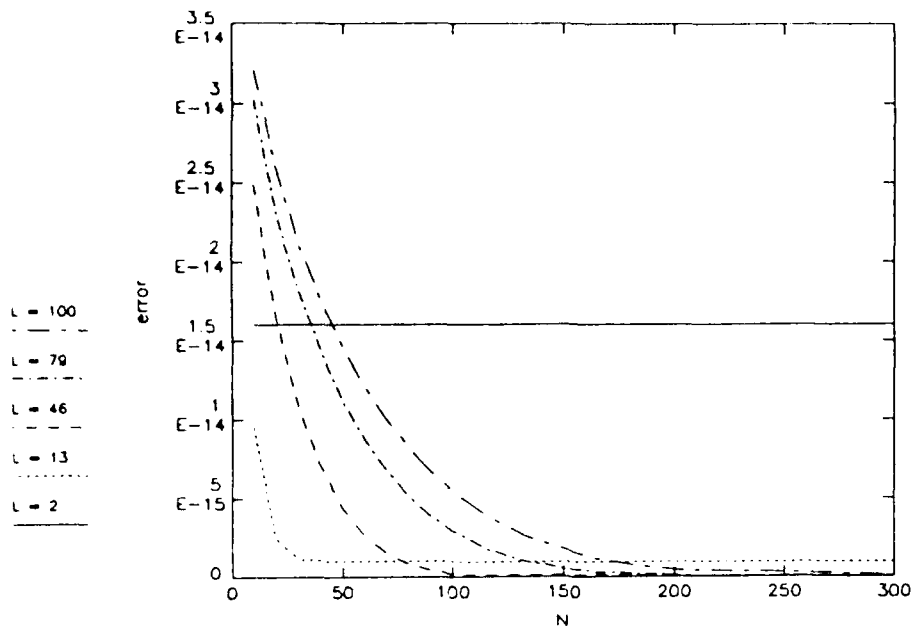
Comparison of Theoretical and Effective Tilt Variances



ATM Conference
p. 22



Error Between Theoretical and Effective Tilt Variances



ATM Conference
p. 23



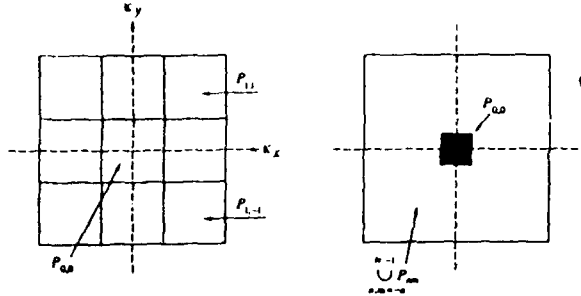
Outline

- Introduction
- Theoretical and Estimated Zernike Modes
- Error Estimation and Effective Zernike modes
- Numerical Example
- > Error Analysis - Theory
- Summary



Error Analysis for 2-D Rectangle Rule

- For $\vec{\kappa} = (\kappa_x, \kappa_y)$, let:



$$g(\kappa_x, \kappa_y) = W_\phi(\vec{\kappa}) F(\vec{\kappa})$$

$$P_{nm} = \left\{ \vec{\kappa} : \left(n - \frac{1}{2} \right) \omega_0 \leq \kappa_x \leq \left(n + \frac{1}{2} \right) \omega_0, \left(m - \frac{1}{2} \right) \omega_0 \leq \kappa_y \leq \left(m + \frac{1}{2} \right) \omega_0 \right\}$$

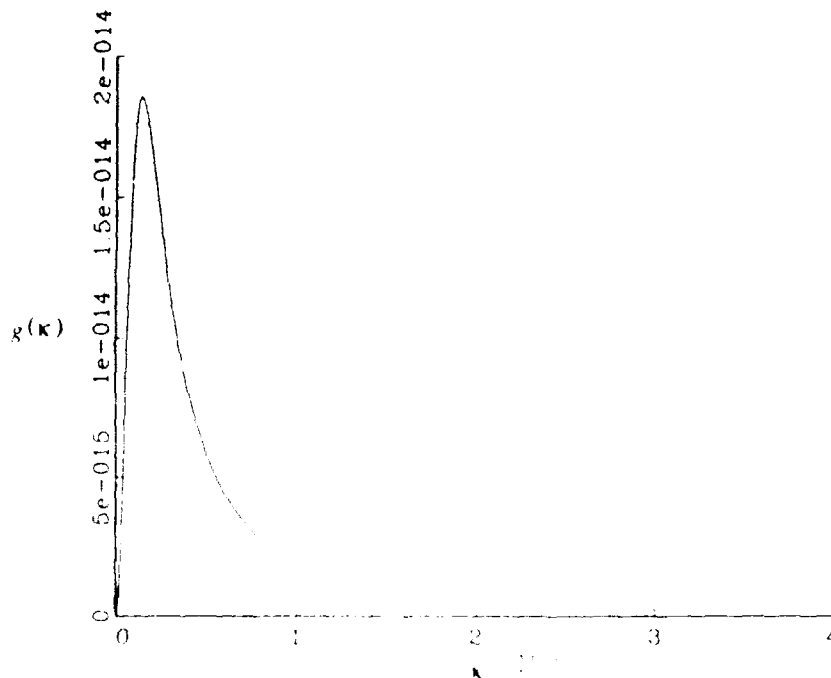
$$\tilde{Q} = \left\{ \vec{\kappa} : -\left(N + \frac{1}{2} \right) \omega_0 \leq \kappa_x, \kappa_y \leq \left(N - \frac{1}{2} \right) \omega_0 \right\} = \bigcup_{n,m=-N}^{N-1} P_{nm}$$

- Expand $g(\kappa_x, \kappa_y)$ in a Taylor Series about the center point $(n\omega_0, m\omega_0)$ of P_{nm} and integrate term by term; valid for n, m not both zero

ATM Conference
p 25



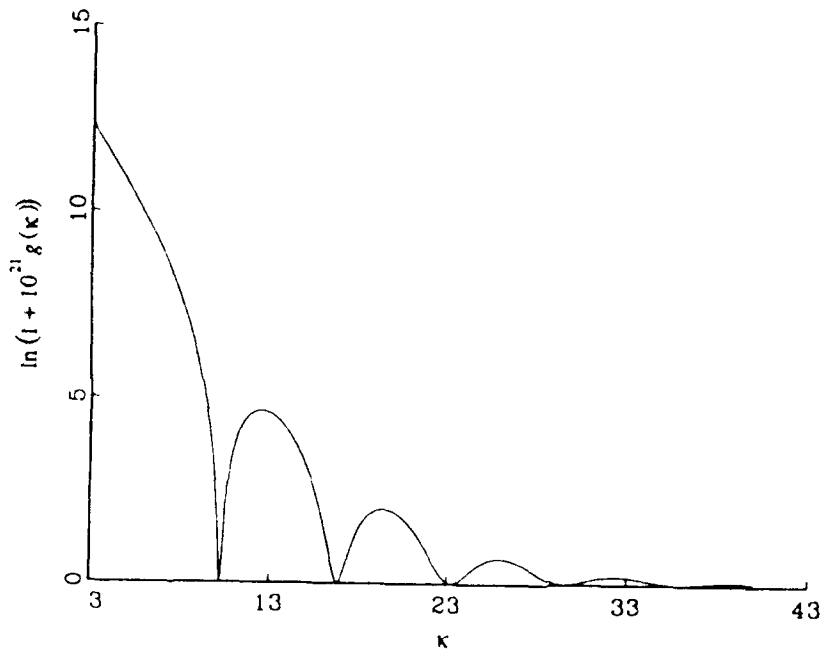
Integrand for Small Values of κ



ATM Conference
p 26



Small Oscillations in Integrand



ATM Conference
p 27



Expansion of Theoretical Variance

- One can show:

$$\begin{aligned}
 \sigma_0^2(a_j) &= \iint_{-\infty}^{\infty} g d\kappa_x d\kappa_y = \sum_{n,m=-N}^{N-1} \iint_{P_{nm}} g d\kappa_x d\kappa_y + \iint_Q g d\kappa_x d\kappa_y \\
 &= \iint_{P_{00}} g d\kappa_x d\kappa_y + \iint_Q g d\kappa_x d\kappa_y + \\
 &\quad \sum_{\substack{n,m=-N \\ n^2+m^2 \neq 0}}^{N-1} \left[\omega_0^2 g(n\omega_0, m\omega_0) + \frac{\omega_0^4}{24} \nabla g(n\omega_0, m\omega_0) \right] + O(\omega_0^6)
 \end{aligned}$$

- Note: Both g and ∇g are functions of $\kappa = |\vec{\kappa}|$ alone



Resultant Error Term

- Now, $g(0, 0) = F(0) = 0, \Rightarrow$

$$\sigma_{\text{eff}}^2(a_j) = \sum_{\substack{n, m = -N \\ n^2 + m^2 \neq 0}}^{N-1} \omega_0^2 g(n\omega_0, m\omega_0)$$

- Therefore, neglecting 6th and higher order terms:

$$\sigma_0^2(a_j) - \sigma_{\text{eff}}^2(a_j) \approx \iint_{P_{0,0}} g d\kappa_x d\kappa_y + \iint_Q g d\kappa_x d\kappa_y + \frac{\omega_0^4}{24} \sum_{\substack{n, m = -N \\ n^2 + m^2 \neq 0}}^{N-1} \nabla g(n\omega_0, m\omega_0)$$

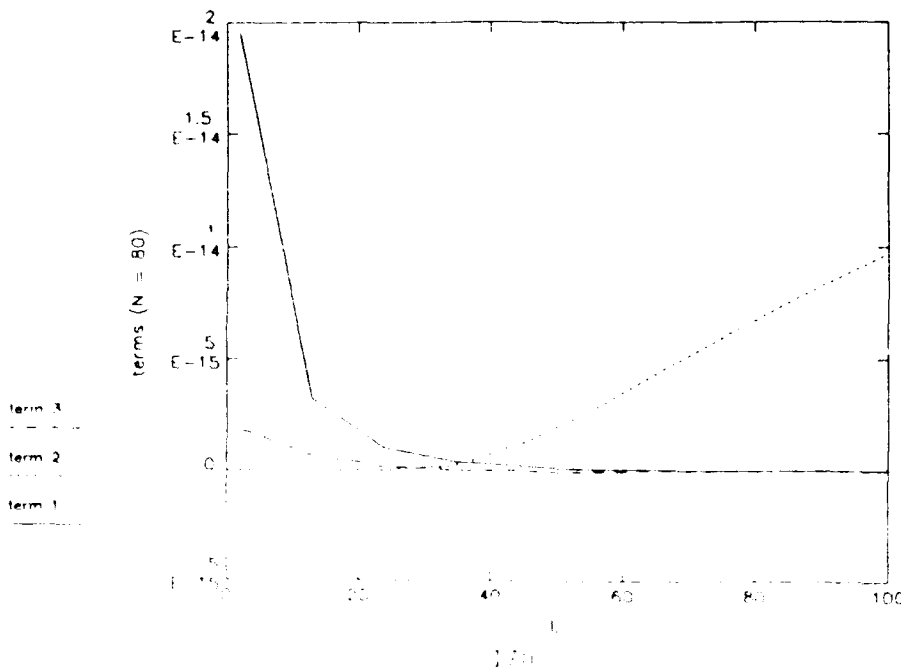
- g is circularly symmetric \Rightarrow

- * Double integrals can be approximated by single integrals in

$$\kappa = \sqrt{\kappa_x^2 + \kappa_y^2}$$



Relative Magnitude of Error Terms





- Introduction
 - Theoretical and Estimated Zernike Modes
 - Error Estimation and Effective Zernike modes
 - Numerical Example
 - Error Analysis — Theory
- ⇒ Summary



- Method for validating phase generators:
 - * Compute Zernike modes from physical phase values
 - * Compare with continuous and discrete theories
- Discrepancy between two theories is intrinsic to computational necessity of using a discrete grid
- Results computed from actual phase screen, at best match up with discrete theory



- Method for quantifying accuracy of Zernike mode variances, given grid size and resolution

- Numerical results for the case of:
 - * FFT phase screen generator
 - * von-Kármán spectrum
 - * Tilt variance

**RECENT ADVANCES IN MODELING OF
BOUNDARY LAYER REFRACTIVITY TURBULENCE**

V. Thiermann and A. Kohnle
FGAN-Forschungsinstitut für Optik
Schloss Kressback, D-7400 Tübingen, F.R. Germany

Monin-Oboukhov similarity is an elegant tool for estimating structure parameters and inner scales of turbulent refractive index fluctuations in the boundary layer. Our recent experiments support slightly different scaling expressions than commonly used. These modified expressions are in better agreement with theoretical considerations and lead to up to 30% larger structure parameters and up to 15% larger inner scales.

The program SPIRIT is presented. It computes structure parameters and inner scales in the lower boundary layer over land from easy-to-estimate input parameters. A listing of the required input quantities and an example of model results in comparison with measurements are given.

RECENT ADVANCES IN MODELING OF
BOUNDARY LAYER REFRACTIVITY TURBULENCE

Volker Thiermann and Anton Kohnle

Forschungsinstitut für Optik (FGAN-FfO)

Schloss Kressbach

D-7400 Tübingen

Federal Republic of Germany

Parameters describing the spatial spectrum of refractive index
in the optically relevant range:

C_n^2 spectral amplitude in the inertial subrange (mm's to m's)

→ important for all turbulence sensitive EO-systems

ℓ_0 high spatial wavenumber cut-off of inertial subrange (mm's)

→ important for communication systems if

- propagation path is short (Fresnel zone $< \ell_0$)

- propagation path is long and turbulence is strong

(coherence length $< \ell_0$)

• important for imaging systems if

optics is small (aperture diameter $< \ell_0$)

$$C_n^2 = a_T^2 C_T^2 + 2 a_T a_q C_{Tq} + a_q^2 C_q^2 \simeq a_T^2 C_T^2$$

over land

$$l_0 \simeq l_T$$

$$C_T^2 = 4 \beta_1 \epsilon_T \epsilon^{-1/3}$$

β_1 Oboukhov-Corrsin-constant

ϵ_T dissipation rate of temperature variance

ϵ dissipation rate of kinetic energy of turbulence

$$l_0 = 7.4 \nu^{3/4} \epsilon^{-1/4}$$

ν kinematic viscosity of air

SCALING in Monin-Obukhov Similarity

$u_* = \sqrt{-\langle u'w' \rangle}$ friction velocity (turbulent velocity scale)

$T_* = -\langle T'w' \rangle / \langle u'w' \rangle$ turbulent temperature scale

z height

k von Kármán constant (0.4)

g/T buoyancy parameter

$\zeta = \frac{z k g T_*}{T u_*^2}$ stability parameter

$\Phi_\epsilon = \frac{\epsilon k z}{u_*^3}$ dimensionless ϵ

$\Phi_{\epsilon T} = \frac{\epsilon_T k z}{u_* T_*^2}$ dimensionless ϵ_T

$\Phi_m = \frac{k z}{u_*} \frac{\partial u}{\partial z}$ dimensionless wind shear

$\Phi_h = \frac{k z}{u_*} \frac{\partial \theta}{\partial z}$ dimensionless lapse rate

$\Phi_{E\epsilon} = \frac{k z}{u_*} \frac{\partial E_\epsilon}{\partial z}$ dimensionless energy flux divergence

$\Phi_{E_T} = \frac{k z}{u_*} \frac{\partial E_T}{\partial z}$ dimensionless temperature
variance flux divergence

$$\Phi \ell_0 \equiv \frac{u_*^{3/4}}{\nu^{3/4} (k z)^{1/4}} \ell_0 = 7.4 \Phi_\epsilon^{-1/4}$$

dimensionless ℓ_0

$$\Phi_{CT} \equiv \frac{(k z)^{2/3}}{T_*^2} C_T^2 = 4 \beta_1 \Phi_{\epsilon T} \Phi_\epsilon^{-1/3}$$

dimensionless C_T^2

Balance equations :

(stationary, homogeneous)

$$\Phi_\epsilon = \Phi_m - \zeta - \Phi_{Fe} \simeq \Phi_m - \zeta$$

$$\Phi_{\epsilon T} = \Phi_h - \Phi_{FT} \simeq \Phi_h$$

Behavior at $\zeta \approx 0$:

$$\frac{\partial \Phi_\epsilon}{\partial \zeta} \approx \frac{\partial \Phi_m}{\partial \zeta} - 1 \approx 2 \quad \left(\bar{\Phi}_\epsilon(0) \approx 1 \right)$$

$$\frac{\partial \Phi_{\epsilon T}}{\partial \zeta} \approx \frac{\partial \Phi_h}{\partial \zeta} \approx 3$$

$$\frac{\partial \Phi_{CT}}{\partial \zeta} \approx 4 \beta_1 \frac{7}{3}$$

$$\bar{\Phi}_{CT}(0) \approx 4 \beta_1 \bar{\Phi}_h(0) \approx 4 \beta_1$$

Behavior at $|\zeta| \rightarrow \infty$:

$$\zeta \rightarrow -\infty: \Phi_\epsilon \approx \zeta \quad (\Phi_{Fe} \approx 0, \bar{\Phi}_m \approx 0)$$

$$\zeta \rightarrow \infty: \Phi_\epsilon \approx 4\zeta \quad (\Phi_{Fe} \approx 0, \Phi_m \approx 5\zeta)$$

$$\zeta \rightarrow -\infty: \Phi_{CT} \propto \zeta^{-2/3}$$

$$\zeta \rightarrow \infty: \Phi_{CT} \propto \zeta^{2/3}$$

Empirical relations, consistent with above considerations:

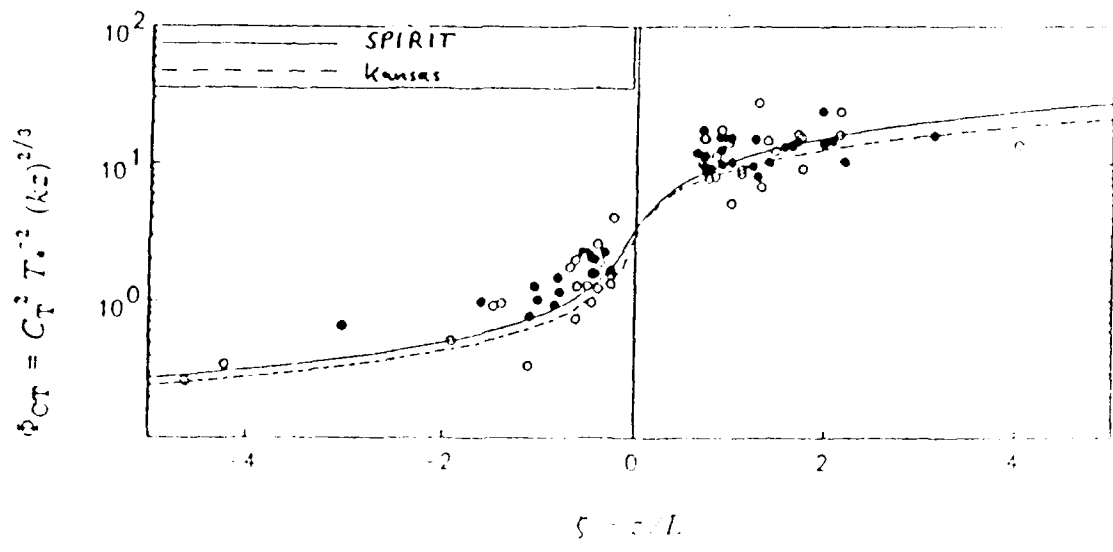
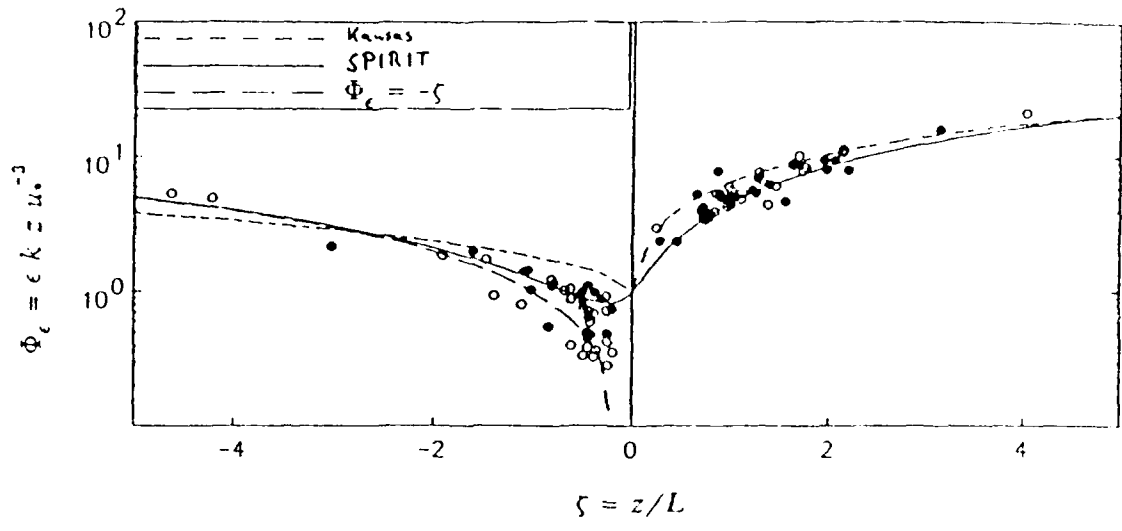
$$\Phi_c = (1 - 3\zeta)^{-1} + \zeta \quad \text{for } \zeta < 0$$

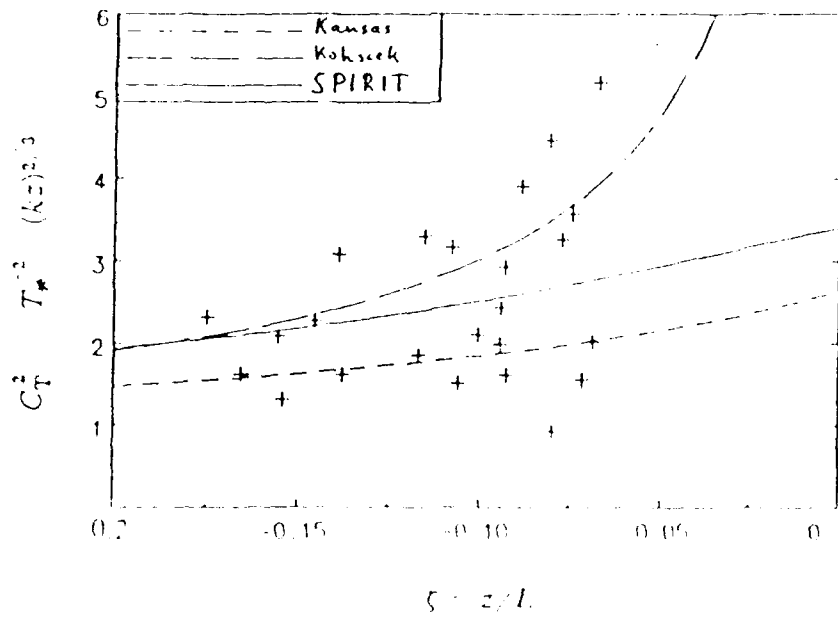
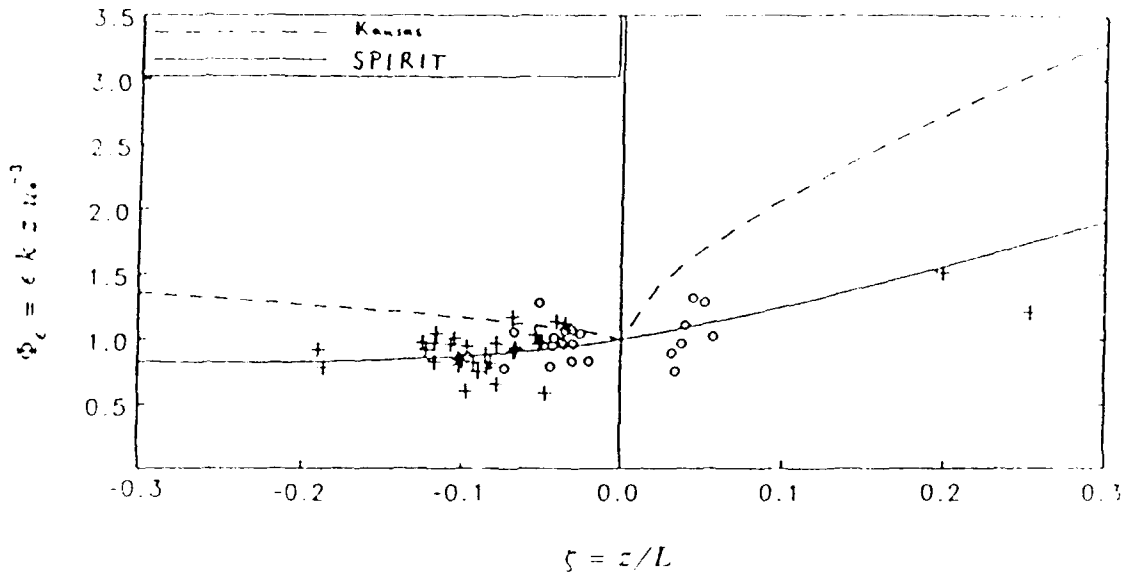
$$\Phi_c = (1 + 4\zeta + 16\zeta^2)^{1/2} \quad \text{for } \zeta > 0$$

$$\Phi_{CT} = 4 \beta_1 (1 - 7\zeta + 75\zeta^2)^{-1/3} \quad \text{for } \zeta < 0$$

$$\Phi_{CT} = 4 \beta_1 (1 + 7\zeta + 20\zeta^2)^{1/3} \quad \text{for } \zeta > 0$$

$$(\beta_1 = 0.86)$$





The program

S P I R I T

computes

Structure Parameters and Inner scales of Refractive Index Turbulence
for optical frequencies in the lower boundary layer over land.

Structure of SPIRIT:

1. Assistance for estimating input parameters (optional)
2. Parameterization of turbulent fluxes of heat, moisture and momentum
3. Application of Monin-Oboukhov-Similarity
4. Relating temperature and humidity to refractivity

INPUT PARAMETERS

Assistance module:

- date, time
- geographical position
- height above sea level
- cloud cover
- wind velocity at a certain height
- coverage of ground by obstacles and vegetation
- height of obstacles and vegetation
- humidity of the ground (humid, moderately humid, dry, very dry)
- brightness of the ground (4 options)
- air temperature
- (relativ humidity)
- wavelength

direct entering:

- solar irradiance (day)
- strong wind heat flux (night)
- surface roughness length
- wind velocity at a certain height
- ground humidity parameter (0...1)
- ground albedo
- air temperature
- temperature derivative of refractivity
- humidity derivative of refractivity

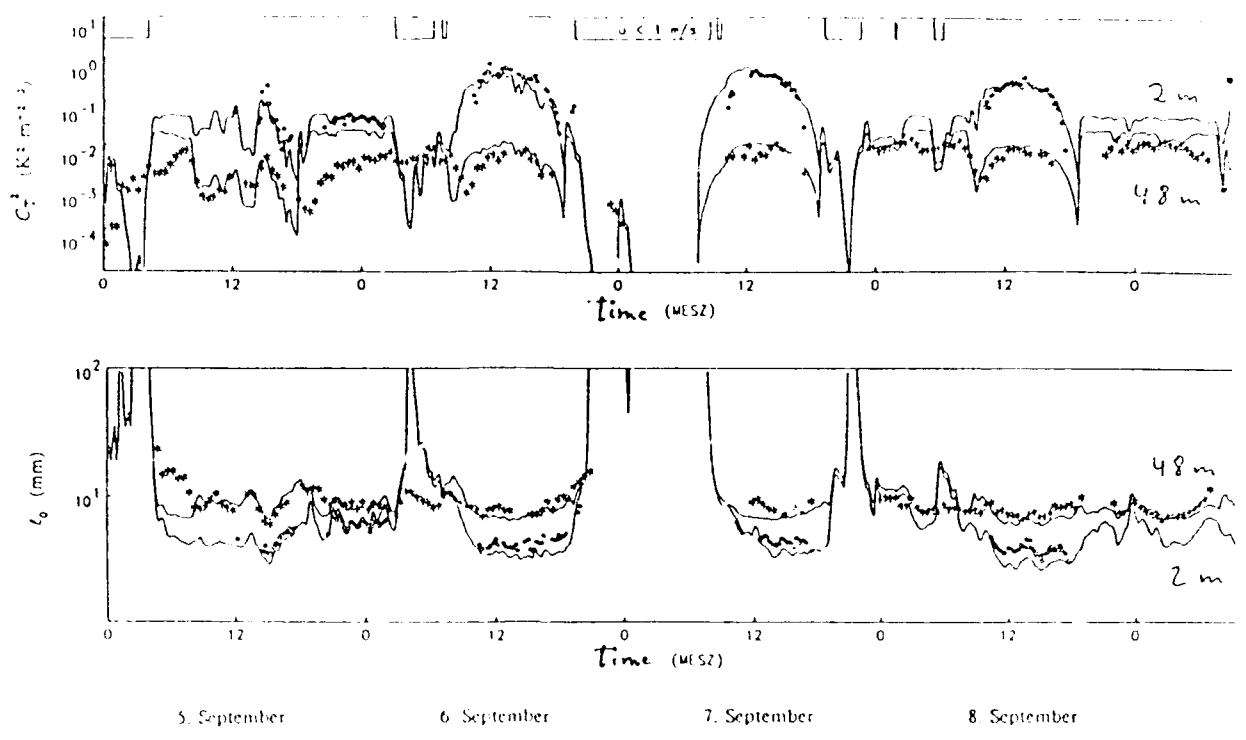
MODEL OUTPUT

Profile of:

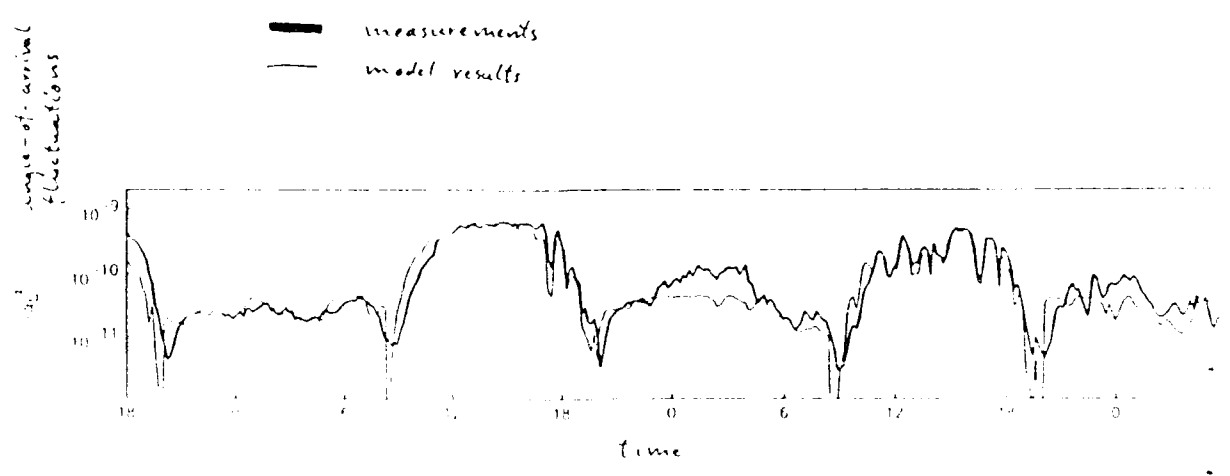
- structure parameters C_n^2 .
- inner scales l_0

Maximum height depends on conditions, day: 200 m

Symbols: measurements, curves: model



1500 m slant path



VISIBILITY DATA FILTERS FOR EUROPE

B.A. Schichtel and R.B. Husar

Center for Air Pollution Impact and Trend Analysis, Washington University, St. Louis, MO 63130

The purpose of the report is to present the methodology for filtering the European meteorological visibility data from undesirable and erroneous data. Seven data filters were devised and imposed on the European synoptic visibility data set. The data set consisted of fourteen years of meteorological data (1973-1986) for about 1600 stations in Europe. The European data set was extracted from the DATSAV global weather database maintained by the U.S. Air Force, ETAC, Scott Air Force Base. The raw meteorological data set consisted of over 1000 magnetic tapes containing about 30 gigabytes of data. The first step in the data processing involved compacting the data set into a binary form, which reduced the data size to 3 gigabytes. Next, from the daily visibility data, the quarterly cumulative distribution functions for extinction coefficient B_{ext} and visibility were computed. Most of the subsequent data filtering was performed using the distribution functions and the Voyager data exploration software. The resulting database is suitable for input to radiative transmission and transfer models, global climate models, air pollution studies, as well as to global biogeochemical explorations.

CUMPKR 008L YU S WIGMIBT183
DATA SPANS THE YEARS 1973-1986

Visibility Data Filters for Europe

Bret A. Schichtel and Rudolf B. Husar

Center for Air Pollution Impact and Trend Analysis
Washington University
St. Louis, MO 63130

GEOPHYSICS LABORATORY
AIR FORCE SYSTEMS COMMAND
UNITED STATES AIR FORCE
HANSCOM AIR FORCE BASE, MA 01731-5000

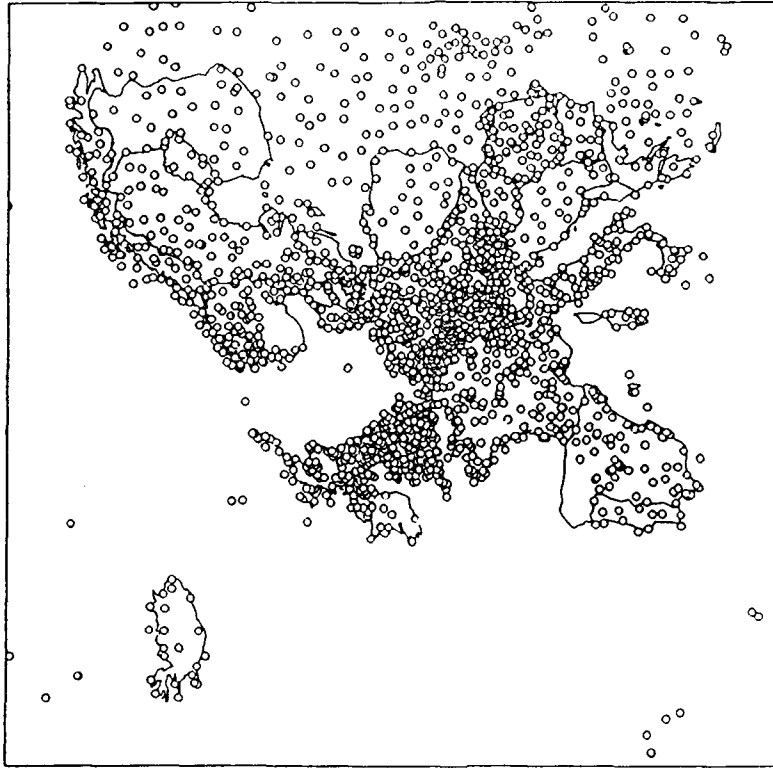
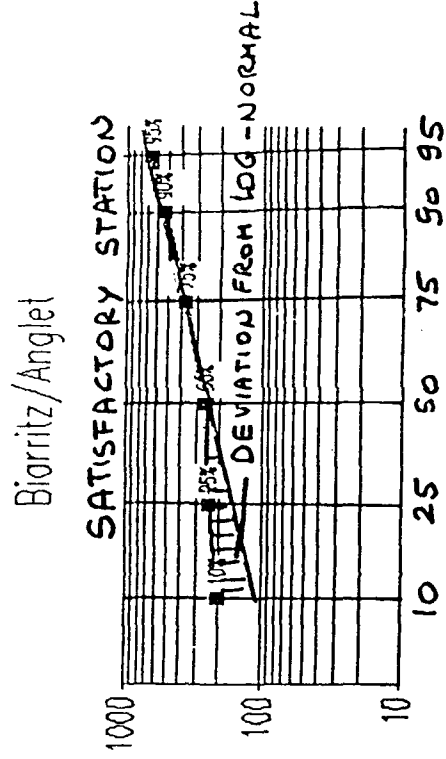
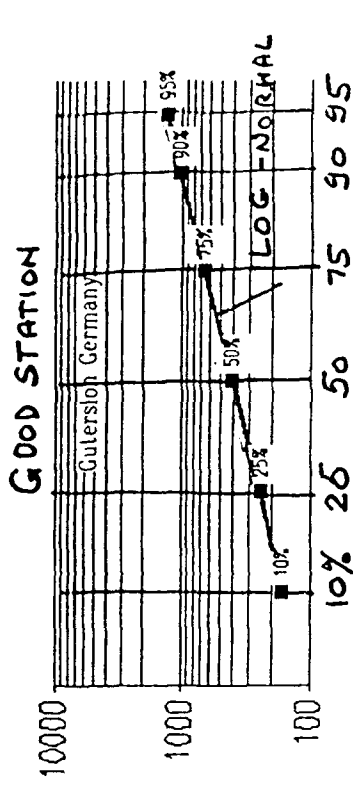


Figure 17. Location of the 1600 stations before the filters were applied.

CUMULATIVE DISTRIBUTION FUNCTIONS
for EXTINCTION COEFFICIENT



B e x i - 1 0 - 6 m c - 1

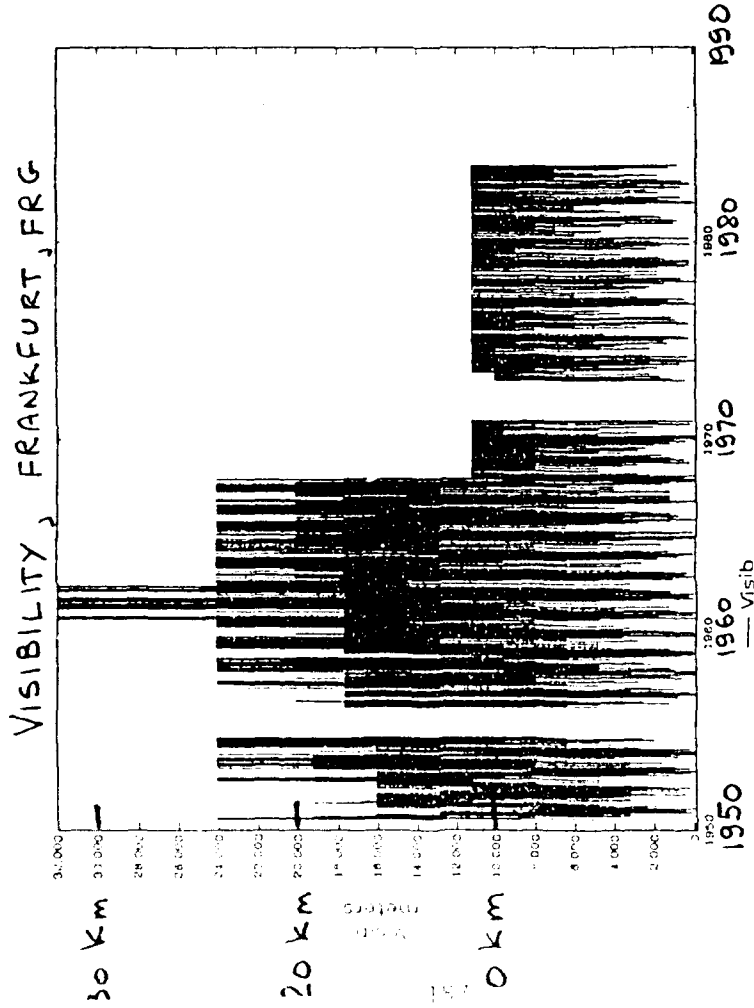


Figure 1. Trend of visual range for Frankfurt, FRG. Note the threshold visibility at 11000 m after 1968. Prior to 1968, the threshold was variable.

TREND OF PERCENTILES

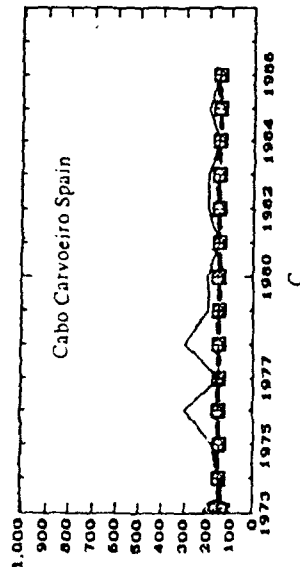
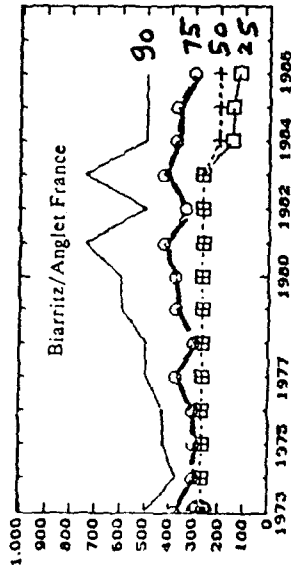
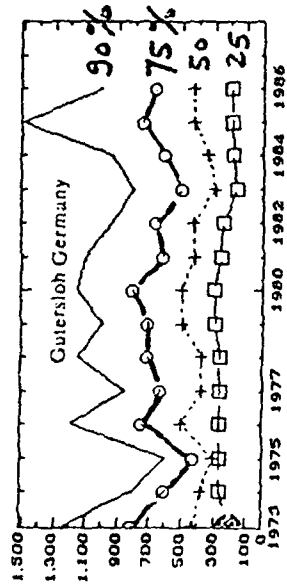


Figure 4. Time trend of Bext percentiles for a good (a), satisfactory (b) and a poor (c) station.

- The data cleaning filters fell into three categories

1. Precipitation and humidity filter.
2. Filters based on the year to year fluctuation of the extinction coefficient.
3. Filters that eliminated entire station.

- The main cause for poor data is found to be the visibility threshold. The threshold is detected by examining the shape and time trend of the distribution function.

- It was determined that the 75 percentile of Bext is generally above the threshold value. Therefore, can be used to find unbiased results.

UNFILTERED DATA

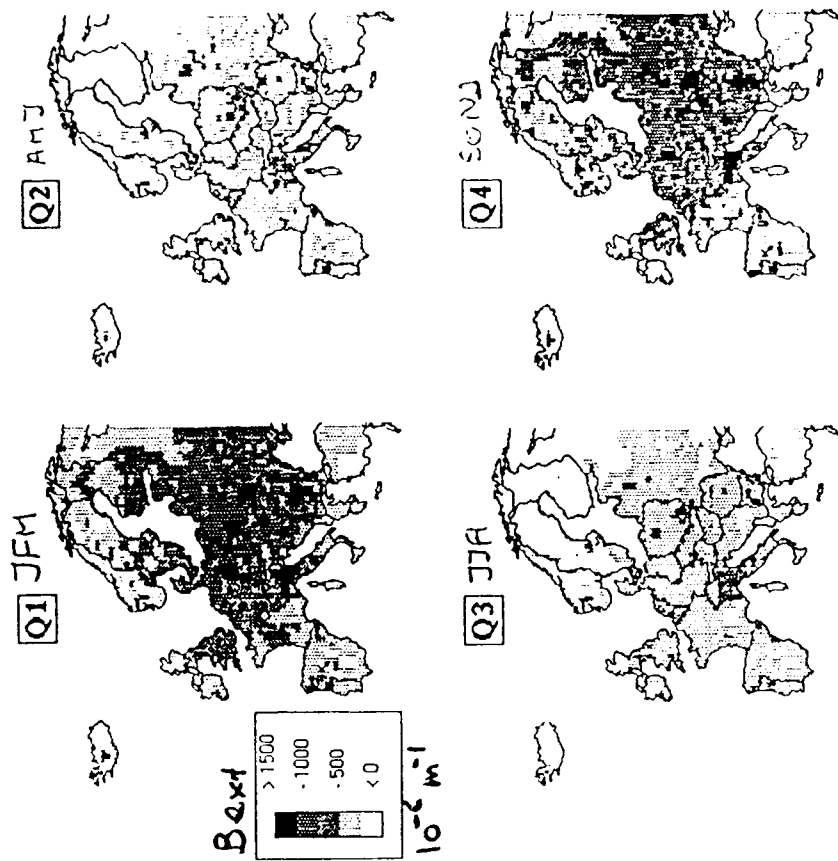


Figure 6. Contour maps of extinction coefficient (10^{-6} m^{-1}) for unfiltered data.

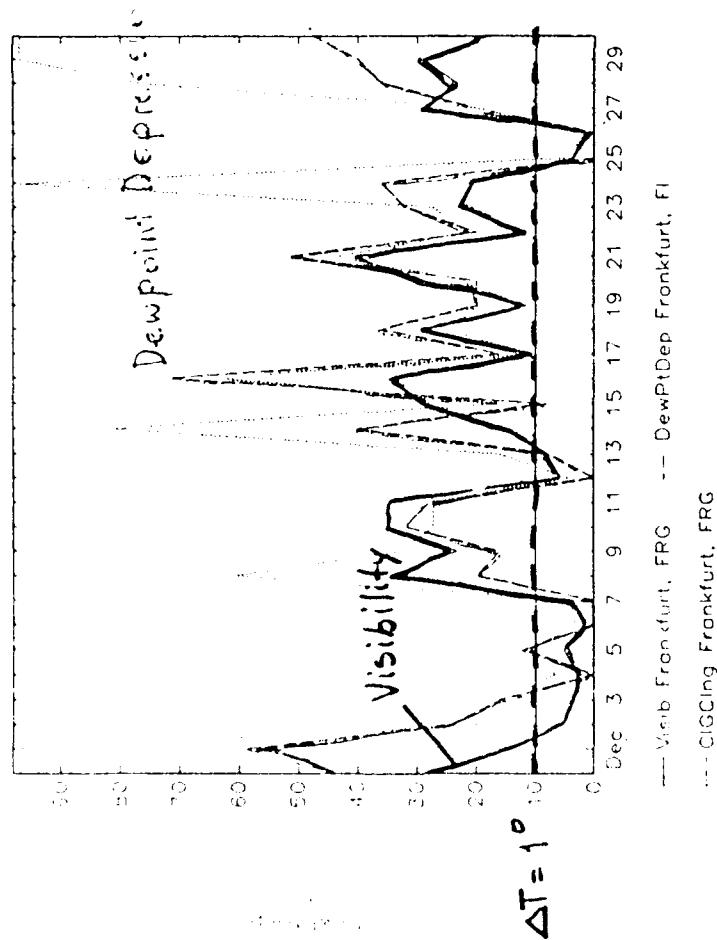


Figure 5. Time series of visibility, dew point depression, and ceiling for Frankfurt, FRG.

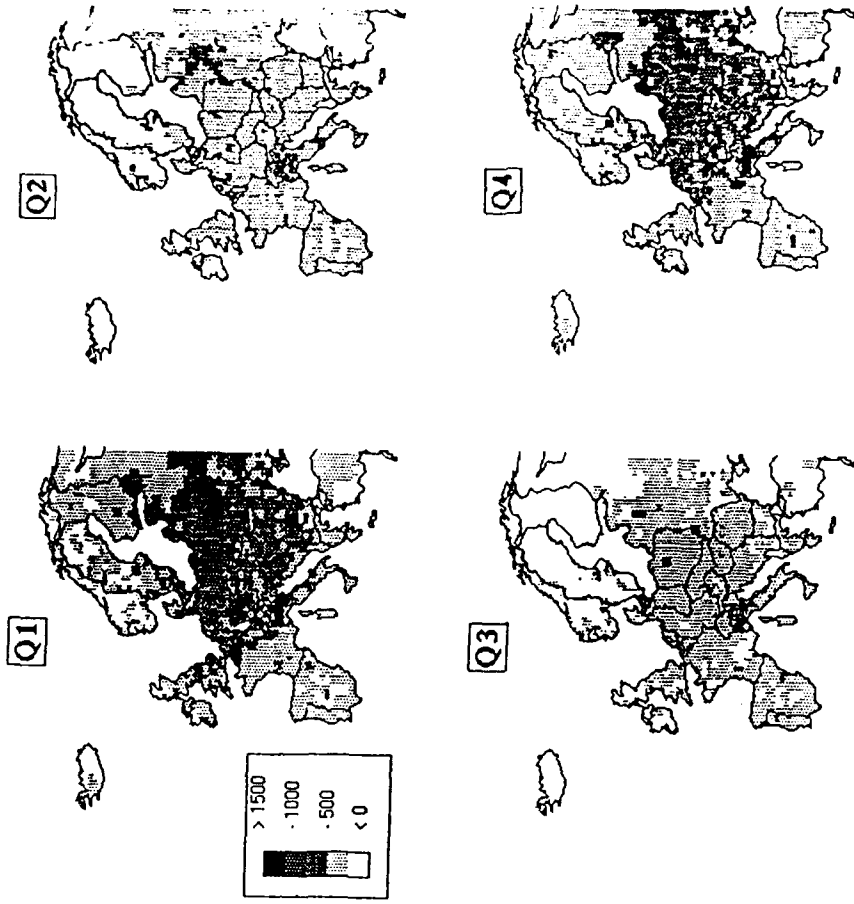


Figure 7. Some contour maps of extinction coefficient (10^{-6} m^{-1}) after imposing the precipitation and humidity filters.

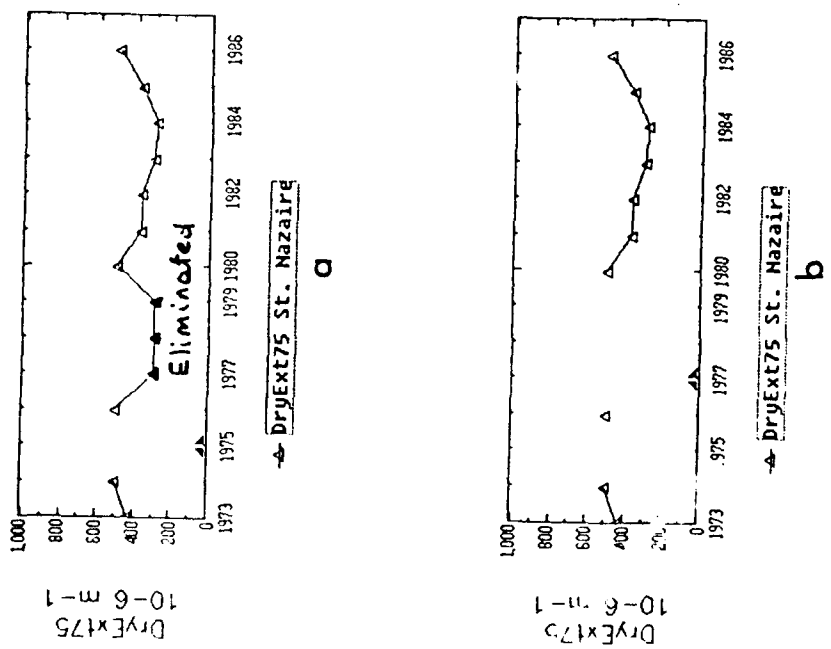
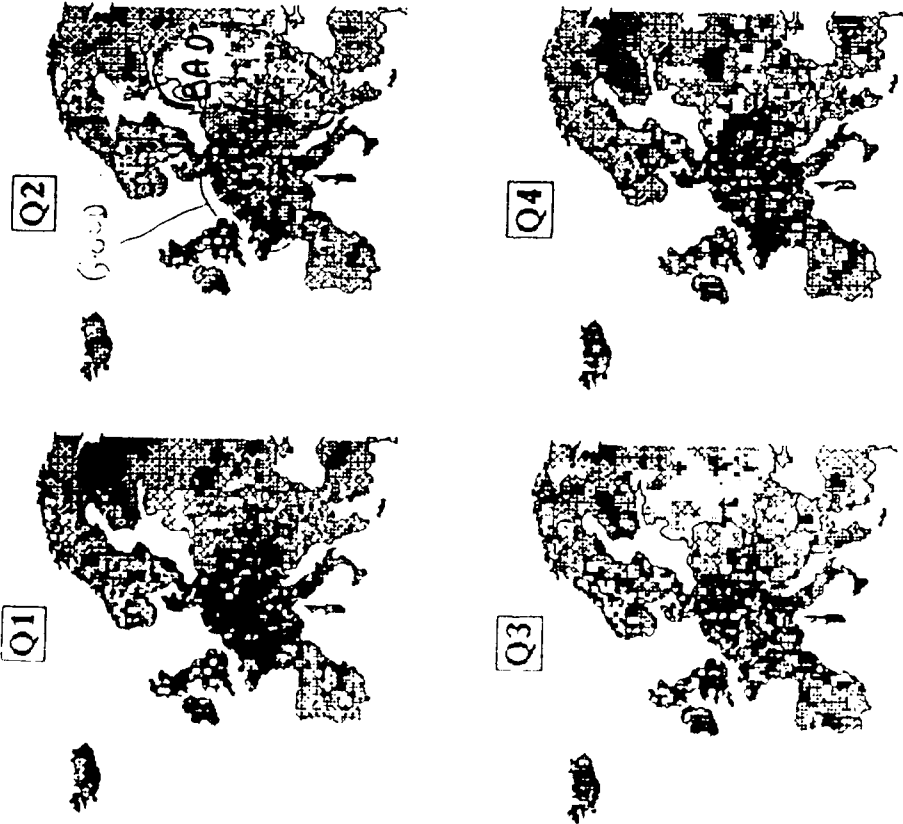


Figure 11. Threshold filter a) a time plot of a station before passing the threshold filter, b) after passing the threshold filter.

FRACTION OF DATA RETAINED
by TIME TREND FILTER



STATIONS REMOVED BY
STATION FILTER

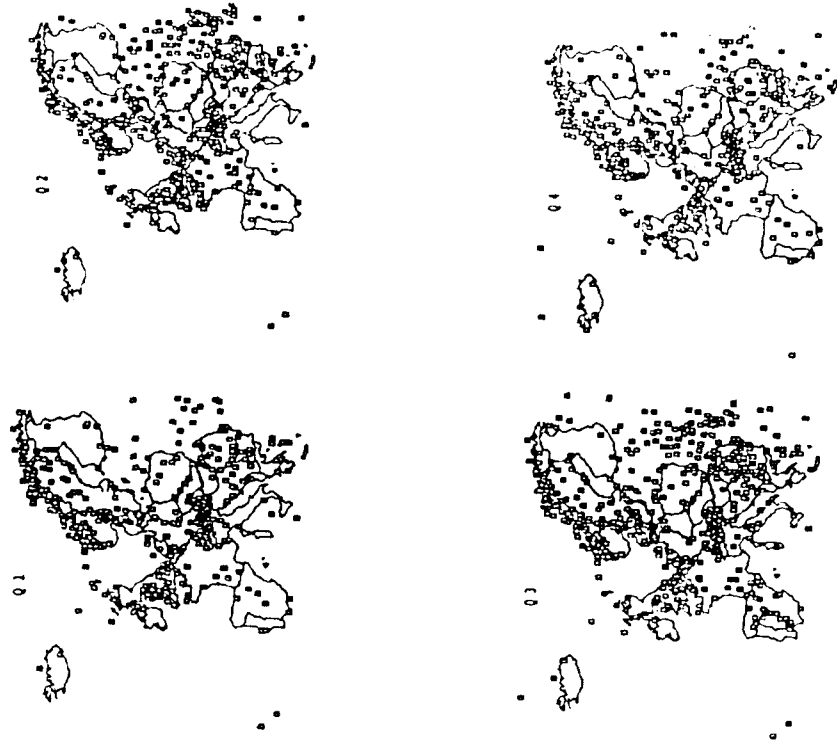
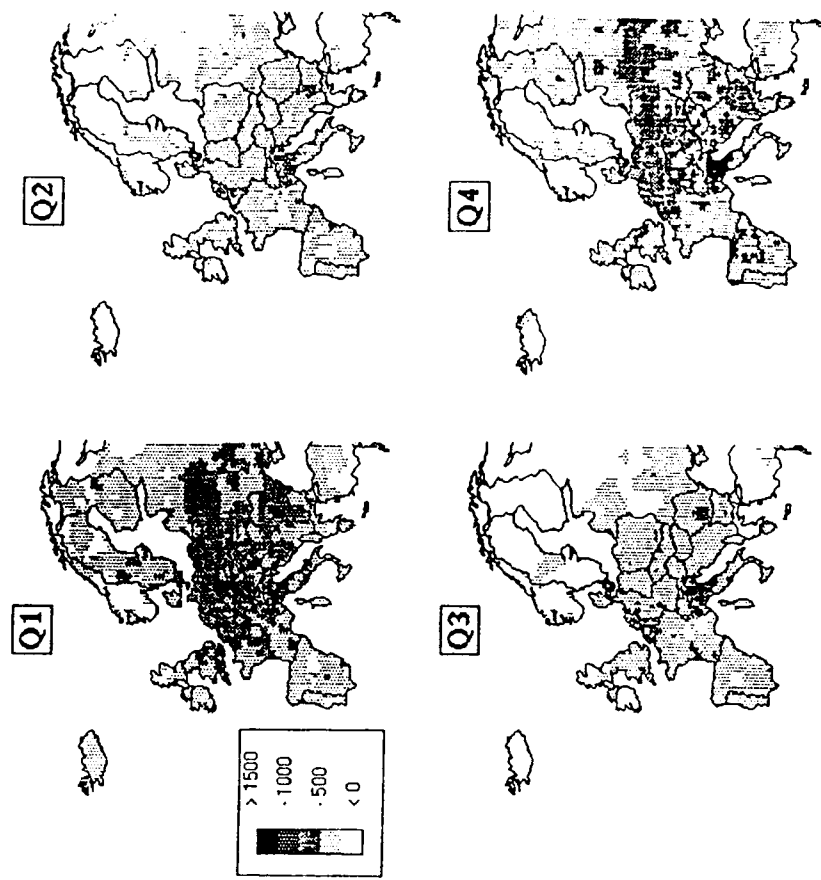


Figure 14. Ratio of the number of points after to the number of points before passing time trend filters.

Figure 18. Location of the stations containing data that were discarded by the station filters.

FINAL CLEANED BEXT MAPS



SUMMARY

Precipitation and humidity filter:

- Reduced the areas of highest Bext.
- Had most pronounced effect on quarters 1 and 4.

Time trend filters:

- Removed approximately 30% of data from each quarter.
- Had the largest effect in Eastern Europe

Station filters:

- About 24% of the stations were removed from each quarter.
- The coast of Norway, Alps region and southeastern Europe were most heavily effected.

Application of all filters:

- The basic contour of extinction over Europe did not change, but Bext was reduced between 20% and 50%.
- The extinction over Europe could be lumped into a hazier cold season and warm season.
- The largest extinction coefficient is observed over N. Italy and the "coal belt of Europe" between Great Britain, Germany and Poland.

Figure 19. Maps of filtered extinction coefficients for Europe.

**COMPARISON OF XSCALE 89 VERTICAL STRUCTURE
ALGORITHM WITH FIELD MEASUREMENTS**

R.P. Fiegel

U.S. Army Laboratory Command, Atmospheric Sciences Laboratory,
White Sands Missile Range, NM 88002

The visible extinction versus altitude data from the Meppen 1980 and Cardington 1984 balloon flight field tests are compared to the recent modifications in the below cloud (Case 2) vertical profile of XSCALE 89. The visibility and humidity data from the Sprakensehl 1983-1985 tower measurements are also compared to the low visibility (Case 1), below cloud (Case 2), and radiation fog (Case 3) model profiles of XSCALE 89. While certain days are not well modeled, we find good agreement overall.

Comparison of XSCALE 89
Vertical Structure Algorithm
with Sprakensehl Measurements

R. P. Fiegel
U.S. Army Atmospheric Sciences Laboratory
White Sands Missile Range, NM 88002-5501

Annual Review Conference
Atmospheric Transmission Models
5-6 June 1990

Comparison of XSCALE 89
Vertical Structure Algorithm
with Sprakensehl Measurements

R. P. Fiegel
U.S. Army Atmospheric Sciences Laboratory
White Sands Missile Range, NM 88002-5501

XSCALE

- The U.S. Army Natural Aerosol Extinction Module of the EOSAEL program package.
- XSCALE calculates the transmittance through hazes, fogs, rain, and snow for wavelengths within the visible and IR regions.
 - The haze and fog models are based on Mie theory applied to particle size distributions.
 - The rain and snow models are based on empirical and semiempirical models.
 - XSCALE also calculates a vertical profile for hazes and fogs based on an empirical model.

This presentation focuses on a comparison of the XSCALE vertical profile with measurements made in the Federal Republic of Germany.

Recent Changes in XSCALE

1. Sub-cloud parameters changed to replace the explicit sub-cloud pedestal
2. The curvature of the sub-cloud relative humidity profile has been reversed (the curvature is now positive, not negative)
3. An inversion/radiation fog layer has been added
4. A clear air region has been appended above cloud and inversion layers
5. The FORTRAN code has been changed to reduce computation time

Does XSCALE now produce reasonable results?

Data Block

Ten minute averages and maximum and minimum values of:

- Ceiling height
 - Temperature
 - Dewpoint
 - Visibility
- at 6 heights: 2, 9, 80, 150, 225, 300 meters.
- Rejected if ceiling over 300 m.
 - 1066 blocks of ten minute averages.
 - 733 blocks with ceiling less than 300 m.

Sprakensehl Episode Characteristics

- Sprakensehl Type III.A.1
- Low visibility at the surface
- High visibility at 300 m
 - The tower spans the low visibility region.
- Episodes of 2 to 40 hour duration.
- From 9 to 225 m thick.
- Occurred during the period from March 1983 to December 1984.
- Primarily in November and December.
- Single episodes were found in January, March, May, July, and September.

XSCALE Input Parameters

- Ceiling height
- Cloud thickness
- Inversion height
- Surface extinction
- 300 m extinction 'clear air'

Test for Goodness of Fit

The reduced chi-square χ_r^2 is used:

$$\chi_r^2 = \sqrt{\frac{\sum_{i=1}^N (a_i (k_i - \bar{k}_i))^2}{\nu}}$$

where

N is the number of data points ($N = 6$)

k_i are the data points representing the extinction at the i^{th} level

\bar{k}_i is the modeled extinction at the i^{th} level, and

ν is the number of degrees of freedom:

$\nu = N - p$, where

p is the number of profile parameters determined from the set of data.

Clouds: $p = 4$.

Inversions: $p = 3$.

Test for Goodness of Fit

Path transmittance is calculated from data and model profile.

$$\bar{k} = \frac{1}{Z} \sum_{i=2}^N \frac{k_i + k_{i-1}}{2} (z_i - z_{i-1}) . \quad (2)$$

$$T = \exp(-\bar{k}Z) . \quad (3)$$

Where

k represents visible extinction,

z represents altitude,

T represents transmittance.

Test for Goodness of Fit

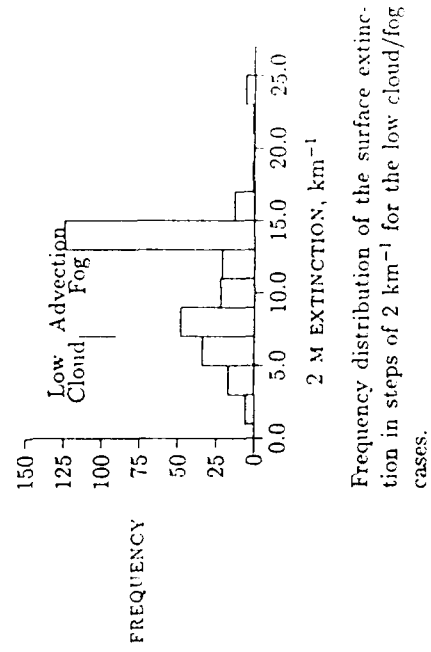
The v_1 is a weighting factor, we take it to be $1/\sigma_1$

The σ_1 is taken as the largest of:

- the manufacturer's stated instrument accuracy of 15 %, or
- the standard deviation estimated from the ten minute average, and extremes of a data block.

Surface Extinction for Clouds/Fogs

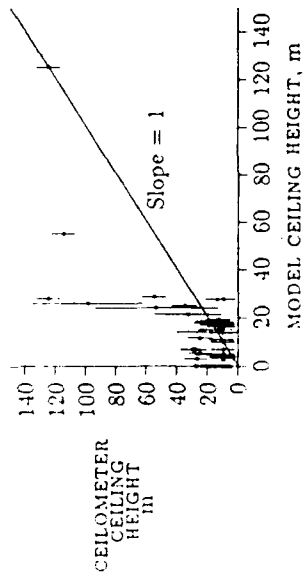
Representative Data Blocks



Of 733 low ceiling blocks

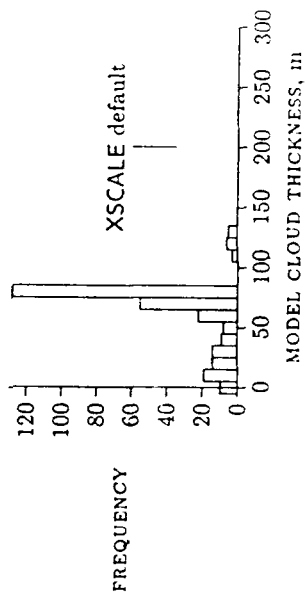
- 293 are representative of XSCALE Low cloud/Advection fogs.
- 119 are representative of XSCALE Inversion layer/Radiation fogs.
- 321 are not well modeled by XSCALE

Ceiling Height: Measured vs. Calculated



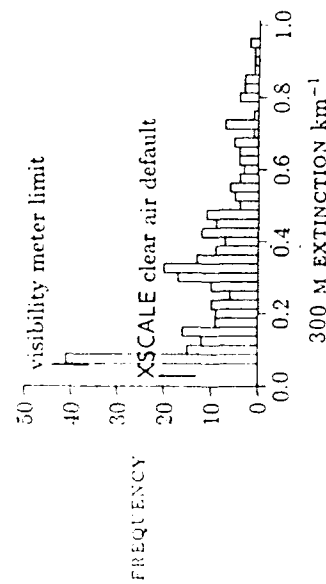
Comparison of the measured ceiling height (y -axis) with the 7 km^{-1} extinction ceiling height (x -axis). Agreement is demonstrated by the error bars overlapping the slope 1 line.

Cloud Thickness



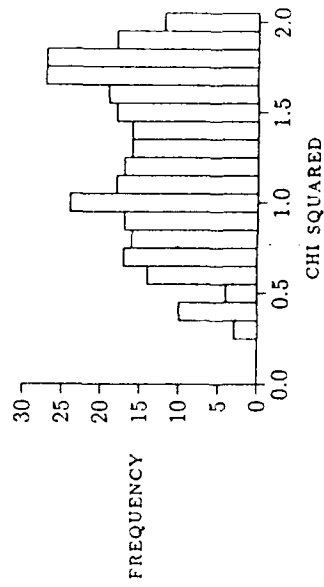
Frequency distribution of the cloud thickness which minimizes χ^2 in steps of 10 m for low cloud/fog cases.

Upper Air Extinction
for Low Clouds



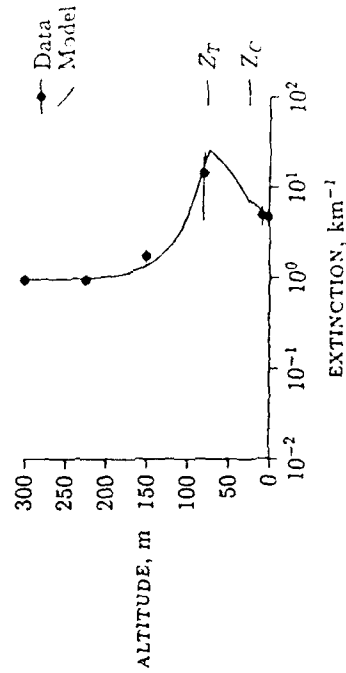
Frequency distribution of the upper air extinction in steps of 0.025 km⁻¹.

Cloud Profile χ^2 Values



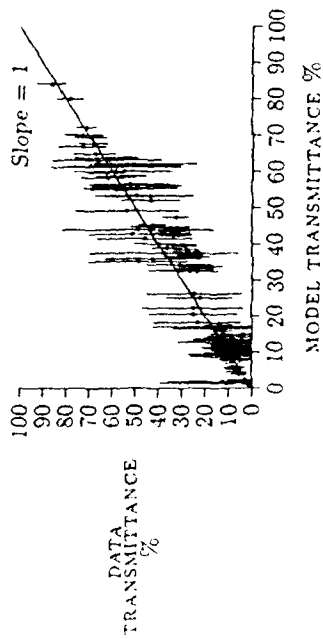
Frequency distribution of the χ^2 value in steps of 0.1 for the low cloud/fog cases.

Low Cloud Profile



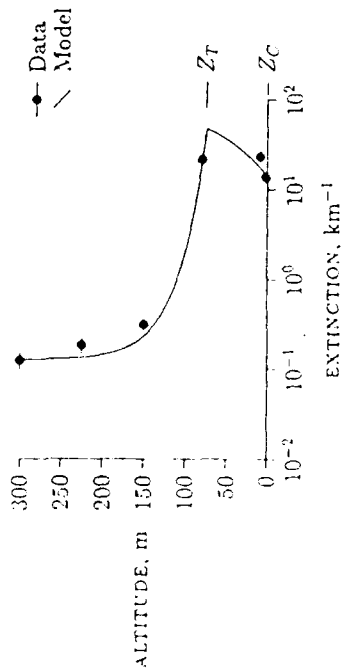
Low cloud profile, $\chi^2 = 1.0$, transmittance calculated from the data is $23 \pm 19\%$, from the model 18% . The measured ceiling is 35 ± 8 m, the calculated ceiling is 25 m, the cloud top is at 76 m.

Transmittance: Data vs. Model for Low Clouds



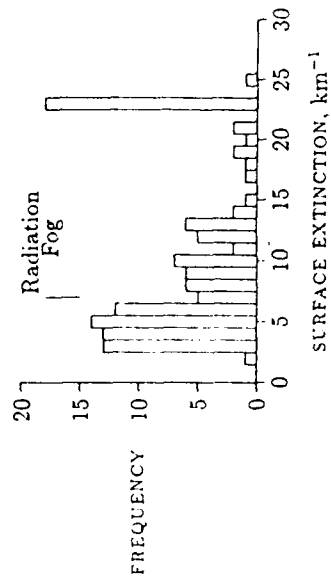
Transmittances determined from the measured visibilities (y-axis) versus transmittance calculated from the model extinction (x-axis), for the low cloud/fog cases. The line has slope 1.

Advection Fog Profile



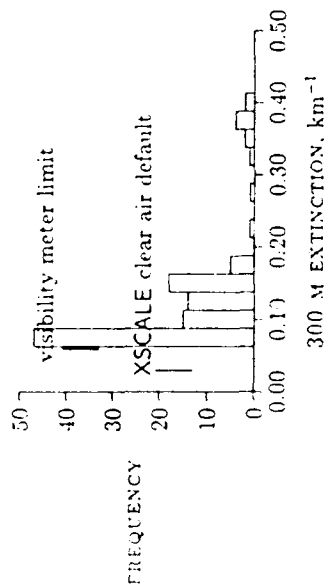
Advection fog profile. $\lambda^2 = 2.0$, transmittance calculated from the data is $8 \pm 3\%$, from the model 11% . The measured ceiling is 10 ± 8 m, the calculated ceiling is 9 m; the cloud top is at 75 m.

Surface Extinction for Inversion Layers



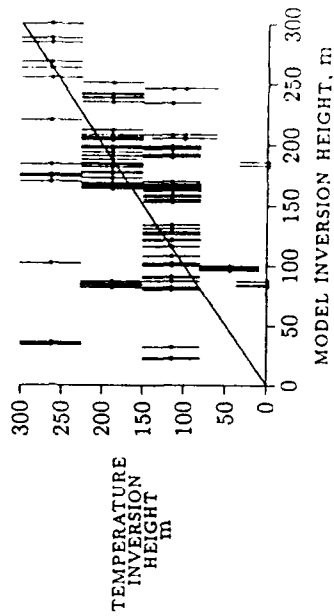
Frequency distribution of the surface extinction in steps of 1 km^{-1} for inversion layer cases.

Upper Air Extinction
for Inversion Layers



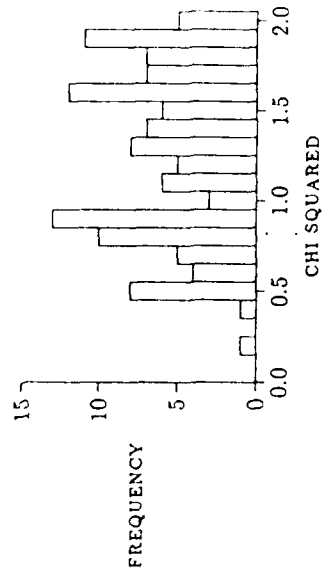
Frequency distribution of the upper air extinction in steps of 0.025 km^{-1} for inversion layer cases.

Inversion height:
Measured Temperature vs. χ^2 Calculation



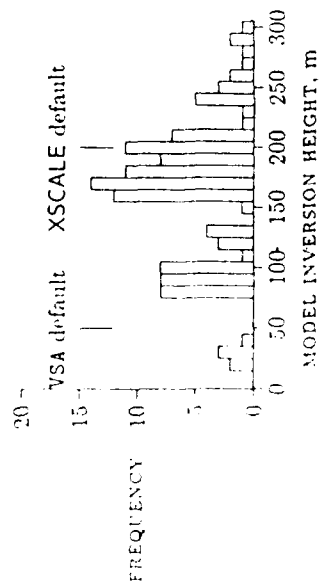
Inversion heights, Z_I , calculated from the measured temperature profile (y -axis) versus those determined to minimize χ^2 (x -axis). The line has slope 1, slightly more; its are within ~ 1 error bar of agreement that are farther away.

Inversion Profile χ^2 Values



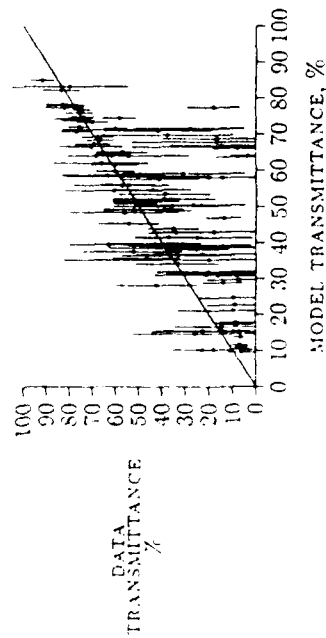
Frequency distribution of the χ^2 values for the inversion layer cases, in steps of 0.1.

Inversion Layer Height



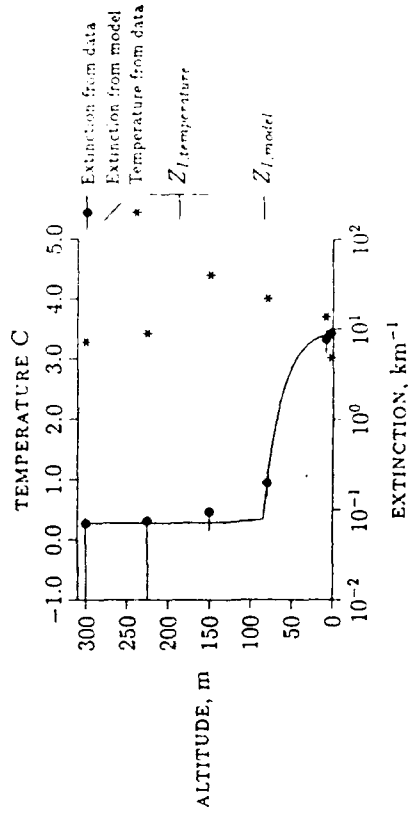
Frequency distribution of the inversion layer height determined to minimize χ^2 in steps of 10 m.

Transmittance: Data vs. Model
for Inversion Layers



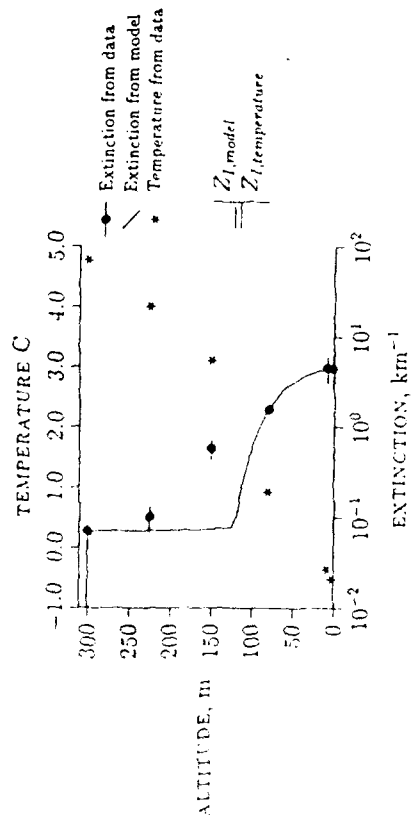
Transmittances determined from the measured visibilities (y-axis) versus transmittance calculated from the model extinctions (x-axis) for the inversion layer cases. The line has slope 1.

Inversion Profile
Good Fit



Inversion profile, $\chi^2 = 0.5$; transmittance calculated from the data is $70 \pm 8\%$, from the model 67% .

Inversion Profile Marginal Fit



Inversion profile, $\chi^2 = 2.0$, transmittance calculated from the data is $70 \pm 7\%$, from the model 73% .

Conclusions

- The profiles calculated by XSCALE are realistic.
 - Caveat: The default values represent only a single possible situation.
- 412 or 56 % of 733 data blocks were accurately modeled by one of the four XSCALE profiles.
- For a particular real situation **all** the input values are important.

SPATIAL NON-UNIFORMITY OF AEROSOLS AT THE 15,500 ft LEVEL

L.A. Mathews

Naval Weapons Center, Code 3892, China Lake, CA 93555

P.L. Walker

Physics Department, Naval Postgraduate School, Monterey, CA 93943

Longjump III meteorology was reported on previously*. This work presents the results of a more detailed analysis of the aerosol data. That data was obtained from aircraft at 15,500 feet over a 100 mile course between mountain peaks. Samples were taken at three minute intervals. In general more haze was associated with the mountain peaks than for the region between them. Extinction fluctuated at shorter intervals (10 miles) along the flight path possibly due to the uplifting action of convection cells, but superimposed on this is noise caused by the short sampling intervals. Visibility was highly nonuniform being dominated by molecular scattering punctuated by regions of lower visibility.

*Characterization of the Atmosphere for Longjump III, Mathews and Walker, IRIS, Ames Research Center, 16 March 1989.

**SPATIAL NON-UNIFORMITY OF AEROSOLS
AT THE 15,500 FOOT LEVEL**

by

I.A. Mathews
Research Department
Naval Weapons Center
China Lake, Calif. 93555

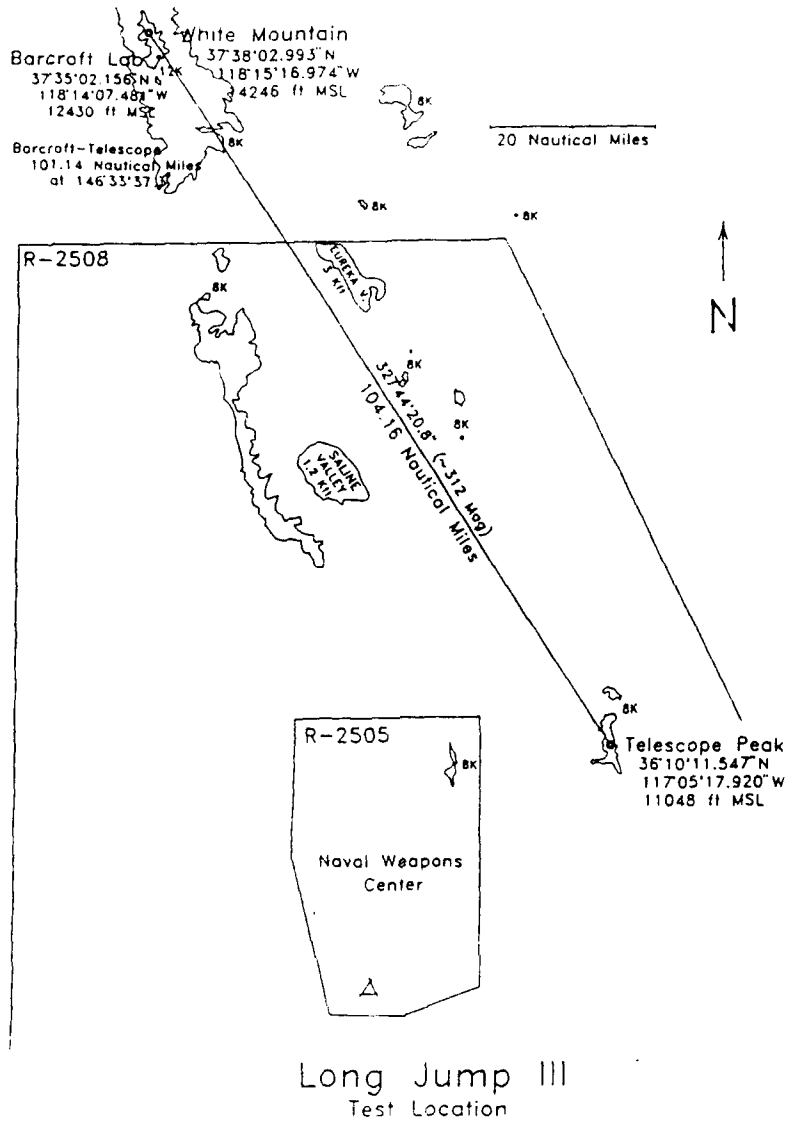
and

P.L. Walker
Physics Department
Naval Postgraduate School
Monterey, Calif. 93943



PROJECT LONG JUMP III

- **FIELD TEST OF VARIOUS DEVELOPMENTAL
INFRARED INSTRUMENTATION**
- **CONTROLLED AIRCRAFT TARGETS**
 - SPECIFIC FLIGHT PROFILES
 - 11,500 TO 15,500 FT
- **BARCROFT LABORATORY (ELEV. 12,470 FT)**
 - ABOVE MAJOR PORTION OF ATMOSPHERIC CONTAMINATES
 - PROVIDES A HORIZONTAL, CLEAR LINE OF SIGHT FOR
OVER 100 MILES



OBJECTIVE

TO DETERMINE:

- (1) OPTICAL PROPERTIES OF ATMOSPHERE ALONG THE FLIGHT PATH AND AT BARCROFT
- (2) OTHER METEOROLOGICAL PARAMETERS AT BARCROFT



BACKGROUND

- **LONG JUMP I**
 - METEOROLOGICAL DATA
 - NEPHELOMETER - VISIBILITY
 - IMMEDIATE BARCROFT AREA
- **LONG JUMP II**
 - METEOROLOGICAL DATA
 - NEPHELOMETER - VISIBILITY
 - AEROSOL SIZE DISTRIBUTION
 - IMMEDIATE BARCROFT AREA
 - MAY NOT REPRESENT LINE OF SIGHT
 - OROGRAPHIC EFFECTS
 - DIFFERENCES IN AIR PARCELS
- **LONG JUMP III**
 - AN INSTRUMENTATED AIRCRAFT WAS USED TO SAMPLE ALONG OR NEAR THE FLIGHT PATH



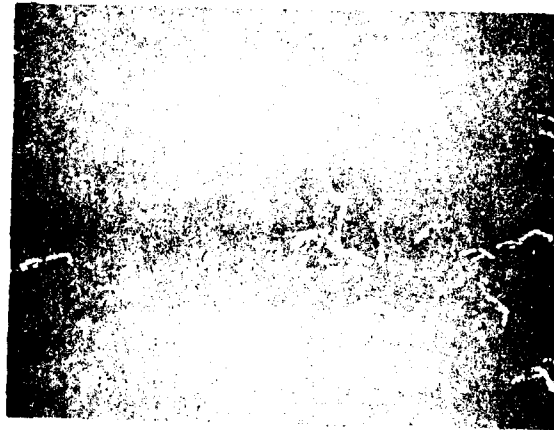
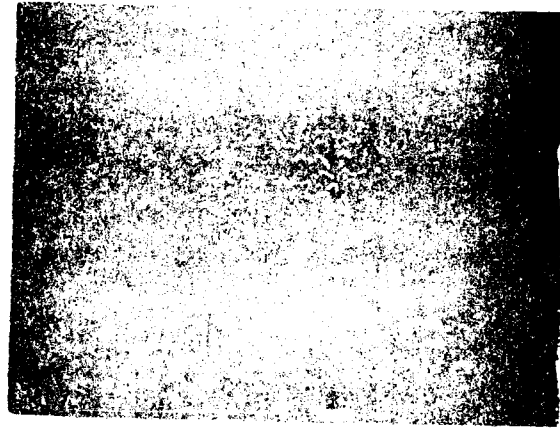
MEASUREMENTS

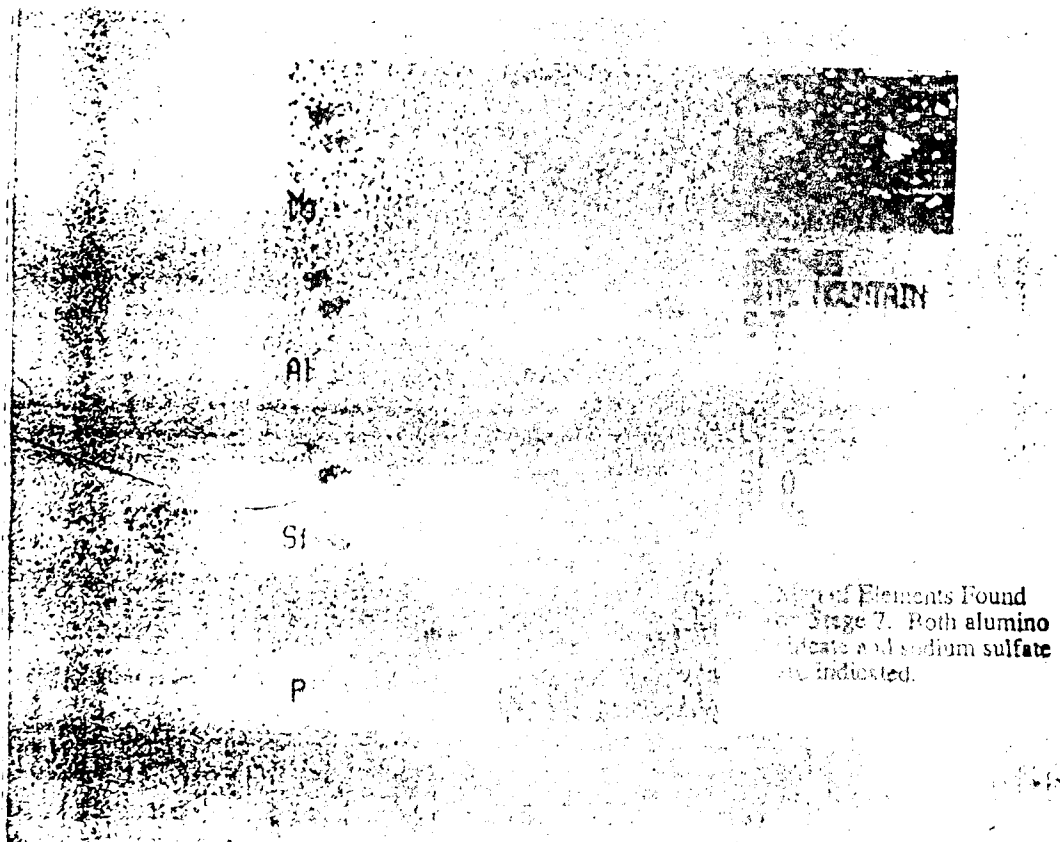
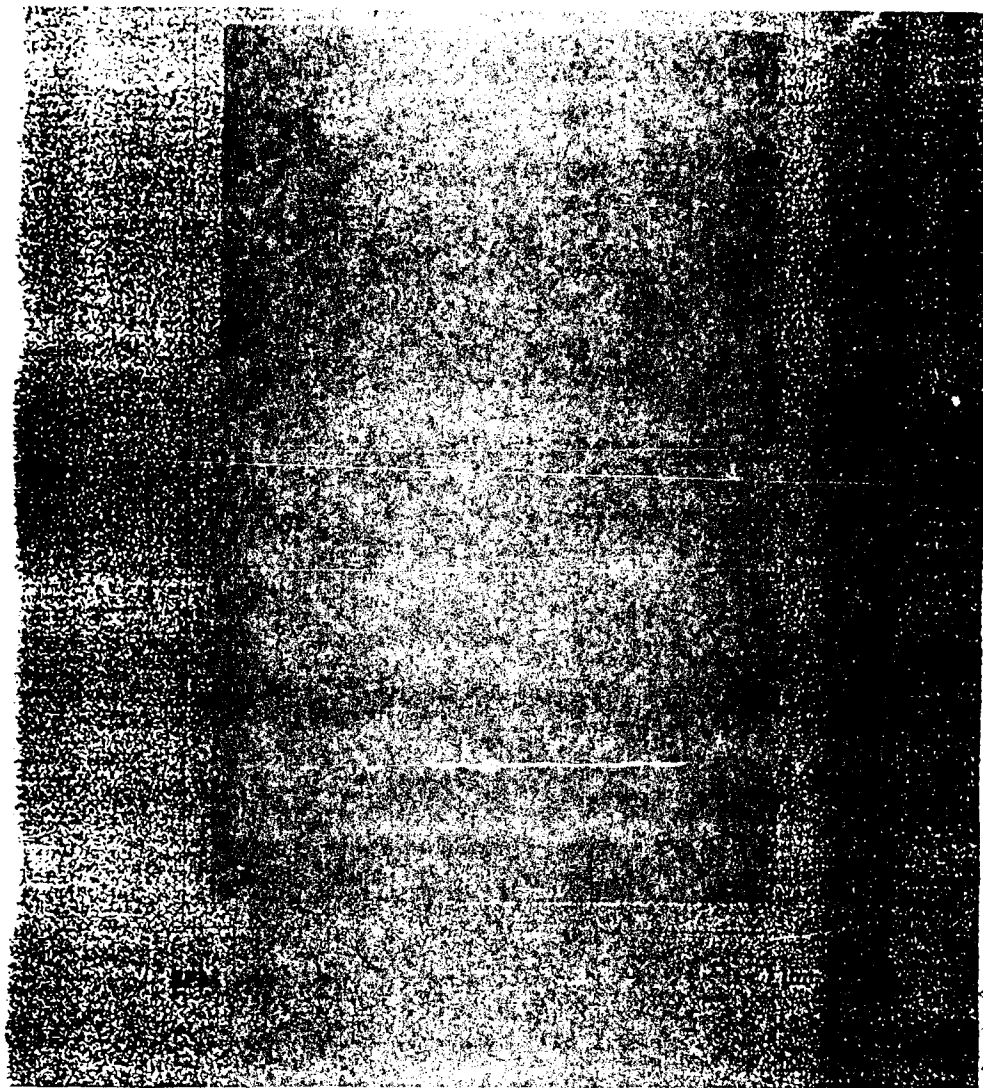
- **AT BARCROFT LABORATORY, THE FOLLOWING PARAMETERS WERE MEASURED**
 - AEROSOL PARTICLE SIZE DISTRIBUTION
 - PARTICLE SCATTERING COEFFICIENT (NEPHELOMETER)
 - RELATIVE HUMIDITY (WET AND DRY BULB TEMPERATURES)
 - AIR TEMPERATURE VERSUS SOIL SURFACE TEMPERATURE
 - INSOLATION
 - WIND SPEED AND DIRECTION
- **OVER BARCROFT AND ALONG THE FLIGHT PATH, THE FOLLOWING PARAMETERS WERE MEASURED:**
 - AEROSOL PARTICLE SIZE DISTRIBUTION
 - AEROSOL CHEMICAL COMPOSITION
 - AIR TEMPERATURE AND DEW POINT
 - CARBON DIOXIDE CONTENT

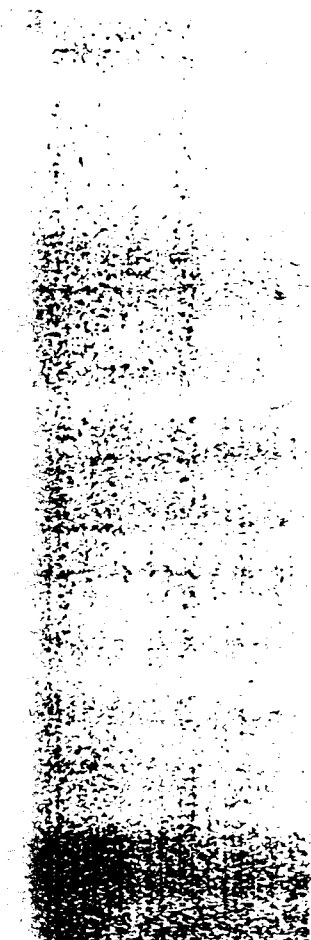


CALCULATED

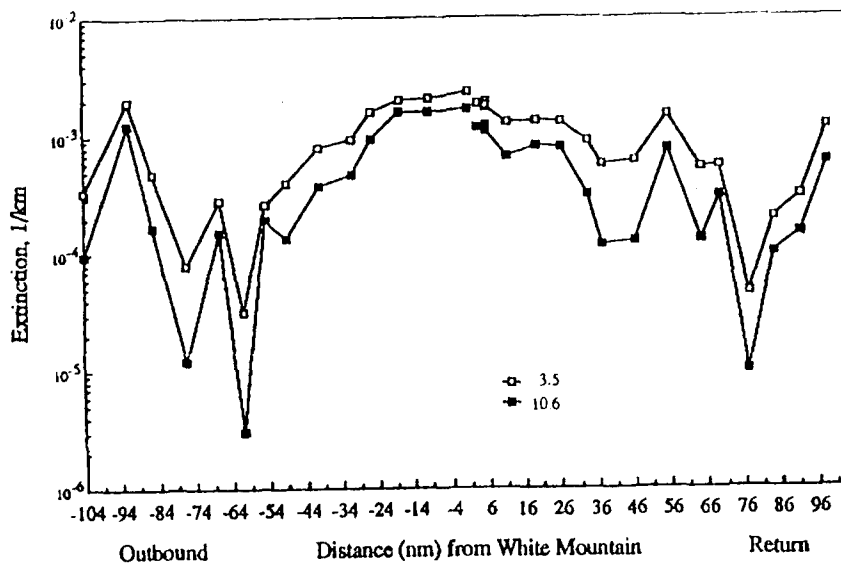
- CALCULATION OF SCATTERING AND ABSORPTION COEFFICIENTS FOR TYPICAL ENVIRONMENTAL PARTICLE WAVELENGTHS
- MIE CODE FROM ECH
- INPUT
 - RELATIVE HUMIDITY
 - PARTICLE SIZE DISTRIBUTION
 - REFRACTIVE INDICES



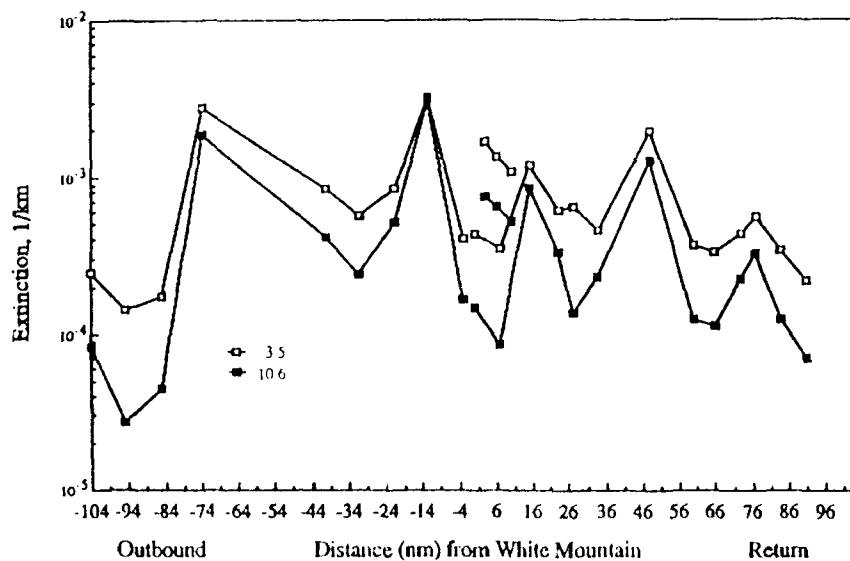




Extinction for Met Flight 5 at 1627 to 1754 PDT on 18 August



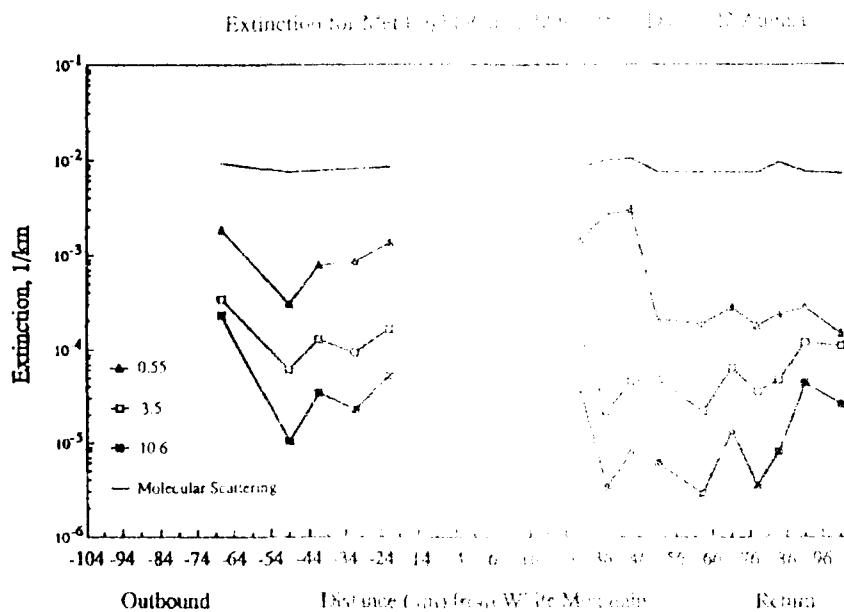
Extinction for Met Flight 6 at 0813 to 0947 PDT on 19 August



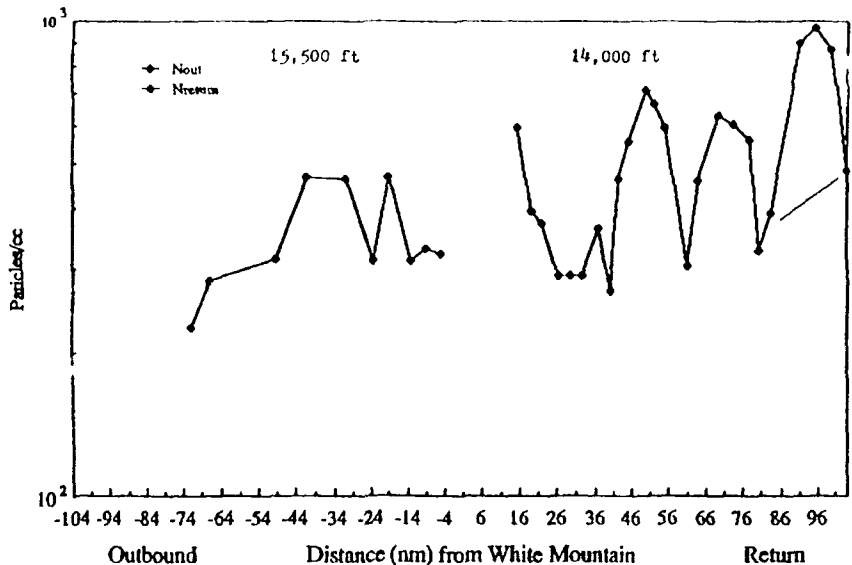


Possible causes of fluctuations are

1. **Noise.** APS33 integration time per data point was 2 min. and that of the EAA was 1 min., but periodicity of the data is about 6 min.
2. **Terrain contour effects.** Aerosols may be concentrated in the vicinity of 7000 ft peaks along flight path and depleted elsewhere.
3. **Convection cells.** Cells can be expected to be 5 to 15 nm wide over the desert, during summertime conditions.



Accumulation Mode Aerosol Concentration from EAA Flight 15 at 1118 to 1238 PDT on 25 August



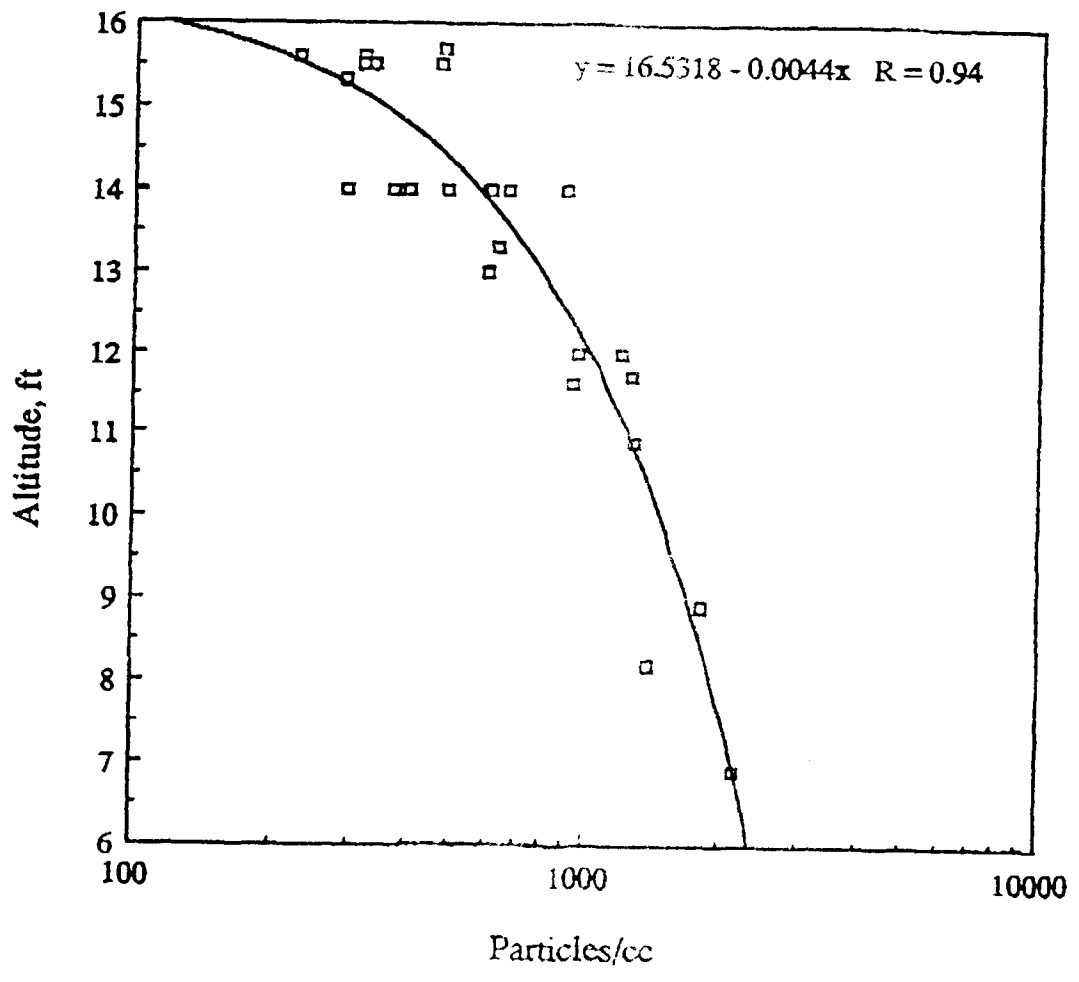
Fluctuation Widths



Week 1. The average fluctuation width was 26.6 nm, which was determined from the extinction minima. The fluctuation widths were determined from the APS33 data.

Week 2. The average fluctuation width was 19.4 nm determined from the particle concentration minima of the higher resolution EAA data.

Accumulation Mode Particle Concentration vs Altitude for Flight 15.



A METHOD OF ESTIMATING SURFACE METEOROLOGICAL RANGES FROM SATELLITE AEROSOL OPTICAL DEPTHS

D.R. Longtin¹, E.P. Shettle^{2*}, and J.R. Hummel¹

(¹SPARTA, Inc., 24 Hartwell Avenue, Lexington, MA 02173, ²Geophysics Laboratory/OPA, Bedford, MA 01731)

Measurements of aerosol optical depth from NOAA Advanced Very High Resolution Radiometers (AVHRR) aboard polar-orbiting satellites have been used to estimate the surface meteorological range over oceans. To do this, a lookup table of optical depth versus meteorological range has been developed which is based on the aerosol extinction profiles in LOWTRAN 7. To better simulate conditions over oceans, the boundary layer height has been lowered to 0.5 km and an extinction profile corresponding to a 150 km meteorological range has been added.

The lookup table has been applied to AVHRR aerosol optical depths near selected island locations where, in turn, the inferred meteorological ranges were validated against surface observations. Results show reasonable success in locating regions where meteorological ranges exceed 30 km, but more precise classification may not be possible due to uncertainties in both the measurements and observations. Unfortunately, the algorithm does not fare as well when the observed meteorological ranges are less than 30 km.

*Now at NRL.

A METHOD OF ESTIMATING SURFACE METEOROLOGICAL RANGES FROM SATELLITE AEROSOL OPTICAL DEPTHS

Presented at
The Annual Review Conference on Atmospheric Transmission Models
June 6, 1990

David R. Longtin¹, Eric P. Shettle² and John R. Hummel¹

¹SPARTA, Inc.
24 Hartwell Avenue
Lexington, MA 02173

²Naval Research Laboratory, Code 6520
Washington, D.C. 20375

Contract F19628-88-C-0038



PURPOSE OF RESEARCH



- Determine Whether Measurements of Aerosol Optical Depth From Polar-Orbiting Satellites Can Be Used to Estimate Surface Meteorological Ranges Over Oceans
- These Are Preliminary Results



METHODOLOGY



- Obtain Experimental Global Sets of Aerosol Optical Depth Over Oceans From NOAA/NESDIS
- Develop a Lookup Table of Surface Meteorological Range Versus Aerosol Optical Depth
- Extract Aerosol Optical Depths Near Islands and Convert Them to Surface Meteorological Ranges
- Validate Inferred Surface Meteorological Ranges with Observed Values



DESCRIPTION OF AEROSOL OPTICAL DEPTHS

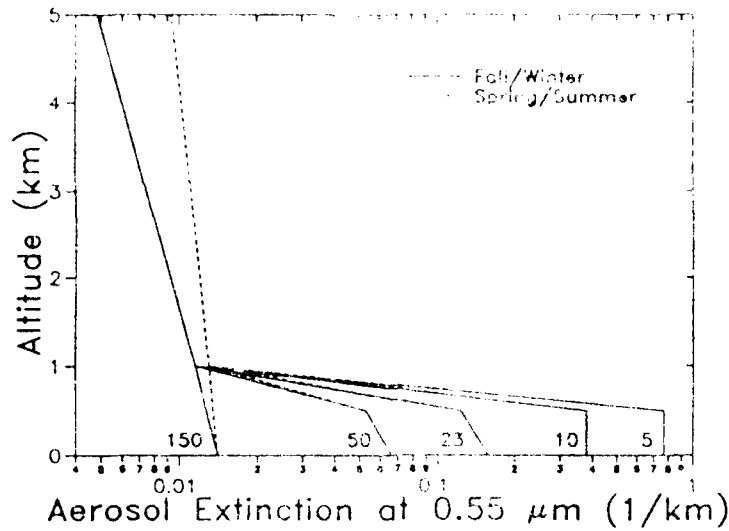


- Based on Radiance Measurements From the Advanced Very High Resolution Radiometer (AVHRR) Aboard NOAA Sun-Synchronous Polar-Orbiting Satellites
- Retrieval Algorithm Relates Aerosol Optical Depth to the Upwelling Radiation in Channel 1 ($0.58 \mu\text{m}$ - $0.68 \mu\text{m}$)
- Measurements Are Taken When NOAA Satellites Cross the Equator (About 13:30 Local Time)
- Reported Aerosol Optical Depths Are Scaled to $0.50 \mu\text{m}$



SPARTA INC.

ASSUMED AEROSOL PROFILES FOR FIXED SURFACE METEOROLOGICAL RANGES



Note: Profiles Based on Modified Shettle and Fenn (1976)

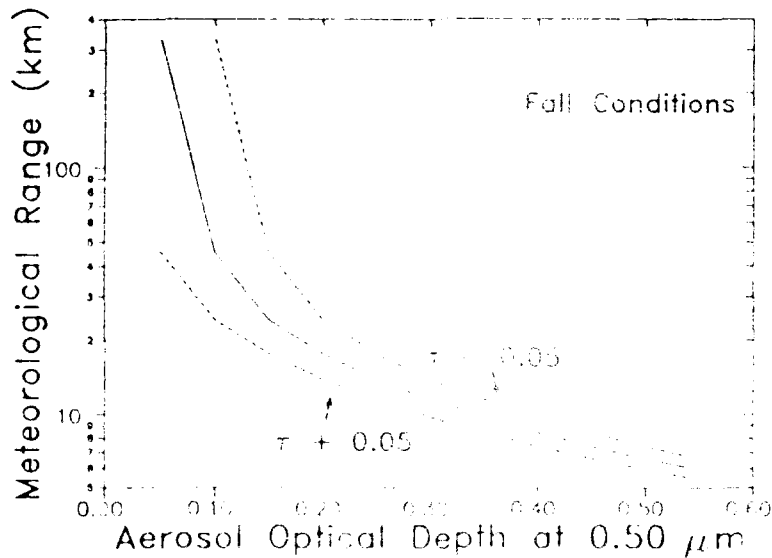
Note: Profiles Are For Surface Meteorological Ranges of 150, 50, 23, 10 and 5 km

Note: Surface Meteorological Range Equals $3.912/\text{Total Extinction at } 0.55 \mu\text{m}$



SPARTA INC.

CALCULATED OPTICAL DEPTH VERSUS SURFACE METEOROLOGICAL RANGE



Note: Dashed Lines Establish a Range of ± 0.05 Disturbances in the AVHRR Measurements ($\tau = 0.05$)



SPARTA INC.

VALIDATION SCHEME

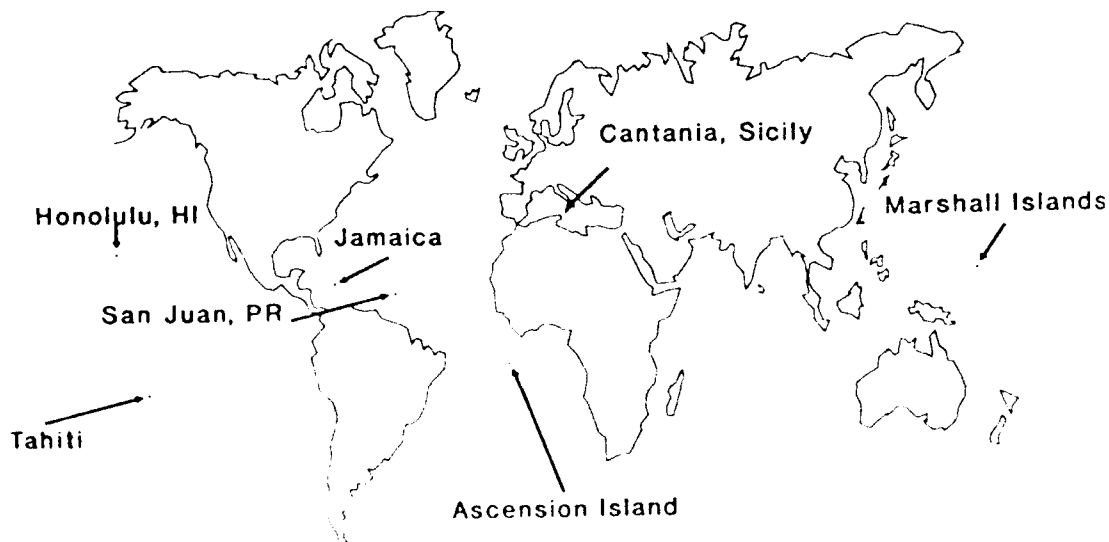


- Compute Daily Averages of Aerosol Optical Depth Near Island Locations
 - Use All Available Data Within 5 Degrees of Each Island
- Omit Those Daily Averages Having Excessive Variability
- Convert Average Optical Depths to Inferred Meteorological Ranges Using Lookup Table
- Obtain Observed Meteorological Ranges For Days When Inferred Values Are Available
 - Based on Observations of Surface Visibility Provided by USAFETAC
- Determine the Number of Times When the Inferred and Observed Meteorological Ranges Are in Agreement



SPARTA INC.

ISLAND LOCATIONS USED FOR VALIDATION STUDIES

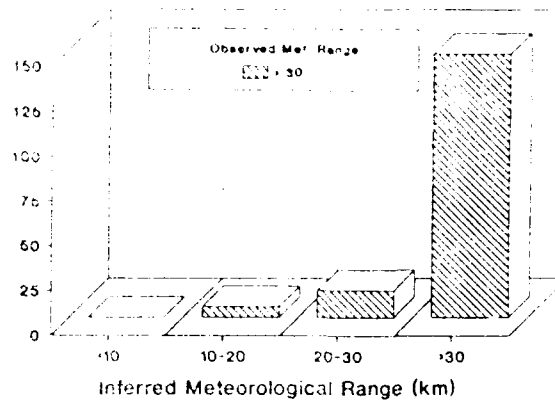
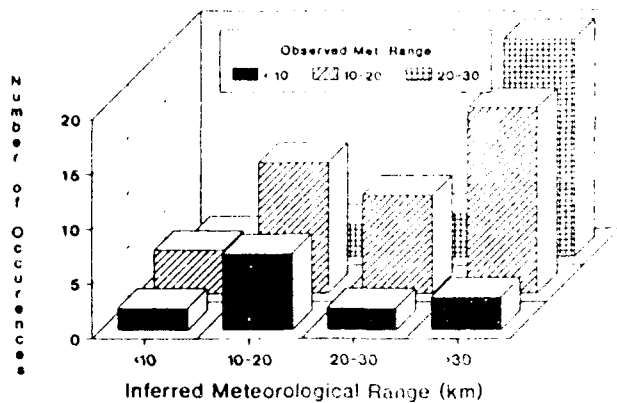




HISTOGRAMS OF INFERRED AND OBSERVED METEOROLOGICAL RANGE



SPARTA INC.



Inferred

	<10	10-20	20-30	>30
Observed < 10	2	7	2	3
Observed 10-20	4	12	9	17
Observed 20-30	2	3	4	20
Observed > 30	0	6	15	147



FACTORS LIMITING VALIDATION FOR METEOROLOGICAL RANGES ≥ 30 KM



- Island Locations Often Lack Reference Points for Very Clear Conditions
- Maximum Reported Meteorological Range Is Station Dependent
 - Marshall Islands: 31 km
 - Honolulu, HI: 52 km
 - Cantania, Sicily: 39 km
 - Jamaica: 39 km
 - San Juan, PR: 46 km
 - Tahiti: 52 km
 - Ascension Island: 97 km
- For Very Clear Conditions, Average Optical Depths Are Similar In Magnitude to the Uncertainty in the AVHRR Aerosol Optical Depths (± 0.05)



SPARTA INC.

CONCLUSIONS



- Reasonable Success in Locating Regions Where Meteorological Ranges Exceed 30 km
 - More Precise Classification May Not Be Possible Due To Uncertainties in Both the Measurements and Observations
- Limited Success in Locating Regions of Low Meteorological Range
 - High Meteorological Ranges Are Often Inferred When the Observed Value is Below 20 km, Possibly Due To Inhomogeneties in Aerosol Loading
 - Improved Results Could Be Expected If It Were Possible to Define the Top of the Boundary Layer More Accurately

A COMPARISON OF THE UVTRAN AND LOWTRAN 7 AEROSOL MODELS

S. O'Brien

Las Cruces Scientific Consulting, Las Cruces, NM 88001

A comparison between aerosol model results used by the AFGL LOWTRAN 7 and ASL UVTRAN models is examined for a variety of surface visibilities. Recent semiempirical results from particle sizing problems operated near the surface at the White Sands Missile Range are also compared with the model results.

A Comparison of the UVTRAN and LOWTRAN 7 Aerosol Models

Sean G. O'Brien
Las Cruces Scientific Consulting
6 June 1990

Summary of Presentation

- Description of UVTRAN aerosol model
- Description of LOWTRAN 7 aerosol models
- Review of past UVTRAN - LOWTRAN aerosol comparisons
- Comparison of UVTRAN and LOWTRAN 7 for sea level aerosols
- Comparison of UVTRAN and LOWTRAN 7 for elevated desert aerosols
- Comparison of model results with measurements made in an elevated desert region
- Conclusions

UVTRAN Aerosol Model

- References: E.M. Patterson, "Ultra-Violet Atmospheric Propagation Model," Final Report on Project DAAL03-86-D-001 Delivery Order 0578 (1988)

E.M. Patterson and J.B. Gillespie, Appl. Opt. 28, p. 245 (1989)
- Aerosol model spans 185 to 700 nm wavelength region
- Aerosol extinction is dominant in the 300 to 700 nm region

UVTRAN Aerosol Model

- Rayleigh molecular scattering $k_{\text{mol}}^{\text{sca}}$ is given by

$$k_{\text{mol}}^{\text{sca}} = \frac{1}{\lambda^4} \frac{0.987}{9.26 \times 10^{18} - (1.07 \times 10^9 / \lambda^2)} \frac{N}{N_0}$$

- Aerosol extinction $k_{\text{aer}}^{\text{ext}}$ is then given by

$$k_{\text{aer}}^{\text{ext}} = \left[\frac{3.912}{V} - k_{\text{mol}}^{\text{sca}}(550 \text{ nm}) \right] \left[\frac{550}{\lambda} \right]^q$$

where $q = 0.585 V^{1/3}$

LOWTRAN 7 Aerosol Models

- References: F.X. Kneizys, et al., LOWTRAN 6 technical report, AFGL-TR-83-0187 (1983)
 F.X. Kneizys, et al., "User's Guide to LOWTRAN 7," AFGL-TR-88-0177 (1988)
 D.R. Longtin, E.P. Shettle, J.R. Hummel, and J.D. Pryce, "A Wind Dependent Desert Aerosol Model: Radiative Properties," AFGL-TR-88-0112

- Models considered here:

<u>Sea Level</u>	<u>Elevated Desert</u>
Urban, 70% RH	Rural, 0% RH
Maritime, 70% RH	Desert, WS=0 m/s
Rural, 70% RH	

A Review of UVTRAN - LOWTRAN 6 Aerosol Comparisons

- From Patterson and Gillespie, 1989
- Conditions: AFGL Rural aerosol model, 70% RH
 P = 1013 mb, T = 288°K
 $V_{550} = 23$ km

• Results:	Wavelength (nm)	k_{ext} (km^{-1})	
		<u>UVTRAN</u>	<u>LOWTRAN 6</u>
	300	0.434	0.275
	550	0.158	0.158
	700	0.106	0.118

UVTRAN - LOWTRAN 6 Comparison (continued)

- Reference: W.A. Baum and L. Dunkelman, "Horizontal Attenuation of Ultraviolet Light by the Lower Atmosphere," JOSA 45, 166 (1955)
- Results shown here are from Patterson and Gillespie, 1989

V_{550} (km)	$k_{ext} (km^{-1})$ at 350 nm		
<u>UVTRAN</u>	<u>LOWTRAN 6</u>	<u>B-D</u>	
100	0.092	0.042	0.097
40	0.212	0.134	0.198
20	0.376	0.288	0.366
10	0.691	0.594	0.702
5	1.21	1.20	1.38

Comparison of UVTRAN with LOWTRAN 7 Sea Level Aerosols

- Conditions: P = 1013 mb, T = 288°K, RH = 70%
- Results for 300 nm:

V_{550} (km)	$k_{ext} (km^{-1})$			<u>UVTRAN</u>
	<u>Urban</u>	<u>Maritime</u>	<u>Rural</u>	
5	1.27	0.966	1.34	1.41
10	0.625	0.475	0.660	0.814
23	0.261	0.198	0.275	0.433
50	0.109	0.0829	0.115	0.244

Comparison of UVTRAN with LOWTRAN 7 Sea Level Aerosols

- Results for 700 nm:

V_{550} (km)	$k \text{ (km}^{-1}\text{)}_{\text{ext}}$			UVTRAN
	Urban	Maritime	Rural	
5	0.594	0.702	0.576	0.605
10	0.292	0.345	0.283	0.280
23	0.122	0.144	0.118	0.106
50	0.0510	0.0602	0.0494	0.0393

Comparison of UVTRAN with LOWTRAN 7 Elevated Desert Aerosols

- Conditions: P = 880 mb, T = 303 °K, RH = 0%

- Results for 300 nm:

V_{550} (km)	$k \text{ (km}^{-1}\text{)}_{\text{ext}}$		UVTRAN
	Rural	Desert	
50	0.120	0.122	0.254
100	0.0517	0.0527	0.154
150	0.0290	0.0295	0.109

Comparison of UVTRAN with LOWTRAN 7 Elevated Desert Aerosols

- Results for 700 nm:

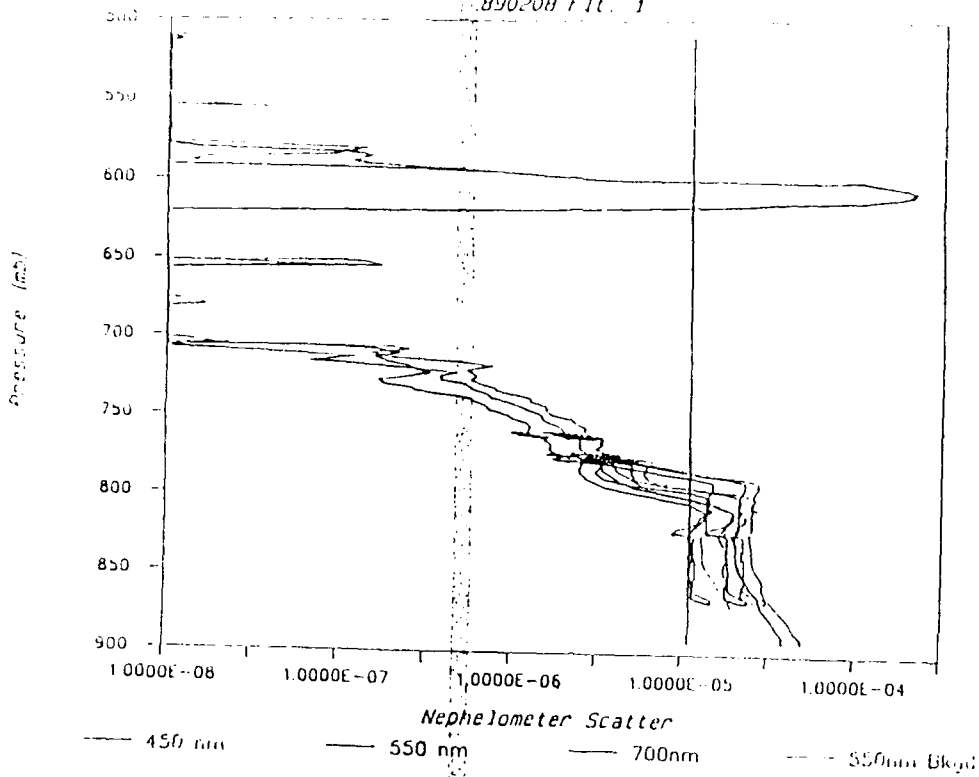
V_{550} (km)	Rural	Desert	UVTRAN
50	0.0514	0.0493	0.0409
100	0.0221	0.0212	0.0154
150	0.0124	0.0119	0.00785

Comparison of Model Results with Elevated Desert Measurements

- References: J. Boatman, D. Wellman, and B. Bodhaine of NOAA/WPL, D. Garvey of ASL, private communications, 1989
S. O'Brien and D. Longtin, OMI-371, 1989
- Measurements examined here are of two kinds:
 - Aircraft three color nephelometer that provided aerosol scattering at 450, 550, and 700 nm
 - Surface Knollenberg particle sizing probes (LAS-X type) that provided size distribution inputs for Mie computations

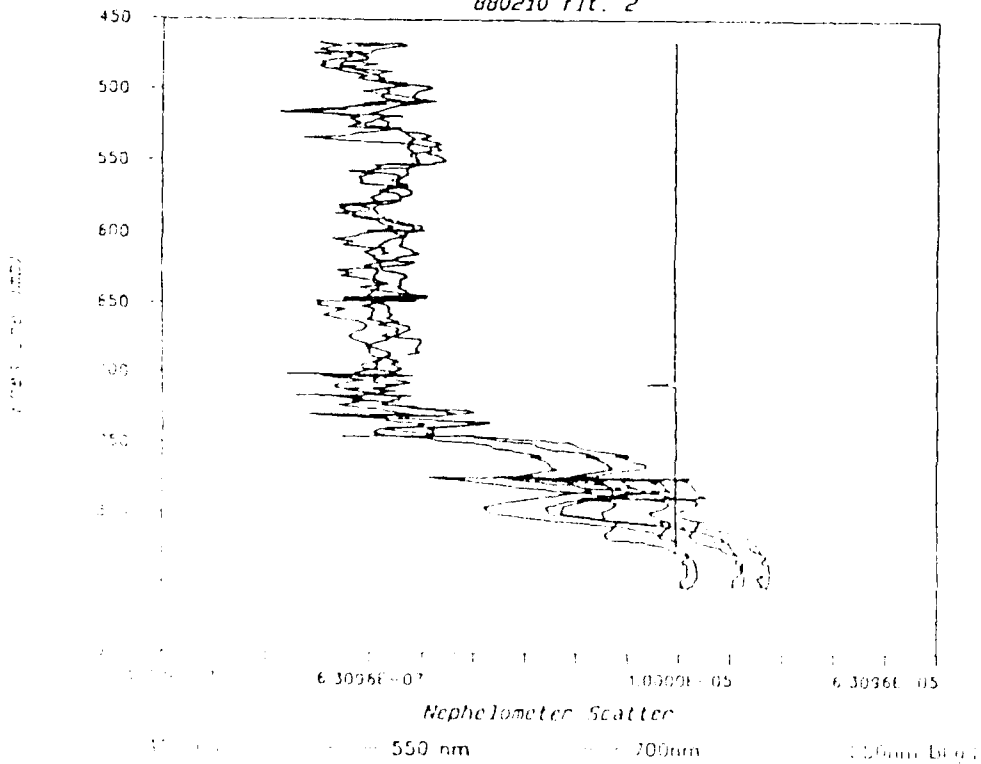
ALIVE '89

890200 fit. 1

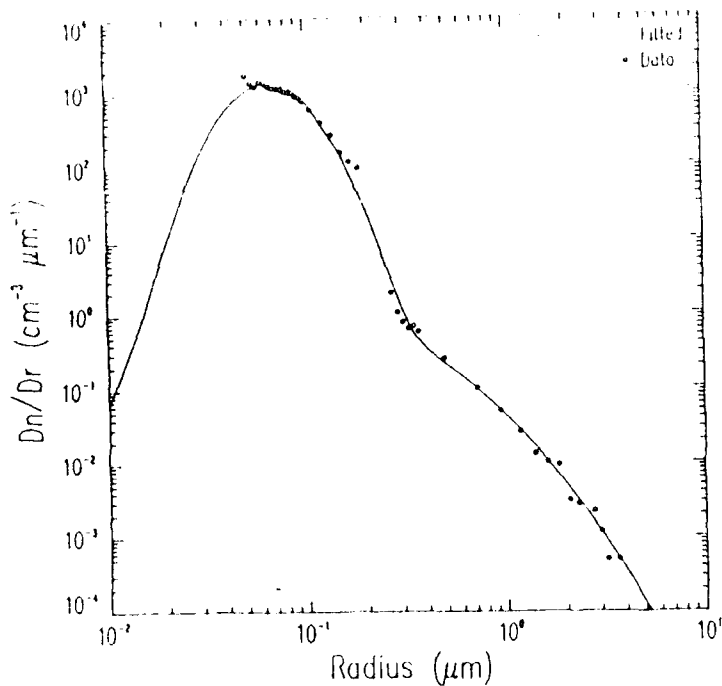


ALIVE '89

880210 fit. 2



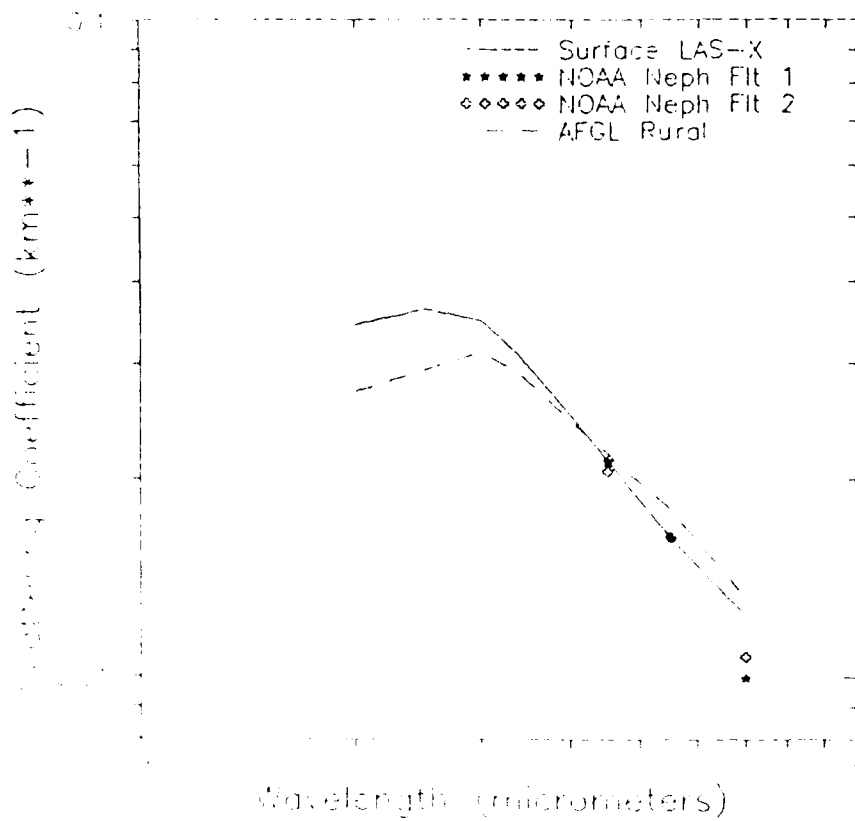
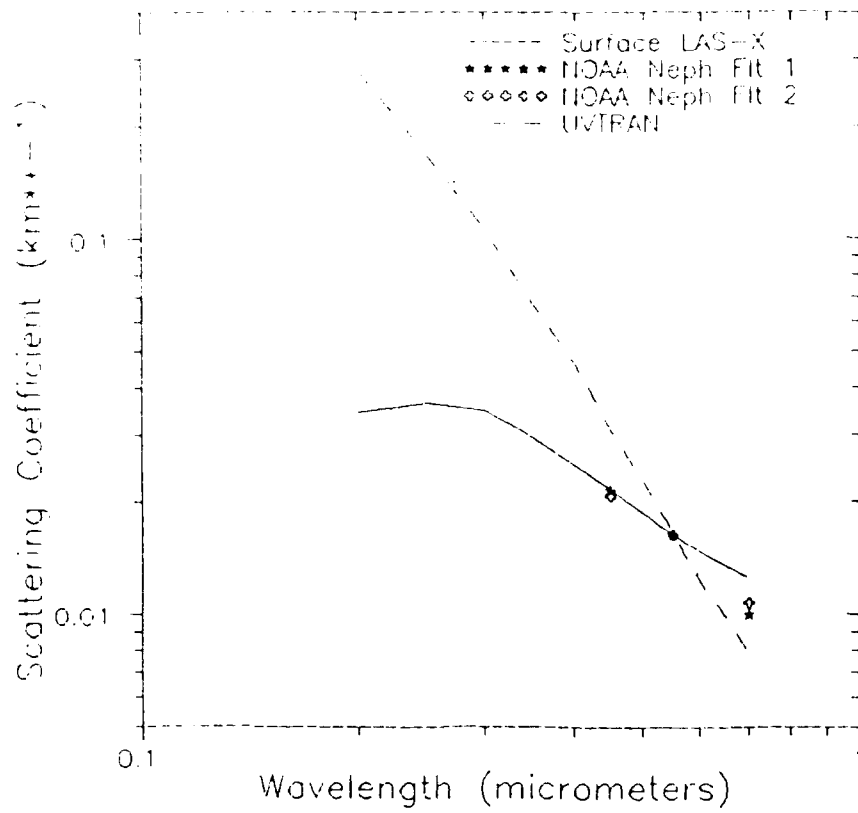
IAS-X Aircraft Data, 22 June 1988

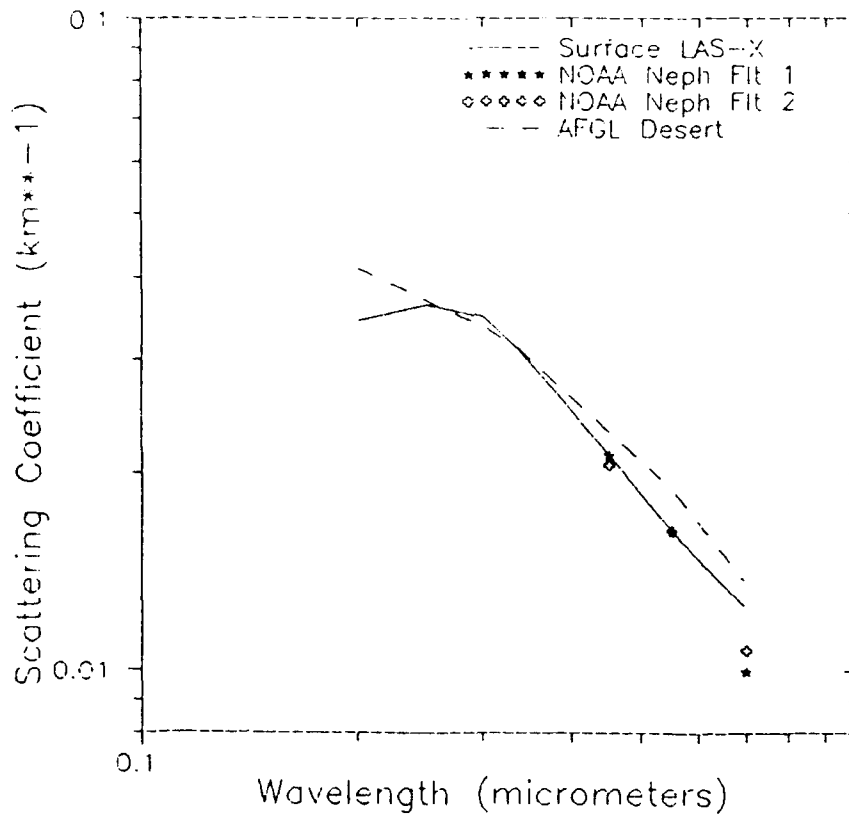


Example of least-squares bimodal lognormal curve fit with automatic edit

Seasonal Size Distribution Parameters Used in Boundary Layer Mie Calculations

Size Distribution Parameter	Minimum	Mean	Maximum
<u>Spring/Summer</u>			
Accumulation mode:			
H	145.78	650.43	2880.86
R	0.07	0.07	0.07
σ	0.385	0.411	0.447
Coarse mode:			
H	0.452	2.376	6.232
R	0.30	0.30	0.30
σ	0.955	0.980	1.00
<u>Fall/Winter</u>			
Accumulation mode:			
H	185.42	608.99	980.23
R	0.07	0.07	0.07
σ	0.401	0.403	0.445
Coarse mode:			
H	0.452	1.341	4.024
R	0.30	0.30	0.30
σ	1.001	1.098	1.150





Conclusions

- For sea level aerosols, visibilities greater than 10 km, and short wavelengths (< 550 nm), UVTRAN predicts a higher aerosol extinction than LOWTRAN 7; limited experimental data tend to support UVTRAN in such conditions
- For sea level aerosols, the two models agree reasonably well when either the visibility is low or the wavelength is long
- For elevated desert aerosols, the two models are in agreement only when both the visibility is relatively low (< 23 km) and the wavelength is above 550 nm
- Under the high visibility conditions of elevated deserts, the UVTRAN model predicts significantly stronger spectral dependence of aerosol extinction than does LOWTRAN 7; limited experimental data indicate that the LOWTRAN 7 desert aerosol model is more accurate in such conditions

HIGH RESOLUTION SOLAR SPECTRUM BETWEEN 2000 AND 3100 ANGSTROMS

L.A. Hall and G.P. Anderson

Geophysics Laboratory/LIM/OPE, Hanscom AFB, MA 01731

Solar spectra in the wavelength range 2000–3100 Angstroms, measured at 40 km in the stratosphere, have been extrapolated to zero optical depth to provide a reference spectrum in 0.1 Angstrom resolution. The wavelength scale has been carefully compared to wavelength standards and a cyclic instrumental effect removed, resulting in a wavelength accuracy to within .04 Angstroms. The absolute intensities have been normalized to a previously released spectrum in 1.0 Angstrom resolution.

HIGH RESOLUTION SOLAR SPECTRUM BETWEEN 2000
AND 3100 ANGSTROMS

L. A. HALL AND G. P. ANDERSON
GEOPHYSICS LABORATORY

Balloon Measurements of Stratospheric Ultraviolet

- O Five Flights: 21 April, 1977
19 April, 1978
27 April, 1980
22 April, 1981
20 April, 1983

- O Results: Absolute irradiance in 2000-3100 A range
at balloon altitudes
Variation of UV irradiance in 11-yr cycle
In situ measurement of Herzberg continuum
cross section
Measurement of O₂ transmission in the
stratosphere
Photodissociation rate coefficients of O₂
in the stratosphere
Extrapolation of absolute irradiance to
zero optical depth

BLACK BOX #1:

The Instrument:

$\frac{1}{2}$ m Ebert Fastie Spectrometer

10 min scan time - 187-310 nm

Single dispersion

Two optical trains -

.012 nm resolution + filter*

.1 nm resolution

Both with EMR 514F Photomultiplier
Tubes

* Interference filter (1983 only)

Scan equivalent altitude -

~ 28, 33, 37, & 40 km

Five Flights:

April 77, 78, 80, 81 & 83

Sampling rate:

50 pts/ \AA ($\pm .005$)

BLACK BOX #2:

The Calibration:

Standard of Irradiance: 250-300 nm

Tungsten filament quartz

halogen lamp calibrated

by Epley against BoJ Stds.

Estimated accuracy:

4% at 300 nm

8% at 250 nm

Relative Calibration: 190-250 nm

Deuterium lamp overlapped

with above

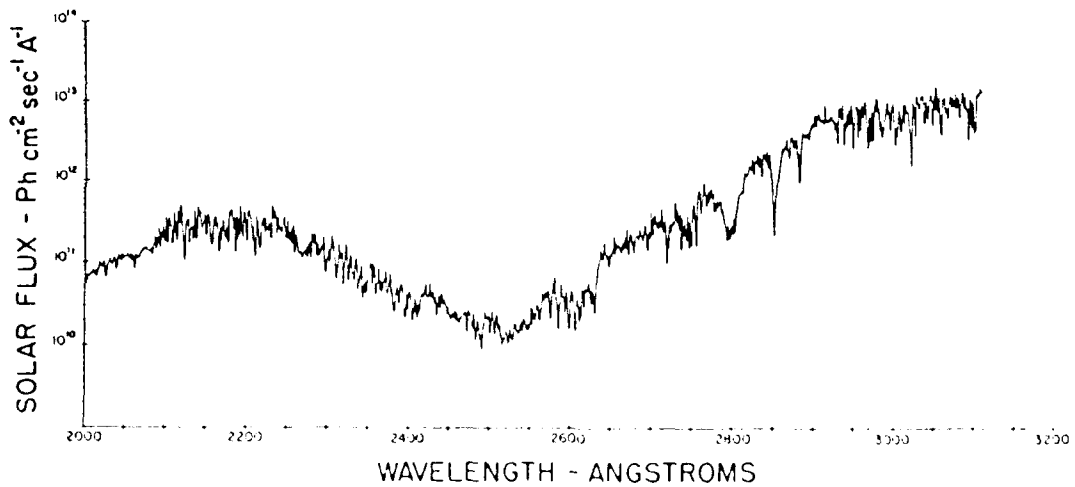
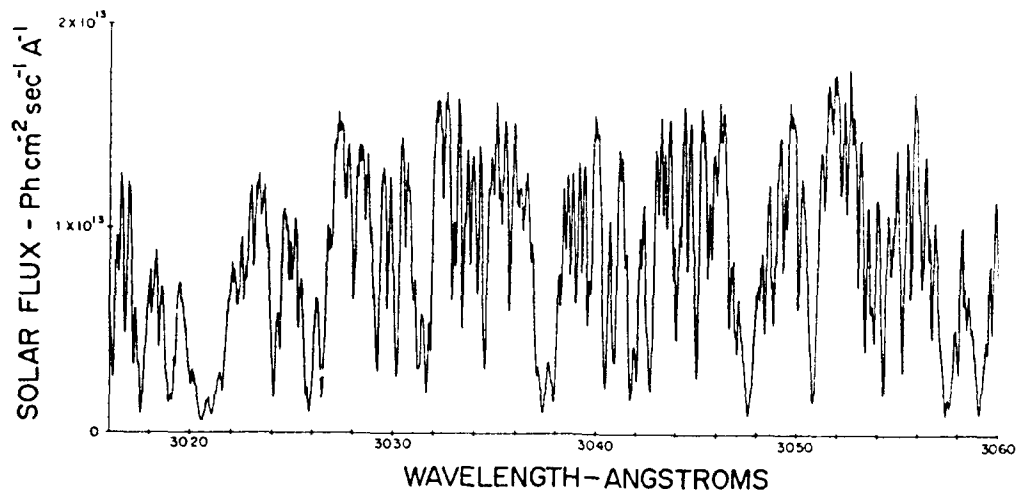
Estimated accuracy:

10% at 200 nm

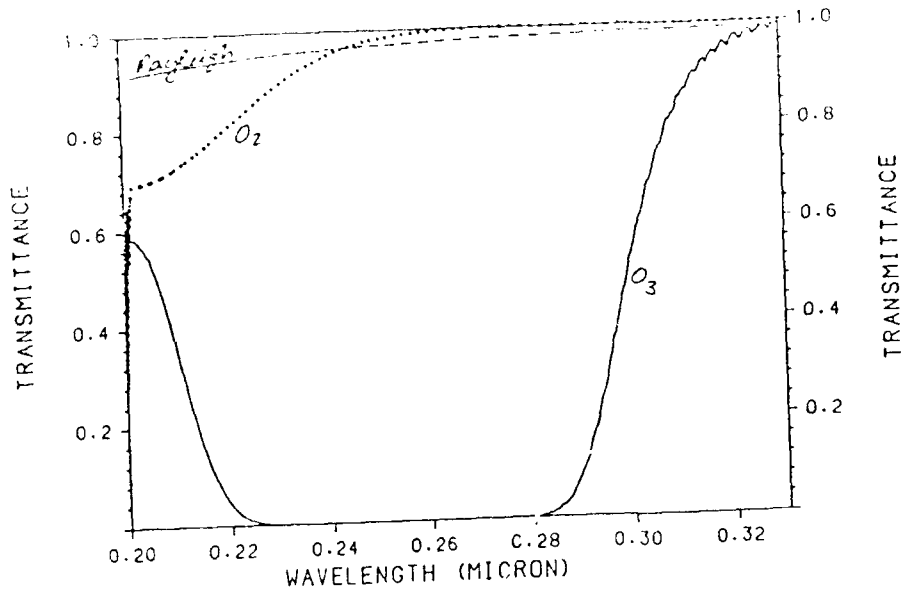
Flight Repeatability:

3% drift between pre & post
flight (with recovery)

long term $\frac{1}{2}$ %/yr drift (corrected)



EXERCISE 7: Transmittances
 vertical path = 30 km → space



In a spectral region where ozone is the dominant absorber:

$$I = I_0 \exp(-\sigma N)$$

where I = irradiance at a point where slant column density is N

I_0 = incident irradiance

σ = absorption cross section of ozone

For two measurements, at different N and perhaps different I_0 :

$$\ln(I_1/I_2) = \ln(I_{01}/I_{02}) - \sigma(N_1 - N_2)$$

Accuracy of Overburden Determinations

O_3 : $3.15e^{17} \text{ cm}^{-2} \pm 1\%$ ($\pm 2\%$)
for 3 different I_0 's

O_2 : on-board pressure sensor
 $\pm 2\%$

[m]: same as O_2 : $\pm 2\%$

Potential Extrapolation Error Estimates

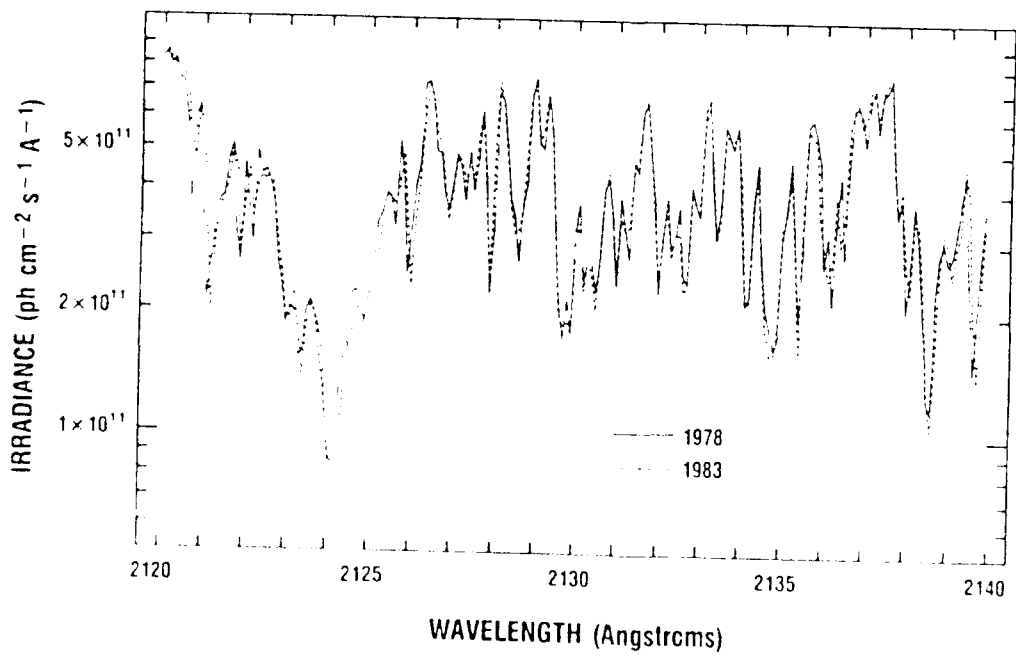
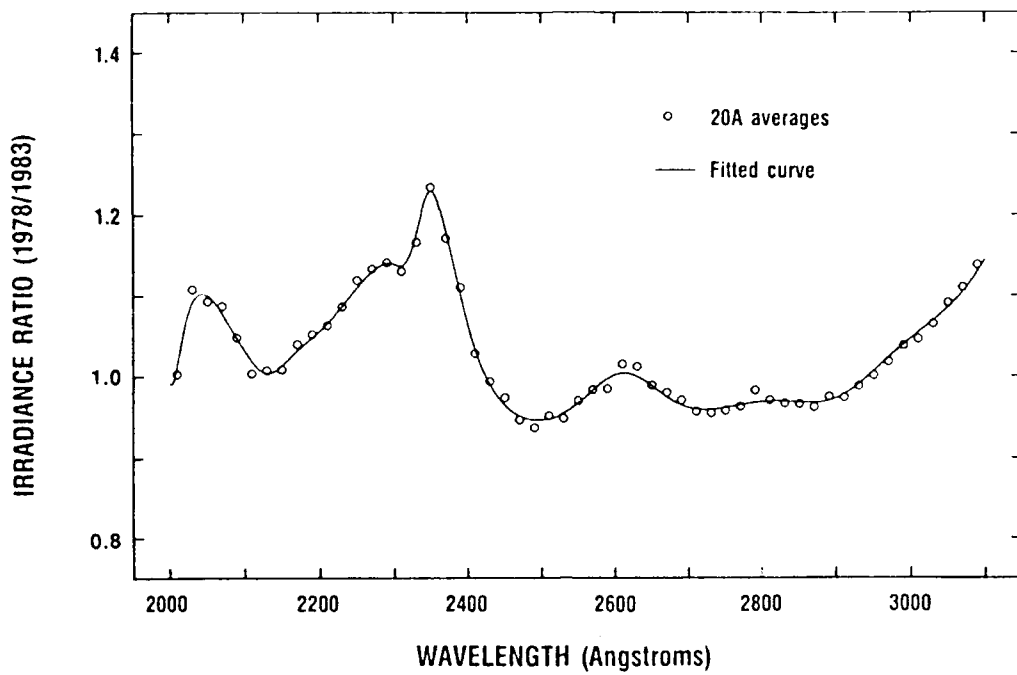
O_3 : 2% abundance
3% cross section (ref)
1-8% attenuation* (fn λ)

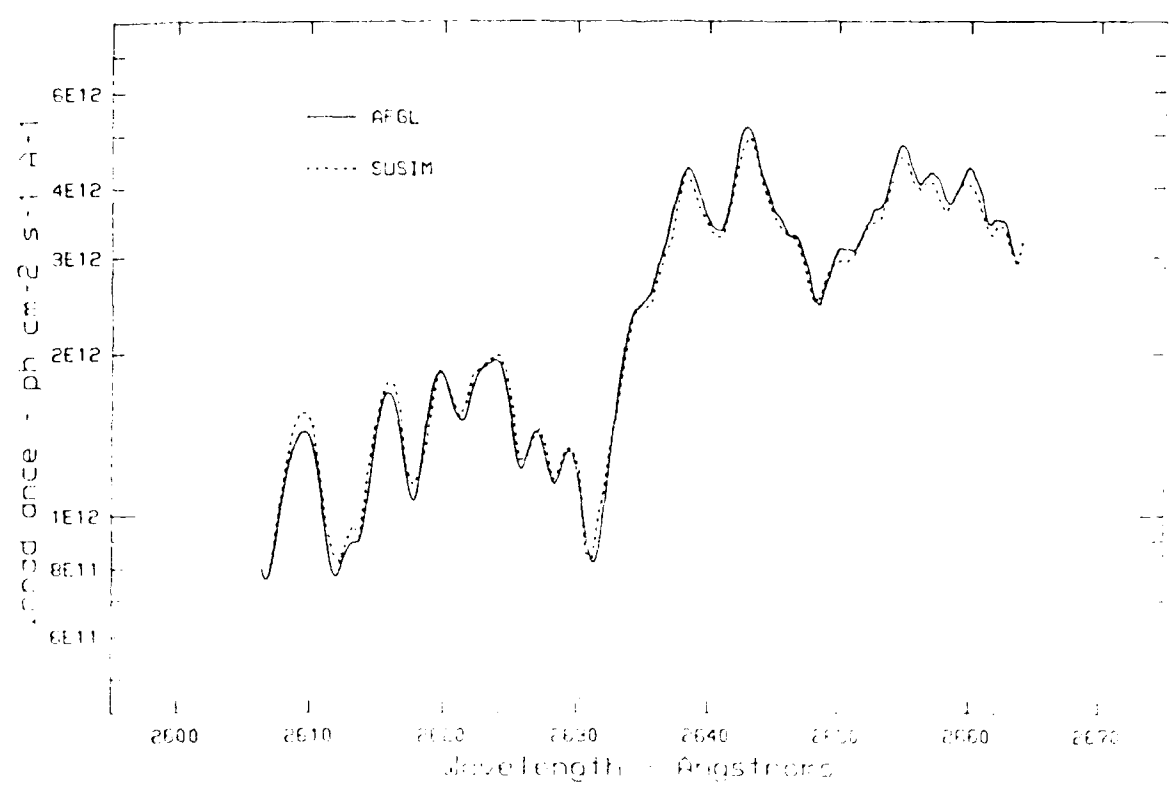
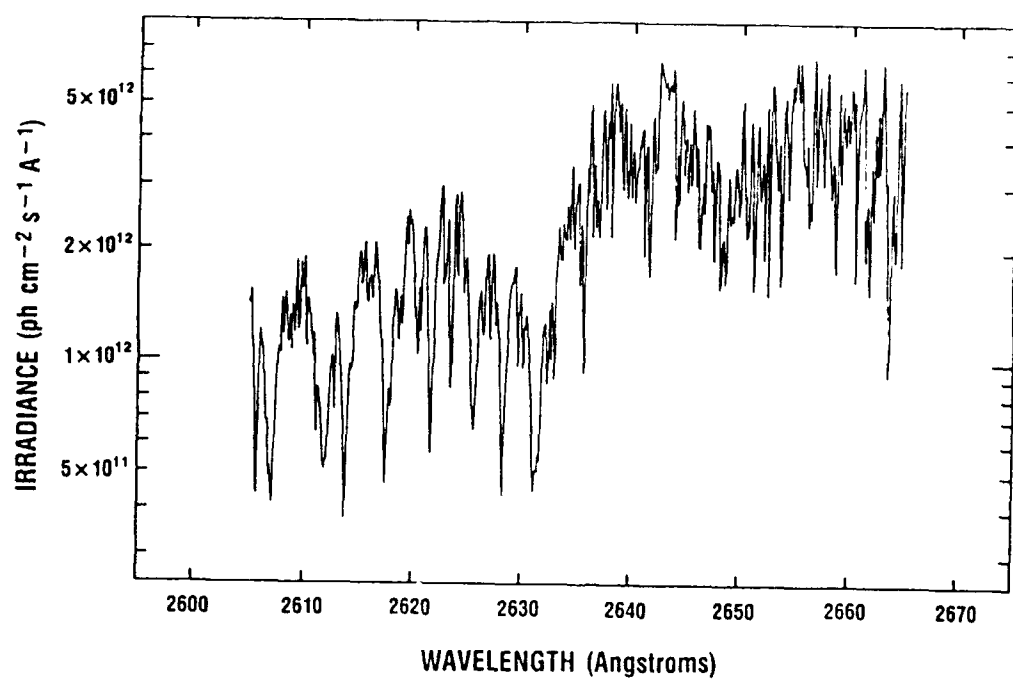
O_2 : 2% abundance
5% cross section (ref)
~3% attenuation*

[m] 2% abundance
1% cross section (ref)
~2% attenuation*

* fractional contribution to final extrapolation

$$T_{\tau} = e^{-\tau_3} e^{-\tau_2} e^{-\tau_1}$$





**PREDISSOCIATION LINE WIDTHS OF THE SCHUMANN-RUNGE
ABSORPTION BANDS OF SOME ISOTOPES OF OXYGEN**

W.H. Parkinson¹, A.S.-C. Cheung², S.L. Chiu², J.R. Esmond¹, D.E. Freeman and K. Yoshino¹

¹Harvard-Smithsonian Center for Astrophysics, Cambridge, MA 02138,

²Chemistry Department, University of Hong Kong, Hong Kong

Predissociation line widths of the (3,0) – (11,0) Schumann-Runge bands of $^{18}\text{O}_2$ and $^{16}\text{O}^{18}\text{O}$ in the wavelength region 189–196 nm have been obtained from the published measurements of the absolute absorption cross sections of Yoshino et al. [Planet. Space Sci., 36, 1201 (1988); 37, 419 (1989)] and spectroscopic constants of these molecules of Cheung [J. Mol. Spectrosc., 131, 96 (1988); 134, 362 (1989)]. The line widths are determined as parameters in the non-linear least squares fitting of calculated to measured cross sections. Predissociation maxima are found at upper vibrational levels with $v'=4, 7$ and 10 for $^{18}\text{O}_2$ and $^{16}\text{O}^{18}\text{O}$. Our predissociation line widths are mostly greater than previous experimental values for both isotopic molecules. This work is supported by NASA grant NAG 5-484 to Smithsonian Astrophysical Observatory.

Predissociation Line Widths of the Schumann-Runge Absorption Bands
of Some Isotopes of Oxygen

W.H. Parkinson¹, A.S.C. Cheung², S.L. Chiu², J.R. Esmond¹, D.E. Freeman¹ and
K. Yoshino¹

¹Harvard-Smithsonian Center for Astrophysics, Cambridge, MA 02138

²Chemistry Department, University of Hong Kong, Hong Kong

Predissociation line widths of the (3,0)-(11,0) Schumann-Runge bands of ¹⁶O₂ and ¹⁶O¹⁸O in the wavelength region 180-196 nm have been obtained from the published measurements of the absolute absorption cross sections of Yoshino *et al.* [Planet. Space Sci. **36**, 1201 (1988); **37**, 419 (1989)] and spectroscopic constants of these molecules of Cheung [J. Mol. Spectrosc. **131**, 96 (1988); **134**, 362 (1989)]. The line widths are determined as parameters in the non-linear least squares fitting of calculated to measured cross sections. Predissociation maxima are found at upper vibrational levels with $v' = 4, 7$ and 10 for ¹⁶O₂ and ¹⁶O¹⁸O. Our predissociation line widths are mostly greater than previous experimental values for both isotopic molecules. This work is supported by NASA grant NAG 5-484 to Smithsonian Astrophysical Observatory.

Predissociation Line Widths of the Schumann-Runge Absorption Bands
of Some Isotopes of Oxygen

W.H. Parkinson, A.S.C. Cheung,^{*} S.S-L. Chiu,^{*} J.R. Esmond,
D.E. Freeman and K. Yoshino

Harvard-Smithsonian Center for Astrophysics
60 Garden Street, Cambridge, MA 02138, U.S.A.

^{*}Chemistry Department, University of Hong Kong, Hong Kong

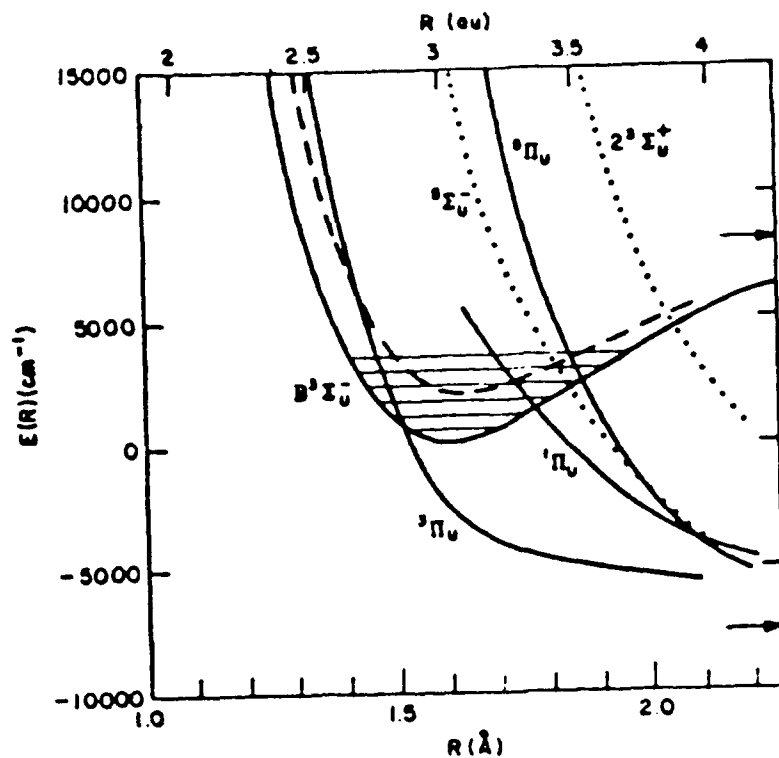
Supported by the NASA Upper Atmospheric Research Program

The Schumann-Runge absorption bands of $^{16}\text{O}_2$ and their extensive predissociation are of considerable atmospheric significance in connection with the transmission of solar radiation and the production of $\text{O}(^3\text{P})$ atoms. The cross sections of the S-R bands consists of hundreds of broadened and often overlapping rovibronic lines, and the predissociation of $^{16}\text{O}_2$ is the main source of odd oxygen in the atmosphere above 60 km. The cross sections are also temperature dependent and can only be obtained from parameters including predissociation line widths at any temperature. The predissociation line widths and, in particular, their variation with the upper level vibrational quantum number v' , are also of importance in the elucidation of the curve-crossing mechanism responsible for the predissociation. The analogous predissociation line widths of the Schumann-Runge bands of $^{18}\text{O}_2$ and $^{16}\text{O}^{18}\text{O}$ would provide valuable supplementary information on the mechanism of predissociation because the predissociating vibronic energy levels, but not the associated bound and repulsive potential energy curves, are isotope-dependent. In addition, $^{16}\text{O}^{18}\text{O}$ constitutes about 0.4% of atmospheric O_2 and is a source, via predissociation, of ^{18}O in the stratosphere.

THE PREDISSOCIATION OF B $^3\Sigma_u^-$ STATE OF O_2 .

The predissociation is caused by four repulsive states, namely, $^1\Pi_u$, $^3\Pi_u$, $^5\Pi_u$ and $^3\Sigma_u^-$, which cross the upper B $^3\Sigma_u^-$ state of the Schumann-Runge system in its bound region. The theoretical investigations of Julienne and Krauss (1975) and Julienne (1976) have shown that both the level shifts and line widths can be attributed to perturbations dominated by the $^5\Pi_u$ state, with other states playing minor roles in the predissociation. Nevertheless, accurate predissociation line width measurements for the various vibrational levels are required to provide a meaningful comparison of different sets of line widths calculated from theoretical parameters.

JULIENNE AND KRAUSS



PARAMETERIZATION OF THE SCHUMANN-RUNGE BANDS (Absorption Cross Section)

1. Boltzman Population

2. Hönl London Factor

3. Band Oscillator Strengths

$^{16}\text{O}_2$; Planet. Space Sci. 35, 1067-1075 (1987).

$^{18}\text{O}_2$; Planet. Space Sci. 36, 1201-1210 (1988).

$^{16}\text{O}^{18}\text{O}$; Planet. Space Sci. 37, 419-426 (1989).

4. Line Center Positions

$^{16}\text{O}_2$; J. Mol. Spectrosc. 119, 1-10 (1986).

$^{18}\text{O}_2$; J. Mol. Spectrosc. 131, 96-112 (1988).

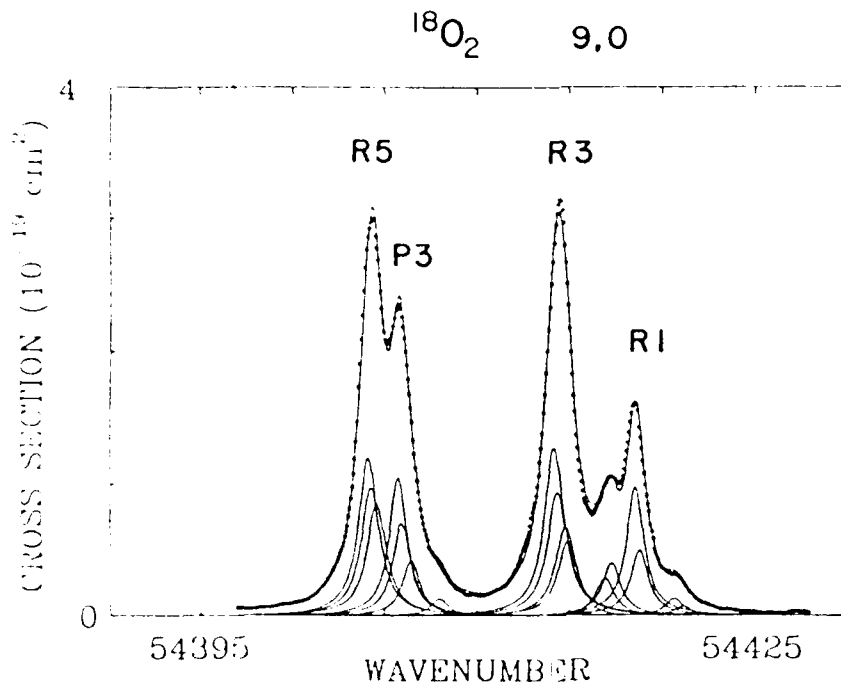
$^{16}\text{O}^{18}\text{O}$; J. Mol. Spectrosc. 134, 362-389 (1989).

5. Predissociation Line Widths

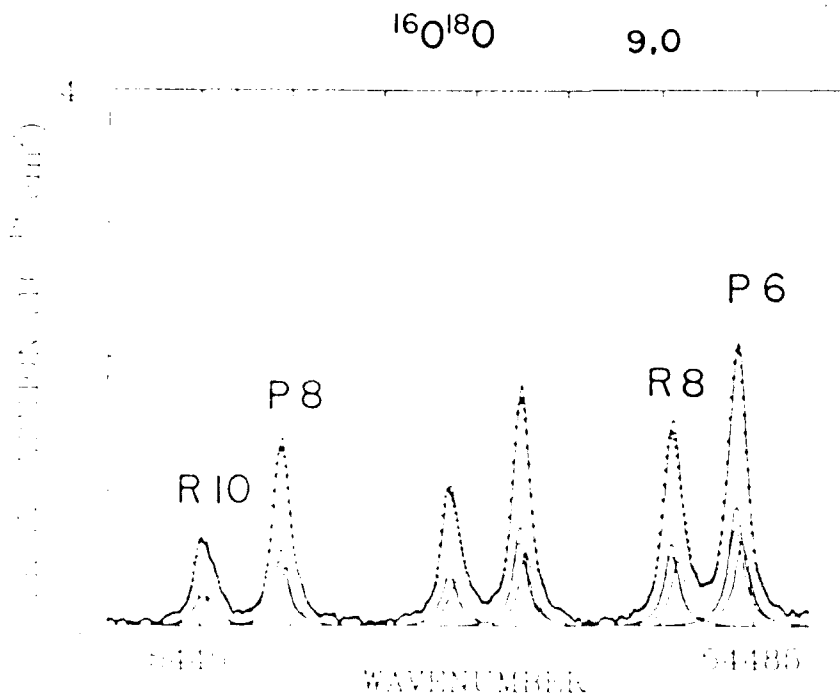
$^{16}\text{O}_2$; J. Chem. Phys. 92, 842-849 (1990).

$^{18}\text{O}_2$; Present work

$^{16}\text{O}^{18}\text{O}$; Present work



Absorption cross section near the band head of the (9,0) Puzos-Runge band of $^{18}\text{O}_2$ at 79 K. The uppermost curve is synthesized from the lower fine structure component (Lorentzian) curves to fit the measured cross sections, represented by dots.

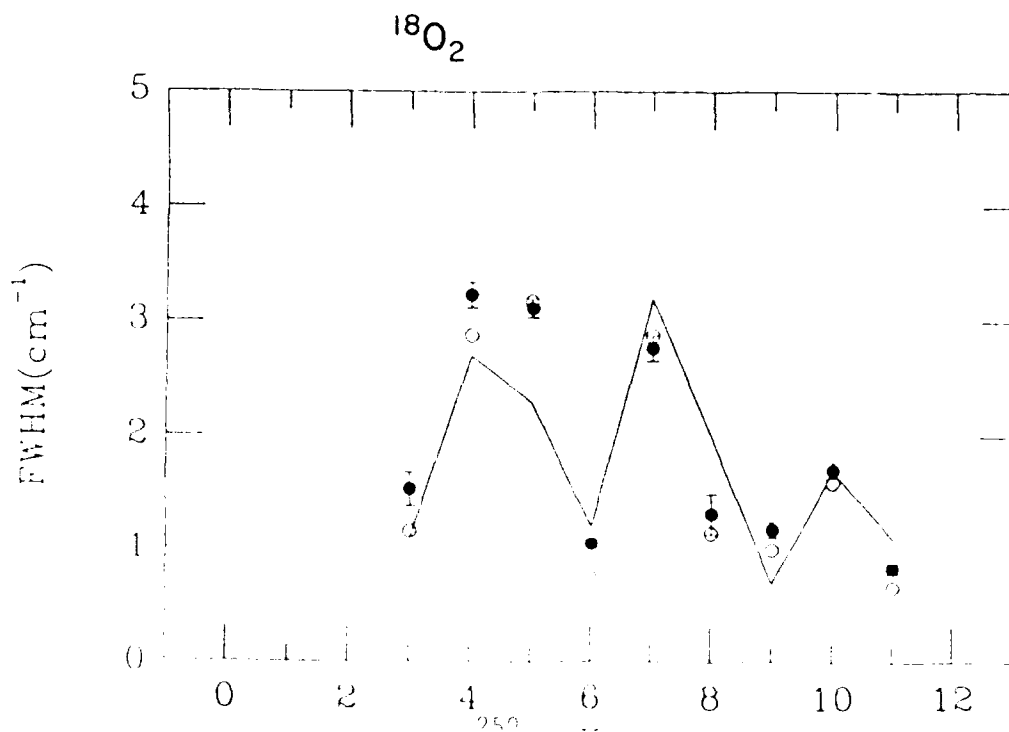


Absorption cross section near the band head of the (9,0) Puzos-Runge band of $^{16}\text{O}^{18}\text{O}$ at 79 K. The uppermost curve is synthesized from the lower fine structure component (Lorentzian) curves to fit the measured cross sections, represented by dots.

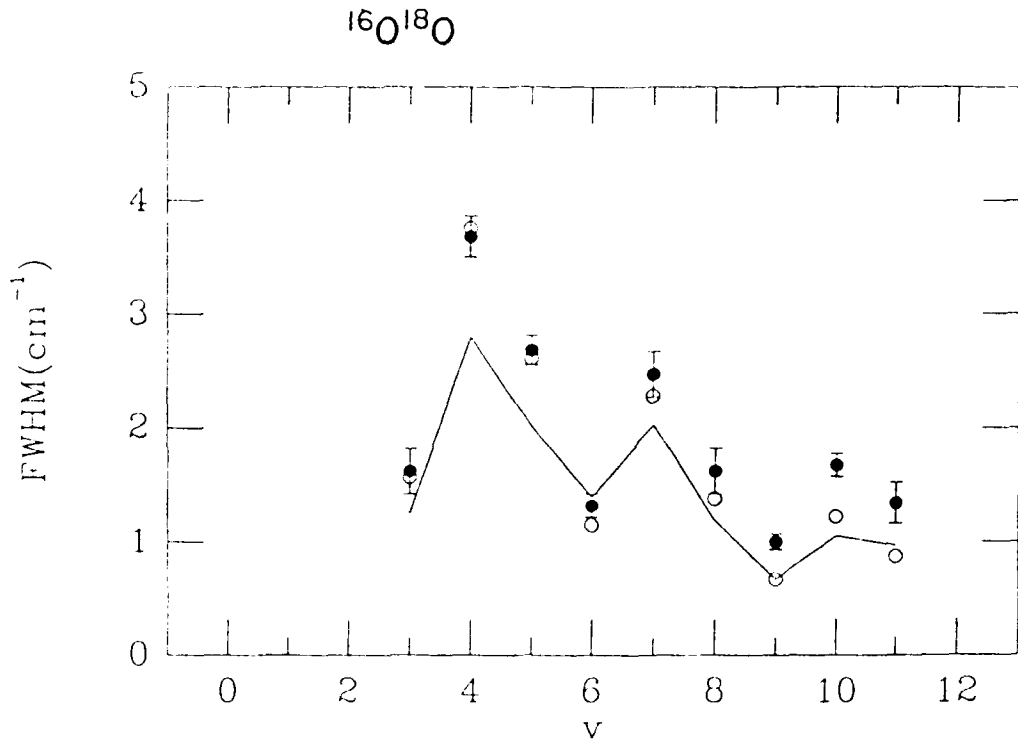
TABLE 1. Predissociation line widths (cm^{-1} , FWHM) of the Schumann-Runge bands of $^{16}\text{O}_2$, $^{18}\text{O}_2$ and $^{16}\text{O}^{18}\text{O}$

v'	$^{16}\text{O}_2$	$^{18}\text{O}_2$	$^{16}\text{O}^{18}\text{O}$
1	0.93 ± 0.18		
2	0.72 ± 0.04		
3	1.78 ± 0.11	1.53 ± 0.15	1.62 ± 0.20
4	3.87 ± 0.27	3.23 ± 0.11	3.69 ± 0.18
5	2.13 ± 0.07	3.12 ± 0.08	2.68 ± 0.13
6	1.79 ± 0.21	1.05 ± 0.03	1.32 ± 0.10
7	2.01 ± 0.10	2.77 ± 0.11	2.47 ± 0.20
8	1.92 ± 0.12	1.32 ± 0.18	1.62 ± 0.20
9	1.01 ± 0.16	1.18 ± 0.07	1.00 ± 0.07
10	1.09 ± 0.08	1.71 ± 0.07	1.67 ± 0.10
11	1.48 ± 0.18	0.84 ± 0.05	1.34 ± 0.18
12	0.88 ± 0.14		

Variation of predissociation line width with vibrational quantum number in the B $^2\Sigma_g^-$ state of $^{18}\text{O}_2$. Filled circles: present average values, open circles: Lewis et al. (11) solid line: Julienne (12)

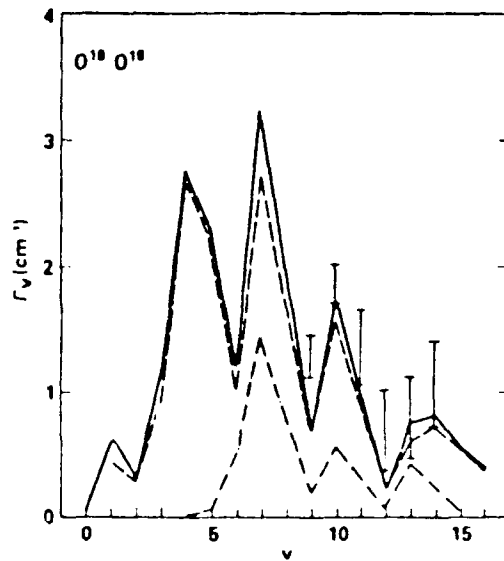
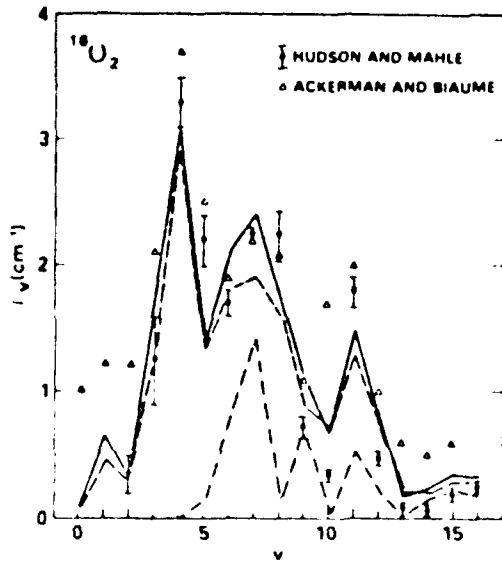


Variation of predissociation line width with vibrational quantum number in the B $^2\Sigma_g^-$ state of $^{16}O^{18}O$. Filled circles: present average values, open circles: Lewis et al.,¹³ solid line: Blake et al.⁸



JUN 73

PAUL S. JULIENNE



AURIC: ATMOSPHERIC ULTRAVIOLET RADIANCE INTEGRATED CODE

R.L. Huguenin, M.A. LeCompte
Aerodyne Research, Inc., 45 Manning Road, Billerica, MA 01821

R.E. Huffman
Geophysics Laboratory/LIM, Hanscom AFB, MA 01731

AURIC is a planned computer simulation model to synthesize background radiance and clutter as viewed by ultraviolet sensors. Radiometrically "accurate" radiance and clutter predictions will be emphasized through inclusion of all relevant phenomenology. Radiances will be fully traceable to underlying phenomenology using parametric first principles radiance models. Included will be the capability to compare AURIC predictions with measured data. Phenomenological models and simulation algorithms will be modularized to accommodate upgrades and substitutions. A relational data base management system will serve as the shell for integration and control of the modules, as well as provide the foundation for a high level user interface that provides ease of use for scientists and system engineers.

AERODYNE RESEARCH, Inc.
SYSTEMS



**AURIC: ATMOSPHERIC ULTRAVIOLET RADIANCE INTEGRATED
CODE**

* R.L. HUGUENIN, *M.A. LeCOMPTE, AND **R.E. HUFFMAN

*AERODYNE RESEARCH, INC.
45 MANNING ROAD
BILLERICA, MA 01821

** IONOSPHERIC MODELING AND REMOTE SENSING BRANCH
IONOSPHERIC RESEARCH DIVISION
AIR FORCE GEOPHYSICS LABORATORY
HANSCOM AFB, MA 01731

45 Manning Road
BillERICA, MA 01821 0976
(508) 663 9500 Fax: (508) 663 4918



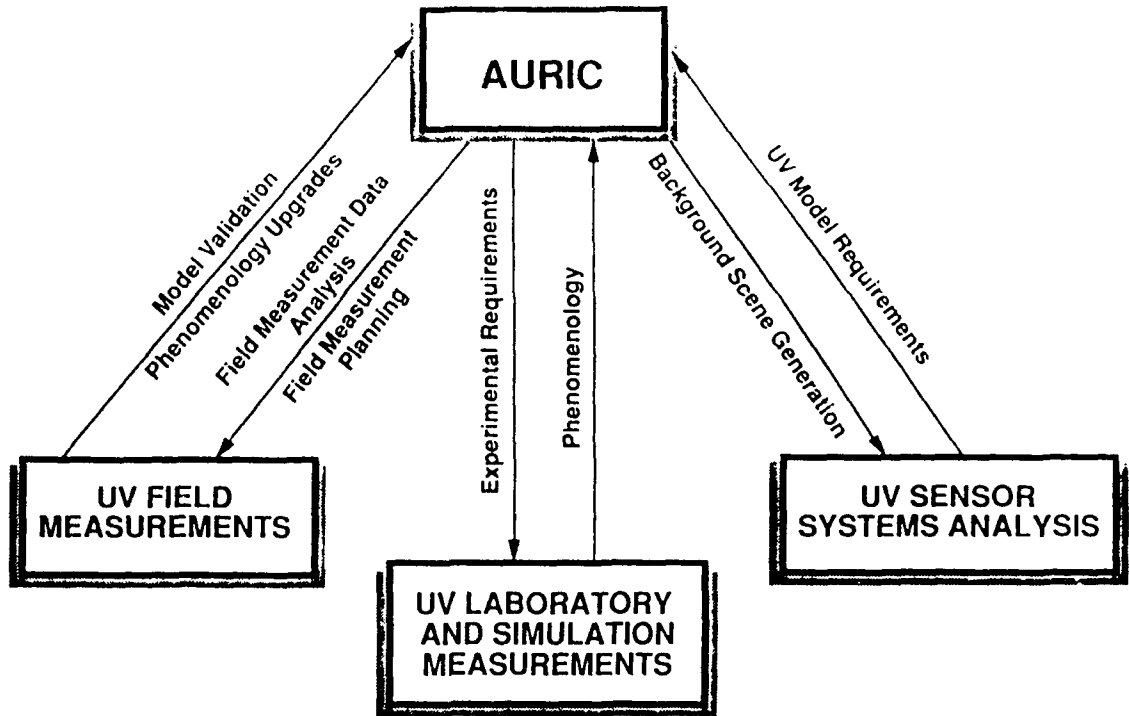
SYSTEMS



PROBLEM BEING ADDRESSED

- MEASUREMENTS LIMITED
 - TEMPORAL COVERAGE
 - SPATIAL COVERAGE
 - SENSOR CHARACTERISTICS
- MEASUREMENTS OF ALL BACKGROUND CONDITIONS UNREALISTIC
- RADIANCE MODELING CAPABILITY NEEDED
 - INTERPOLATE AND EXTRAPOLATE MEASURED RADIANCES TO OTHER CONDITIONS
 - SYNTHESIZE RADIANCES FOR SCENARIOS SENSORS FOR WHICH NO DATA EXIST
 - ANALYZE AND TEST CURRENT UNDERSTANDING OF SOURCES OF ULTRAVIOLET BACKGROUND RADIANCE AND CLUTTER
 - PROVIDE INTEGRATED SYNTHETIC SCENES, WHERE RADIANCE INTERACTIONS ARE TOTALLY CONSISTENT AND RADIOMETRICALLY ACCURATE





M90-039eB H



AURIC PROGRAM OBJECTIVE

DEVELOP AND PROVIDE TO AIR FORCE GEOPHYSICS LABORATORY
A COMPUTER SIMULATION MODEL TO SYNTHESIZE BACKGROUND
RADIANCE AND CLUTTER AS VIEWED BY USER SPECIFIED ULTRA-
VIOLET SENSORS



AURIC REQUIREMENTS (CONT'D)

- HIERARCHICAL DEVELOPMENT STRATEGY
 - NEED TO ACCOMMODATE FUNDING LEVEL/SCHEDULE UNCERTAINTIES
 - COMPLETE "ACCURATE" MODEL FOR RESTRICTED SETS OF MEASUREMENT SCENARIOS
 - ADD MEASUREMENT SCENARIO VERSATILITY ACCORDING TO FUNDING AVAILABILITY
- ACCESSIBLE DESK-TOP CAPABILITY
 - ANALOGOUS TO PC LOWTRAN, PC SPIRITS
 - EASE OF USE FOR SCIENTISTS, SYSTEMS ENGINEERS
- FULLY SUPPORTED, DOCUMENTED
- RESPONSIVE BUT CONTROLLED UPDATE RELEASES/VERSIONS
 - ENCOURAGE USER CONTRIBUTIONS
 - CONTROLLED RELEASES TO PERMIT UNIFORM COMPARISONS
 - PERIODIC USER MEETINGS

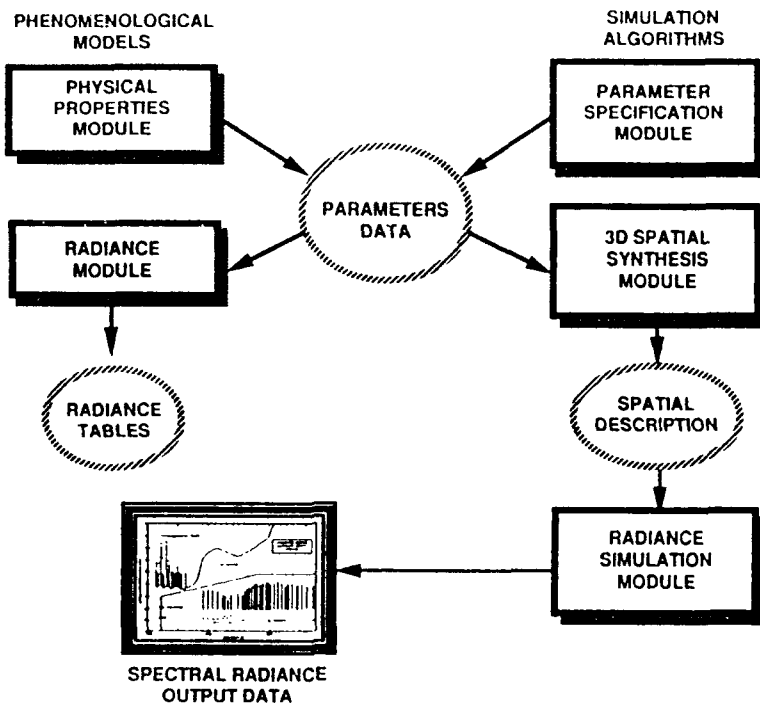
**AURIC REQUIREMENTS**

- RADIOMETRICALLY "ACCURATE" RADIANCE AND CLUTTER PREDICTIONS
 - ALL RELEVANT PHENOMENOLOGY NEEDED FOR USER-SPECIFIED SCENARIOS
 - ENTRANCE-APERTURE SPECTRAL RADIANCES NEED TO EXCEED SENSOR SPECIFICATIONS
 - CAPABILITY NEEDED TO SPECIFY SENSOR MODEL AND APPLY TO RADIANCE PREDICTION
 - INCLUSION OF LOCAL ENVIRONMENT CONTAMINANTS DESIRED
- RADIANCE FULLY TRACEABLE TO UNDERLYING PHENOMENOLOGY
 - REQUIRES FULLY PARAMETRIC FIRST-PRINCIPLES RADIANCE MODELS
 - AB INITIO CALCULATIONS
 - PARAMETRIC PERTURBATION
- CAPABILITY TO COMPARE AURIC PREDICTIONS TO MEASURED DATA
 - REQUIRES CAPABILITY TO DISPLAY BOTH DATA SETS
 - REQUIRES CAPABILITY TO COMBINE BOTH DATA SETS
 - VALIDATION/CALIBRATION MODEL REFINEMENT CAPABILITY DESIRED



SYSTEMS

AURIC: ATMOSPHERIC ULTRAVIOLET RADIANCE INTEGRATED CODE



M90-039ee/B.H.



SYSTEMS

AURIC SYSTEM DESIGN/DEVELOPMENT APPROACH

- SEPARABLE MODULAR DESIGN
 - PHENOMENOLOGY UPDATE/SUBSTITUTION ACCOMMODATION
 - HIERARCHICAL DEVELOPMENT ACCOMMODATION
 - EXPANDABILITY
 - SHARED DEVELOPMENT EFFICIENCY
- SIMULATION MODELING
 - COMPUTATIONAL EFFICIENCY REQUIREMENT
 - RADIOMETRIC ACCURACY NOT MEASURABLY COMPROMISED
 - PHENOMENOLOGICAL TRACEABILITY NOT MEASURABLY COMPROMISED
- RULE-BASED SCENE SPECIFICATION AND MODELING
 - ACCOMMODATES COMPLEX PHENOMENOLOGY CONSISTENCY REQUIREMENTS
 - PERMITS HIGH LEVEL SCENE SPECIFICATION WITH OPTIONAL LOWER LEVEL ACCESS



PHYSICAL PROPERTIES MODULE TABLE ENTRIES

- RELEVANT CROSS-SECTIONS WITH SPECTRAL DEPENDENCE FOR EACH ATMOSPHERIC SPECIES
 - PHOTOABSORPTION
 - PHOTODISSOCIATION
 - PHOTOIONIZATION
 - ELECTRON IMPACT
 - ION IMPACT
 - NEUTRAL IMPACT
 - METEORITIC IMPACT
 - COSMIC RAY (SOLAR, GALACTIC) IMPACT
- BRANCHING RATIOS FOR RELEVANT ATMOSPHERIC SPECIES
- OTHER

**AURIC CODE MODULES**

- PHYSICAL PROPERTIES MODULE
 - SETS OF LOOK-UP TABLES FOR RELEVANT PHYSICAL PROPERTIES
 - LOOK-UP INTERPOLATORS
 - SELECTION RULES RESIDE IN PARAMETER SPECIFICATION CODE



RADIANCE MODULE (CONTINUED)**RADIANCE LOOK-UP TABLES**

- **COMPUTATIONALLY MOST EFFICIENT RADIANCE SOURCE**
- **PREDETERMINED SPECTRAL RADIANCES VS. KEY PHYSICAL PARAMETERS**
 - **COMPUTATIONALLY INTENSIVE CALCULATIONS SHIFTED TO OFF - LINE SYSTEM**
 - **MEASURED/CALIBRATED SPECTRAL RADIANCE DATA FOR KNOWN CONDITIONS**
 - **CALIBRATED TO COMMON RADIANCE UNITS**
 - **REVISIONS/UPDATES PROVIDED AS CONTROLLED RELEASES**
- **PARAMETRIC INTERPOLATION EXPRESSIONS**
 - PARAMETRICALLY SEPARABLE APPROXIMATION FORMULAS**
- **SELECTION RULES/CONTROLLER IN PARAMETER SPECIFICATION CODE**

**AURIC CODE MODULES**

- **RADIANCE MODULE**
 - **RADIANCE LOOK-UP TABLES GENERATED BY OFF - LINE CODE**
 - **RADIANCE CALCULATION CODES**
 - **RADIANCE PERTURBATION CODES**
 - **SELECTION RULES/CONTROLLER IN PARAMETER SPECIFICATION CODE**



3D SPATIAL SYNTHESIS MODULE

- ANALYTICAL SPECIFICATIONS OF MEAN VALUE FOR EACH RELEVANT PHYSICAL PROPERTY
 - LATITUDE, LONGITUDE, ALTITUDE POINT SPECIFICATION
 - CONTINUOUS RATHER THAN ARTIFICIALLY LAYERED
 - SPATIAL RESOLUTION FINER THAN SENSOR IFOV
- SPATIAL CLUTTER
 - SPATIALLY DISCREET PHENOMENA MODELED WITH BOUNDED TEXTURE MODEL
 - SPATIALLY NON-DISCREET PHENOMENA PERTURBED FRACTALLY
 - EMPIRICALLY/THEORETICALLY DERIVED FRACTAL TEXTURE DIMENSION
- LINE-OF-SIGHT INTERSECTION OF PHYSICAL PROPERTIES
 - VOXEL/SCENE ELEMENT ANALYTICAL INTERSECTION MODEL
 - RAY TRACE PHYSICAL PROPERTIES SAMPLING ALGORITHM
 - 1/4 - VOXEL PHYSICAL PROPERTIES AVERAGING ALGORITHM

**RADIANCE MODULE (CONTINUED)**

- RADIANCE CALCULATION CODES
 - DIRECT CALCULATION FOR COMPUTATIONALLY EFFICIENT CODES
- RADIANCE PERTURBATION CODES
 - PARAMETRIC RADIANCE EXPRESSIONS FOR EACH RELEVANT PHENOMENON
 - CLUTTER RADIANCES FROM PHYSICAL PROPERTY TEXTURES
 - COMPUTATIONALLY EFFICIENT
 - SLANT PATH MANIPULATION
 - IMAGE PIXEL INTERPOLATION (FUTURE)



PARAMETER SPECIFICATION MODULE

- **USER INTERFACE TO OVERALL MODULE**
 - HIGH LEVEL SCIENTIFIC/ENGINEERING SPECIFICATIONS**
 - OPTIONAL LOWER LEVEL SPECIFICATIONS**
 - CONSTRAINED USER INPUTS - PHYSICAL CONSISTENCY**
 - TRANSFORMATION OF USER INPUTS TO CODE INPUTS**
- **SYSTEM CONTROLLER**
 - 3D SPATIAL DISTRIBUTION MODELS/RULES**
 - RADIANCE MODELS/CALCULATION RULES**
 - INTERNAL CONSISTENCY RELATIONSHIPS**
 - MODULE DRIVER/SEQUENCE RULES**
- **RELATIONAL DATA BASE MANAGEMENT SHELL**



RADIANCE SIMULATION MODULE

- **RADIANCE ASSIGNMENT TO LINE-OF-SIGHT PATH**
 - SEGMENTED PATH (VOXEL) RADIANCE CALCULATIONS**
 - LINE-OF-SIGHT PATH RADIANCE PROPAGATION**
 - TWO RADIANCE FORMATS**
 - SPECTRAL RADIANCE AT SENSOR ENTRANCE APERTURE**
 - SPECTRAL RADIANCE CONVOLVED WITH SENSOR MULTISPECTRAL TRANSFER FUNCTION**



PARAMETER SPECIFICATION MODULE

- 3D SPATIAL DISTRIBUTION MODEL SOURCES

MSIS THERMOSPHERE MODEL

INTERNATIONAL IONOSPHERE MODEL

US STANDARD ATMOSPHERE

OTHER



PARAMETER SPECIFICATION MODULE (CONT'D)

- 3D SPATIAL DISTRIBUTION MODELS

NUMBER DENSITY DISTRIBUTION MODELS FOR RELEVANT ATMOSPHERIC SPECIES (NEUTRAL, CHARGED)

NEUTRAL ATMOSPHERIC TEMPERATURE DISTRIBUTION MODEL

ION TEMPERATURE DISTRIBUTION MODELS

PHOTOELECTRON SPECTRUM MODEL

EXOSPHERIC TEMPERATURE MODEL

SOLAR CYCLE, SOLAR ACTIVITY MODELS

CORPUSCULAR RADIATION MODELS

MAGNETIC FIELD MODEL



OUTPUT AND DISPLAY

- **PARAMETER SPECIFICATIONS**
INTERACTIVE MENU, PROMPTS, FLAG,
OUTPUT SUMMARY
- **SPECTRAL RADIANCE PLOT**
WITHOUT SENSOR FUNCTION APPLIED
WITH SENSOR FUNCTION APPLIED
SELECTABLE RADIANCE UNITS, INCLUDING SENSOR
UNITS (COUNTS, DATA NUMBER)
SELECTABLE WAVELENGTH/WAVENUMBER UNITS
NORMALIZED, SCALED, RATIO, DIFFERENCE OPTIONS
SPECTRUM SEQUENCE, OVERLAY OPTIONS
- **CLUTTER METRICS, POWER SPECTRAL DENSITIES**
- **RASTER IMAGE DISPLAY (FUTURE)**
- **IMAGE MANIPULATION/STATISTICS/TRANSFORMS (FUTURE)**



PARAMETER SPECIFICATION MODULE

RADIANCE MODELS/CALCULATION RULES

- **SEASONAL CYCLE MODEL**
- **DIURNAL CYCLE MODEL**
- **PATH ATTENUATION MODELS FOR EACH RELEVANT SPECIES**
ABSORPTION
SCATTERING
- **PATH EMISSION MODELS FOR EACH RELEVANT SPECIES**
- **PATH SCATTERED RADIANCE MODELS**
SINGLE/MULTIPLE SCATTERING
RESONANCE SCATTERING
- **OUTPUT RADIANCE INTERPOLATOR**

λ 1000 - 4000 Å (100,000 - 25000 CM^{-1}) INITIAL RANGE

5 CM^{-1} (0.05 - 0.80Å) INITIAL SPECTRAL RESOLUTION



AURIC MODEL DEVELOPMENT SEQUENCE

1-D (LINE-OF-SIGHT) 2-D (IMAGERY)

MID-LATITUDE NADIR	PHASE I	PHASE II
MID-LATITUDE LIMB		
DISTURBED/AURORAL	PHASE III	PHASE V
HIGH SPECTRAL RESOLUTION	PHASE IV	PHASE VI



AURIC CODE DEVELOPMENT ENVIRONMENT

- EVEREX PC (80386) /MICROVAX II
- OFF - THE - SHELF RDBMS (DEVELOPMENT)

ORACLE RDBMS

UNIX WITH X - WINDOWS/MOTIF

FORTRAN COMPILER

- PORTABILITY



**MEASUREMENT NEEDS FOR AURIC: ATMOSPHERIC
ULTRAVIOLET RADIANCE INTEGRATED CODE**

R.E Huffman

Geophysics Laboratory, Hanscom AFB, MA 01731

The development of the AURIC model for ultraviolet radiance and transmission will require the availability of a wide variety of both laboratory and field measurements. These measurements or phenomenology needs are available for many of the areas of interest, but a number of space measurements have not been conducted over a sufficient period of time (solar cycles) and with well-calibrated sensors. The current and near-future availability of airglow, auroral, and scattering space measurements of use for the validation and improvement of the AURIC model will be discussed. Improved measurements of solar radiation, atmospheric density and composition, and celestial sources will all contribute to an improved model. Laboratory measurements of the photon cross sections for the Schumann-Runge bands of oxygen that have recently become available are an example of the measurements needed for the model at wavelengths shorter than the current limit of LOWTRAN 7 of 200 nm.

MEASUREMENT NEEDS FOR AURIC:
ATMOSPHERIC ULTRAVIOLET RADIANCE INTEGRATED CODE

ANNUAL REVIEW CONFERENCE ON ATMOSPHERIC MODELS
5-6 JUNE 1990
GEOPHYSICS LABORATORY

ROBERT E. HUFFMAN
GEOPHYSICS LABORATORY
(617) 377-3311

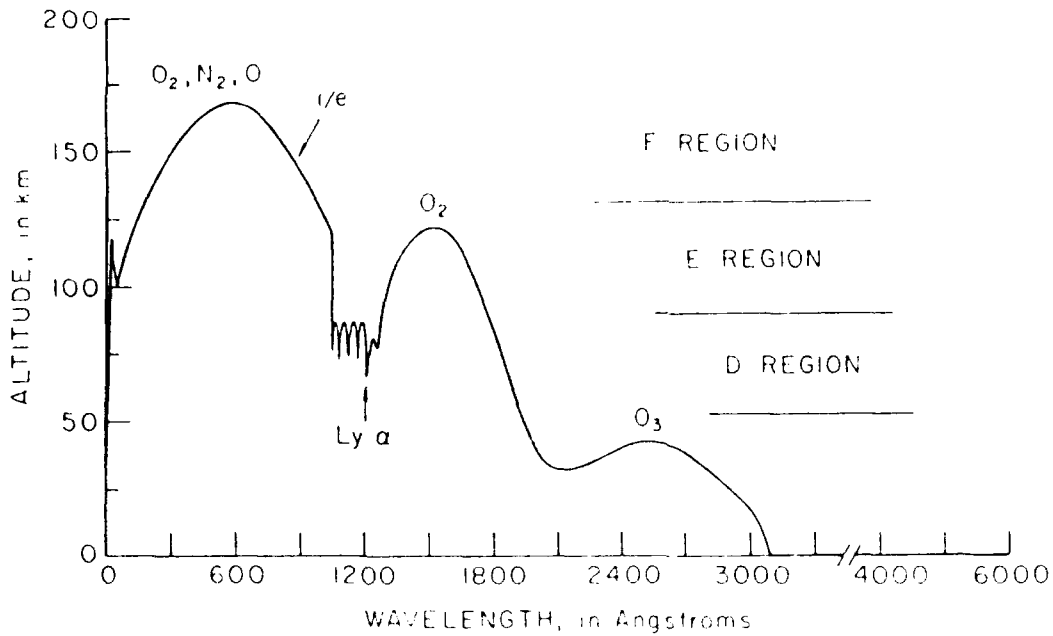
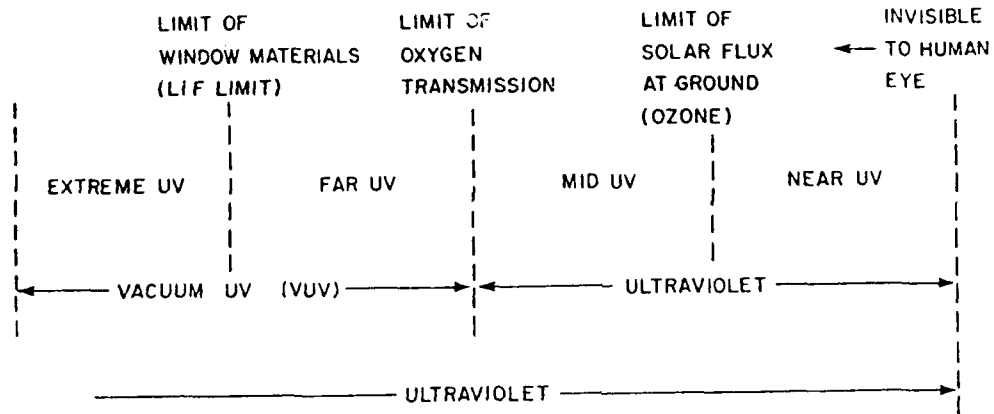
MEASUREMENT NEEDS FOR AURIC:
ATMOSPHERIC ULTRAVIOLET RADIANCE INTEGRATED CODE

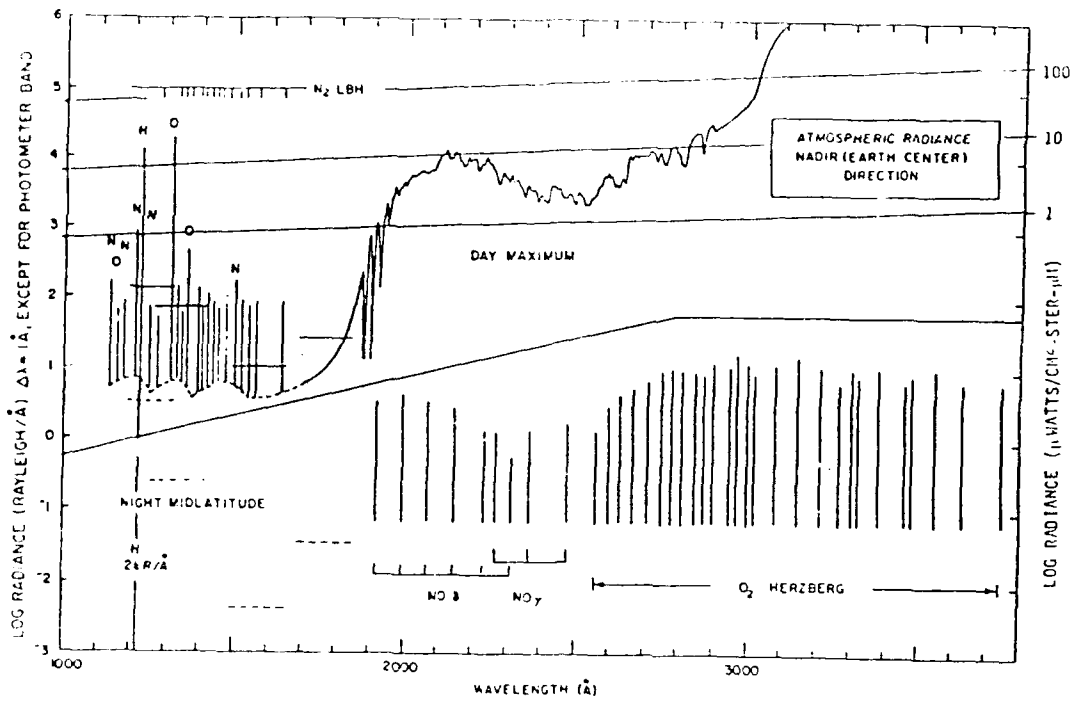
OUTLINE

- * ATMOSPHERIC ULTRAVIOLET RADIATION
- * COMPARISONS WITH LOWTRAN 7
- * AURIC OVERVIEW
- * MEASUREMENTS NEEDS

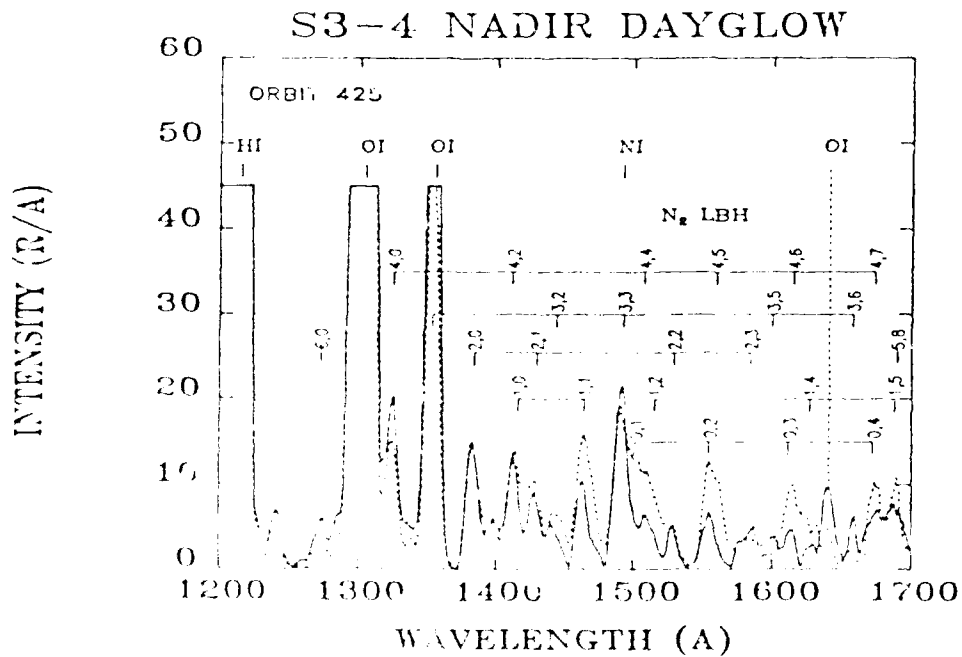
ULTRAVIOLET WAVELENGTH REGIONS

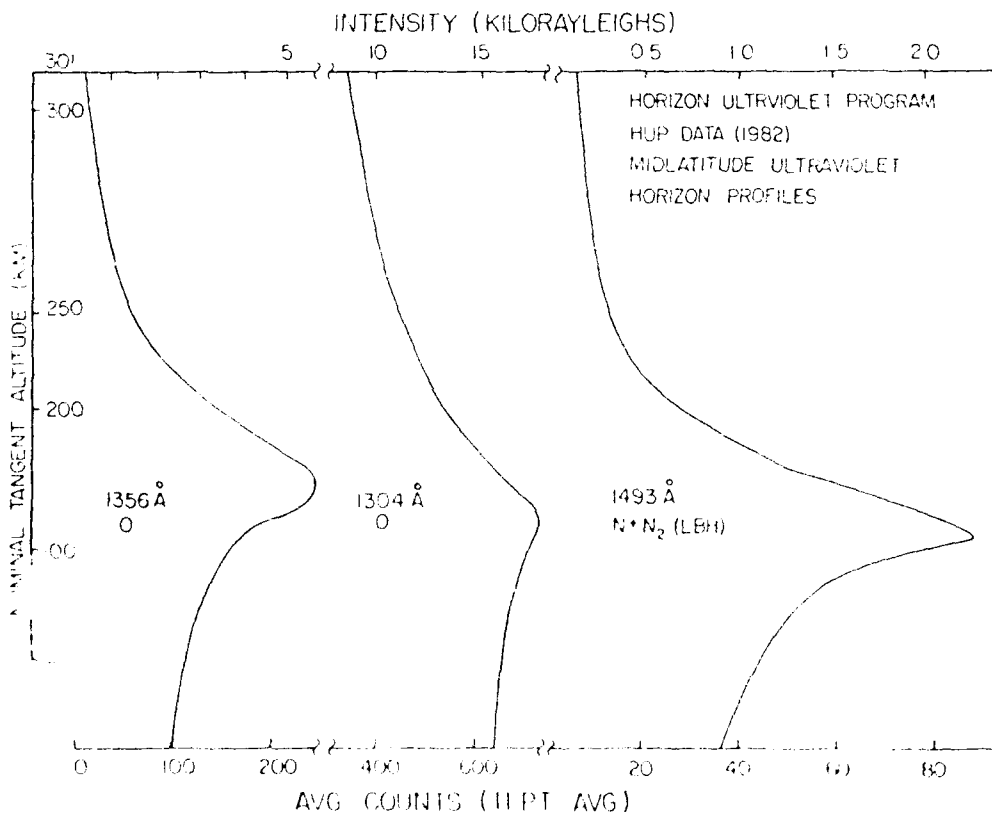
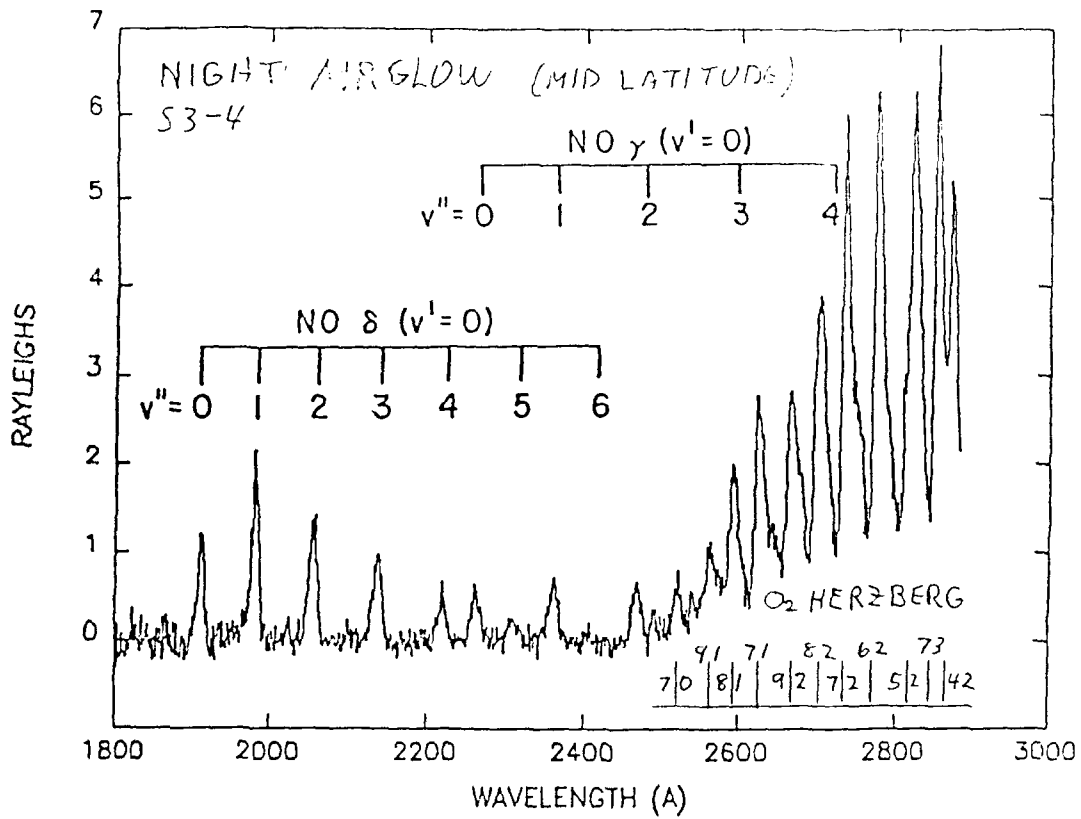
MICROMETER	0.1	0.2	0.3	0.4
NANOMETER	100	200	300	400
ÅNGSTRÖM	1000	2000	3000	4000

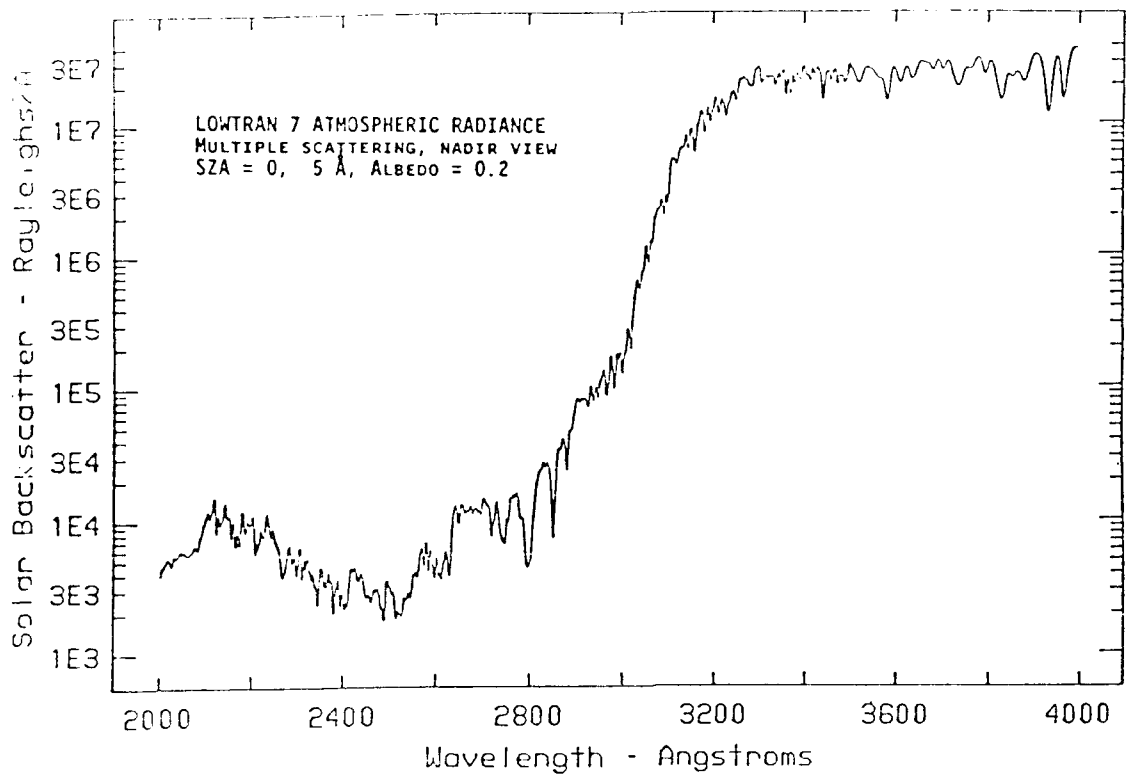




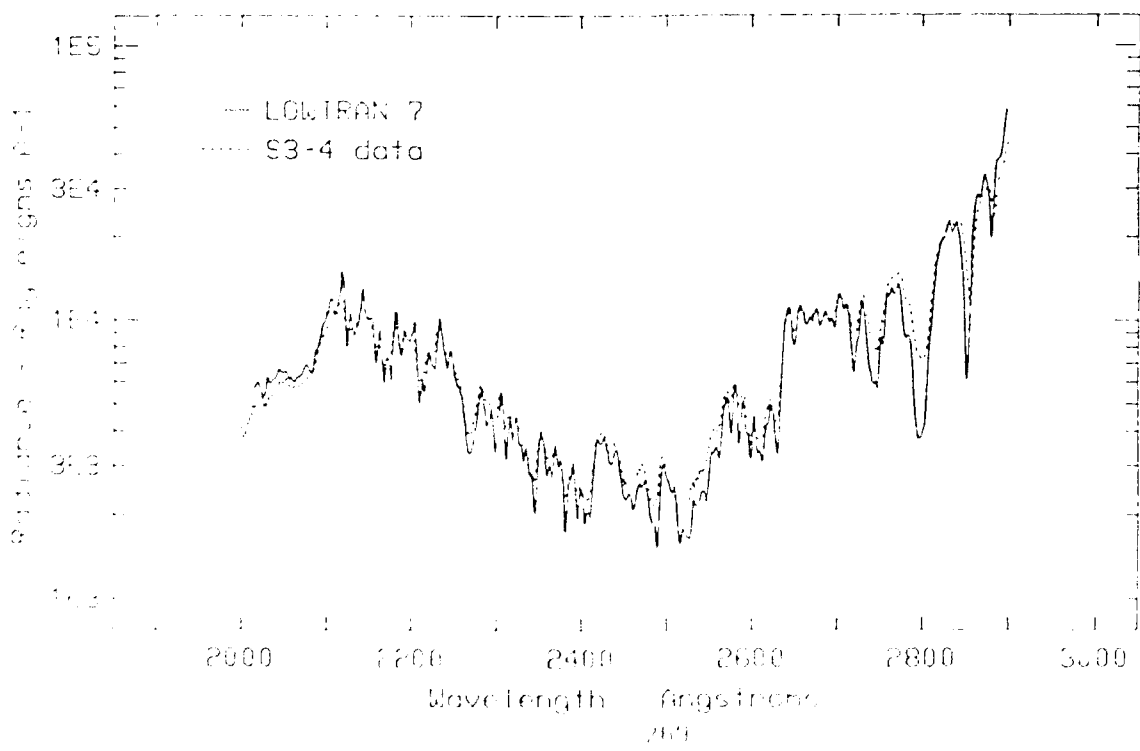
Based on
 Robert E. Huffman, "Handbook of Geophysics"
 Air Force Geophysics Laboratory, 1986
 AFGL(LIU) Hanscom AFB MA 01731/(617-377-3311)



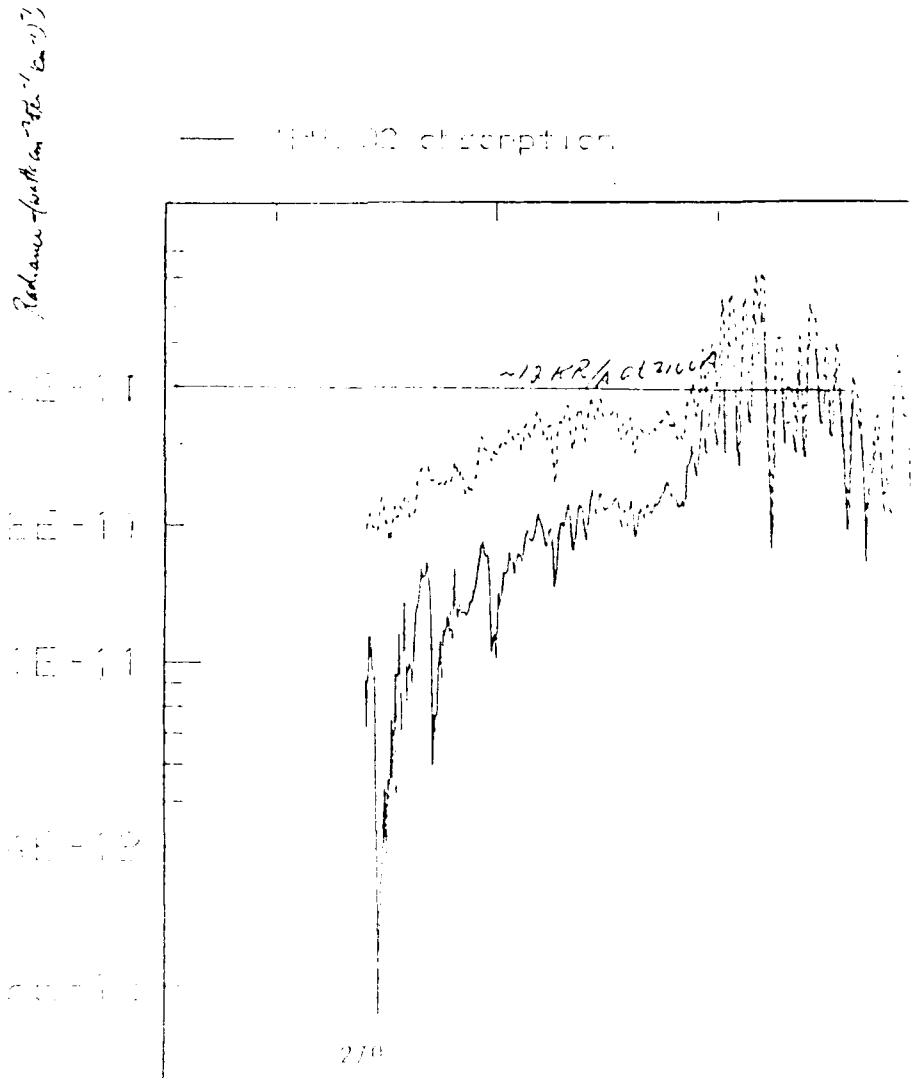
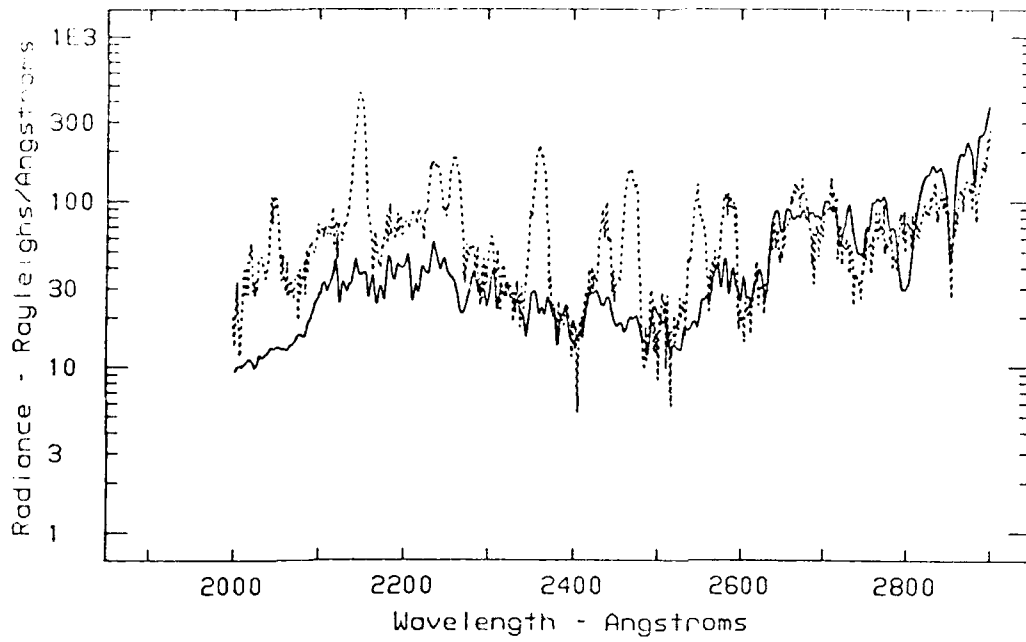




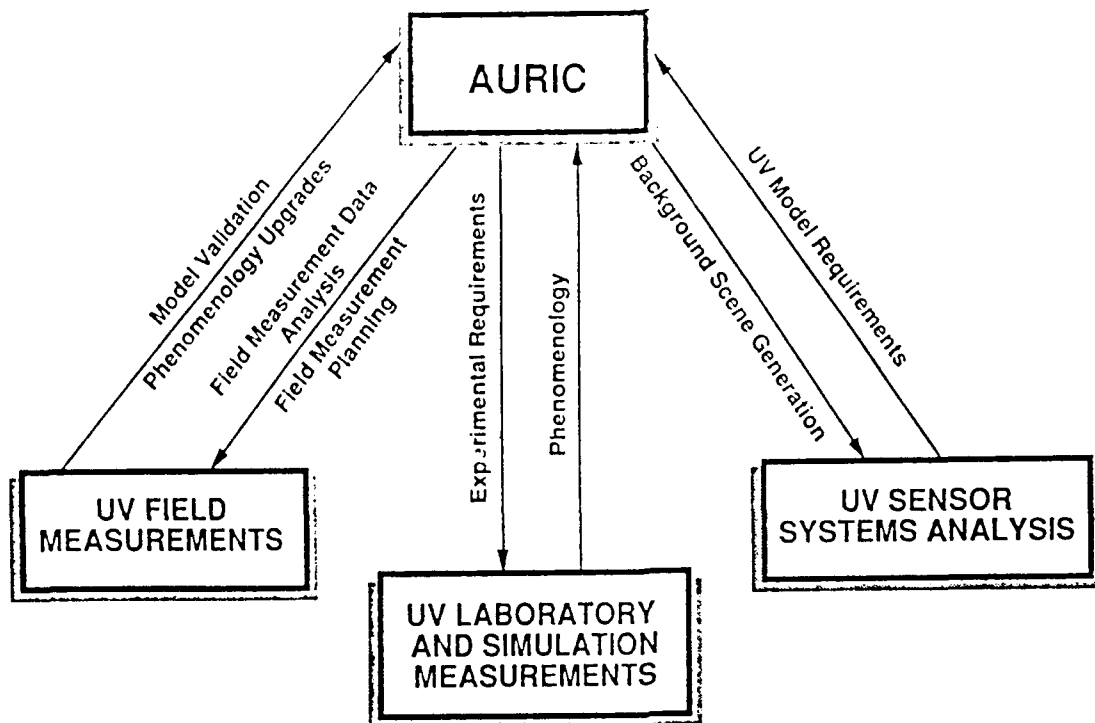
Earth Radiance - SZA 24 deg



LOWTRAN7 (solid line) and S3-4 data (dashed line), SZA=94 deg



Atmospheric Ultraviolet Radiance Integrated Code (AURIC)



MEASUREMENT NEEDS FOR AURIC: ATMOSPHERIC ULTRAVIOLET RADIANCE INTEGRATED CODE

MEASUREMENTS NEEDS

- * ATMOSPHERIC DENSITY, COMPOSITION, TEMPERATURE, ETC.
- * CROSS-SECTIONS FOR ABSORPTION, IONIZATION, ETC.
- * REACTION RATES FOR AIRGLOWS
- * SOLAR FLUX AND VARIABILITY (THROUGH EUV)
- * TRANSPORT, SCATTERING, FLUORESCENCE
- * DAY/NIGHT; SOLAR CYCLE; GEOPHYSICAL VARIABILITY
- * AURORAL REGIONS, PARTICLE EXCITATION PROCESSES
- * FIELD, LABORATORY, ASSOCIATED MODELS
- * LIMB, NADIR, TEMPORAL VARIABILITY

MODELING OF ULTRAVIOLET & VISIBLE TRANSMISSION WITH THE UVTRAN CODE

E. Patterson

School of Geophysical Sciences, Georgia Institute of Technology, Atlanta, GA 30332

J. Gillespie

U.S. Army Atmospheric Sciences Laboratory, WSMR, NM 88002

We have developed a model, UVTRAN, which allows the calculation of transmittance of visible and ultraviolet wavelengths as well as the calculation of lidar returns from backscattering or fluorescing targets. The transmission model is designed for relatively short ranges in the lower troposphere and incorporates gaseous scattering and absorption as well as aerosol attenuation. Of special note is the treatment of aerosol attenuation. The aerosol attenuation is parameterized with a wavelength dependence that depends on the visual range. The usefulness of this parameterization relative to the more usual parameterization in terms of aerosol microphysical properties whose wavelength dependence is independent of concentration will be discussed. A set of measurements is in progress that is designed to verify the transmittance models will also be discussed.

**MODELING OF ULTRAVIOLET AND VISIBLE
TRANSMISSION USING THE UVTRAN CODE**

by

**E. M. Patterson
School of Earth and Atmospheric Sciences and GTRI/EML
Georgia Institute of Technology
Atlanta, Georgia 30332**

and

**J. B. Gillespie
U. S. Army Atmospheric Sciences Laboratory
White Sands Missile Range, NM 88002**

WHY UVTRAN

Simple, user friendly model for transmission.

Includes major molecular absorbers.

Direct parameterization for wavelength dependence.

**Modular, suitable for inclusion in lidar simulations for
both DIAL and fluorescence measurements.**

TRANSMISSION MEASUREMENTS TO MODEL VERIFICATION

There is a relatively small data base for lower tropospheric UV transmission along horizontal paths.

Additional measurements under a variety of conditions are needed for model assessment and verification.

ASL has a program for model verification:

Urban measurements in the eastern U.S.

Co-operative measurements in desert areas of Middle East.

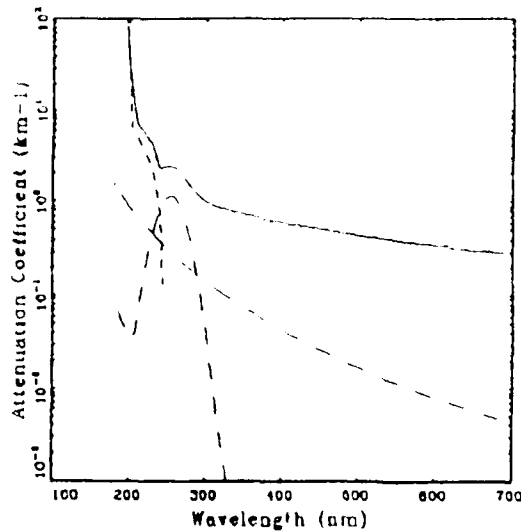
Table II. Comparison of Observed and Calculated Attenuation Coefficients at 300 nm for Different Visibilities

Visual range (km)	σ_{obs} (UVTRAN) (km^{-1})	σ_{obs} (LOWTRAN) (km^{-1})	σ_{obs} (B&D emp) (km^{-1})
100	0.137	0.047	0.213
40	0.244	0.150	0.340
20	0.476	0.320	0.553
10	0.809	0.662	0.978
5	1.41	1.34	1.83

Table III. Comparison of Observed and Calculated Attenuation Coefficients at 350 nm for Different Visibilities

Visual range (km)	σ_{obs} (UVTRAN) (km^{-1})	σ_{obs} (LOWTRAN) (km^{-1})	σ_{obs} (B&D emp) (km^{-1})
100	0.092	0.042	0.097
40	0.212	0.134	0.198
20	0.376	0.288	0.366
10	0.621	0.594	0.702
5	1.21	1.20	1.38

COMPARISONS OF MODEL PREDICTIONS FOR UV TRANSMITTANCE FOR UVTRAN, LOWTRAN, AND THE EMPIRICAL PARAMETERIZATION OF BAUM AND DUNKELMAN ARE SHOWN IN THE TABLES. SIGNIFICANT DIFFERENCE IN TRANSMISSION ARE SEEN - DIFFERENCES WHICH WILL BE ADDRESSED WITH OUR TRANSMISSION WORK.



ATTENUATION CALCULATIONS FOR STANDARD CONDITIONS AT SEA LEVEL FOR AN ASSUMED VISIBILITY OF 10 KM USING THE UVTRAN MODEL. THE TOTAL ATTENUATION COEFFICIENT IS GIVEN BY THE SOLID LINE, THE AEROSOL ATTENUATION BY THE DOTTED LINE, THE MOLECULAR SCATTERING ATTENUATION BY THE DASHED AND DOTTED LINE, THE OZONE AND OXYGEN ATTENUATIONS BY THE LONG AND SHORT DASHED LINES, RESPECTIVELY.

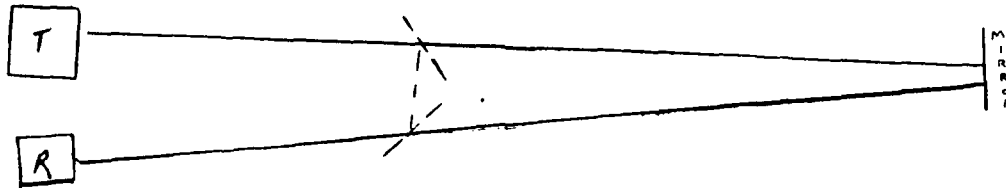
OBJECTIVES OF WORK

VERIFY PERFORMANCE OF UV-VISIBLE FILTER WHEEL TRANSMISSOMETER

MEASURE ATMOSPHERIC TRANSMITTANCE AT UV AND VISIBLE WAVELENGTHS UNDER A VARIETY OF ATMOSPHERIC CONDITIONS

VERIFY MODELS AND PARAMETERIZATION OF ATMOSPHERIC UV TRANSMITTANCE

TRANSMISSOMETER PATH GEOMETRY



ANCILLARY MEASUREMENTS NEEDED FOR MODEL VERIFICATION

Visual Range

Ozone

Atmospheric Pressure and Temperature

Aerosol Size-Number Characterization

SOFTWARE REQUIREMENTS

CONTROL FILTER WHEEL POSITIONING

DATA ACQUISITION

INITIAL DATA PROCESSING

CALCULATION OF MEANS AND STD DEVIATIONS

EVALUATION OF DATA

TRANSMISSION CALCULATIONS

FILTER WAVELENGTHS

POSITION	CENTER WAVELENGTH (NM)
0	BROAD BAND NEUTRAL DENSITY
1	200
2	220
3	240
4	260
5	280
6	320
7	360
8	400
9	440
10	550
11	BLOCKED

EXPERIMENTAL CONSIDERATIONS

CALIBRATION NEEDS

EFFECTS OF UNEQUAL PATH LENGTHS
BEAM DIVERGENCE
AMOUNT OF BEAM SEEN BY RECEIVER

ALIGNMENT STABILITY

SOURCE STABILITY

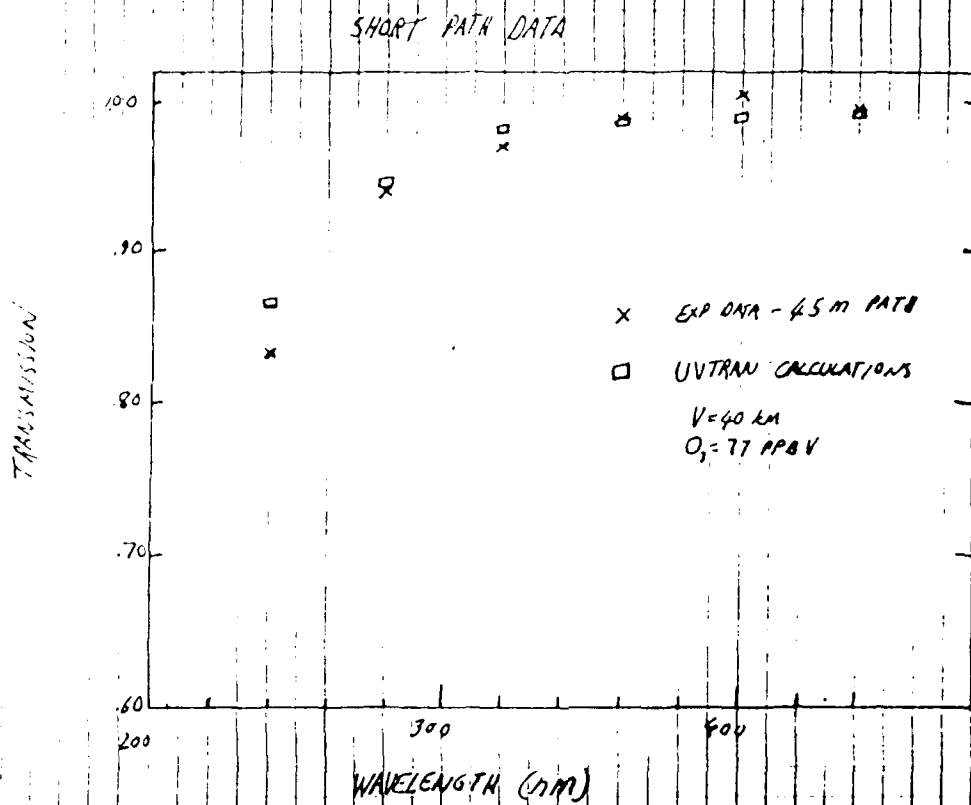
ATMOSPHERIC REFRACTION AND TURBULENCE

CALIBRATION TECHNIQUES

SIGNAL IS MEASURED FOR TWO PATH LENGTHS UNDER HIGH VISIBILITY CONDITIONS

LONG WAVELENGTH DATA AT TWO DISTANCES IS USED TO ESTIMATE A GEOMETRICAL CORRECTION FACTOR

SIMULTANEOUSLY MEASURED SCATTERING CAN BE USED TO CORRECT LONG WAVELENGTH DATA



SUMMARY

AUTOMATED UV TRANSMISSOMETER SYSTEM HAS BEEN USED FOR INITIAL MEASUREMENTS OF ATMOSPHERIC TRANSMITTANCE BETWEEN 200 AND 550 NM.

FULLY CALIBRATED MEASUREMENTS HAVE NOT YET BEEN MADE, BUT INITIAL DATA INDICATE THAT SYSTEM WILL BE SENSITIVE TO VARIATIONS IN OZONE, ATMOSPHERIC DENSITY, AND AEROSOL CHARACTERISTICS.

SYSTEM IS SUITABLE FOR DESIRED MODEL VERIFICATIONS.

SABLE: A SOUTH ATLANTIC AEROSOL BACKSCATTER MEASUREMENT PROGRAM

S.B. Alejandro, G.G. Koenig
Geophysics Laboratory/OPA, Hanscom AFB, MA 01731

J.M. Vaughn, P.H. Davies
Royal Signal & Radar Establishment, St. Andrews Road,
Great Malvern, Worcs., WR143PS, United Kingdom

The plans for an atmospheric aerosol field measurement experiment are described. The South Atlantic Backscatter Lidar Experiment (SABLE) is an important step in determining the feasibility of obtaining space-based lidar measurements for the determination of atmospheric winds, and the spatial and temporal variation of aerosol backscatter. Two field campaigns operating from Ascension Island (a British colony of St. Helena) have been completed. The first field campaign obtained lidar backscatter measurements utilizing an airborne platform during a 3-week period from mid-October through mid-November 1988. The second SABLE program was expanded to include measurements utilizing airborne particle-measurement probes, ground-based lidars, radiosondes, and supporting meteorological equipment. This program was conducted during a 4-week period from mid-June through mid-July 1989. This is the first time that such a comprehensive aerosol-measurement program has been undertaken in the Southern Hemisphere. SABLE-type measurements are not only pertinent to the development of space-based sensors, but also have direct utility in the study of aerosols and their effect on climate.

THE RSRE LASER TRUE AIRSPEED SYSTEM (LATAS)

J.M. Vaughn

Royal Signal & Radar Establishment,

St. Andrews Road, Great Malvern, Worcs., WR143PS, United Kingdom

LATAS is a compact robust airborne lidar incorporating a 10.6 μm cw CO_2 waveguide laser of 3-4 Watt output and currently installed in a Canberra B-57 aircraft. Doppler shifted radiation scattered from atmospheric aerosols is detected by coherent heterodyne techniques. Signal processing is carried out in a surface acoustic wave spectrum analyser, A/D converter and fast integrator. Integrated spectra and aircraft parameters are recorded on a high density MODAS tape recording unit. Detailed absolute calibration studies have been carried out, together with extensive algorithm development for data extraction. In a typical flight to ~15km altitude up to $\sim 10^4$ individual measurements of atmospheric backscatter may be made. Backscatter sensitivity extends to a value of $\sim 8 \times 10^{-12} \text{m}^{-1} \text{sr}^{-1}$ as currently operated. Features of the design, calibration and performance will be discussed.

**MEASUREMENTS OF AEROSOL AND CLOUD LIDAR
BACKSCATTER PROFILES IN THE EQUATORIAL SOUTH ATLANTIC**

Lt. Col. G.G. Koenig, E.P. Shettle* and S.B. Alejandro
Geophysics Laboratory/OPA, Hanscom AFB, MA 01731

J. M. Vaughn

Royal Signal & Radar Establishment,
St. Andrews Road, Great Malvern, Worcs., WR143PS, United Kingdom

Aerosol, cloud, and clean air lidar backscatter information obtained using a continuous wave coherent 10.6 micrometer CO₂ laser system flown on a B-57 Canberra aircraft will be presented. These data were collected during the South Atlantic Backscatter Lidar Experiment (SABLE) in the fall of 1988. SABLE is a cooperative aerosol lidar backscatter measurement program between the Royal Signals and Radar Establishment (RSRE) of the United Kingdom, and the Geophysics Laboratory (AFSC) of the United States. The program was organized to address a mutual interest in establishing a database of atmospheric aerosol backscatter coefficients in and around a remote (Ascension) island location in the Southern Hemisphere. Of special interest are the lidar signal levels associated with high altitude visible and sub-visible cirrus. Visible and sub-visible cirrus and marine stratocumulus lidar backscatter coefficients will be presented. The observed stratocumulus lidar backscatter coefficients will be compared with model computed backscatter coefficient information. Finally, the backscatter coefficients associated with a documented case of sub-visible cirrus will be described. This is the first time that such a comprehensive aerosol measurement program has been undertaken in a remote location in the Southern Hemisphere.

*Now at NRL.

**COMPARISONS BETWEEN SAGE II 1.02 μm EXTINCTION
AND SABLE 10.6 μm BACKSCATTER MEASUREMENTS**

E.P. Shettle*, G.G. Koenig, and S.B. Alejandro
GL/OPA, Hanscom AFB, MA 01731

J. M. Vaughn and D.W. Brown
Royal Signal & Radar Establishment, St. Andrews Road,
Great Malvern, Worcs., WR143PS, United Kingdom

The South Atlantic Backscatter Lidar Experiment (SABLE) was designed to provide a database of atmospheric aerosol backscatter coefficients in remote sensing of the South Atlantic. Such data would be utilized in evaluating the feasibility of using space-based lidar systems to obtain global measurements of aerosols and winds. Several of the SABLE flights were planned to give temporal and spatial coincidence with SAGE II (Stratospheric Aerosol & Gas Experiment) measurements of aerosol extinction. SAGE, which is a satellite based instrument, derives the aerosol extinction profiles from measurements of solar irradiances through the atmosphere during sunrise and sunset. Comparisons of the two measurements provide a partial validation of the SABLE measurements and a validation of the use of aerosol models to relate the SAGE 1.02 μm extinction to the 10.6 μm backscatter measurements. These aerosol models can then be employed with the full SAGE aerosol database to extend the spatial and temporal coverage of the SABLE measurements.

*Now at NRL.



DEPARTMENT OF THE AIR FORCE
GEOPHYSICS LABORATORY (AFSC)
HANSCOM AIR FORCE BASE, MASSACHUSETTS 01731-5000

REPLY TO
ATTN OF: OP (F.X. Kneizys, 617-377-3654/E.P. Shettle, 617-377-3665)

SUBJECT: Annual Review Conference on Atmospheric Transmission Models

TO: DISTRIBUTION

5 February 1990

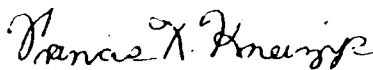
1. The extended DoD Plan for Atmospheric Transmission Research and Development tasks the Air Force to conduct an annual review conference to provide for tri-service discussion of model deficiencies and recommend corrective action.

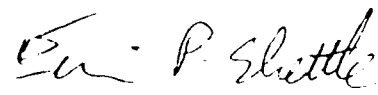
2. The 13th Annual Review Conference will be held at GL, Hanscom Air Force Base, Bedford, Massachusetts, during the first week in June (5-7 June 1990). The objectives of the meeting are to review the current status of the transmittance/radiance models and the need and plans for future developments. Areas of interest include molecular and aerosols effects on atmospheric propagation, propagation measurements using lidar, and turbulence measurements and modeling. We are interested in learning about comparisons between models and experimental data and in hearing your recommendations regarding how we can overcome any identified deficiencies.

3. This letter is intended to solicit contributions to this conference. If you would like to present a paper, please provide an unclassified abstract which should be double-spaced and no more than 12 lines. Please send abstracts to G.P. Anderson, GL/OPE (AFSC), Hanscom AFB, MA 01731-5000 by 13 April 1990. (Telephone 617-377-2335).

4. Note all sessions will be open, and it is anticipated that foreign nationals will be permitted to attend this year. Allow sufficient time to obtain the necessary clearances for your papers.

5. If you plan to participate in the conference, but not make a presentation, please notify us in writing, by 20 April 1990 (non-US citizens should allow at least 6 weeks for visit approval). Seating accommodations are limited. Send your letter to L.W. Abreu, GL/OPE (AFSC), Hanscom AFB, MA 01731-5000, (Telephone 617-377-2337). If you have any questions contact us at the numbers listed. AUTOVON prefix for Hanscom AFB is 478.


FRANCIS X. KNEIZYS
Atmospheric Effects Branch
Optical/Infrared Technology Div.


ERIC P. SHETTLE
Atmospheric Optics Branch
Optical/Infrared Technology Div.



DEPARTMENT OF THE AIR FORCE
GEOPHYSICS LABORATORY (AFSC)
HANSCOM AIR FORCE BASE, MASSACHUSETTS 01731-5000

REPLY TO OP/F. Kneizys/617-377-3654/E. Shettle/617-377-3665
ATTN OF

1 May 90

SUBJECT: Annual Review Conference on Atmospheric Models
(5-6 June 90) (AFGL/OP Ltr, 5 Feb 90, same subject)

DISTRIBUTION
TO

1. On the basis of responses to our February 5th letter announcing the Annual Review Conference on Atmospheric Transmission Models, we have constructed the enclosed tentative agenda for a two-day meeting on 5-6 June 1990. In general, we have reduced some initial time requests slightly to allow for adequate discussion. Speakers should plan on a maximum presentation time of 15 minutes. Vugraphs are preferable as visual aids in the talks. The meeting will be unclassified.

2. We ask that all conference speakers provide us with hard copies of viewgraphs used in your presentation at the meeting. You can either mail them to F.X. Kneizys GL/OPE, Hanscom AFB, MA 01731, or bring a copy to the meeting.

3. We will meet on 5-6 June (starting at 0845 on the 5th and 0830 on the 6th in the GL Science Center, Bldg 1106, Hanscom AFB. (See attached map). Please plan to arrive by 0830 on the fifth to allow time for registration on the first day.

4. We do not intend to make motel reservations for any participants, but we have enclosed a list of motels which are reasonably close to Hanscom AFB (although you will need a car for transportation). On-base government quarters are limited, so if you require VOQ accommodations, please make your reservations early by calling 617-377-2112. The AUTOVON prefix for Hanscom AFB is 478.

Francis X. Kneizys
FRANCIS X. KNEIZYS
Atmospheric Effects Branch
Optical/Infrared Technology Div.

Eric P. Shettle
ERIC P. SHETTLE
Atmospheric Optics Branch
Optical/Infrared Technology Div.

- 3 Atchs
1. Agenda
2. Map
3. List of Motels

ANNUAL REVIEW CONFERENCE ON ATMOSPHERIC TRANSMISSION MODELS

5-6 June 1990

**Geophysics Laboratory (AFSC)
Hanscom Air Force Base
GL Science Center, Building 1106**

PROGRAM

**Tuesday, 5 June 1990
(0845 - 1200)**

WELCOME - Col. Robert J. Hovde (GL)

KEYNOTE - Col. T.S. Cress, USAF(OUSDA)

SESSION 1 - ATMOSPHERIC PROPAGATION MODELS

(Co-Chair Persons: R. Picard (GL), C.M. Randall (Aerospace), R.G. Isaacs (AER))

"Status of the LOWTRAN and MODTRAN Models"

L.W. Abreu, F.X. Kneizys, G.P. Anderson, E.P. Shettle, J.H. Chetwynd (Geophysics Laboratory)

"Modeling Solar and Infrared Radiation Fields for BTI/SWOE"

J.R. Hummel (SPARTA, Inc.)

COFFEE BREAK (1020 - 1040)

**"PCTTRAN 7 - An Implementation of the GL's LOWTRAN 7 Model
for the Personal Computer"**

J. Schroeder (ONTAR Corporation)

"Spectral Modeling of Off-axis Leakage Radiance Using the MODTRAN Code"

N. Grossbard (Boston College), D.R. Smith (Geophysics Laboratory)

"Cloud Opacity Retrievals Using LOWTRAN and the Stamnes Scattering Model"

B.L. Lindner, R.G. Isaacs (Atmospheric and Environmental Research, Inc.)

"Calculated Cloud Edge SWIR Radiance Gradients as Viewed by Satellite"

L.L. Smith (Grumman Corporate Research Center)

LUNCH (1200 - 1330)

Tuesday, 5 June 1990
(1330 – 1700)

(1330 – 1450)

SESSION 2a – ATMOSPHERIC PROPAGATION MODELS (CONTINUED)

(Co-Chair Persons: R. Picard (GL), C.M. Randall (Aerospace), R.G. Isaacs (AER))

“The Department of Energy Initiative on Atmospheric Radiation Measurements (ARM): A Study of Radiative Forcing and Feedbacks”

R.G. Ellingson (University of Maryland), G.M. Stokes (Pacific Northwest Laboratories), A. Patrinos (US Department of Energy)

“The HITRAN Molecular Database in 1990”

Lt. S. Shannon, L.S. Rothman (Geophysics Laboratory)

“Line Coupling Calculations for Infrared Bands of Carbon Dioxide for FASCOD3”

M.L. Hoke, F.X. Kneizys, J.H. Chetwynd (Geophysics Laboratory); S.A. Clough (Atmospheric and Environmental Research, Inc.)

“FASCOD3: An Update (with NLTE Emphasis)”

G.P. Anderson, F.X. Kneizys, E.P. Shettle, J.H. Chetwynd, L.W. Abreu, M.L. Hoke (Geophysics Laboratory); S.A. Clough, R.D. Worsham (Atmospheric and Environmental Research, Inc.)

COFFEE BREAK (1450 – 1510)

Tuesday, 5 June 1990
(1330 – 1700)

(1510 – 1700)

SESSION 2b – LINE-BY-LINE APPLICATIONS

(Co-Chair Persons: R. Picard (GL), C.M. Randall (Aerospace), R.G. Isaacs (AER))

“RAD: A Line-by-Line Non-LTE Radiative Excitation Model”

R.H. Picard, R.D. Sharma, J.R. Winick (Geophysics Laboratory); P.P. Wintersteiner, A.J. Paboojian, R.A. Joseph (ARCON Corp); H. Nebel (Alfred University)

“Non-LTE CO₂ Vibrational-Temperature Profiles for FASCOD3”

P.P. Wintersteiner, A.J. Paboojian (ARCON Corporation); J.R. Winick, R.H. Picard, (Geophysics Laboratory)

“Non-LTE CO Infrared Emission in the Mesosphere and Lower Thermosphere and Its Effect on Remote Sensing”

J.R. Winick, R.H. Picard (Geophysics Laboratory); P.P. Wintersteiner (ARCON Corp.)

“Path Characterization Algorithms for FASCODE”

R.G. Isaacs, S.A. Clough, R.D. Worsham, J.-L. Moncet, B.L. Lindner, L.D. Kaplan (Atmospheric and Environmental Research, Inc.)

“Temperature Retrievals with Simulated SCRIBE Radiances”

J.-L. Moncet, S.A. Clough, R.D. Worsham, R.G. Isaacs, L.D. Kaplan (Atmospheric and Environmental Research, Inc.)

SOCIAL HOUR – (1730 – 1900) Officer's Club

Wednesday, 6 June 1990
(0830 - 1200)

SESSION 3a - TURBULENCE
(Chairperson: J.H. Brown (GL))

"Validation of Random Phase Screens"

A.E. Naiman, T. Goldring (W.J. Schafer Associates, Inc.)

"Recent Advances in Modeling of Boundary Layer Refractivity Turbulence"

V. Theimann, A. Kohnle (FGAN-Forschungsinstitut für Optik)

SESSION 3b - AEROSOLS

(Co-Chair Persons: E.P. Shettle (NRL), R.B. Husar (Wash. U.))

"Visibility Data Filters for Europe"

B.A. Schichtel, R.B. Husar (Washington University)

COFFEE BREAK (0950 - 1010)

Wednesday, 6 June 1990
(0830 - 1200)

(1010 - 1200)

SESSION 3b - AEROSOLS (Continued)

(Co-Chair Persons: E.P. Shettle (NRL), R.B. Husar (Wash. U.))

"Comparison of XSCALE 89 Vertical Structure Algorithm with Field Measurements"

R.P. Fiegel (U.S. Army Atmospheric Sciences Laboratory)

"Spatial Non-Uniformity of Aerosols at the 15,500 ft Level"

L.A. Mathews (Naval Weapons Center), P.L. Walker (Naval Postgraduate School)

"A Method of Estimating Surface Meteorological Ranges from Satellite Aerosol Optical Depths"

D.R. Longtin, J.R. Hummel (SPARTA, Inc.); E.P. Shettle (Geophysics Laboratory)

SESSION 4a - UV MODELING

(Co-Chair Persons: R.E. Huffman (GL), J.B. Gillespie (ASL))

"A Comparison of the UVTRAN and LOWTRAN7 Aerosol Models"

S. O'Brien (Las Cruces Scientific Consulting)

"High Resolution Solar Spectrum Between 2000 and 3100 Angstroms"

L.A. Hall, G.P. Anderson (Geophysics Laboratory)

LUNCH (1200 - 1330)

Wednesday, 6 June 1990
(1330 – 1700)

(1330 – 1510)

SESSION 4a – UV MODELING (Continued)
(Co-Chairpersons: R.E. Huffman (GL), J.B. Gillespie, (ASL))

“Predissociation Line Widths of the Schumann–Runge Absorption Bands of Some Isotopes of Oxygen”

W.H. Parkinson, J.R. Esmond, D.E. Freeman, K. Yoshino (Harvard-Smithsonian Center for Astrophysics);
A.S-C. Cheung, S.L. Chiu (University of Hong Kong)

“AURIC: Atmospheric Ultraviolet Radiance Integrated Code”

R.L. Huguenin, M.A. LeCompte (Aerodyne Research, Inc.); R.E. Huffman (Geophysics Laboratory)

“Measurement Needs for AURIC: Atmospheric Ultraviolet Radiance Integrated Code”

R.E. Huffman (Geophysics Laboratory)

“Modeling of Ultraviolet and Visible Transmission with the UVTRAN Code”

E. Patterson (Georgia Institute of Technology), J. Gillespie (U.S. Army Atmospheric Sciences Laboratory)

COFFEE BREAK (1510 – 1530)

Wednesday, 6 June 1990
(1330 – 1700)

(1530 – 1700)

SESSION 4b – LIDAR

(Co-Chairpersons: Lt. Col. G.G. Koenig, S.B. Alejandro (GL))

“SABLE: A South Atlantic Aerosol Backscatter Measurement Program”

S.B. Alejandro, G.G. Koenig (Geophysics Laboratory); J.M. Vaughn, P.H. Davies (Royal Signals and Radar Establishment)

“The RSRE Laser True Airspeed System (LATAS)”

J.M. Vaughn (Royal Signals and Radar Establishment)

**“Measurements of Aerosol and Cloud Lidar Backscatter Profiles
in the Equatorial South Atlantic”**

Lt. Col. G.G. Koenig, E.P. Shettle, S.B. Alejandro (Geophysics Laboratory); J.M. Vaughn (Royal Signals and Radar Establishment)

**“Comparisons Between SAGE II 1.02 μm Extinction and SABLE
10.6 μm Backscatter Measurements”**

E.P. Shettle, G.G. Koenig, S.B. Alejandro (Geophysics Laboratory); J.M. Vaughn, D.W. Brown (Royal Signals and Radar Establishment)

Appendix

**Annual Review Conference on Atmospheric Transmission Models
5-6 June 1990
Attendance List**

Name	Affiliation	Phone Number
Mr. Leonard Abreu	GL/OPE Hanscom AFB, MA 01731-5000	617-377-2337
Dr. Steven B. Alejandro	GL/OPA Hanscom AFB, MA 01731-5000	617-377-4774
Ms. Gail Anderson	GL/OPE Hanscom AFB, MA 01731-5000	617-377-2335
Mr. Dave Anderson	GL/LIU Hanscom AFB, MA 01731-5000	
Mr. Terry E. Battalino	Geophysics Division (Code 3253) Pacific Missile Test Center Point Mugo, CA 93042-5000	805-898-8115
Dr. Donald E. Bedo	GL/OPA Hanscom AFB, MA 01731-5000	617-377-3667
Cynthia Beeler	Visidyne, Inc. South Bedford Street Burlington, MA 01803	617-273-2820
Dr. Alexander Berk	Spectral Sciences, Inc. 111 S. Bedford Street Burlington, MA 01803	617-273-4770
Dr. Larry Bernstein	Spectral Sciences, Inc. 111 S. Bedford Street Burlington, MA 01803	617-273-4770
Col. A. Blackburn	GL/OP Hanscom AFB, MA 01731-5000	
Mr. James H. Brown	GL/OPA Hanscom AFB, MA 01731-5000	617-377-4412

**Annual Review Conference on Atmospheric Transmission Models
5-6 June 1990
Attendance List**

Name	Affiliation	Phone Number
Mark W.P. Cann	Centre for Research in Experimental Space Science York University 4700 Keele Street Downsview, Ontario M3J 1P3 Canada	416-736-2100 ext 33508
Dr. Ken Champion	GL/LY Hanscom AFB, MA 01731-5000	617-377-3033
David T. Chang	AER, Inc. 840 Memorial Drive Cambridge, MA 02139	617-547-6207
Pierre Chervier	Oerlikon Aerospace 225 Blvd. Seminaire South St. Jean, Quebec J3B 8E9 CANADA	514-358-2000
Dr. Michael G. Chieftetz	SPARTA, Inc. 21 Worthen Road Lexington, MA 02173	617-863-1060
Mr. James H. Chetwynd	GL/OPE Hanscom AFB, MA 01731-5000	617-377-2613
Maureen Cianciolo	TASC 55 Walkers Brook Drive Reading, MA 01867	617-942-2000
Mr. Shepard A. Clough	AER, Inc. 840 Memorial Drive Cambridge, MA 02139	617-547-6207
Dr. William M. Cornette	Photon Research Associates, Inc. 9393 Town Center Drive San Diego, CA 92121	619-455-9741
Col. Ted Cress	OUSDA (R&AT/E&LS) The Pentagon/Room 3D1219 Washington, DC 20301	AV225-9604

Annual Review Conference on Atmospheric Transmission Models
5-6 June 1990
Attendance List

Name	Affiliation	Phone Number
Dr. Gilbert Davidson	PhotoMetrics, Inc. 4 Arrow Drive Woburn, MA 01801	617-938-0300
Dr. Martine de Maziere	Institut d'Aeronomie Spatiale de Belgique 3 Avenue Circulaire Bruxelles B-11800 Belgium	32-8-3730363
Mr. Anthony Dentamaro	GL/LIU Hanscom AFB, MA 01731-5000	617-377-3484
Dr. Edmond Dewan	GL/OPE Hanscom AFB, MA 01731-5000	617-377-4401
Dr. Robert G. Ellingson	Department of Meteorology University of Maryland College Park, MD 20742	301-454-5088
Mr. Vincent Falcone	GL/LYS Hanscom AFB, MA 01731-5000	617-377-4029
Robert Farley	GL/LIS Hanscom AFB, MA 01731-5000	617-377-3090
Mr. R. Fiegel	Atmospheric Sciences Lab. White Sands Missile Range, NM 88002-5501	
Marvin Vaun Frandsen	SVERDRUP/TEAS Grp. PO Box P135 Eglin AFB, FL 32542	904-678-2001
Dr. Daryl E. Freeman	Harvard Smithsonian Center for Astrophysics 60 Garden Street Cambridge, MA 02138	617-495-2783
Ms. Joan-Marie Freni	ST Systems Corporation 109 Massachusetts Avenue Lexington, MA 02173	617-862-0405
Mr. William O. Gallery	AER, Inc. 840 Memorial Drive Cambridge, MA 02139	617-547-6207

Appendix

**Annual Review Conference on Atmospheric Transmission Models
5-6 June 1990
Attendance List**

Name	Affiliation	Phone Number
H. Gardiner	GL/OPE Hanscom AFB, MA 01731-5000	617-377-2672
Dr. James B. Gillespie	U.S. Army Atmospheric Sciences Lab.. Attn: SLCAS-AR-P (Dr. James Gillespie) White Sands Missile Range, NM 88002-5501	508-678-6609
Steven Adler Golden	Spectral Sciences, Inc. 111 S. Bedford Street Burlington, MA 01803	617-273-4770
T. Goldring	W.J. Schafer Associates Arlington, VA 22209	
Dr. R. Earl Good	GL/OP Hanscom AFB, MA 01731-5000	
Mr. Donald Grantham	GL/LYA Hanscom AFB, MA 01731-5000	617-377-2982
Dr. M. Griffin	GL/LYS Hanscom AFB, MA 01731-5000	617-377-2961
Neil Grosbard	Boston College 885 Centre Street Newton, MA 02159	617-377-3752
Dr. L.A. Hall	GL/LIU Hanscom AFB, MA 01731-5000	617-377-3322
Ms. Larrene Harada	W.J. Schafer Associates, Inc. 1901 North Fort Meyer Drive, Suite 800 Arlington, VA 22209	703-558-7900
Kenneth R. Hardy	Lockheed Missiles and Space Co., Inc. Org 9/01 B/201 3251 Hanover Street Palo Alto, CA 94304	415-424-2825
Dr. Richard Hendl	GL/CA Hanscom AFB, MA 01731-5000	

**Annual Review Conference on Atmospheric Transmission Models
5-6 June 1990
Attendance List**

Name	Affiliation	Phone Number
Glen J. Higgins	ST Systems Corporation 109 Massachusetts Avenue Lexington, MA 02173	617-862-0405
Dr. Mike Hoke	GL/OPI Hanscom AFB, MA 01731-5000	377-3614
Ann S. Hollis	SSD Meteorology Department 50, 2nd Weather Squadron Los Angeles AFB, PO Box 92960 Los Angeles, CA 90009	213-643-0304
Col. Robert J. Hovde	GL/CC Hanscom AFB, MA 01731-5000	
Mr. Robert E. Huffman	GL/LIU Hanscom AFB, MA 01731-5000	617-377-3311
R.L. Huguenin	Aerodyne Research, Inc. 45 Manning Road Billerica, MA 01821	508-663-9500
Dr. John R. Hummel	SPARTA, Inc. 21 Worthen Road Lexington, MA 02173	617-863-1060
Charles Humphrey	Visidyne, Inc. South Bedford Street Burlington, MA 01803	617-273-2820
Dr. Rudolf B. Husar	CAPITA Washington University Campus Box 1124 St. Louis, MO 63130	
Dr. Keith Hutchinson	TASC 55 Walkers Brook Drive Reading, MA 01867	617-942-2000
Dr. Ronald G. Isaacs	AER, Inc. 840 Memorial Drive Cambridge, MA 02139	617-547 6207

Appendix

**Annual Review Conference on Atmospheric Transmission Models
5-6 June 1990
Attendance List**

Name	Affiliation	Phone Number
Frank W. Jenks	ASD/WE WPAFB, OH 45433-6503	AV 785-2207
Dr. Douglas W. Johnson	AER, Inc. 840 Memorial Drive Cambridge, MA 02139	617-547-6207
Mr. Robert A. Joseph	ARCON Corporation 260 Bear Hill Road Waltham, MA 02154	617-890-3330
Mr. Frank T. Kantrowitz	Atmospheric Sciences Laboratory White Sands Missile Range, NM 88002	505-678-4313
Dr. Lewis D. Kaplan	AER, Inc. 840 Memorial Drive Cambridge, MA 02139	617-547-6207
Stefan Kinne	NASA Ames Research Center Mail Stop 245-4 Moffett Field, CA 94035	515-604-5505
Mr. Francis X. Kneizys	GL/OPE Hanscom AFB, MA 01731-5000	617-377-
Lt. Col. George Koenig	GL/OPA Hanscom AFB, MA 01731-5000	
David Lees	SPARTA, Inc. 21 Worthen Road Lexington, MA 02173	617-863-1060
Dr. Bernhard L. Lindner	AER, Inc. 840 Memorial Drive Cambridge, MA 02139	617-547-6207
Mr. David R. Longtin	OptiMetrics, Inc. 50 Mall Road Burlington, MA 01803	617-863-1060
Sam Makhlouf	GL/OPE Hanscom AFB, MA 01731-5000	617-377-3766

**Annual Review Conference on Atmospheric Transmission Models
5-6 June 1990
Attendance List**

Name	Affiliation	Phone Number
John E. Malowicki	RADC/OCSP Griffis AFB, MA 13441-5700	315-330-3055
Mr. Joseph Manning	107 W. Henry Street Salina, MI 48176	313-429-2043
Mr. Larry A. Mathews	Research Department, Code 3895 Naval Weapons Center China Lake, CA 93555	619-939-3368
Dr. Robert A. McClatchey	GL/LY Hanscom AFB, MA 01731-5000	
Susan M. McKenzie	Mission Research Corporation 1 Tara Boulevard, Suite 302 Nashua, NH 03062	603-891-0070
Jean-Luc Moncet	AER, Inc. 840 Memorial Drive Cambridge, MA 02139	617-547-6207
Aaron E. Naiman	W.J. Schafer Associates Arlington, VA 22209	703-558-7900
Paul Noah	Ontar Corporation 129 University Road Brookline, MA 02146	617-739-6607
Meg Noah	Ontar Corporation 129 University Road Brookline, MA 02146	617-739-6607
Dr. Sean G. O'Brien	3373 Solar Ridge Street Las Cruces, NM 88001	382 505- 522 -0285
Dr. Robert O'Neil	GL/OPE Hanscom AFB, MA 01731-5000	617-377-3688
Armand J. Paboojian	ARCON Corp. 260 Bear Hill Road Waltham, MA 02154	617-890-3330

**Annual Review Conference on Atmospheric Transmission Models
5-6 June 1990
Attendance List**

Name	Affiliation	Phone Number
Dr. W.H. Parkinson	Harvard Smithsonian Center for Astrophysics 60 Garden Street Cambridge, MA 02138	617-377-4865
Dr. Duane Paulsen	GL/OPB Hanscom AFB, MA 01731-5000	617-377-3618
Mr. Paul W. Pellegrini	RADC/ESE Hanscom AFB, MA 01731-5000	617-377-3699
Dr. William A. Peterson	U.S. Army Atmospheric Sciences Lab Attn: SLCAS-AS-D (Dr. William Peterson) White Sands Missile Range, NM 88002-5501	505-678-1465
Ms. Angela Phillips	E-O & Data Systems Group Hughes Aircraft Company PO Box 902 El Segundo, CA 90245	213-616-0124
Dr. Richard H. Picard	GL/OPE Hanscom AFB, MA 01731-5000	617-377-2222
Dr. Alan B. Plaut	MIT/Lincoln Laboratory MS N259 244 Wood Street Lexington, MA 02173-0073	617-981-5500
A. Pritt	Aerospace Corporation PO Box 92957 Los Angeles, CA 90009-2957	213-336-6701
Mr. Charles M. Randall	Chemical Physics Department Aerospace Corporation PO Box 92957 Los Angeles, CA 90009-2957	213-336-5977
Dr. Anthony Ratkowski	GL/OPB Hanscom AFB, MA 01731-5000	617-377-3630
Dr. David C. Robertson	Spectral Sciences, Inc. 111 S. Bedford Street Burlington, MA 01803	617-273-4770

**Annual Review Conference on Atmospheric Transmission Models
5-6 June 1990
Attendance List**

Name	Affiliation	Phone Number
Mr. Ron Rodney	WRDC/WEA WPAFB, OH 45433-6543	513-225-1978
Dr. Laurence S. Rothman	GL/OPI Hanscom AFB, MA 01731-5000	617-377-
Crystal Schaff	GL/LYA Hanscom AFB, MA 01731-5000	617-377-2963
Dr. John Schroeder	Ontar Corporation 129 University Road Brookline, MA 02146	616-739-6607
Dr. Bertram D. Schurin	MS E-55-MS/G-223 Hughes Aircraft Company PO Box 902 El Segundo, CA 90245	213-544-4494
Dr. John E. A. Selby	Research Department, MS A08-35 Grumman Aerospace Corporation South Oyster Bay Road Bethpage, NY 11714	
Lt. Scott D. Shannon	GL/OPI Hanscom AFB, MA 01731-5000	617-377-3694
Mr. Eric P. Shettle	Code 6522 Optical Sciences Division Naval Research Laboratory Washington, DC 20375-5000	202-404-8152
Mr. Richard C. Shirkey	Atmospheric Sciences Laboratory DELAS-EO-S White Sands Missile Range, NM 88002	
Donald R. Smith	GL/OPB Hanscom AFB, MA 01731-5000	617-377-3203
Dr. Lewis L. Smith	Mail Stop A01-26 Grumman Corporate Research Center Bethpage, NY 11714-3580	516-575-2196

Appendix

**Annual Review Conference on Atmospheric Transmission Models
5-6 June 1990
Attendance List**

Name	Affiliation	Phone Number
Donald M. Stebbins	RADC/OCSP Griffis AFB, NY 13441-5700	315-330-3056
Robert Sundberg	Spectral Sciences, Inc. 111 S. Bedford Street Burlington, MA 01803	617-273-4770
Mr. Frank Suprin	GL/OPA Hanscom AFB, MA 01731-5000	617-377-3664
Capt. Andrew Terzakis	WL/WE Kirtland AFB, NM 87117-608	508-844-0451
Volker Thiermann	Forschungsinstitut fur Optik FGAN Schloss Kressback D-7400 Tubinger 1 Federal Republic of Germany	707-709161
Peter B. Ulrich	W.J. Schafer Associates Arlington, VA 22209	703-558-7900
Dr. George A. Vanasse	GL/OPI Hanscom AFB, MA 01731-5000	
J. Michael Vaughn	Royal Signals & Radar Establishment Malvern, WORCS, WR143PS United Kingdom	0684-895759
Dr. Fred Volz	GL/OPI Hanscom AFB, MA 01731-5000	
Ron Wachtmann	ST Systems Corporation 19 Massachusetts Avenue Lexington, MA 02173	617-862-0405
Dr. Richard Wattson	Visidyne, Inc. 10 Corporate Place Burlington, MA 01803	617-273-2820

Annual Review Conference on Atmospheric Transmission Models
5-6 June 1990
Attendance List

Name	Affiliation	Phone Number
Sandi Weaver	WRDC/WEA WPAFB, OH 45433-6543	513-225-1978
Steven P. Weaver	FTD/WE WPAFB, OH 45433-6503	513-257-6525
Alan Wetmore	US Army Atmos. Sci. Lab. Attn: SLCAS-AE-T (Alan Wetmore) White Sands Missile Range, NM 88002-25501	505-678-5563
Dr. Jeremy R. Winick	GL/OPE Hanscom AFB, MA 01731-5000	617-377-3619
Mr. Peter P. Wintersteiner	ARCON Corporation 260 Bear Hill Road Waltham, MA 02154	617-890-3330
Mr. R.D. Worsham	AER, Inc. 840 Memorial Drive Cambridge, MA 02139	617-547-6207
Dr. A.S. Zachor	Atmospheric Radiation Consultants 59 High Street Acton, MA 01720	508-263-1931

AUTHOR INDEX

Abreu, Leonard W.	1, 88	Lindner, Bernhard L.	45, 137
Alejandro, Steven B.	280, 282, 283	Longtin, David R.	219
Anderson, Gail P.	1, 88, 237	Mathews, Larry A.	3
Brown, D.W.	283	Moncet, Jean-Luc	137, 145
Chetwynd, James H.	1, 80, 88	Naiman, Aaron E.	155
Cheung, A.S-C.	245	Nebel, Henry	99
Chiu, S.L.	245	O'Brien, Sean G.	226
Clough, Shepard A.	80, 88, 137, 145	Paboojian, Armand J.	99, 112
Davies, P.H.	280	Parkinson, W.H.	245
Ellingson, Robert G.	62	Patrinos, Ari	62
Esmond, J.R.	245	Patterson, E.M.	272
Fiegel, R.P.	193	Picard, Richard H.	99, 112, 125
Freeman, Daryl E.	245	Rothman, Laurence S.	71
Gillespie, James B.	272	Schichtel, Bret A.	185
Goldring, T.	155	Schroeder, John	26
Grossbard, Neil	34	Shannon, Scott	71
Hall, L.A.	237	Sharma, R.D.	99
Hoke, Michael L.	80, 88	Shettle, Eric P.	1, 88, 219, 282, 283
Huffman, Robert E.	252, 264	Smith, Donald R.	34
Hugueinin, R.L.	252	Smith, Lewis L.	54
Hummel, John R.	13, 219	Stokes, Gerald M.	62
Husar, Rudolf B.	185	Theirmann, Volker	173
Isaacs, Ronald G.	45, 137, 145	Vaughn, J. Michael	280, 281, 282, 283
Joseph, Robert A.	99	Walker, Philip L.	208
Kaplan, Lewis D.	137, 145	Winick, Jeremy R.	99, 112, 125
Kneizys, Francis X.	1, 80, 88	Wintersteiner, Peter P.	99, 112, 125
Koenig, George G.	280, 282, 283	Worsham, Robert D.	88, 137, 145
Kohnle, A.	173	Yoshino, K.	245
LeCompte, Malcolm A.	252		